The role of deep-seated landsliding in the geomorphic evolution of the Esk Valley, Hawke's Bay: An innovative approach to hazard evaluation

---

A thesis

submitted in partial fulfilment

of the requirements for the degree

of

Master of Science in Engineering Geology

at the

University of Canterbury

by

Kerry John Leith

UNIVERSITY OF CANTERBURY

2003

ABSTRACT

An engineering geomorphological investigation of the Esk River catchment has been undertaken to quantify the relationships between the valley's geomorphic evolution, the many 1-10km^2 deep-seated landslides present within the catchment, and a significant flood event that inundated the lower valley in April 1938. The identification of key geomorphic processes enabled the assessment of catchment's geomorphic stability, the development of generalised models for landsliding, and the delineation of a pre-disposed zone of instability. This information is then applied to assess key geomorphic controls on the flood event.

The region lies within the forearc basin of the obliquely convergent Hikurangi Margin, and is underlain by soft, gently eastward dipping Pliocene marine strata. Structurally it is dominated by its close proximity to the Mohaka Fault, as well as two westward-dipping blind thrusts beneath the valley identified in this study: the Wakarara Fault – Trelinnoe Sector, and the Eastern Patoka Fault. Evidence from seismic reflection surveys indicates that these have both been active since the early Mangapanian (2.8 – 3.2 Ma), and an analysis of stream longitudinal profiles and plan form suggests limited displacement may have taken place within the last 10,000 years.

A survey of rock mass defects within a representative sample area in the centre of the valley highlights four sub-vertical joint sets; conjugate sets strike 153° and 246°, and another sub-parallel to the folding strikes 033°. These defects correlate well with lineaments identified in aerial and satellite photographs and are attributed to extension of the sediments across the top of fault-propagated folds. The generally low power streams have exploited these defects and highly incised channels now run almost exclusively along them.

Deep-seated landslides occur generally within the area of folding and their extents are defined by lineaments inferred to correspond to persistent joints in the rock mass. The slides are translational, and are facilitated by up to 80m of incision – ongoing since the abandonment of an extensive terrace inferred to be Ohakean (18-10ka) in age. Basal failure surfaces commonly dip at angles as low as 6°, and a combination of tectonically induced flexural shears sub-parallel to bedding and very low shear strength tuffaceous horizons are inferred to provide planes of sufficiently low shear strength to facilitate failure. While most deep-seated landslides appear active, there is no evidence to suggest they were substantially affected by recent major tectonic (e.g. 1931 M_s7.8 Hawke's Bay Earthquake) or climatic events (e.g. 1938 c.1:1000yr Esk Valley Storm).

The headwaters of the catchment are located on the Maungaharuru Range. This rises from 500m – 1300m and provides baseflow to the Esk River. Extensive deep-seated landslides dominate the eastern face of the range. These are inferred to have been triggered by the removal of lateral support at the foot of the range following significant incision and denudation in the last interglacial c.125ka. A deep-seated gravitational slope deformation is proposed to extend to 1.2km below sea level, and provide a driving mechanism for the slides.

While the 1938 Esk Valley flood was primarily a result of an exceptional three day storm event, suspended sediment load was also an important factor. This is inferred to have resulted primarily from channel erosion in soft colluvial sediments on the Maungaharuru Range. Combined with significant sediment load from shallow landsliding and possible tectonic subsidence preconditioning the lower reaches of the aggradational valley, this lead to c.1m of silt being deposited in the lower reaches of the aggradational valley. Rapid stream incision in response to uplift in 1931 and aggradation in 1938 is returning the lower reach of the river to grade and decreasing the flood hazard.

TABLE OF CONTENTS

LIST OF FIGURES AND TABLES

ACKNOWLEDGEMENTS

Firstly I would like to thank my supervisors Jarg Pettinga and Jim McKean for putting in such a well orchestrated tag-team effort. Your enthusiasm, patience, and ability to take each new idea with a completely open mind (no matter how far-out the previous one was) has been key to allowing this project, and me, to continue to develop to the stage it has today. I would also like to thank Joc Campbell, who always had a few minutes to lend suggestions whenever the need arose, and managed to somehow make writing a thesis seem like an everyday undertaking.

The instigation of this project came from a suggestion by Gary Clode at the Hawke's Bay Regional Council, without this I would probably never have made it out to such a fantastic part of the country. The HBRC not only provided considerable funding and logistical support to this project, but also a great place to work and I am grateful to all the staff who so often went out of their way to give me a hand. In particular I'd like to thank Gary for his interest and support, and providing such a flexibile project; Garth Eyles for subjecting me to some interesting debates, Karen Roberts for the fantastic place to live, Simon Stokes and Craig Goodier for giving up so much of their time to get me up to speed, Jan for the Christmas present, and Mike Adye for giving me the run of the truck.

The remainder of the funding for this project came from the Mason Trust Fund for which I am sincerely grateful.

Speaking of financial assistance, I'd like to thank my parents Ross and Jill for getting me to this stage. Blind faith can go a long way, and I hope you guys know how much your unwavering support has meant.

I'd like to thank Kyle Bland and Nicola Litchfield for participating in some rather lengthy e-mail conversations. It was invaluable to get your input, and without your prompt responses I don't know what I would've done some days.

To all the farmers of the Esk Valley, and Pan Pac and Carter Holt Forests I would like to say thankyou for providing such free access, and being so hospitable on some of the more inclement days. I would particularly like to thank John and Fiona Wills of Trelinnoe Station – first off, for saving my bacon more than once, and secondly for being so hospitable and welcoming on my many visits.

To Tans – the hardest working identity crisis on the block – thanks for all the good times, and here's to many more!

Finally I'd like to thank some of the people responsible for continually providing a taste of that "real world" outside of the confines of the office, particularly in the latter months. To Leen, and the boys from Hansons Ln., Em, Nash, all the girls that ever called Brockworth home, Verne, Andrew, Andy, Jim, and Sam (ya...) - I think now's time to start following up on some of those plans...

1 INTRODUCTION

1.1 PREAMBLE

The geomorphic evolution of a landscape involves the generation of landscape form by the complex interaction of constructive, destructive, and sediment transport processes. While constructive processes relate almost solely to volcanic and tectonic activity, landscape degradation can be the result of fluvial, aeolian, and glacial processes as well as various forms of mass wasting. The latter involves the transport of material downslope under the influence of gravity, and can take the form of falls, topples, slides, spreads and flows (Varnes, 1978). The contribution of mass wasting to landscape evolution depends on the scale, frequency, and duration of the instability; these factors can vary over many orders of magnitude depending on the nature of the instability process.

Deep-seated landslides are defined in this investigation as those that undergo failure in unweathered bedrock, they are typically large (hundreds of metres to kilometre scale), long-term (thousands of years) processes. In areas such as the Esk Valley in central Hawke's Bay, where deep-seated landslides are common, they can be both a product of, and key geomorphic contributor to, the environment in which they are located. They are therefore important processes in landscape evolution. An understanding of the relationship between mass wasting and the evolution of an active geomorphic system such as the Esk River catchment, especially the mechanics and processes involved, can provide valuable insight into the stability, activity, and mechanics of the landslide(s) as well as the relative roles of other active processes in defining the stability of the system.

The Esk River Valley offers an excellent opportunity to investigate the role of mass wasting in the geomorphic evolution of a landscape. It is located in a tectonically active region of New Zealand, and is underlain by a relatively homogeneous sequence of soft, Plio-Pleistocene marine sedimentary strata. The combination of these factors has produced a rapidly evolving, structurally simple landscape containing a number of medium and large-scale deep-seated landslides.

The valley covers an area of 238km^2 and is located immediately north of Napier on the east coast of the North Island. Flooding in the lower reaches of the valley related to high suspended sediment loads, possibly derived from these deep-seated landslides, has in the

past put people and property at risk. An engineering geomorphological investigation into the relationship between the deep-seated slides and other geomorphic processes active within the Esk Valley has the potential to provide a rapid, cost effective means of evaluating the stability of the slides, as well as valuable information regarding their role in the flooding hazard.

1.2 THESIS AIMS AND OBJECTIVES

The primary aims of this project are to: (1) assess the role of deep-seated landsliding in valley evolution by evaluating active processes, and investigating key relationships between deep-seated landsliding and other geomorphic processes within the Esk Valley (e.g. drainage evolution or tectonic forcing); and (2) assess the contribution of deep-seated landsliding to the long-term flooding hazard in the lower Esk Valley. In order to achieve these aims a number of specific objectives have to be met, initially to investigate the relationships between deep-seated landsliding and geomorphic processes in the catchment:

- Identify and delineate the extents of deep-seated landsliding in the valley
- Determine key geomorphic processes and their likely development over time
- Identify and quantify structural controls
- Relate landforms to geomorphic processes, both ancient and present-day
- Classify landslides based on morphology and likely failure style; and
- Determine the relationship between landsliding and key geomorphic processes.

Then, to assess the role of landsliding in generating potentially hazardous flood conditions:

- Quantify key aspects of the 1938 flood including climatic contributors, duration, flow characteristics, and sediment output.
- Quantify sediment input from deep-seated landsliding.
- Identify alternative sediment sources and estimate volume contributions; and
- Assess the current activity of geomorphic processes – including deep-seated landsliding – and their relationship to the long-term flood hazard.

A wide range of Engineering Geomorphological techniques were used to achieve these objectives, including aerial photo interpretation, digital terrain model analysis,

geomorphological mapping, rock mass defect surveys, and seismic reflection interpretation. While – as with many earth science investigations – individual techniques rarely provide an unambiguous answer; the strength of this investigation lies in the combination of results from each technique. This integrated approach allowed the following specific research questions to be answered:

- Are there fundamental controls associated with the activity and mechanics of deep-seated landsliding in the area, and if so what are they?
- Did deep-seated landsliding contribute significantly to the 1938 flood hazard?
- Did a severe earthquake in 1931 significantly destabilise deep-seated landslides in the catchment?
- Is the Esk Valley at steady-state, and if not, was the flooding observed in 1938 simply a reflection of this and therefore likely to be part of a long-term, ongoing process?
- What is the probability of a similar flood event occurring today?
- Is an investigation into the geomorphology of landslides and the surrounding environment a viable means of assessing the associated hazard at a regional scale?

1.3 STUDY AREA

The Esk Valley reaches the coast about 10km north of Napier. The river occupies the eastern side of a narrow, northward trending catchment and is fed by short E-W trending tributary streams. Topography in the lower valley is characterised by low hills and lithologically controlled ridges; in the upper valley the low hills give way to broad terraces while highly incised drainages dissect the topography throughout the region. These drainages act as effective natural barriers, often making travel through the catchment difficult. Limestone capped ridges define the northern and eastern bounds of the valley and have a significant orographic effect on local rainfall distribution.

Despite problems posed by the highly incised streams, access to the valley is good and the majority of the area is within 40 minutes drive from Napier city. State Highways 2 and 5 run through the valley, as does the main rail link to Gisborne.

Economic activities in the valley are varied. Intensive horticulture is the main activity in the floodplain near the mouth of the valley, and a marae, pulp and paper mill, and

electricity substation lie toward the coast. The majority of the Esk Valley is, however, developed in equal parts forestry and pastoral farming.

The Esk Valley lies in a tectonically active region of New Zealand, this is responsible for the uplift of the weak, Plio-Pleistocene sandstones and siltstones that dominate bedrock lithologies in the valley today. The tectonic activity is also associated with frequent seismic activity; since 1848 there have been 19 earthquakes with Modified Mercalli intensities of greater than 7 in Hawke's Bay (Johnson and Pearce, 1999). These factors have undoubtedly contributed to the extensive deep-seated landsliding in the valley, and around 20% of the land area is currently affected by these instabilities.

1.4 PREVIOUS RESEARCH

There has been much recent interest in east coast North Island tectonics (eg. Cutten *et al.*, 1988; Kelsey *et al.*, 1995; Neall *et al.*, 1995; Beanland and Haines, 1998; Beanland *et al.*, 1998; Barnes *et al.*, 2002), Quaternary development (eg. Berryman *et al.*, 2000; Hicks *et al.*, 2000; Crosby and advised by K. Whipple, 2001; Litchfield, 2002), landsliding (eg. Pettinga, 1987a; Pettinga, 1987b; Crozier *et al.*, 1992; Reid and Page, 2003), and petroleum exploration. However, prior to an analysis by Bland (2001) little geological work has been undertaken in the Esk Valley. This is particularly true in terms of late Quaternary geology and geomorphology where, other than work on the valley hydrology (Williams, 1986; Harrison, 1988; Black, 1991) and the production of a map of soil cover, no published investigation precedes this study.

The role of Engineering Geomorphology is rapidly becoming recognised as a "suitable, cost-effective aid to land-use planning" (Guzzetti *et al.*, 1999), but it is still at a formative stage in terms of recognised techniques. Geomorphologists have previously concentrated on describing and analysing processes involved in landscape formation (Adams, 1980; Bull, 1991; Clapp and McConchie, 2000; Gupta and Virdi, 2000), this has been used to develop methods of event prediction (Parise *et al.*, 1997; Clapp and McConchie, 2000; Glade, 2000; Agliardi *et al.*, 2001), and is now being applied as a means of hazard evaluation. Research based on a geomorphic assessment of hazards has largely been driven by the significance of hazards and is focused on the most common types. As a result a large proportion of literature is directed toward the evaluation of geomorphic techniques for fluvial hazard investigations (Dunne, 1988; Patton, 1988; Marutani *et al.*, 1999) while

their application for landslide hazards is only now becoming more popular (Hansen, 1984; Hutchinson, 1992; Petley, 1998; Guzzetti *et al.*, 1999; Wasowski *et al.*, 2000).

1.5 THESIS OUTLINE

The remainder of this thesis is divided into six chapters that broadly reflect the order in which the investigation was carried out. While each of the first four chapters assume no prior knowledge of Esk Valley geomorphology, each builds on the knowledge gained in the previous chapter(s) to provide a comprehensive overview of deep-seated landsliding and geomorphology within the Esk Valley. The final two chapters bring together observations made in these previous sections, and discuss interactions and implications in terms of controls on the geomorphic evolution of the valley, landslide formation and activity, and the aforementioned flooding hazard. Brief outlines of each chapter are given below.

Chapter 3 (Geomorphic Overview) provides a background for the investigation and briefly outlines the structure and geomorphology of the region. This also details the findings of an investigation into the 1938 Esk Valley flood.

Chapter 4 (Reconnaissance) describes analyses undertaken during the initial stages of the investigation. Remote sensing techniques are applied here and include the use of aerial photos, satellite imagery, and digital terrain models.

Chapter 5 (Field Investigations) summarises observations made in the field regarding valley geomorphology and landslide mechanics.

Chapter 6 (Structural investigation) discusses identified active tectonic structures within the valley based on an analysis of around 75km of seismic lines shot within the area. These findings are then related to the regional structure of the forearc basin.

Chapter 7 (Discussion) draws data from all aspects of the investigation and discusses key interactions in terms of deep-seated landsliding and their implications regarding the flood hazard.

Chapter 8 (Conclusion) answers questions posed at the beginning of the investigation and assesses the applicability of Engineering Geomorphology for regional hazard investigations.

2 GEOMORPHIC OVERVIEW

2.1 INTRODUCTION

In order to investigate the geomorphic development of the Esk Valley, its influence on the many deep-seated landslides within the region, and it's possible impact on flooding processes, it is important to first understand relevant geologic, hydrologic, and cultural processes. This chapter gives a brief overview of what are deemed to be the most important factors contributing to the evolution of the Esk Valley landscape.

2.2 REGIONAL GEOLOGY

2.2.1 TECTONIC SETTING

Hawke's Bay lies within the contractional forearc basin of the Hikurangi Margin, a tectonically active region created by the oblique subduction of the Pacific plate beneath the Australian Plate (see Figure 2.1). The plate boundary lies in the Hikurangi trough approximately 160 km east of Hawke's Bay (Lewis, 1980; Lewis and Pettinga, 1993). Here the Pacific plate gradually slips below the overriding Australian plate, descending at an angle of ~6°. This angle increases to approximately 20° in the region below the axial ranges (Bannister, 1988). The process creates a region of intense faulting and folding that can be traced from the Hikurangi trough westward to the axial ranges (Lewis, 1980; Cashman *et al.*, 1992; Lewis and Pettinga, 1993; Kelsey *et al.*, 1995; Barnes *et al.*, 2002). The margin can be subdivided into three tectonic domains; the frontal ridge, forearc basin, and accretionary slope (Lewis, 1980; Cole and Lewis, 1981).

The faults that delineate the western margin of the forearc basin belong to the **North Island Shear Belt** (NISB) (Ballance, 1993; Beanland, 1995; Neall *et al.*, 1995), and are considered a continuation of the dextral strike-slip motion present in the South Island Alpine Fault (Neall *et al.*, 1995).

The Esk Valley lies within the western third of the forearc basin (Figure 2.1). The Mohaka Fault to the west of the Maungaharuru Range marks the transition from the ranges of the uplifted frontal ridge to sedimentary sequences of the forearc basin (Cutten, 1988). The valley displays many tectonic and geomorphic features typical of the East Coast forearc basin (Table 2.1).

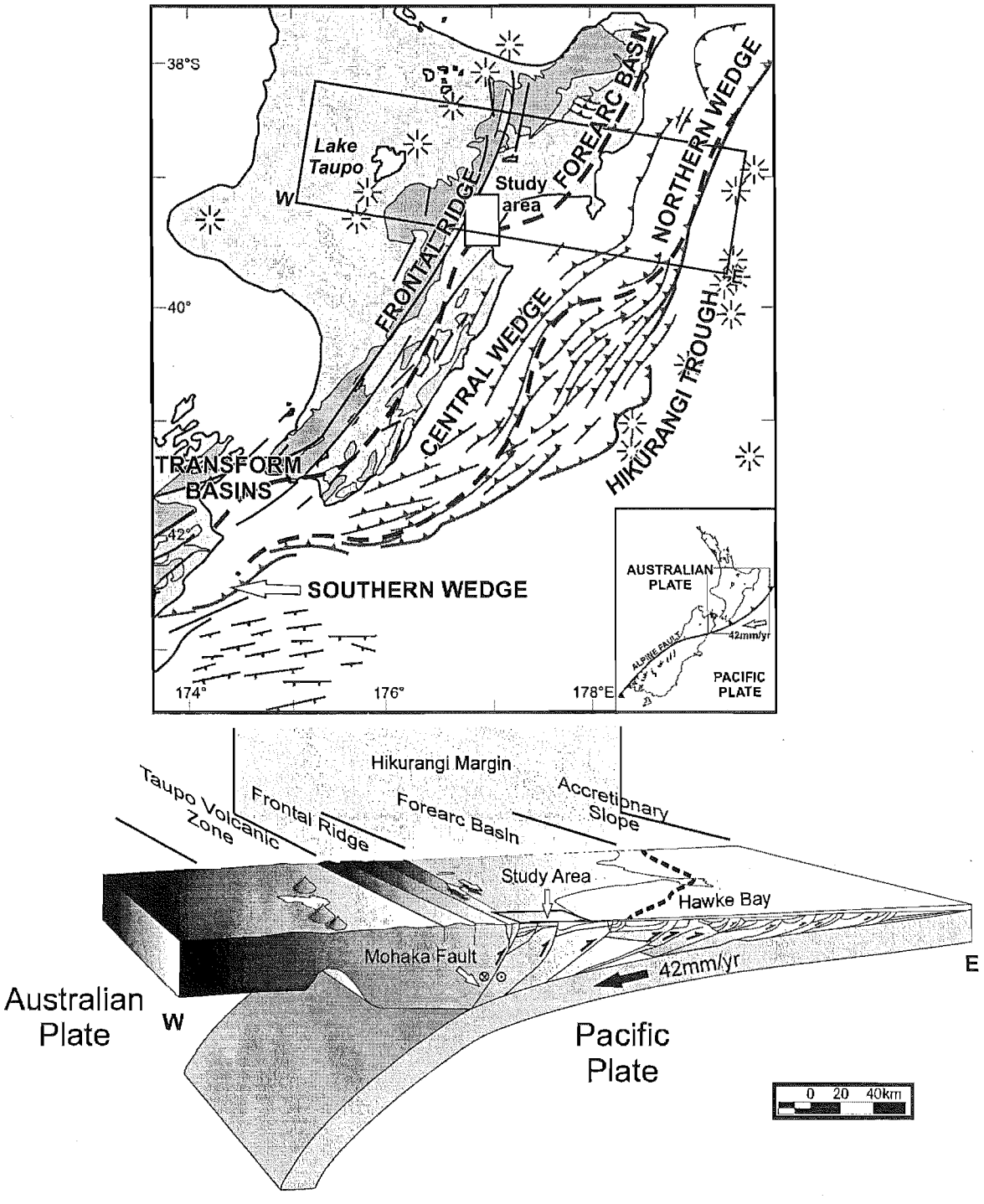

Figure 2.1 Tectonic setting of Esk Valley

The map (after Lewis and Pettinga (1993)) details the main structural features of the Hikurangi Margin and defines boundaries between the frontal ridge, forearc basin, and three wedge sectors of the accretionary slope. Note the pronounced broadening of the forearc basin around the latitude of Hawke Bay. Shaded areas indicate early accreted terranes, the dark indicates Jurassic to Triassic in age, while the lighter area indicates Lower Cretaceous. The block diagram is based on that given in Barnes *et al.* (2002) and is approximately true-scale. The location of the diagram is given in the map above. This is based largely on offshore seismic data and clearly shows the subduction-related imbricate thrusts of the accretionary wedge, the transfer to broadly spaced thrusts in the forearc basin, and the continental backstop structures of the frontal ridge. The presence of faults within the field area is based on inference.

Table 2.1 Occurrence of tectonic and geomorphic features within domains of the forearc setting (adapted from Berryman, 1998)).

Tectonic Domain	Tectonic Features	Geomorphic Features
Accretionary Slope	Growing anticlines and synclines Reverse faults Angular unconformities in sedimentary sequences Slope basins	Uplifted and generally landward tilted marine terraces Stream capture common Tilting and reverse gradient of fluvial terraces common Cliffed coastlines Superficial and deep-seated mass movement common Mud diapirs and mud volcanoes
Forearc basin	Westward-dipping reverse and oblique slip faults Complex pattern of subsidence and uplift during Holocene Moderate regional uplift during Pleistocene Broad synclinal structure Strong uplift and formation of asymmetric syncline adjacent to western boundary faults	Low lying coastline Estuaries Barrier bars Low gradient rivers in coastal areas Fluvial terrace sequences caused by aggradation and downcutting in inland areas Large landslides, perhaps caused by large earthquakes Landslide dammed lakes Abundant superficial mass movement Sparse hot springs
Frontal ridge	Oblique slip faults bounding region with horizontal to vertical slip ratio commonly 5:1 Intra-mountain oblique faults Infaulted Neogene rocks along intra-mountain faults Down-stepped, faulted western margin	Horizontally offset topography including streams and ridges Formation of shutter ridges Remnants of late Tertiary marine erosion surface General summit height accordance Ignimbrite plateau onlapped at western margin Landforms and deposits of periglacial conditions including solifluction lobes, rock glaciers and shaved surfaces

2.2.2 STRUCTURE OF THE FOREARC BASIN

Structural elements such as active faults and folds, internally strained rock, bedding, and lithology can have a strong influence on the geomorphic processes operating within a region. The structure of the onshore region of western Hawke's Bay from Hastings north to the mouth of the Mohaka River is underepresented in the literature. Studies of the forearc region have concentrated in southern Hawke's Bay (Kamp, 1988; Cashman *et al.*, 1992; Erdman and Kelsey, 1992; Beanland *et al.*, 1998), the Wairarapa in the south (Kelsey *et al.*, 1995; Neef, 1999; Nicol *et al.*, 2002; Formento-Trigilio *et al.*, 2003), and around Wairoa to the north (Mazengarb, 1983) (Figure 2.2). Offshore seismic exploration (Lewis and Kohn, 1973; Lewis and Pettinga, 1993; Barnes *et al.*, 2002), driven by the hydrocarbon potential of the East Coast Basin, has played an important part in these studies and a number of surveys have been carried out in Hawke Bay itself, off the coast, and onshore along much of the East Coast. Notable are two surveys, one within the Esk Valley Region (Westec, 1997), and the other over the Te Waka – Maungaharuru Range (Petrocorp Exploration Ltd. 1991).

The lack of structural investigation undertaken in western Hawke's Bay is partly evident in geological maps of the region which show a marked decrease in tectonic features, particularly from the Heretaunga Plains north to the Mohaka River (see Figure 2.2). This cannot be wholly explained by a change of tectonic input. As a result of this, the extrapolation of structural characteristics into the Esk region is essential in order to understand the tectonic processes taking place.

2.2.2.1 Quaternary Deformation history

The tectonic regime contributing to deformation observed today began around 1.6 million years ago (Beanland *et al.*, 1998). Prior to this the region was part of an offshore basin and accumulated sediment eroded from coastal ranges to the west (Lewis, 1980). Shortening of the basin was ongoing, however, structures present in basement greywackes seen today were most active after the end of the Miocene (c. 5 Ma) (Begg *et al.*, 1994), probably from 3.7-2.5 Ma (Beanland *et al.*, 1998). The initiation of uplift and deformation within the forearc southwest of Cape Kidnappers has been investigated by Edwards (1987) and Erdman (1990) (Cashman *et al.*, 1992). They describe a repeating cycle of increasing rates of uplift followed by transgressions and periods of stability. The first uplift event recorded occurred in the late Pleistocene (Mangapanian, 3.1 - 2.4 Ma) (Edwards, 1988). This was

followed by a marine transgression, then a second (late Nukumaruan to early Castlecliffian, c.1.4-1.0Ma) uplift event producing prominent conglomeratic interbeds east of the newly uplifted ranges, before the most rapid uplift occurred in the late Pleistocene (Castlecliffian, ~0.8 Ma). Contractional structures within the eastern margin of the basin formed contemporaneously with this final event (Erdman, 1990). Structures associated with this final event are some of the most prominent features in the region and are clearly apparent in the landscape today.

2.2.2.2 General Stratigraphy

Uplift of the overriding Australian plate is possibly the most influential process actively shaping the forearc morphology. This produces relatively young exposed marine sediments, steep topography, and the intensive erosion of sub-aerially exposed bedrock (Kamp, 1992) contributing to a rapidly evolving landscape. Sediment eroded off the uplifting sub-aerial regions is deposited in the adjacent forearc basin and over the accretionary slope (Lewis and Kohn, 1973).

The sequence of sediments in the forearc basin thickens to the north (Berryman, 1998) and contains a bedrock sequence of compacted, generally uncemented sediments (Pettinga and Bell, 1992). These sediments have been laid down since the Miocene (Beanland *et al.*, 1998) and contain both marine and terrestrial deposits. Due to the large proportion of uncemented mudstones, siltstones, and sandstones generally displaying uniaxial compressive strengths below 10 Mpa, these sediments are referred to as a "soft rock terrain" (Pettinga and Bell, 1992). A gradual decrease in landscape dissection moving north toward Wairoa is attributed largely to lithology. Mudstones present to the south have been removed in northern areas leaving only the more resistant underlying limestone and decreasing the rate of stream incision (Kamp, 1992). The basin fill lies unconformably on indurated Mesozoic sandstones and argillites (greywackes) similar to those that make up the axial ranges.

Figure 2.2 Hawke's Bay regional locality map detailing major structural elements
Structural features are based on data compiled in Kamp (1992), Beanland *et al.* (1998), and Begg *et al.* (1994). This illustrates the strong NE-SW structural trend parallel to the Ruahine and Mohaka continental backstop structures. It also illustrates the distinct lack of faulting and/or structural data north of the Heretaunga Plains, and gentle SE dip of the uplifted strata north of Napier. Structures marked in red are compiled in Begg *et al.* (1994), and are regarded as having ruptured in the last 125,000 years.

1) Kairakau - Waimarama Regional slump
2) Kaiwhakapiripiri Range
3) Pah Hill landslide
4) Waipoapoa landslide
5) Ponui landslide
6) Tiniroto landslide
7) Te Putere landslide
8) Tutira landslide dam
9) Ngatapa landslide dam
10) Te Pohue landslide
11) Te Waka splinter fault
12) Ahuateatua peak
13) Rangiora fault
14) Rukumoana fault (Patoka fault zone)
15) Poukawa fault zone

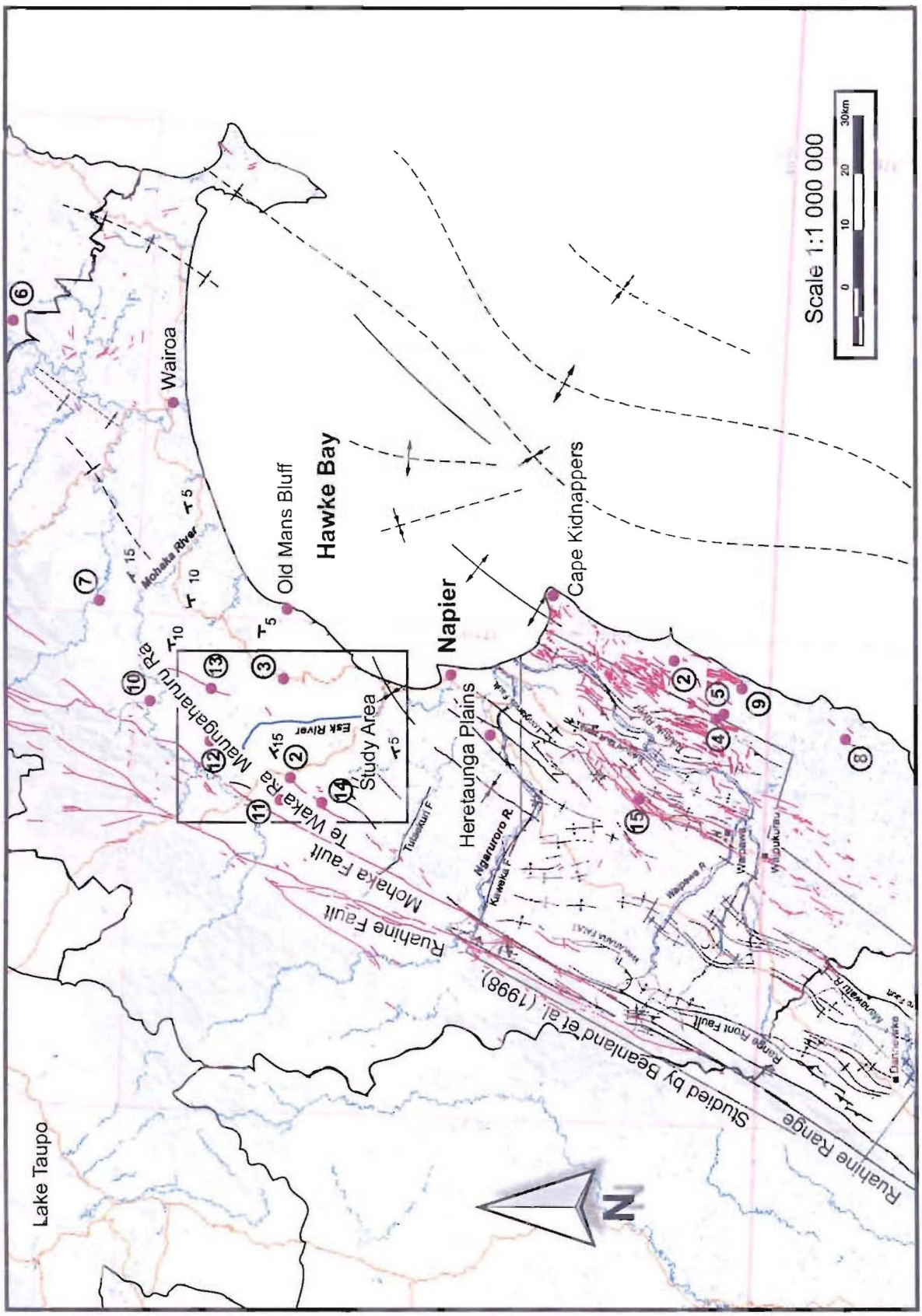
Scale 1:1 000 000
30km
20
10
0
Wairoa
Hawke Bay
Old Mans Bluff
Napier
Cape Kidnappers
Heretaunga Plains
Study Area
Esk River
Mohaka River
Mohaka Fault
Te Waka Ra
Manganahanui Ra
Ruahine Fault
Ruahine Range
Studied by Beanland et al. (1998)
Lake Taupo
N

2.2.2.3 Internal structure

The forearc basin displays a distinct NE-SW structural trend, and the characteristics of the basin change both laterally (from east to west), as well as longitudinally along the strike of the NISB. Two areas of the basin are discussed here, that south of the latitude of Cape Kidnappers, and north of the latitude of Wairoa.

Moving from Cape Kidnappers south to the southern end of the Ruahine Range (Figure 2.2) the basin narrows from a width of 20km to 10km (Cashman *et al.*, 1992). The basin fill is asymmetric and is deepest along its northwest margin (>2.5 km) (Beanland *et al.*, 1998). Sediments in this region appear to be strongly affected by both the convergent nature of the plate margin and the strike-slip motion of the adjacent NISB structures. Around the latitude of Cape Kidnappers the basin contains low, rolling contractional anticlinal ridges that gently plunge north below the gravels of the Heretaunga Plains (Cashman *et al.*, 1992) (Figure 2.2). Just south of this area, toward the eastern side of the basin, is the Poukawa Fault Zone (Figure 2.2). This predominantly contains westward-dipping thrust faults and can be traced approximately 20km along strike. Offset on faults within this zone is reported to have occurred during the 1931 Hawke's Bay earthquake (Cashman *et al.*, 1992). Other than these features tectonic disturbance in the predominantly Pleistocene basin sediments south of Cape Kidnappers is minimal until near the southern end where the depth to basement reduces, and is reflected in an increase of structural disruption. Dips of overlying sediments begin to steepen, and reverse faults and synsedimentary folds relating to these faults become common (Kamp, 1988).

To the north of the Esk Valley, around Wairoa, is the central part of the forearc basin (Kamp, 1988). The basin here is around 140 km wide and appears less directly affected by the contractional nature of the margin. This area is dominated by the presence of the Wairoa Basin. This contains a 10km thick autochthonous regressive sequence of Miocene-Pliocene marine sediments (Kamp, 1988). Although the regression was tectonically induced (Kamp, 1988), the sequence is remarkably undisturbed. There is evidence to suggest this portion of the basin may be under contraction at times, and extension in others (Mazengarb, 1983).

North of the Wairoa Basin, the forearc continues to the NE and joins with the Tonga-Kermadec system (Kamp, 1988).

2.2.2.4 Western boundary faults

Major strike-slip faults define the western margin of the forearc. While much of the inter-plate motion is taken up in the offshore subduction zone, and some margin-parallel strain is accommodated within the forearc (Raub *et al.*, 1987). These western structures accommodate the majority of margin-parallel strain not absorbed in the subduction zone. The Ruahine and Mohaka faults lie immediately to the west of the forearc basin (Figure 2.2) and the latter generally marks the boundary between Tertiary forearc basin sediments and basement Mesozoic greywackes of the continental backstop (Cutten *et al.*, 1988) (Figure 2.1). These predominately dextral strike-slip faults are approximately parallel and are a continuation of the NNE trending Wellington Fault Zone. The Ruahine fault lies approximately 10 km to the NW of the Mohaka. Initial movements probably began in the early Miocene about 24Ma, and activity definitely took place on the Mohaka fault prior to 11Ma, however, most lateral displacement has taken place in the last 5Ma (Cutten, 1994). Both of these faults have shown strike-slip displacements in the Quaternary (Erdman and Kelsey, 1992) and are actively uplifting the axial ranges at a rate of ~3mm/yr (Kamp, 1992). They have horizontal slip rates 5-10 times that of their vertical displacement (Raub *et al.*, 1987; Beanland *et al.*, 1998; Berryman, 1998). Total strike-slip displacement on these faults is unknown but has been inferred to be as much as 200 km (Cutten, 1988). Recent studies by Beanland *et al.* (1998) suggest strike-slip movement on the Mohaka fault may be less than 300m in the last 3 m.y., and possibly restricted to the Quaternary, indicating most lateral movement prior to this has been on the Ruahine fault.

2.2.2.5 Selected active structures

While little mapping of active faults within the Esk Catchment has taken place, it is likely that many features within the region are related to the continuation of structural styles identified outside its boundaries. This section discusses the identified active forearc basin structures adjacent to the Esk Valley. This includes those identified by Beanland *et al.* (1998) in a study undertaken to the south of the Heretaunga Plains, and three documented active faults identified on the margins of the Esk Valley (the Rukumoana Fault, the Te Waka Splinter Fault, and the Rangiora Fault).

Forearc basin faults southeast of the Heretaunga Plains

A detailed study of the structure and deformational history of the inner forearc was undertaken by Beanland et al. (1998). This study incorporated over 400 km of seismic

survey data and provides the most comprehensive illustration of tectonic deformation within the inner forearc available today. The location of this study is given in Figure 2.2. While ~30 km south of the Esk Valley, many of the features described may correlate to structures within the Esk study area.

Rangefront contractional structures form a zone 2-4 km in width approximately 5 km SE of the Mohaka Fault (Erdman and Kelsey, 1992; Beanland *et al.*, 1998) (Figure 2.2). These reverse faults generally dip 60-80° to the northwest. Striations on the planes are within 20° of the fault dip and indicate predominately dip-slip movement (Erdman and Kelsey, 1992). Strong reflectors marking the unconformable top of the basement sit 4 km higher on the ranges to the west of the faults than in the forearc indicating the net vertical displacement across the rangefront in the last 3.7 my (Beanland *et al.*, 1998). This displacement may, however, not have been entirely on rangefront faults as the currently predominantly strike-slip Ruahine, Mohaka, and Wellington Faults between the ranges and the forearc may have once also had a significant dip-slip component contributing to the net vertical displacement (Beanland *et al.*, 1998). Evidence suggests that this vertical displacement may reduce significantly toward the Esk Valley in the north (Erdman and Kelsey, 1992; Beanland *et al.*, 1998).

As mentioned in section 2.2.2.1, few faults deform upper Cenozoic sediments in the north of the area studied by Beanland *et al.* (1998). The Pliocene-Pleistocene strata are instead gently folded with bedding generally dipping at less than 5°. En echelon reverse faults noted in a seismic section to the north (C89-02) displace Miocene sediments and gently fold younger Mangapanian (2.8-3.2 Ma) deposits. These are overlain by horizontal strata indicating significant tectonic activity ceased soon after this time (Beanland *et al.*, 1998).

Toward the southern end of this study area NNW trending reverse faults within the forearc have a spacing of approximately 2-8 km. The intensity of faulting decreases to the north as the average spacing increases to c. 20 km. This decrease in intensity is greatest between Dannevirke and Hastings where many traces abruptly terminate (Beanland and Haines, 1998) (Figure 2.2). This corresponds to a widening of the forearc and may be a result of the greater area available for strain distribution. The fault planes are well defined and generally dip 30-80° to the NW. Overlying strata are typically folded into steep monoclines (Beanland *et al.*, 1998).

Rukumoana Fault (Patoka fault zone)

A 21 km long trace of the Rukumoana Fault is the strongest trace of the Patoka Fault Zone, and has been mapped almost to the southern border of the Esk catchment (Figure 2.2, location 14). The Patoka Fault Zone was first identified by Henderson (1933), and was suggested to be the source of a strong earthquake felt at Te Pohue a week after the 1931 Hawke's Bay earthquake. The Rukumoana Fault was first identified by Stoneley *et al.* (1958) and has subsequently been recognised by several other authors (Bland, 2001). It is a prominent structure now classed as part of the Patoka Fault Zone and related to the Ruahine/Mohaka Fault system (Petrocorp Exploration Ltd, 1991; Begg *et al.*, 1994).

The fault can be traced in seismic reflection profiles from near where it splays from the Mohaka Fault at a slight compressional jog west of Patoka (Figure 2.2), and is inferred to cross through the Maungaharuru Range at SH5 (Wylie, 1993; Bland, 2001). However, this may not be the case and is discussed in more depth in Section 5.3.

The fault dip flattens at depth and is projected to intersect the Mohaka fault (Wylie, 1993). It is inferred from surface investigations to be dominantly dextral strike-slip (Begg *et al.*, 1994), however, a significant component of westward dipping thrust displacement is evident in seismic section and vertical offset has been estimated from field mapping at between 20m and 100m (most recently 60-100m; Bland (2001)). There is also a significant c.25° increase in dip of sediments adjacent to the fault (Bland, 2001) indicating further dip-slip motion.

Te Waka Splinter Fault

This is a relatively minor structure that lies to the south of the Esk Valley between the Mohaka and Raukomoana Faults (Figure 2.2, location 11). Around 15 km strike-length has been mapped by Neall and Hanson (1995), and the fault is described as an extensional splinter trace of the Mohaka fault. In the southern section the fault has an orientation of 034°/85°W, and can be traced to below the Te Waka Range trig station where it splays and appears to terminate. At this locality the western block is downthrown by 30m, however as this is near the terminus of the fault, total displacement is likely to increase to the south. Possible horizontal displacement is between 60 and 100m, and faulting events have been identified both pre- and post- the 11,850 yr.BP Waiohau Tephra (Neall *et al.*, 1995).

Rangiora Fault

The Rangiora fault is a 14 km long NE trending dextral strike-slip structure mapped by Cutten *et al.* (1988) to the NE of the Esk Valley (Figure 2.2, location 10). A 5 km length of this fault has been recently active with three faulting events, each offsetting features by 4-6 m and showing reversal of the upthrown side. These are dated at 3300-1900yr.BP, and two at less than 1900yr.BP. Corresponding rates of movement for the Rangiora fault and NISB structures for the Holocene indicate that the Rangiora Fault may be related to this system and, in fact, may be evidence for the eastward propagation of the NISB into the forearc basin (Cutten *et al.*, 1988).

2.2.2.6 Deep-Seated landslides

Deep-seated landslides are defined in this study as those that undergo failure in unweathered bedrock. Deep-seated landsliding is a relatively common occurrence within the Hikurangi Margin. A number of such landslides have been identified within the Esk Valley, although these have remained largely uninvestigated prior to this study. This section briefly outlines some of the key characteristics of deep-seated landslides investigated within the Hikurangi Margin.

The Hikurangi Margin contains some of the largest documented landslides in New Zealand (Crozier *et al.*, 1992). Some of the most notable slides occur south of Hastings around the Maraetotora Plateau, and include the 30km wide Kairakau – Waimarama Regional Slump (Crozier *et al.*, 1992), the Kaiwhakapiripiri Range – a 3km long mudstone and limestone block slide (Crozier *et al.*, 1992), Pah Hill, Mt. Kahuranaki (Spörli and Pettinga, 1980), Ponui (Pettinga, 1987a), and Waipoapoa (Pettinga, 1987b). Lake Waikaremoana was dammed by a very large, probably earthquake induced, landslide over 3280 years ago. Other documented extremely large landslides to the north of Hawke's Bay include the Waikaretei Lakes landslide (c. 11,000 B.P.), Tiniroto, Te Putere, and Tutira (Johnson and Pearce, 1999). The location of each of these landslides is given in Figure 2.2 (localities 1-8). Countless other deep-seated slides in this region remain uninvestigated.

The Waipoapoa and Pounui Landslides are seated in weak Upper Miocene sedimentary strata, an alternating well-bedded sandstone-mudstone sequence of accretionary slope basin origin (Pettinga, 1982; Pettinga, 1987a, b). Both slides represent the reactivated portion of larger, pre-existing landslide complexes, and reactivation occurred in 1976 following a period of above average rainfall. The slides have estimated volumes of

$8.35x10^6m^3$ and $2.5x10^6m^3$ respectively and are of comparable size to those seen in the Esk Valley. Typical failure style at each site involved initial bedding-controlled block sliding. At Waipoapoa this was followed by flowage and the incorporation of multiple defect-controlled blocks, whereas at Ponui rapid movement and partial disintegration followed.

Near vertical joints and faults at the Waipoapoa Landslide allowed the propagation of the crown escarpment, and while bedding dips gently against the direction of movement, evidence suggests that these contacts facilitated the formation of a sub-horizontal basal shear surface. High pore-water pressures resulting from infiltration along defects and permeability contrasts in the alternating sandstone and mudstone beds are also indicated as an important contributor to the failure. (Pettinga, 1987b)

The Ponui Landslide occurs in a succession of alternating sandstone-mudstone and amalgamated sandstone and is a reactivation of a slide initiated by the 1931 Hawke's Bay earthquake. Defects around the Ponui landslide enabled the propagation of the lateral escarpment. The principal failure surface, a thin, tectonically induced montmorillonitic clay gouge zone paralleled the bedding orientation. Sliding occurred along the intersection of bedding (10° - 36°) and lateral (near vertical) defects, producing a very low angle failure surface (6° to 20°) (Pettinga, 1987a).

Lake Ngatapa (Figure 2.2, locality 9) was formed at the confluence of the Te Hoe and Mohaka Rivers (Johnson and Pearce, 1999) by a landslide dam resulting from the 1931 Hawke's Bay earthquake. This was around 40km away from the earthquake epicentre and created a lake 2km long. The dam was considered permanent until it was washed out during the 1938 flood (Grant, 1939; Adams, 1981; Neall *et al.*, 1995; Johnson and Pearce, 1999). Unfortunately there is no documented investigation into the landslide itself.

2.2.3 1931 HAWKE'S BAY EARTHQUAKES

The main Mw 7.6 Hawke's Bay Earthquake and the Mw 7.3 aftershock occurred on the 3rd and 11th of February 1931 respectively, and played an important role in shaping the historic geomorphology of the Napier area. The epicentre of the Hawke's Bay earthquake was initially thought to be located around 5km NW of Patoka (Figure 2.4, grid ref. 2820500,6200500) (Bullen (1938) in (Hull, 1990; Begg *et al.*, 1994)). However, McGinty *et al.* (2001) recently revised this location and using geodetic data calculated it to be near Lake Poukawa. This is coincident with recorded surface faulting. The earthquake produced a 90km long dome that extended from Hastings NNE to the Mohaka River (Figure 2.3).

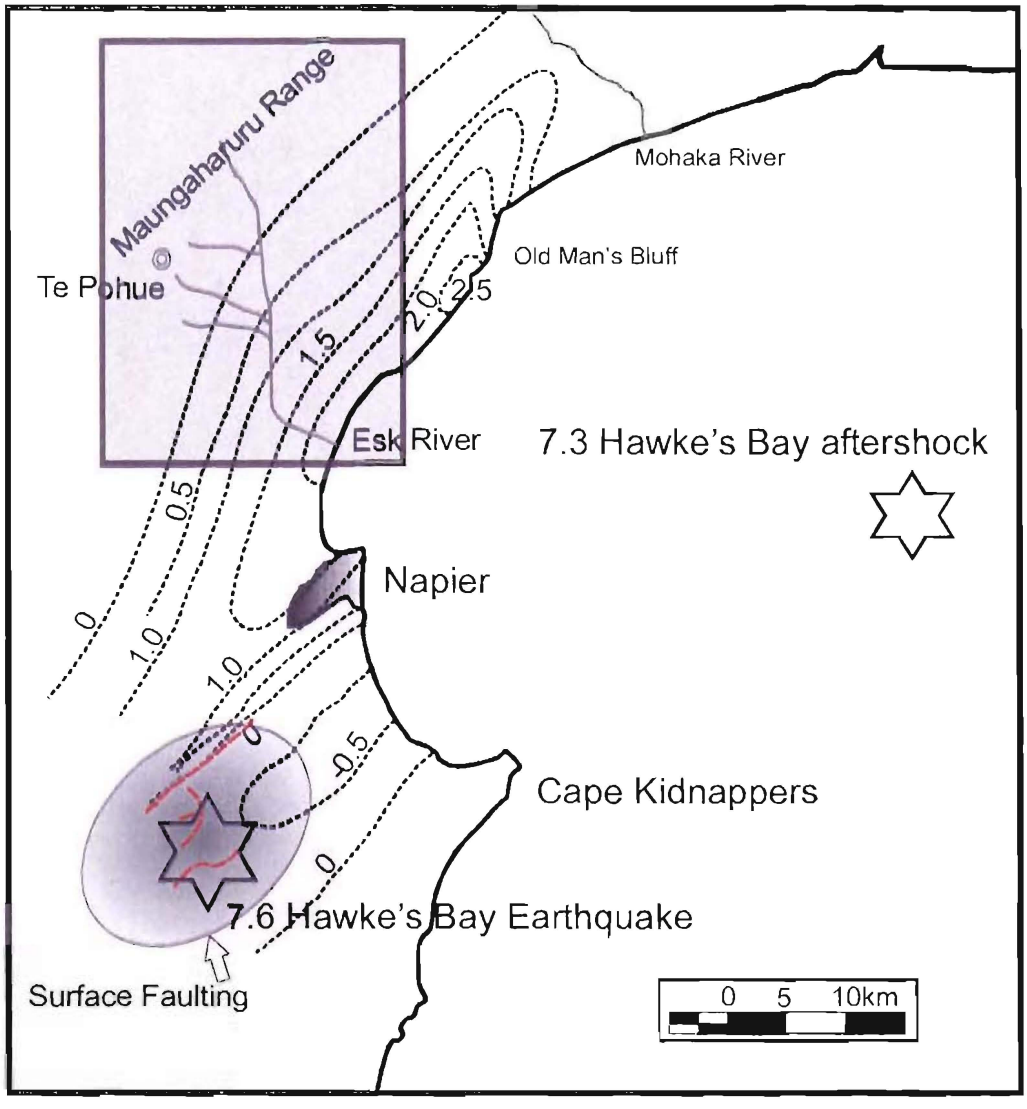

Figure 2.3 Contours of elevation change (m) as a result of 1931 earthquakes (from (Hull, 1990)).

Revised epicentres are from McGinty *et al.* (2001). Surface rupture traces are indicated in red in the region of the Hawke's Bay earthquake.

The Hawke's Bay earthquake is inferred to have occurred along a segment of a steeply dipping reverse-dextral fault. This is likely to be an imbricate thrust propagated up from the decollement at a depth of around 15-20km (Hull, 1990; McGinty *et al.*, 2001). While the fault may be traced onshore in the region of the Poukawa Fault Zone, a lack of primary surface rupture is likely to be due to fault termination at depth, and overlying soft surface sediments deforming elastically (Hull, 1990; McGinty *et al.*, 2001). The epicentre of the Hawke's Bay aftershock 11 days after the initial earthquake is recorded as being near the centre of Hawke Bay. This is, however, poorly constrained and may be in error by tens of kilometres. Rupture is considered to have occurred on a separate fault trace to the Napier

event (McGinty *et al.*, 2001). Residents in Te Pohue describe this earthquake as being stronger than the earlier event (Parsons, 1997).

Doming was measured by re-levellings along the Napier-Gisborne railway in the weeks following the earthquakes (Hull, 1990; McGinty *et al.*, 2001). Maximum uplift was 2.7m around Old Mans Bluff in the north, the mouth of the Esk River was raised 2m. Ahuriri Lagoon, immediately north of Napier was raised about 1m draining the lagoon and diverting the tributary of the Tutaekuri River southward. This uplift contrasts a pattern of Quaternary subsidence in the lagoon (Hull, 1986, 1990) (see Section 6.3.4.2 for further discussion).

2.2.4 SYNTHESIS

From the information outlined in this section, it is evident that the Esk Valley is located in a tectonically active emergent setting. The geological history of this area, including tectonic and depositional processes since its inception, are well documented and provide a relatively straightforward model of increasing tectonic activity with the formation of an accretionary prism and structures to accommodate increasing strain from subduction at an obliquely convergent plate margin. The increase in tectonic activity is matched with an increase in basin sedimentation derived from Mesozoic basement rock in the uplifting ranges of the Australian Plate to the west.

Many of the processes described in the formation of the forearc are continuing today and new structures are constantly forming. While few tectonic structures have been mapped, the Esk Valley is potentially susceptible to disruption from a number of structural sources. These include the continuation of the structural trend identified by Beanland *et al.* (1998) 30km to the south, the reactivation of pre-existing faults linked to an earlier period of activity, other structures related to the Rangiora and Rukumoana Faults, or the eastward propagation of the NISB as suggested by Cutten *et al.* (1988).

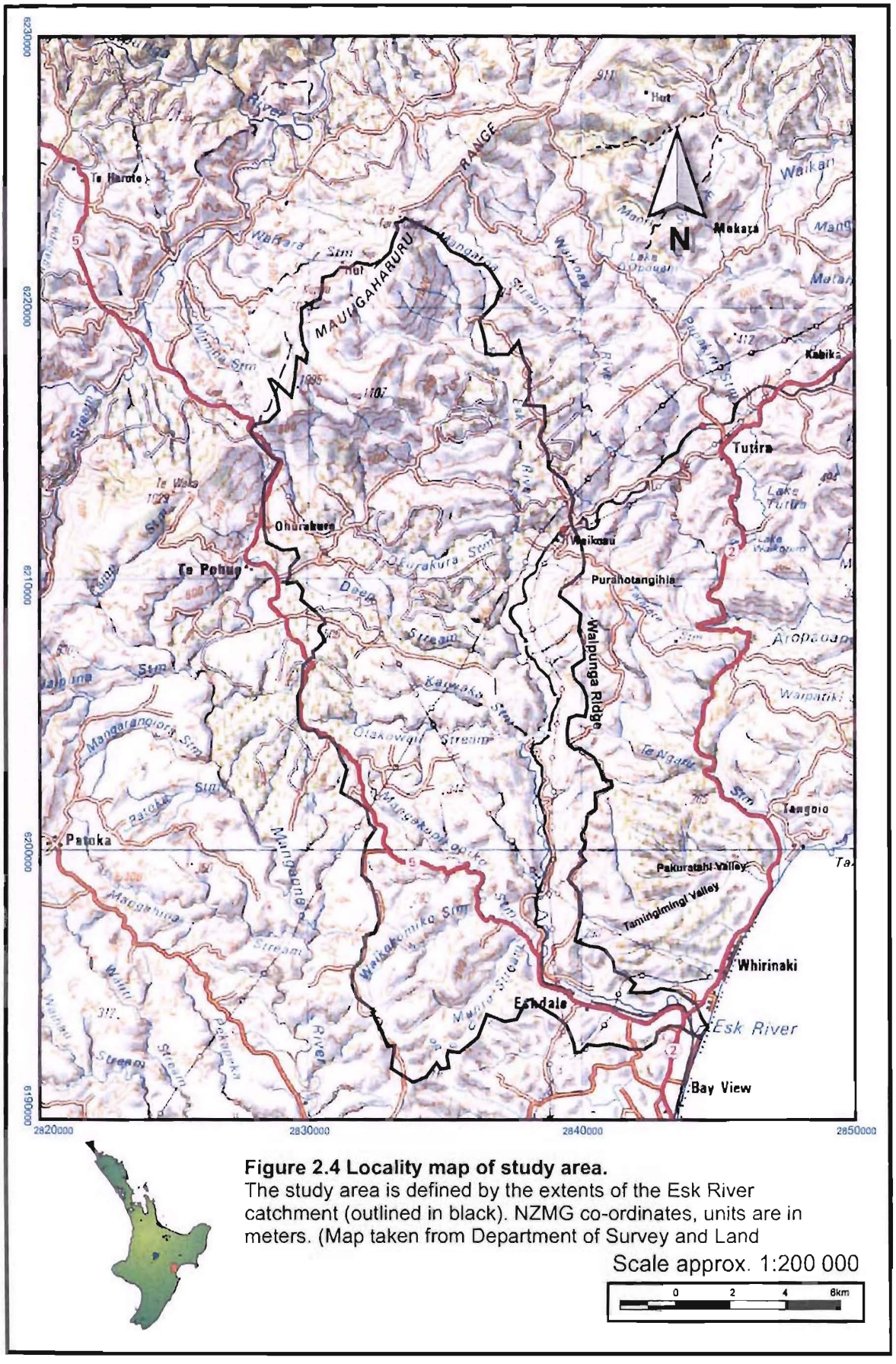

Figure 2.4 Locality map of study area.
The study area is defined by the extents of the Esk River catchment (outlined in black). NZMG co-ordinates, units are in meters. (Map taken from Department of Survey and Land

Scale approx. 1:200 000

2.3 ESK VALLEY GEOMORPHOLOGY

2.3.1 GEOMETRY

The Esk River catchment covers an area of over 238km^2 and stretches as a 10km wide N-S trending corridor 25km north onto the crest of Maungaharuru Range (Figure 2.4). Excluding Purahotangihia and the Maungaharuru Range, which rapidly rises to over 1200m, relief in the catchment is relatively low with a maximum elevation of 500m and an average valley gradient of 0.4°. The valley is characterised by steep, linear hillslopes surrounded by extensive broad terraces and largely detached from a highly incised drainage system. Factors important in the shaping of these slopes include lithology, degree of catchment maturity, deep-seated landslides, and shallow regolith failures.

The lower catchment forms a distinct "L" shape as the Esk River stretches from the coast in a west–northwesterly direction for around 6km before turning sharply north and following the trend of Waipunga Ridge. This form is repeated immediately to the west in Tamingimingi Valley and Pakuratahi Valley and is likely to be related to structural control within the Kaiwaka limestone which forms a cap over much of the area.

Drainage within the valley is highly asymmetric as the combined effects of bedding and tectonic uplift have lead to the entrenchment of the main channel against the eastern limestone capped cliffs of Waipunga Ridge. Major tributaries to the Esk River intersect at regular intervals and stretch from the confluences WNW across the catchment. Only those from Okurakura Stream north have their headwaters located in the Maungaharuru Range.

Interpretation of a satellite image by Wylie (1993) has identified a large number of lineations created by surface features within the valley. Many of these lineations closely match stress directions identified through the investigation of tectonic features elsewhere in the forearc, as well as bedding orientations within the valley. The source or relevance of these lineations has not previously been investigated, though Spörli (1987) undertook an analysis of lineaments in Torlesse basement rocks immediately to the west of this study. Lineament patterns are strongly developed in the basement, and he identifies three main trends: 020°-030°, 045°-050°, and the most prominent, 060°-070°. While these are generally believed to be fault related, he puts forward a number of possibilities for their formation – including a possible transition from E-W compression in the Hawke's Bay monocline to E-W extension in the Taupo Rift. The relationship between these lineations and those identified in the Plio-Pleistocene strata within the Esk Valley is not known.

Hypsometric Curve

The hypsometric curve is a useful means of summarising basin morphology and comparing degrees of basin maturation irrespective of basin scale. It indicates the total proportion of basin area above a proportion of total elevation (Keller and Pinter, 1996). The hypsometric curve for the Esk Valley is given in Figure 2.5.

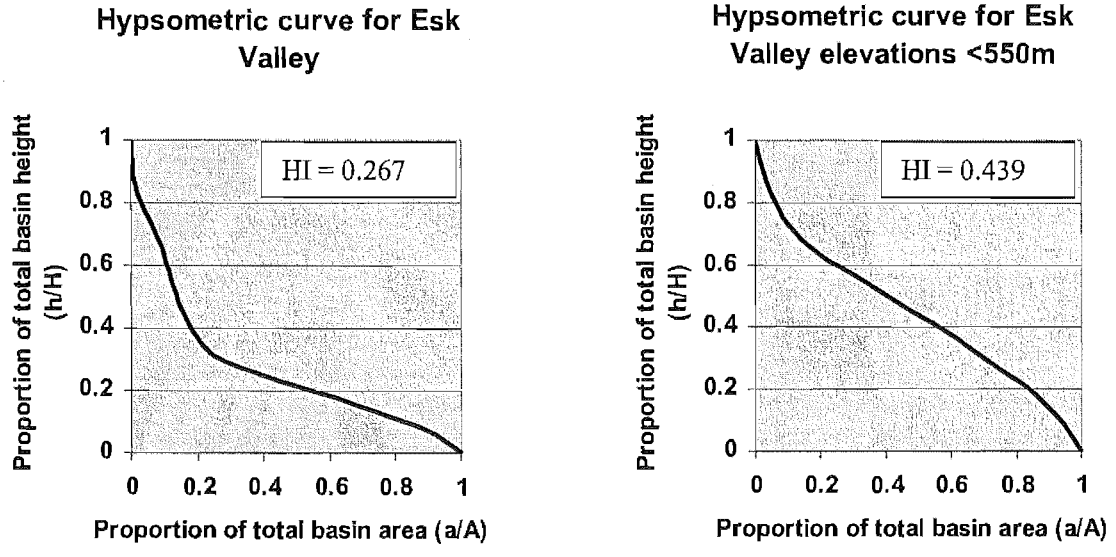

Figure 2.5 Hypsometric curves for the whole Esk Valley (left), and with Maungaharuru Range removed (right).

The hypsometric curve indicates that by far the majority of the basin area is relatively low-lying and that elevations within the basin are generally concordant. The integral of this curve, known as the **Hypsometric Integral** (HI), is used to indicate basin maturation. A value of between 1 and 0.6 describes a youthful basin in which deep incising rivers are present in an elevated landscape. A mature basin in which landscape processes are in equilibrium will have a lower HI, between 0.6 and 0.35 (Strahler, 1952; Keller and Pinter, 1996). For the Esk Valley the value of this integral is 0.267, typical of a "transitory" stage of basin development, a mature stage in which remnants of the young basin remain (Strahler, 1952). In this case the "remnants" are in fact the slopes of the Maungaharuru Range. When these are removed, the mature hypsometric curve and integral on the right of Figure 2.5 is produced. This has a relatively low HI, and is indicative of a basin with "strong relief, steep slopes, steep stream gradients, and high drainage density" (Strahler, 1952). However, this interpretation is complicated by the superposition of high magnitude aggradation and degradation events within the Esk Valley. Low planform, highly incised

streams are underrepresented in the analysis and only slightly reduce the HI. The hypsometry is therefore a reflection of the relict landscape – formed prior to the current period of incision – with a bias toward exaggerated relief. It indicates likely tectonic adjustment around the Maungaharuru Range.

2.3.2 ESK VALLEY GEOLOGY

The Esk Valley region of the forearc basin contains a 900m thick succession of Mid to Late Pliocene mainly marine sediments lying unconformably on the Mesozoic greywacke basement (see Attachment 1). These sediments are characterised by rapid lateral facies changes and generally dip gently (~8°) to the SE (Bland, 2001). The sequence is composed of two groups as in Figure 2.6. The older Maungaharuru Group (late Kapitean to late Mangapanian) strata outcrop in the northern region of the catchment and are mainly comprised of sandstone and carbonate sediments (Bland, 2001). These include the Te Waka and Titiokura Formations, calcareous sandstones that are key structural elements on the Te Waka – Maungaharuru Range. The Petane Group contains all younger strata deposited to the end of the Pliocene and incorporates some non-marine sediments such as iron cemented greywacke gravels, as well as tephras sourced from the Taupo Volcanic Zone which has been active since the Late Pliocene (Bland, 2001). The gravels units form prominent flat-topped hills and ridges throughout the valley as their high resistance to weathering and erosion shelters the less resistant underlying rock. The lack of tectonic disruption within the Esk Valley is evident in the lack of variation in dips throughout the region; these strike around 41° NE and dip c. 8° to the SE. The exceptions to this are on the Maungaharuru Range where rangefront faults have uplifted the basin fill, in particular immediately to the west of the Rukumoana Fault where dips steepen dramatically (c.30°) (Bland, 2001). Units within the valley are often tens of metres thick with much smaller scale internal bedding (Bland, 2001).

Sedimentary strata forming Waipunga Ridge that defines the eastern margin of the Esk Valley have been described by Haywick *et al.* (1991) and were probably deposited during glacio-eustatic sea-level fluctuations in the late Pliocene. These are part of a laterally continuous

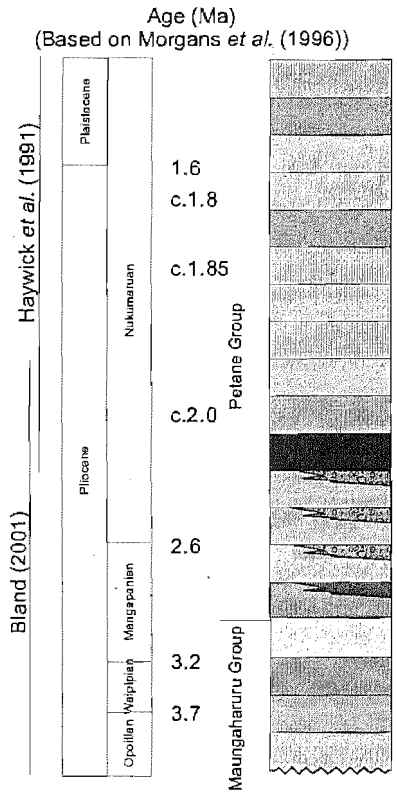

Kaiwaka Formation	Pebbly coquina, shelly sand and limestone; pumice and greywacke conglomerate in mid formation.
Devils Elbow Formation	Calcareous blue-grey silty mudstone; grades up into sand.
Waipatiki Formation	Fine calcareous sand grading up into limestone and coquina.
Te Ngaru Formation	Calcareous blue-grey silty mudstone; grades up into sand.
Tangoio Formation	Fine calcareous sand grading up into limestone and coquina.
Mairau Formation	Calcareous blue-grey silty mudstone; grades up into sand.
Darkys Spur Formation	Laminated fine siliciclastic sand with shell beds and scattered calcareous concretions.
Aroapaonui Formation	Massive blue-grey silty mudstone grades up into fine sand.
Tutira Formation	Poorly sorted greywacke conglomerate, fine sand and silt. Thick pumice near top.
Esk Formation	Massive blue-grey silty mudstone, fine sand and pumice layers.
Waipunga formation	Siliciclastic fine sand, rare pumice and silt beds. Scattered calcareous concretions.
Matahorua Formation	Succession of siliciclastic sandstone and siltstone with prominent greywacke beds.
Grassy Knoll Member	Siliciclastic sandstone and siltstone grading into a greywacke conglomerate. Tephra layers common.
Papakiri Member	Siliciclastic micaceous sandstone and siltstone grading into a greywacke conglomerate.
Trelinnoe member	Thin siliciclastic siltstone grading into sandstone . Capped by greywacke conglomerate.
Deep Stream Member	Siliciclastic siltstone and fine grained sandstone grading into greywacke conglomerate.
Pohue Formation	Alternating siliciclastic siltstone and sandstone beds with occasional shellbeds. Some tephric materials present.
Te Waka Formation	Interbedded coquina and sandstone.
Titiokura Formation	Pale grey to yellow-brown barnacle plate grainstone with interbeds of silt, sand, and mud.
Mokonui Formation	Pale brown to grey-brown, fine to medium grained, poorly cemented, slightly to moderately concretionary sandstone.

Figure 2.6 Composite stratigraphic column for Esk Valley (Haywick *et al.*, 1991; Bland, 2001)

sequence of non-marine to inner shelf sediments (consisting of greywacke gravel, siliciclastic and carbonate sand/siltstone and bioclastic limestone) with some mid-shelf sandy/muddy silts (Haywick *et al.*, 1991). The ridge is capped by the 50m thick Kaiwaka Limestone and contains remnants of Castlecliffian strata.

The effect of lithology on catchment morphology is obvious as uniform dips, and strong resistance contrasts produce similar erosional patterns throughout. Hillslopes are generally steep and linear and are often capped by sharp, lithologically controlled ridges (Black, 1991). Isolated conglomerate-capped remnants are common and form prominent landmarks. South-easterly facing (down dip) slopes are generally much shallower than those inclined against dip to the north-west, and an obvious increase in topographic dissection is evident between Maungaharuru Group sediments and the younger Petane Group.

Prominent dip slopes are evident in the ranges to the west, particularly in the Te Waka and Maniaroa Ranges where the upper limestone cap defines the entire eastern slope of the hills. In the Maungaharuru Range the sediments are more deformed, and considerably more eroded, however, the overall form of the eastern face is still directly related to bedding attitude.

2.3.2.1 Landscape Maturity

The maturity of a landscape describes the degree of geomorphic equilibrium attained between erosional processes and earthbuilding/resistant forces (Strahler, 1952; Bull, 1991). Morphologically a mature landscape is one in which the rate of hillslope degradation equals that of uplift (or baselevel lowering) (Bull, 1991). While the detachment of hillslopes from the fluvial system in the Esk Valley has reduced the rate of fluvial degradation in much of the catchment to imperceptible levels, the occurrence of shallow landslides provides an indication of areas in which disequilibrium is greatest. This instability may be a remnant of the pre-incision landscape, or related to geomorphic processes operating in the region today.

The timing of terrace formation within the valley indicates the cessation of major hillslope denudation and provides time for the landscape to reach steady-state. Extensive terrace sequences in the upper Esk catchment indicate hillslopes are likely to be more stable than in lower parts of the catchment where a greater connection between streams and adjacent slopes has produced convex hillslope profiles with a greater degree of dissection.

2.3.2.2 Deep-Seated landslides

Very little work has been undertaken on deep-seated landslides within the Esk Valley, though deep-seated failures were recognised and mapped at reconnaissance level by Black (1991), and are identified in a landslide database maintained by The Institute of Geological and Nuclear Sciences (IGNS).

The Te Pohue block slide is the only documented slide in the Esk region and lies on the border of the Esk Valley (Figure 2.2, locality 10). Inferred to have been triggered by tectonic activity, debris from the slide blocked drainage and produced the lake at Te Pohue. This event has been dated at post 1850 yrs BP, shortly after the deposition of the Taupo tephra (C. Hannan, pers comm. in Neall *et al.* (1995)). This is consistent with a period of activity on the Te Waka Splinter fault that crosses near the headscarp of the slide. While the mechanics of the landslide have not been investigated, this is almost certainly a bedding controlled failure. Sharp, linear lateral and head scarps strongly suggest pre-existing defect control on release.

2.3.2.3 Shallow Regolith slides

The widespread occurrence of shallow regolith failures on the East Coast of the North Island is well documented (Eyles, 1971; Black, 1991; Crozier *et al.*, 1992; Dunlop, 1992; Pettinga and Bell, 1992; Marden and Rowan, 1993; Merz and Mosley, 1998; Trustrum *et al.*, 1999; Clapp and McConchie, 2000; Hennrich, 2001). The problem is widespread, and is commonly attributed to recent deforestation and conversion of much of the land to pasture (see Section 2.3.4 for more on vegetation change). While the problem was recognised early (Henderson and Ongley, 1920), and severe erosion during a flood event in the Esk Valley in 1938 lead to the formation of the Hawke's Bay Catchment Board (Dunlop, 1992) specifically to investigate methods of dealing with the problem, in the 1960's erosion had reached a degree regarded by some as "the worst example of soil erosion on pastoral hill country anywhere in the world" (Marden and Rowan, 1993).

Typically the shallow failures occur in a geomorphically rejuvenating landscape where river incision and slope processes are active. These failures commonly involve the upper 2m of soil cover and occur on steeper slopes (20-36°+) (Pettinga and Bell, 1992). Soils are typically composed of weathered bedrock and airfall tephras derived from the Taupo Volcanic Zone. While in an undisturbed state these are unlikely to reach saturation during a rain event (70-81% saturation), remoulded soils in landslide scars and deposits can have

a far lower degree of saturation (50-93%) (Merz and Mosley, 1998) and slides may be reactivated by even moderate intensity rainstorms (Pettinga and Bell, 1992).

Antecedent moisture conditions are important in terms of slope stability as these define the base pore pressure level prior to a major precipitation event, and therefore the level of rainfall required to destabilise slopes. The structure of the undisturbed soils means they are able to retain moisture well after a rainfall event (Merz and Mosley, 1998). However, after several months of little rainfall, shrinkage can cause crack networks to develop in the soils. This too can increase slope susceptibility as it allows rainfall to infiltrate rapidly and become concentrated along permeability barriers, leading to the triggering of landslides (Pettinga and Bell, 1992).

While severe sliding has been reported in the Esk Valley, the distribution or current activity of these slides has not been investigated. Black (1991) notes shallow landsliding is particularly widespread in the mid-catchment around Otakowai, Deep Stream, and Mangakopikopiko Stream (Figure 2.4). The slopes of the Maungaharuru Range in the upper catchment have also been severely affected. Flat to moderate rolling land in the upper Kaiwaka Stream catchment, however, shows little evidence of such slides.

2.3.3 HYDROLOGY

2.3.3.1 Climate

A westerly airflow dominates weather patterns in New Zealand. This produces a sequence of eastward moving anticyclones followed by troughs across the country and, combined with the mountain ranges to the west, determines the major climatic features of Hawke's Bay (Thompson, 1987a). It ensures that the Hawke's Bay has the greatest percentage variation of rainfall in New Zealand as hot, dry conditions are followed by periods of heavy rainfall (Johnson and Pearce, 1999).

During west to north-west airflows Hawke's Bay experiences hot, dry conditions as the ranges shelter the region and precipitation falls to the west. This effect is, however, reversed during southerly and easterly conditions where the ranges enhance rainfall in the region. The latter pattern is commonly associated with flood-causing events as precipitation can be heavy at the rangefront and headwaters of many river systems.

North to north-east airstreams bring mild, humid airmasses down from mid-latitudes. These are often slow-moving – particularly when blocked by an anticyclone to the south –

and generally produce mild, cloudy conditions with very little precipitation. (Thompson, 1987a)

Two climatic regimes bring major flooding to Hawke's Bay: depressions formed in the Tasman Sea or Tropics, and tropical cyclones. These have an average return period of 3 years (F.M.Kelliher, M.Marden, A.J.Watson, unpubl. data in Marden and Rowan, 1994). Depressions moving over the North Island bring humid air masses east. As the depression moves eastward north of Hawke's Bay, strong moist easterly airflows south of the trough are forced up over the ranges. This condenses the airmass and subsequent precipitation is very heavy and localised (Thompson, 1987a). Tropical cyclones also play an important role, with storms often passing in close succession every four or five years. The tropical cyclone season lasts from November to April and cyclones are often accompanied by heavy rain and gusty conditions (Thompson, 1987a).

2.3.3.2 Basin geometry and morphology

Basin geometry and morphology can affect processes ranging in scale from regional precipitation distribution down to localised slope runoff and infiltration characteristics. Particularly important in the Esk Valley, are the orographic effects of the bounding topography, the form of hillslopes and terraces, and the long, narrow asymmetric basin shape.

Morphology controls both the distribution of precipitation, and the way it is passed through the system prior to entering the stream network. The most dominant morphological factor is the orographic effect of the Maungaharuru Range (Grant, 1939; Cowie, 1957; Black, 1991; Johnson and Pearce, 1999) and Purahotangihia (Black, 1991). These produce high rainfalls in the headwaters of the catchment (Johnson and Pearce, 1999): 2800mm and 1800mm annually at the summits of the Maungaharuru Range and Purahotangihia respectively, and 1000mm in the lower valley (Black, 1991) (Figure 2.7). As well as introducing a large amount of precipitation to the system, the effect of these ranges means rainfall distribution is low and resultant runoff rapidly drains from the steep slopes into main and tributary channels preventing ponding or other primary storage.

There is very little storage within waterways of the Esk Valley; the few small, isolated lakes present are most likely a result of perched watertables over impermeable lithologies, or springflow – often associated with backtilting within active deep-seated landslides. Relief is characterised by sharp ridges and steep, linear slopes, as well as short, steep,

highly incised rivers (Grant, 1939; Johnson and Pearce, 1999). This ensures rapid runoff and high channel flows, with few areas for infiltration or ponding (Black, 1991).

Terraces form broad sub-horizontal surfaces between hillslopes and the river system. While these provide little natural subaerial storage, they are composed of thick gravel sequences overlain by porous volcanic soils, and offer good opportunities for infiltration and subsurface flow. Possibly a more important effect of the terraces, combined with the highly incised streams, is the reduction of two-way connectivity between hillslope sediment transport processes and erosional stream processes. This means both sediment production and sediment transport into the fluvial system is reduced as the lack of direct fluvial erosion allows hillslopes to adjust to a stable equilibrium. And shallow slope angles prevent mass wasting and significant bedload transport.

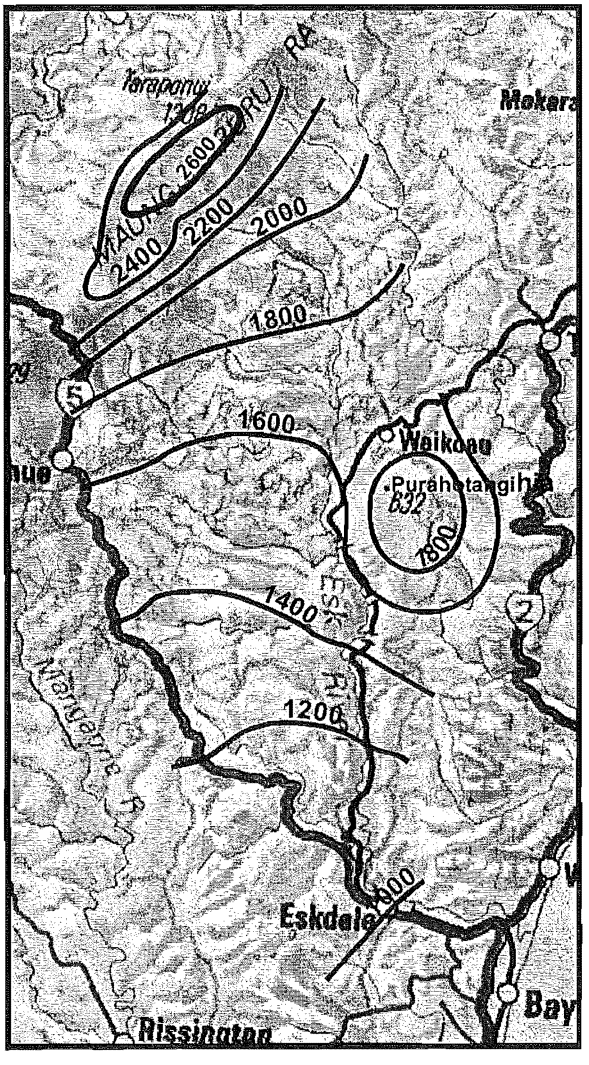

Figure 2.7 Annual rainfall isohyet (from Black, 1991)

A flood hydrograph is a graphical representation of river output against time for a rainfall event. Basin geometry is an important factor in the formation of a flood hydrograph, especially in the Esk Valley where required variables such as basin slope, bed roughness, and hydraulic radius are constant for much of the valley. Major features of the Esk Valley flood hydrograph include:

- Rapid response – the lack of storage in the catchment means the river quickly responds to rainfall, and peak flows on the hydrograph closely match the timing of maximum event intensity.
- Steady increase of flood flow – The long, asymmetric form of the Esk Valley means drainage path lengths for the valley increase linearly (see Figure 2.8). This means flood flows rise and fall linearly relative to the contribution from the catchment. A strong flood peak as a result of the concentration of lengths around 30-40km is compounded by this area being the highest rainfall area (the Maungaharuru Range).
- Immediate return to baseflow – The lack of storage and infiltration capacity within the catchment means residual flows return almost immediately following a flood.

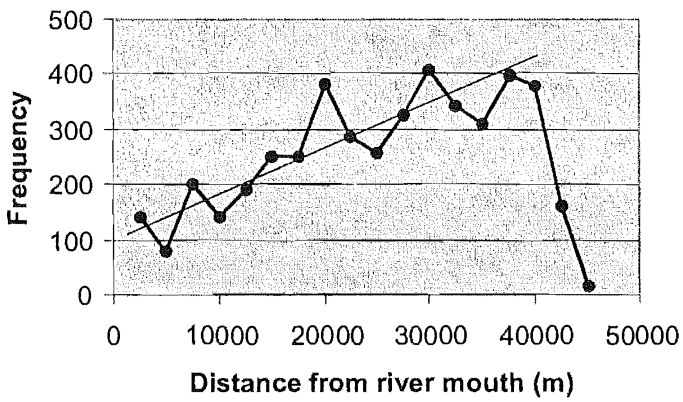

Figure 2.8 Summary of drainage path lengths for Esk Valley

2.3.3.3 Lithology and the Fluvial System

The fluvial system within the Esk Valley is very closely related to basin lithology and morphology. In particular, lithology strongly controls baseflow within the catchment.

The Esk River and its tributaries are for the most part accommodated in narrow, highly incised, sinuous channels. The mid to upper reaches of the valley contain the most pronounced examples of this – commonly 60-80m deep and c.200m wide – the height to width ratio in some valley sections is as low as 1:1. Sinuosity increases from the headwaters to the mouth of the Esk and is matched by a transition from bedrock to alluvial channel fill. After turning the bend at the southern end of Waipunga Ridge the last few kilometres of channel are relatively straight. Prior to European settlement, the outlet to the river was further to the south into Ahuriri Lagoon (Williams, 1986).

Baseflow for the Esk River is around 2.5m^3/sec. and much of this (58%) is supplied from the limestone capped Maungaharuru Range (Black, 1991). Deep-seated landslides also

contribute significantly as mixed sandstone/limestone debris provides excellent storage and transmission structures. Harrison (1988) indicates the prominent cemented conglomerate beds of the lower Petane Group may also add a component of baseflow. Though above average levels of fracturing in siltstones in Ohurakura to Otakowai Stream catchments, and the presence of broad, uncemented gravel terraces in these areas may also be important factors.

Quaternary sediments play an important part in the valley hydrology. In a study of two small zero order catchments immediately outside the Esk Valley, Merz *et al.* (1998) found undisturbed soils were unlikely to reach saturation and produce overland flows except in the most extreme storms, though, high proportions of macropores within the soil may produce rapid subsurface flow. Alternatively, shallow landslide scars reduce regolith cover to negligible depths, and overland flows within these areas are high.

Deep-seated landslides provide storage within the Esk Valley, and probably contribute significantly to baseflow. Irregular terrain on the surface of the slides promotes ponding and infiltration, and fractures in the often poorly consolidated slide material support subsurface flow. Conversely, instability on the surface of deep-seated slides – particularly those on Maungaharuru Range – leads to increased levels of shallow landsliding and subsequently enhances runoff, decreasing catchment storage.

Streams do not contain a lot of sediment, particularly in the upper valley. Bedrock channels are common and the fine silt and sandstones offer little resistance to erosion. Channel fill is generally composed of fine gravels derived from conglomerate beds in the Matahorua Formation. Some siltstone boulders are also present in upper reaches, but these rapidly degrade and silts are deposited in pointbars and overbank deposits in the lower, less constrained sections of the river. The investigation by Williams (1986) gives d_{50} values for bed and armouring layers in the lower Esk Valley around 9mm and 35mm respectively, and suspended sediment around 0.7mm.

2.3.4 VEGETATION AND LAND USE

Vegetation plays a key role in the hydrologic cycle of a catchment. Plants intercept precipitation, limit overland flow, and help reduce latent soil moisture conditions by absorption and evapotranspiration. These effects help dampen peak flood flows, and prevent soil loss – and its subsequent build-up in channels. When combined with the added soil stability provided by root cohesion, the vegetation also helps improve hillslope

stability and reduce the frequency of shallow regolith landslides. The current vegetation, and vegetation history within the Esk Valley is therefore an important consideration when investigating active geomorphic processes.

A warming climate between 14,500 BP and 11,500 BP followed the last glacial period and lead to the afforestation of much of the North Island and transformation from scrub and grassland to broadleaf forests (McGlone, 1995). Around Poukawa, in southern Hawke's Bay Matai and Totora-type hardwoods created a dense forest that is inferred to have completely covered the region. This forest was in place until around 1000yr BP when probable burning by Polynesian settlers quickly reduced the forest to levels similar to that seen today and bracken and scrubby plants colonised the land (McGlone, 1995).

European colonisation of the Hawke's Bay region began around 1840, and at this time 43% of Hawke's Bay forest remained. Bush and scrublands in the Esk were converted to pastoral runs in the late 1850's and English grass was sown. The remaining forest at Te Pohue was milled between 1870 and 1900 (Grant, 1996; Parsons, 1997) leaving small remnants of indigenous forest in the upper Ohurakura catchment (Black, 1991). It was not until the late 1940's, when the Hawke's Bay Catchment Board began investigating serious erosional problems within the Esk Valley, that the progressive destruction of vegetation was halted (Dunlop, 1992). At this time there was little or no riparian vegetation along streams, and intensive areas of shallow failures within the middle catchment (Black, 1991).

Today, the use of modern farming practices and fertilisers, widespread riparian planting, and afforestation of over a quarter of the catchment in exotic pines appears to have addressed many of these issues. Substantial vegetation can aid slope stability by reducing soil moisture levels through rainfall interception and transpiration, as well as reinforcement through interlocking root networks (Pearce *et al.*, 1987; Forest Research Institute, 1990). Marden and Rowan (1993) investigated the effect of different types of vegetation on the stability of slopes in Tertiary bedrock following Cyclone Bola (917mm of rainfall in 72 hours), which hit the East Coast of the North Island in March 1988. They found by far the best protection was provided by closed canopy forests (indigenous forest and exotic pine plantations >8 years old); land occupied by regenerating scrub and exotic pines 6-8 years old was four times more susceptible to landsliding than that with a closed canopy, while young exotic pines (<6 years) and pasture provided the least protection and land was 16 times more susceptible to sliding.

2.4 FLOODING HAZARD

2.4.1 1938 ESK VALLEY FLOOD

A natural hazard is a natural process that puts people's life or property at risk. The Esk Valley has a history of hazardous floods, the most significant of these being the 1938 Esk Valley Flood (Williams, 1986; Johnson and Pearce, 1999). This occurred as a response to three days of heavy rainfall and caused serious damage to much of the Esk Valley, in particular the more populated lower reaches where on average 1m of silt was deposited over the entire valley floor (Grant, 1939; Cowie, 1957). Washouts and slips caused considerable damage to road and rail throughout the region (Cowie, 1957), and telephone communications were cut (Hawke's Bay Daily Mail, 1938).

While the Esk River was not the only river to flood during this storm, the discharge of the Esk Valley was the highest per unit area of any in Hawke's Bay (Grant, 1939). A hydrograph based on rainfall records in Grant (1939) and eye witness accounts in Cowie (1957) is given below in Figure 2.9.

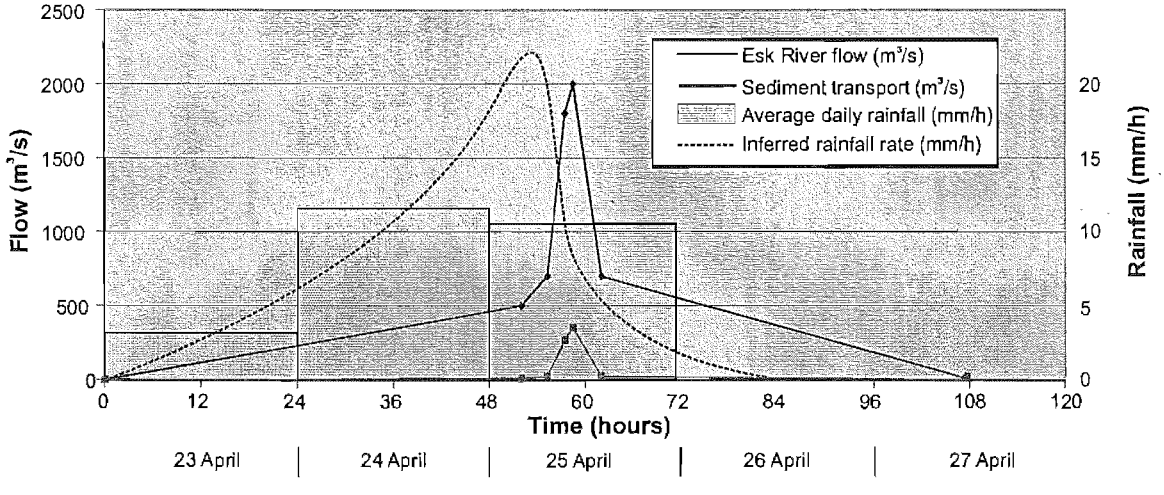

Figure 2.9 Inferred hydrograph for April 1938 Esk Valley Flood

The hydrograph form is inferred from accounts of the water level at various stages during the flood given by residents in the lower Esk Valley and recounted in Cowie (1957). These were then tied to stage-rating curves calculated for the lower Esk River and given in Williams (1986). Daily rainfall records are derived from Grant (1939), and the inferred curve describes the temporal distribution of the rainfall. Peak precipitation rates were almost certainly much higher. However, the daily records this is derived from do not allow more frequent variability to be resolved, and the curve therefore only broadly describes the rainfall pattern.

Time	Record	Approximate flow
23 April	Rainfall began	5m^3/s
25 April 4 a.m.	Rise commenced	500 m^3/s
7:15 a.m.	Bank high	700 m^3/s
9:30-10:30 a.m.	Rising near peak	1800-2000 m^3/s
10:00-10:30 a.m.	At peak	2000 m^3/s
10:30 a.m.-2:00 p.m.	Falling slowly to bank high	2000-700 m^3/s
Two days later	Down to normal	5m^3/s

Table 2.2 Local settler account of Esk Valley flood peak (Cowie, 1957) and associated approximate flows (Williams, 1986)

The peak flood discharge of 2000m^3/s lasted just over half an hour, and this corresponded to a record of peak rainfall in the upper reaches of the catchment 2-3 hours earlier (Grant, 1939; Cowie, 1957; Williams, 1986).

24 and 72 hour rainfalls recorded at Lake Tutira (Cowie, 1957) equate to a c.1000 year storm at Esk Forest, the nearest government recording station (based on logarithmic extrapolation of current records in Thompson (1987a) – see Appendix A). Flood flows in the lower Esk River were also over twice the calculated 100yr design flood (Williams, 1986).

2.4.2 HYDROLOGIC FACTORS

Floods in the Esk Valley are accentuated by factors relating to its climate, morphology, geology, geometry, and land use.

2.4.2.1 Climatic control

The highly variable climate in Hawke's Bay is possibly the single greatest contributor to flooding hazards in the Esk Valley. Intense storm events infrequently punctuate the normally warm, dry conditions experienced in the region. This offers little opportunity for landscape self-regulation or adjustment (see Bull, 1991).

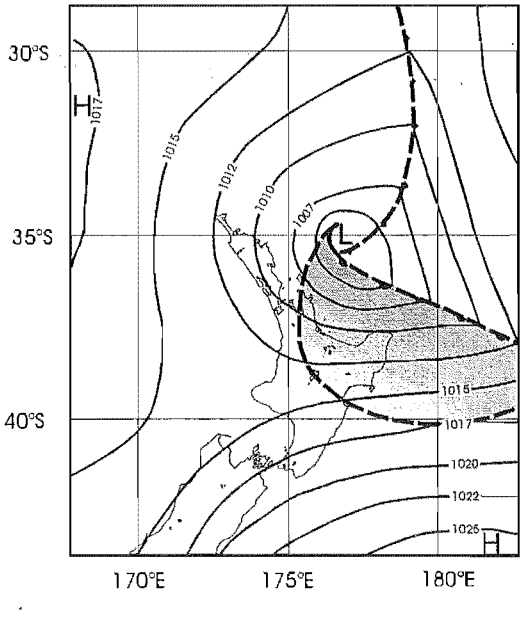

Figure 2.10 Situation on 24 April 1938 during Esk Valley flood (adapted from Cowie, 1957)

The two potentially hazardous climatic regimes (depressions formed in the Tasman Sea or Tropics, and tropical cyclones) discussed in section 2.3.3.1 have notably different signatures within the Esk Valley. Tropical cyclones move across the valley rapidly and rainfall distribution, while affected by orographic elements, is largely determined by the cyclone path. The onset of flood conditions is rapid with only a moderate influence from catchment geometry. Shallow landsliding is common; however, storm duration limits the transportation of sediment into the stream system. Flood flows also reduce quickly as total precipitation and infiltration is relatively low.

Conversely, depressions can be very slow moving. Rainfall distribution from these systems is in direct response to topography and is therefore concentrated along the Maungaharuru Range. Combined with event duration, this ensures prolonged peak flood flows, complete saturation of the catchment, high landslide input, and possibly the activation of deep-seated landslides as groundwater levels and pore pressures increase.

The 1938 event provided an extreme example of a depression-related storm. In this case the effect was accentuated, however, as a south-easterly front related to an anticyclone to the south brought cool air up to meet the warm, moist north-easterly front and increased the rate at which the air was being forced up (Cowie, 1957) (see Figure 2.10). The importance of the orographic effect is highlighted in the 1938 event where rainfall distribution was similar each day – indicating the movement of the system was not a major factor – and by far the heaviest falls occurred by the ranges (1000mm at Puketiriti (7km SW of the Te Waka Range) and 274mm in Napier for the same three day period) (Grant, 1939; Thompson, 1987a).

2.4.2.2 Geometric and Morphologic contributors

Morphology in the Esk valley generally accentuates flooding processes. Steep, linear hillslopes maximise runoff and reduce the opportunity for infiltration and storage. This is compounded by the presence of the steepest slopes in areas of maximum precipitation – the Maungaharuru Range and Purahotangihia. The highly incised, relatively clean, linear channels have a low hydraulic resistance and offer little opportunity for ponding, ensuring high flows. These factors, while decreasing the duration of a flooding event, lead to an increase in potentially hazardous peak flood flows.

While terraces at the foot of hillslopes reduce the degree of hydraulic connection between many steep valley slopes and the fluvial system, it is assumed efficient drainage within

ephemeral streams and terrace sediments significantly diminishes this effect and a high proportion of slope runoff and subsurface flow is transferred into the stream system during a flood event. The effect of terraces and stream incision on sediment production and transport within the valley is emphasised during flooding events, where slopes surrounded by terraces may be less likely to fail, and sediment produced by such failures is unlikely to reach the stream system.

The effect of the geometric and morphologic controls on the Esk Valley flood is most notable when comparing the short (2-3hr) delay between the peak rainfall in the upper catchment and maximum flows in the lower Esk River (Section 2.4.1) indicating high throughput. Evidence for the lack of storage can be seen when comparing the calculated total outflow for the event based on the inferred hydrograph ($1.4x10^8m^3$) with the total precipitation recorded in the catchment over the three days (based on isohyets derived in Grant (1939)), which totals $1.3x10^8m^3$. While errors involved in this comparison are high (see Appendix B), this indicates virtually all precipitation was immediately drained from the valley.

2.4.2.3 Lithologic and Fluvial Factors

Sediment entrained as suspended and bedload during flood flows contributes to flood hazard processes by controlling channel processes, and inundating land following the recession of waters. Sediment mobilised during flood flows provides tools for scour and erosion in bedrock channels (Whipple *et al.*, 2000). However, very high sediment loads can saturate the flow and prevent normal erosional processes from taking place during floods, particularly in alluvial channels. This can enhance the effect of flood events by holding bed level constant and effectively raising water levels. Following the 1938 flood there was very little incision noted in the mid- to lower channels and significant aggradation occurred in the Esk River channel within the aggradational valley (Grant, 1939; Williams, 1986). Siltation of the lower Esk Valley caused the most damage to property during the 1938 flood.

This siltation can be attributed to landslides within the catchment (discussed later), erosion of bedrock banks, and the mobilisation of sediment stored in the fluvial system. It is difficult to determine the greatest sources of sediment, however, some indication can be gained by investigating the type and volume of sediment mobilised in the 1938 flood, and comparing basin characteristics immediately after the flood and subsequent adjustments.

Inspection of sediments deposited during the 1938 flood by Grant (1939) shows by far the majority (83%) was fine-medium sand between 0.15mm and 0.5mm, although the silt component rose to >30% in lower reaches presumably due to waning flow rates and less bedload transport. This is in contrast to much coarser sediments measured in the lower Esk by Williams (1986) (see Section 2.3.3.3), and may indicate a low proportion of siltation came from remobilised bedload in larger Esk Valley channels. Extreme scouring of beds in "small tributaries in the high reaches of the valley" (Grant, 1939), probably around Okurakura Road at the foot of the Maungaharuru Range is likely to have produced the greatest bed load contribution to the siltation in the lower Esk.

The volume of material able to be carried as bed or suspended load within a flow is dependant on the type of sediment being transported, channel characteristics, and flow rates. There are a number of empirical formulae that can be used to calculate maximum bed load transport rates for a given flood condition. These are based on excess shear stresses, excess discharge per unit width, or excess stream power per unit width. However, these equations perform poorly, and usually a combination of results for all three types is adopted (Knighton, 1998). Sediment rating curves for the Esk River were produced by Williams (1986) using a combination of three popular empirical formulae: Meyer-Peter Muller, Englund-Hansen, and Einstein-Brown. These were then checked against actual sediment recordings from the $725m^3/s$ July 1985 flood.

The resulting curves are given in Appendix B and indicate maximum sediment concentrations for the 1938 event were around 17.5% of the total water volume. Based on flow rates derived from slope – area analysis, and assumptions including excess sediment supply to channels, accurate reports of flood staging (Cowie, 1957), and the validity of the sediment rating curve for a flood of this magnitude, this would equate to a total sediment output of approximately $4.51x10^6m^3$. While $6.5x10^6m^3$ was apparently deposited on the valley floor, errors involved in these calculations are high, the former being based on eye witness accounts, and a huge extrapolation of calculated data; and the latter based on estimations of sediment thickness by Grant (1939). At best the magnitude of these figures illustrates the degree of sediment transported, and the close agreement suggests that almost all the sediment was deposited in the valley (see Appendix B for calculations).

2.4.2.4 Landslide input

Introduction

Landslide processes have the potential to compound flooding hazards. Generally the most extreme effect of landsliding is the formation and subsequent breach of landslide dams. This is an example of a process that is a direct contributor to a flood hazard and has been extensively researched. Less direct effects are, however, very poorly understood – possibly due to the difficulty in quantifying them and the huge variability depending on event characteristics. Examples of these indirect effects include severe aggradation in channels and floodplains, increased overland flow as slide scars provide channels of low hydraulic resistance, damage to engineering structures due to mechanical tooling or pressure from debris mobilised by landslides (eg. coarse bedload or logs caught upstream), redirection of stream channels and bank erosion due to lateral sediment input, and the lessened ability of rivers to alter form and efficiently carry debris due to infilled channels and high bed resistance.

Deep-seated slides

Deep-seated landslides can play an important role in determining flood processes both in their immediate vicinity and in the downstream channel reaches. Minimal landslide displacement can generate large volumes of very coarse sediment. This can dam or deflect streams and severely limit stream power, especially in narrow, confined waterways such as those in the Esk Valley. Perturbations on the surface of deep-seated landslides lead to instability and accelerate localised mass wasting processes. This also leads to increased sediment outputs from landslide complexes.

Of the $8km^2$ of deep-seated landslides within the Esk Valley (excluding those on the Maungaharuru Range), a total 13km of toe slope intersects rivers in the Esk Valley and is able to discharge debris directly into the channels. A movement of 1m per slide would equate to an input of c.$0.5x10^6m^3$ of sediment to the system.

While there is no record of historical movement on any of these slides, possibly due to the low population density and lack of records from the early 1930's (Parsons, 1997), the likelihood of movement as a result of the 1931 earthquake and/or the 1938 storm is high. The potential for these slides, along with the landslide complexes of the Maungaharuru Range, to contribute considerable amounts of sediment and affect fluvial processes within the Esk Valley therefore warrants investigation.

Shallow Failure Contribution

The majority of silt deposited during the 1938 flood has been attributed to the "thousands" of shallow failures in the catchment (Hawke's Bay Daily Mail, 1938). These were reportedly most intense in areas with the greatest rainfall, and at the time were largely attributed to the 1931 earthquake (Cowie, 1957). As mentioned in Section 2.3.2.3, while the exact nature of shallow landslides in the 1938 event has not been investigated, the mechanism and distribution of these slides in elsewhere in Hawke's Bay has been studied in detail. These failures are not likely to have produced significant landslide dams. However, shallow landslides triggered by ground shaking during the 1931 earthquakes and heavy precipitation in the 1938 storm, produced a large amount of sediment and been a major indirect contributor to the 1938 flood. An illustration of the magnitude of landsliding can be seen in Figure 2.11 below:

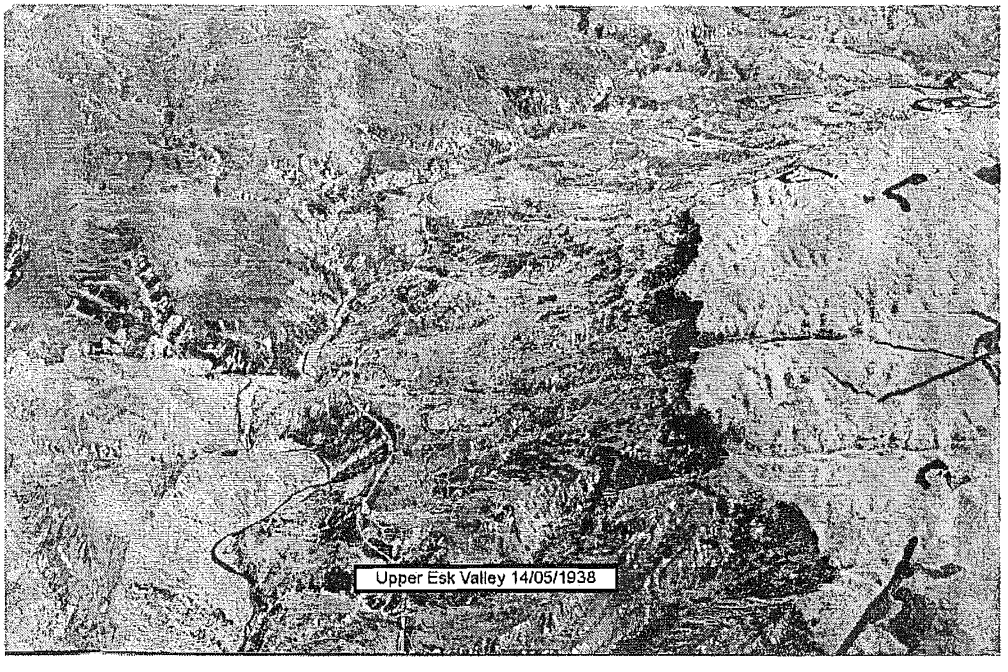

Figure 2.11 Upper Esk Valley 14/05/1938

Taken soon after the Esk Valley Flood, this photo clearly illustrates the lack of substantial vegetation cover at the time, and the extreme degree of shallow landsliding. The photo is taken looking north above Island Farm, The Esk River runs up the centre of the photograph, and the junction with Deep Stream can be seen approximately halfway up the image. Photo courtesy HBRC archives.

2.4.3 EARTHQUAKE EFFECTS

Earthquakes are indirect contributors to flooding processes, their primary effect being the triggering of large numbers of landslides. This effect is seen both during the event, and in

the long-term destabilisation of hillslopes - these often fail in years following the event (Wasowski *et al.*, 2000). The landslide-causing effects of earthquakes are well documented, and have been linked both to shallow (Keefer, 1994; Luzi and Pergalani, 2000), and deep-seated failures (Keefer, 1994; Crozier *et al.*, 1995). Despite this we have only a basic understanding of the process that takes place during an earthquake to cause slope failure (Wasowski *et al.*, 2000).

Evidence for the initiation of rockfalls and shallow landslides in the 1931 earthquake is commented on by Henderson (1933) and Marshall (1933) as well as many eye-witness accounts (Grant, 1939; Cowie, 1957; Parsons, 1997). None, however, attempt to quantify the extent of landsliding. Deep-seated landslides were also described by Marshall (1933) on the coast at Old Mans Bluff, as well as those documented by Adams (1981) and Pettinga (1987a; 1987b) discussed in section 2.2.2.6. These last examples include a slide over 100km away from the earthquake epicentre and indicate a real likelihood of deep-seated failures occurring in the Esk.

Earthquakes can also alter, and therefore destabilise, stream paths. Surface rupture can create knickpoints or dams in river courses, and tectonic uplift instantly re-grades a stream's profile and can force rapid channel aggradation, degradation, or avulsion. Each of these effects can be hazardous to people or structures and enhance the effect of subsequent floods by prompting rapid change in the fluvial system. Examples of these effects can be seen in Hawke's Bay in the migration of the Tutaekuri River (Begg *et al.*, 1994), and possibly high levels of incision occurring in the mouth of the Esk River described by Williams (1986).

2.5 SUMMARY

The Esk Valley has been subject to a diverse range of processes, acting both modern and prehistoric. It is important to have an understanding of processes acting in similar regions in order to attempt to quantify their interactions with, and effect on, landforms in the Esk Valley.

Features and processes common to the forearc basin are particularly important. These include soft Pliocene marine sediments, active tectonic uplift and associated thrust faults, broad, continuous fluvial terraces, and common deep-seated and shallow landsliding.

3 REMOTE SENSING AND FIELD RECONNAISSANCE

3.1 INTRODUCTION

An initial reconnaissance investigation was undertaken to determine the extent of deep-seated landsliding within the Esk Valley and attempt to identify dominant geomorphic controls. This investigation utilized a combination of 1:50,000 topographic maps (Stirling, 1979), a panchromatic LANDSAT image (Landsat 7 enhanced thematic mapper, 1999), geological maps (Haywick *et al.*, 1991; Bland, 2001), and c.1:25,000 scale aerial photographs (New Zealand Aerial Mapping, 1944). Structural anomalies identified within the field area were then quantified with the use of a Digital Elevation Model (DEM) based on 20m contour data derived from Department of Lands and Survey topographic maps. Results from these investigations were compiled in a GIS database and then used to identify areas in which to concentrate the field investigation.

3.2 SATELLITE AND AIR PHOTO INTERPRETATION

3.2.1 INTRODUCTION

Extensive satellite and air-photo interpretation formed the basis of the reconnaissance study. The 1:25,000 scale aerial photo stereo pairs were used to identify deep-seated landslides and assess their likely geometry, mechanism of failure, and activity. Stream patterns were also examined in these photographs as well as any lineaments that may be evidence of dominant underlying structures such as joint systems, faults, and bedding orientation. The air-photo study was backed up with the use of a DEM and 17.5m/pixel resolution rectified LANDSAT imagery. These enabled the quantification of larger features identified in aerial photos as they can be mapped to NZMG co-ordinates. They were also used for the identification of more regional structures (>10 km in extent).

The combination of these sources was found to produce good results, and provided a comprehensive overview of structures at vastly different scales. The majority of mapping was undertaken from high quality aerial photographs, however, relief and geometric distortion in these made the production of a true-scale geomorphic map for the region infeasible. The referenced satellite image was used mainly to identify regional trends and

investigate the relationship between features covering more than a third of the area of each aerial photograph, for example the aerially extensive landslide complexes on the Maungaharuru Range. The low resolution of the satellite image limits its use for the identification of features under 300m long, and geomorphic features appear "flat" due to the lack of shadowing. The DEM, while providing no data on surface cover and having a coarse vertical resolution, is useful as relief could easily be exaggerated – simulating aerial photos; and larger features can be measured directly off the projection – as with the satellite image. Other benefits of the DEM include the ability to vary illumination and vertical exaggeration, as well as manipulate data to emphasise specific morphologic features or properties.

While both stereo and aerial oblique photographs were taken of the Esk River immediately after the 1938 flood (see Figure 2.11), the first full coverage of the area was undertaken in 1943 by New Zealand Aerial Mapping. In order to identify historical changes in the valley morphology and its contributing geomorphic processes, these early aerial photographs of the Esk catchment were contrasted with a later high quality 1:25 000 series from 1981. The series numbers, and individual photos used are listed in Appendix C.

3.2.2 RESULTS

A large landslide complex is identified as part of the Maungaharuru Range on the western margin of the catchment. This consists of both rotational and translational failures in the order of 10km^2. Several smaller deep-seated translational slides (c.1km^2) are also identified within the catchment, as well as many shallow failures, particularly in early photographs. Bedding orientation can be determined and many indurated beds (commonly conglomerate) are delineated. Streams generally appear to be of low power and sinuous, although on close inspection these are very highly incised (~80m) and apparent sinuosity is derived from sharp, angular bends (see Berry Rd. Stream in Figure 3.1A). Three main sets of lineaments are identified, generally marked by corresponding channel orientations. Traces of the dextral strike-slip Patoka Fault Zone are also apparent outside the catchment to the southwest (see Appendix C).

3.2.3 SPECIAL INVESTIGATION: SHALLOW LANDSLIDE DISTRIBUTION AND ASSOCIATED SEDIMENT PRODUCTION

3.2.3.1 Introduction

The striking degree of shallow landsliding evident in the early 1943 aerial photos is one of the most distinctive characteristics of the Esk Valley at that time. Here it is suggested that nearly all shallow landslides visible in the 1943 series are a direct result of the 1938 storm. These photos therefore offer a means of calibrating a slope stability model for the 1938 storm such as that developed for the Tutira area by Hennrich (2001). This section describes the development of a basic shallow landslide distribution map for the 1938 storm based on the observation that most steep slopes in the area were subject to intensive landsliding as a result of the event.

While no information is available on the state of the catchment prior to the 1938 storm, bright white scars evident on aerial photographs taken soon after the event illustrate the degree of landsliding in the region at the time (Figure 2.11). Based on the rapid recent deforestation prior to 1938 (described in Section 2.3.4), and the strong reaction from local authorities to the degree of landsliding (see Dunlop, 1992), it is reasonable to assume the majority of these scars are a direct result of this event. Comparisons of shallow slides evident in these oblique images with 1943 photos (as in Figure 3.1) indicates very little modification or reestablishment of vegetation on the scars, and therefore suggests all those visible in the later photos can also be attributed to the 1938 storm. From these images it is clear that the failures are generally restricted to steep slopes, of these, commonly over 60% of the surface has failed.

This investigation is similar to that undertaken by Eyles (1971) in the adjacent Tangoio Conservation Reserve where landslides identified in the same series of aerial photographs were also attributed to the 1938 storm. He found approximately 17% of slopes in the reserve failed during the 1938 storm to an average depth of 0.6m. Failures typically occurred on slopes between 26° and 36°, and were more frequent on northern facing slopes due to a greater climatically-related variation in soil wet/dry cycles.

3.2.3.2 Method

The density of failures on slopes on which slides are present, and consistency of failures on steep slopes indicates a strong relationship between slope angle and stability during the

1938 event. Conversely, there appears to be very little variation that may imply a dependence on factors typically required in deterministic stability models such as soil depth, antecedent moisture conditions, and contributing catchment area (e.g. Shalstab Montgomery and Dietrich, 1994). This may reflect a combination of the homogeneity of the mixed weathered-bedrock and volcanically-derived soils, and the intensity of rainfall which may have lead to saturated conditions throughout the catchment.

This relationship was tested by converting digital elevation data taken from the LINZ DEM to a digital slope map using Golden Software Surfer. The critical slope was then adjusted by inspection to obtain a best fit to the landslide distribution evident in aerial photos. An upper and lower bound was selected to account for oversteepened slopes where no surficial soils will develop, and those apparently too shallow for landsliding to occur.

Unfortunately no allowance could be made for slope aspect. However, as a result of bedding orientation in the valley the majority of steep slopes are on the NW (scarp) side of topography. This means failures on the SE (dip) side of topography are therefore in the minority, and a decrease in the frequency of failures in these slopes is unlikely to substantially affect results.

3.2.3.3 Results

There is a very good correlation between slope angle as defined by the LINZ DEM and shallow landslide distribution as a result of the 1938 storm. For slopes between 27° and 31° there is approximately an 80% failure rate. However, on slopes where failures do occur, the slope map under represents the area over which sliding took place. This relationship in two locations where 1943 photographs have been manually rectified to match NZMG co-ordinates can be seen in Figure 3.1. Due to their location in relation to the Maungaharuru Range, these areas are likely to have been subject to distinctly different rainfalls during the 1938 storm, however, landslide conditions appear similarly related to slope, and the increased rainfall in the vicinity of the range does not appear to have played a significant part in the instability as suggested in early reports (see section 2.4.2.4). This analysis indicates these failures occupy approximately 0.4% of the total catchment land area.

The slope window in which sliding occurs is steep for the Esk catchment where the greatest slopes are typically on the scarp side of topography and are consistently around 20° (see Figure 4.16), notably below the 27° failure angle suggested by the DEM. This

window may represent the upper limit at which slopes are able to develop a significant soil profile. Slides appear to be occurring on geomorphically active areas, such as oversteepened "soft" bedrock slopes below indurated conglomerate ridges, areas that have maintained soil cover and are now being affected by the extreme fluvial incision such as terrace edges, and dissected topography in the Mangakopikopiko catchment. The lack of landsliding on shallower slopes in apparently inactive regions may suggest the destabilising effects of the 1931 earthquake are not particularly significant.

This strong correlation between slope angle and landslide frequency has been used to develop a landslide susceptibility map for the Esk catchment during the 1938 storm (see Appendix E). Based on this, approximate volumes of sediment production have been derived for the event. The total landslide plan form area from this map is around $1.16 \times 10^6 m^2$; considering an average slope of 29°, and landslide depth of 2m (Pettinga and Bell, 1992; Merz and Mosley, 1998), this gives a total sediment production of $2.67 \times 10^{6\ +1.33 \times 10^6}_{\ -0.38 \times 10^6}\ m^3$ (see Appendix E for calculations).

While it is difficult to estimate how much of the sediment generated by landsliding during the 1938 storm reached stream channels and therefore became a factor in the resulting flood; it is reasonable to assume that because a large number of the slides were in areas of apparently rapid geomorphic change primarily driven by stream incision, the connection between slopes and streams in these areas facilitated a high degree of fluvial sediment transport.

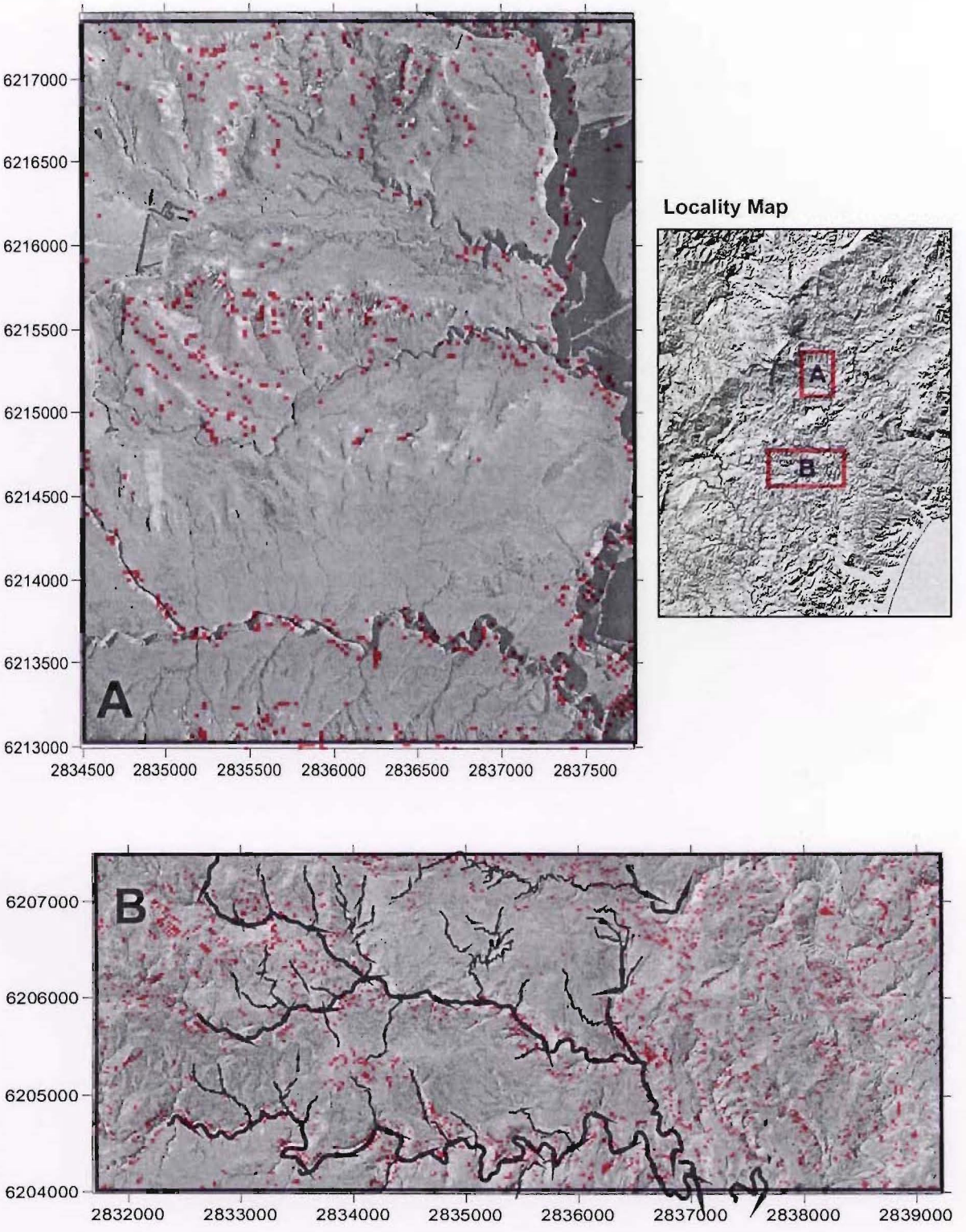

Figure 3.1 Comparison between slope map and shallow landslide distribution in 1943

Berry Rd. Stream can be seen toward the bottom of 3-1 A, 3-1 B details the Trelinnoe study area. Despite some distortion in the photos, a very good correlation can be seen between the location of bright white landslide scars resulting from the 1938 storm, and slope angles indicated between 27° and 31°.

3.3 FLUVIAL GEOMORPHOLOGY

"...rivers have all the makings of a scientific obsession – they are tremendously varied and complex, but also systematic – as if just one more crucial insight would explain all the variety and complexity"

Keller and Pinter (1996)

It has long been recognized that natural watercourses are one of the most sensitive indicators of geomorphic environmental change. Their plan form and longitudinal profile is remarkably sensitive to minor environmental perturbations related to climatic and tectonic forcing. Such perturbations include variations in flow, sediment flux, and baselevel change.

This stage of the investigation aimed to first identify key channel characteristics, then link these characteristics to geomorphic processes. Rivers in the Esk Valley are instantly characterized by two key features; their sinuosity, and the high degree of incision. Key geomorphological knowledge is combined with quantitative morphologic analyses in order to identify and quantify relevant aspects including their longitudinal profile, sinuosity, and later – the relationship between fluvial processes and the extensive river terraces throughout the valley.

3.3.1 LONG RIVER PROFILES

3.3.1.1 Introduction

The long profile of a river is simply a plot of bed elevation against the path length of the stream to its outlet. While this is generally one of the least adjustable factors in a stream system (Knighton, 1998) – particularly in bedrock channels – the study of long river profiles has proved a useful indicator of long-term geomorphic processes including sediment transport mechanisms, discharge, and tectonic forcing.

Rubey (1952) summarized the key factors controlling channel grade and therefore profile shape, in the equation below:

$$s^3 X = k \frac{Q_s^2 M}{Q^2}$$ **Equation 3.1**

Where:

s = channel gradient

X = cross-sectional shape (=depth/width ratio)

k = constant (determined by inspection)

Q_s = sediment load

M = sediment size

Q = discharge

This equation forms the basis of many studies of fluvial systems, and clearly shows the direct relationship between sediment characteristics and channel grade, and the inverse relationship between discharge and grade. This equation, as with many studies, is based on an assumption of "steady state" conditions – where a balance exists between long-term uplift and erosion producing statistically invariant topography.

As well as variations in the magnitude of these factors, their effect also varies depending on bed morphology or channel dynamics. Whipple and Tucker (2002) divide channels into three main groups:

- transport-limited; where the gradient of the channel is defined by the rivers ability to transport sediment load. While these channels are generally alluvial, Howard (1980) points out limited bedrock incision is also possible.
- detatchment-limited; where channel grade is defined by the balance between the rivers ability to erode its bed and the rate of uplift/base level fall. These are almost exclusively bedrock channels and are considered to be limited by stream power and bed erodability.
- hybrid channels; channel gradient in these systems is defined by both transport capacity, and the rate of bedrock detatchment. These mixed bedrock-alluvial channels are common, and are characterised by "frequent outcrops of bedrock but largely blanketed by a thin layer of alluvium" (Whipple and Tucker, 2002).

As well as these three groups, further complexity is introduced when considering steady state and non steady state systems (Whipple and Tucker, 2002).

An investigation into river bed morphologies in the Esk Valley suggests these are predominantly hybrid channels; bedrock outcrop is frequent, particularly in the upper reaches of streams, where the proportion of bedrock exposed in the channels commonly exceeds that with thin alluvial cover, however the proportion of alluvial cover increases toward the outlet of the system, and the channel that extends through the aggradational valley at the bottom of the system is transport-limited, the mouth of the river regularly having to be opened by machinery to overcome the strong aggradation (Williams, 1986). Further comment on channel features identified within the valley is given in Chapter 4.

3.3.1.2 Review

It has long been recognized that the profile described along the length of a stream channel can often be correlated to simple mathematical functions. The applicability of exponential, logarithmic, and power functions has been investigated by many authors (eg. Krumbein, 1937; Snow and Slingerland, 1987; Morris and Williams, 1997, 1999; Knighton, 2000) with varying results. Generally, exponential functions of the form given below in Equation 3.2 have been found to best match stream profiles.

$$H = H_o e^{-k_1 L}$$ **Equation 3.2**

(cited in Knighton, 1998)

Where H and H_0 are final and initial median grainsizes, L is channel length

Transport-limited systems

Correlations of long profiles to exponential functions are, however, merely the most generalised expressions of a complex literature. They are based on investigations of what are assumed to be transport-limited systems, that is: systems in which sediment transport processes dominate, and were fundamental in defining the form of the profile. Such assumptions are suited to silt, sand, and gravel-bedded alluvial systems where a downstream reduction in sediment size is inferred to be a controlling factor on channel slope. This is a logical conclusion and is based on the observation that the particle size model in Equation 3.3 mirrors that for channel elevation along any exponentially graded stream (Equation 3.2).

$$D = D_0 e^{-\alpha L}$$ **Equation 3.3**

D and D_0 are final and initial channel elevations.

However, studies using a simple particle size correlation produced poor results unless discharge was also included in the analysis (Knighton, 1998). By incorporating this third factor into the equation, Hack (1957) showed a clear relationship for a range of exponentially graded channels given by the equation:

$$s = 0.006\left(\frac{D_{50}}{A_d}\right)^{0.6}$$ **Equation 3.4**

Where

s = local channel slope

D_{50} = median grainsize

A_d = drainage area

The exponent in the above equation describes the degree of profile concavity. Drainage area is used as a proxy for discharge, which is notoriously difficult to measure due to large spatial and temporal fluctuations.

Morris and Williams (1997), in a theoretical proof, showed that exponential profiles are prevalent in channels with low lateral inflows and in which bed loads are subject to communition or hydraulic sorting. The low lateral inflows factor is important as this situation is analogous to long, narrow valleys in which stream length can therefore be a proxy for drainage area, and by implication, stream power. This is highlighted in their study where actual stream data deviates from modelled conditions at junctions where drainage area (and therefore stream power) is instantly increased. A later study correlating bed concavity and particle size on 137 transport-limited channels ranging from 0.0010-1770 km in length gives a strong linear correlation with a coefficient of variability (R) of -0.980 (Morris and Williams, 1999).

The complexity inferred in Rubey's (1952) equation (Equation 3.1) where sediment load, size and discharge are all variables – combined with the variability in stability state of

natural channels becomes apparent when comparing studies on each factor. Knighton (2000) suggests from field studies that "channel gradient is most strongly related to discharge", whereas Whipple and Tucker (2002), while investigating factors that control the rate of incision in bedrock, found theoretical variations in sediment flux produced good results and exponential profiles. These studies are in turn both in direct contrast to the previously presented findings of Morris and Williams (1997).

The findings of Whipple and Tucker (2002) are based on a model of transport-limited incision proposed by Willgoose *et al.* (1991) and Tucker *et al.* (1998) in which volumetric sediment transport capacity is written as a power function of bed shear stress. This is presented below:

$$Q_c = K_t A^{m_t} S^{n_t} \qquad \textbf{Equation 3.5}$$

Q_c = volumetric sediment transport capacity

K_t = dimensional transport coefficient

A = catchment area

S = local channel gradient

m,n = positive constants that depend on basin hydrology, hydraulic geometry, and erosion process. These are extremely difficult to calibrate, and very few field studies have derived values for them (Sklar and Dietrich, 1998).

By incorporating uplift rate (U), and a variable (β) to quantify the proportion of sediment delivered to the channel as bed load, an equation can be derived from Equation 3.5 to predict channel gradient and therefore profile shape in a steady state transport-limited system (Equation 3.6 and Equation 3.7) (Willgoose *et al.*, 1991).

$$S_t = \left(\frac{\beta U}{K_t}\right)^{\frac{1}{n_t}} A^{-\theta_t} \qquad \textbf{Equation 3.6}$$

$$\theta_t = (m_t - 1)/n_t \qquad \textbf{Equation 3.7}$$

The importance of stream power is considered so great by Whipple and Tucker (2002), that they define an *intrinsic concavity index* (θ) (Equation 3.7) in order to better describe the form of the exponential curve excluding other external factors (e.g. nonuniform uplift

(Kirby and Whipple, 2001), variations in substrate (Moglen and Bras, 1995), and downstream variations in sediment flux (Sklar and Dietrich, 1998)). This is derived from the slope of a line of best fit projected through points for a single channel on a log-log plot of drainage area against gradient.

Detachment-limited systems

Our understanding of processes operating in bedrock and hybrid bedrock-alluvial channels is nowhere near as good as those for alluvial channels, and only recently have attentions begun to be turned to these systems (e.g. Foley, 1980; Howard and Kirby, 1983). Bedrock channels have generally been assumed to be detachment-limited systems, where erosion of the substrate is the primary controlling variable on channel grade.

There are a number of mechanisms proposed to facilitate bedrock erosion including simple bed load abrasion, dissolution, cavitation, quarrying, and mechanical instabilities associated with knickpoint migration. The fundamental control on these processes and the rate of incision has long been assumed to be stream power, however, the importance of sediment flux in providing tools and access to bedrock has recently been recognised (Sklar and Dietrich, 1998; Whipple and Tucker, 2002). These controls have lead to the use of a bedrock channel stream power incision model based on bed shear stresses as given in Equation 3.8 (Howard and Kirby, 1983; Howard *et al.*, 1994; Whipple and Tucker, 2002).

$$E = Kf(q_s)A^m S^n \qquad \text{Equation 3.8}$$

Where:

E = vertical incision rate

K = dimensionless erosion efficiency factor (increases with erodability)

$f(q_s)$ = represents models describing dependence of river incision rate on sediment flux, generally:

=1 in detachment limited system where sediment transport capacity (Q_c) > (Q_s) sediment flux

<1 with decreasing Q_s/Q_c capacity

An expression to define detachment-limited steady state channel gradient (S_d) can be derived from this equation using a similar method to that outlined for transport-limited systems (Equation 3.9 and Equation 3.10) (Howard, 1980; Whipple and Tucker, 2002).

$$S_d = (\frac{U}{K})^{\frac{1}{n}} A^{-\theta_d}$$ **Equation 3.9**

$$\theta_d = m/n$$ **Equation 3.10**

Hybrid channels

The profile of hybrid channels such as those in the Esk Valley is largely dependant on the model used to define $f(q_s)$ for variations of Q_s/Q_c, and the degree of disparity between the intrinsic concavity indices of the system in a transport- and detachment-limited state (θ_t and θ_d) (Whipple and Tucker, 2002).

Whipple and Tucker concentrate on two models presented for $f(q_s)$:

1) The linear decline model (Beaumont *et al.*, 1992) – where $f(q_s)$ decreases to zero with increasing Q_s/Q_c (Equation 3.11)

$$f(q_s) = 1 - Q_s / Q_c$$ **Equation 3.11**

This assumes more energy is required in to transport bed load in lower reaches, and the amount available for incision is therefore reduced (Whipple and Tucker, 2002).

2) The parabolic model (Sklar and Dietrich, 1998) – where $f(q_s)$ increases to a maximum around $Q_s/Q_c = 0.5$, and decreases to zero at the upper and lower limits of Q_s/Q_c (Equation 3.12).

$$f(q_s) = 1 - 4(Q_s / Q_c - 1/2)^2$$ **Equation 3.12**

This attempts to describe the role of sediment in both providing tools for erosion at low relative sediment flux ($Q_s/Q_c < 0.5$), and then providing a cover to protect the bed from erosion at high relative sediment flux levels ($Q_s/Q_c > 0.5$) (Whipple and Tucker, 2002).

The disparity between intrinsic concavity indices for the transport- and detachment-limited systems affects the degree to which the stream gradient flattens or steepens through the hybrid region. If a rapid transition occurs from transport- to detachment-limited, then the difference in the intrinsic concavity index determines the strength of the break in steady state channel gradient that will occur at this point. In hybrid systems, however, the presence of shallow alluvium in the channel allows this transition to occur along the length of the channel (Whipple and Tucker, 2002).

Whipple and Tucker use these solutions to derive models for steady state hybrid channel gradient that apply for various geomorphic conditions. In the simplest case, where the intrinsic concavity index for the transport-limited system is less than that for the detachment- limited system (a commonly argued case), and the linear decline model is applied for f(qs), the steady state gradient model for the channel is simply given by the sum of the models for the transport- and detachment-limited systems (Equation 3.6 and Equation 3.9). This is given below:

$$S = (\frac{U}{K})A^{-m} + \frac{\beta U}{K_t}A^{1-m_t} \qquad \textbf{Equation 3.13}$$

Esk Valley

Of the models presented for channel gradient in Whipple and Tucker (2002), the hybrid channel is considered to be analogous to the situation in the Esk Valley, though a lack of data regarding the catchment and the question of temporal process variations prevents the confident selection of a model. However, Whipple and Tucker (2002) show that for all of the models as K is increased, describing the soft, readily erodable bedrock in the Esk Valley, the detachment-limited factor each model rapidly decreases, and the hybrid channel slope approaches that for the transport-limited state (Whipple and Tucker, 2002). Profiles defined by this equation, or indeed those defined by the hybrid equations approximate exponential curves, particularly at high intrinsic concavity values (Whipple and Tucker, 2002). More research has to be undertaken to derive an intrinsic concavity index for the Esk Valley.

3.3.1.3 Method

Long river profiles for the Esk Valley were manually digitised off a 20m DEM. This method was chosen primarily for the rapidity of measurement, and has been used in a

number of studies (Dietrich *et al.*, 1993; Montgomery and Foufoula-Georgiou, 1993; Snyder *et al.*, 2000). Sources of error for this method are, however, considerable and given below:

- Data to produce this DEM was taken from 20m contours and interpolated to fit a rectilinear grid. This process produced a stepped surface at low gradients, because for widely spaced contours the region between contours is assigned elevation values only slightly below those of the upper bounding contour. Near the lower bounding contour, elevations sharply decrease (see Figure F.1).
- Due to the coarseness of digitised points, and the effect on the grid of high degrees of incision in river valleys, the initial data is very "dirty", with many spikes due to contamination from valley walls. These are removed by simply rounding all data down to the nearest 20m, effectively negating the effect of poor vertical interpolation of the grid.
- The degree of incision is likely to have also hampered the production of contour maps off aerial photos. In some sections the bottom of valleys is not visible in aerial photos, and in others only poorly. This may have lead to a significant error and effectively raised the stream channel in the narrowest sections.
- Digitising invariably shortens the path length of the rivers by cutting corners on the actual path. Although this effect compounds along the digitised length, the effect on data for this study is considered negligible.

Individual streams were digitised and plotted on a composite graph of long profile length vs. elevation (see Figure 3.2). This plot is used in preference to that of Whipple and Tucker (2002) primarily because of the simplicity of the data acquisition compared to inherent difficulties involved in calculating drainage area variation along the stream profiles. The linear nature of most of the catchments in some ways negates the need to plot drainage area, as with the narrow valleys investigated by Morris and Williams (1997), path length effectively becomes a proxy for drainage area. The increased stream power related to the orographic effect of the Maungaharuru Range as discussed in (Chapter 2) would also be severely underestimated by a simple area-power correlation. Exponential curves of the form in Equation 3.2 were automatically fitted to the profile curves (Figure 3.2). Fit statistics are given in Appendix F.

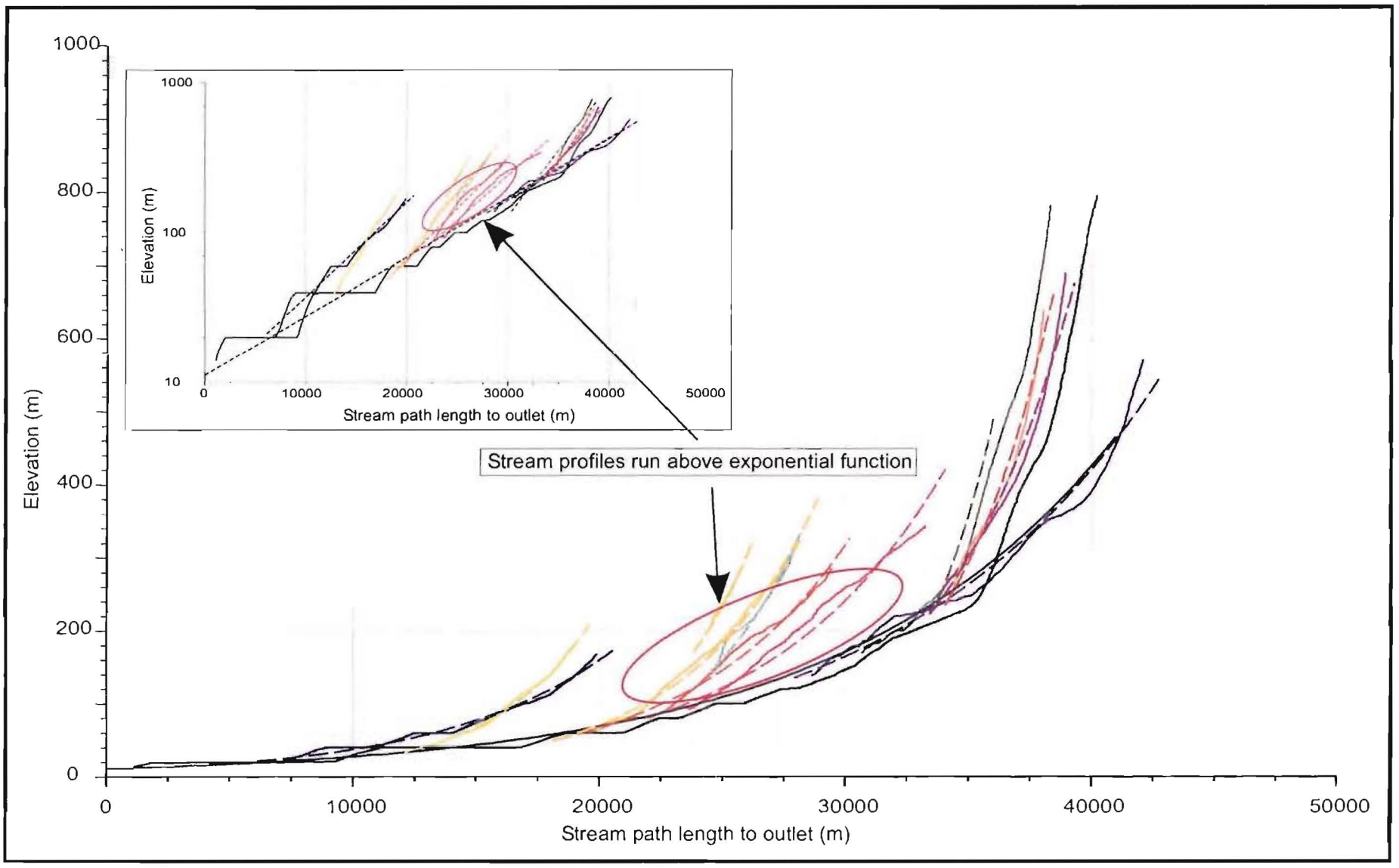

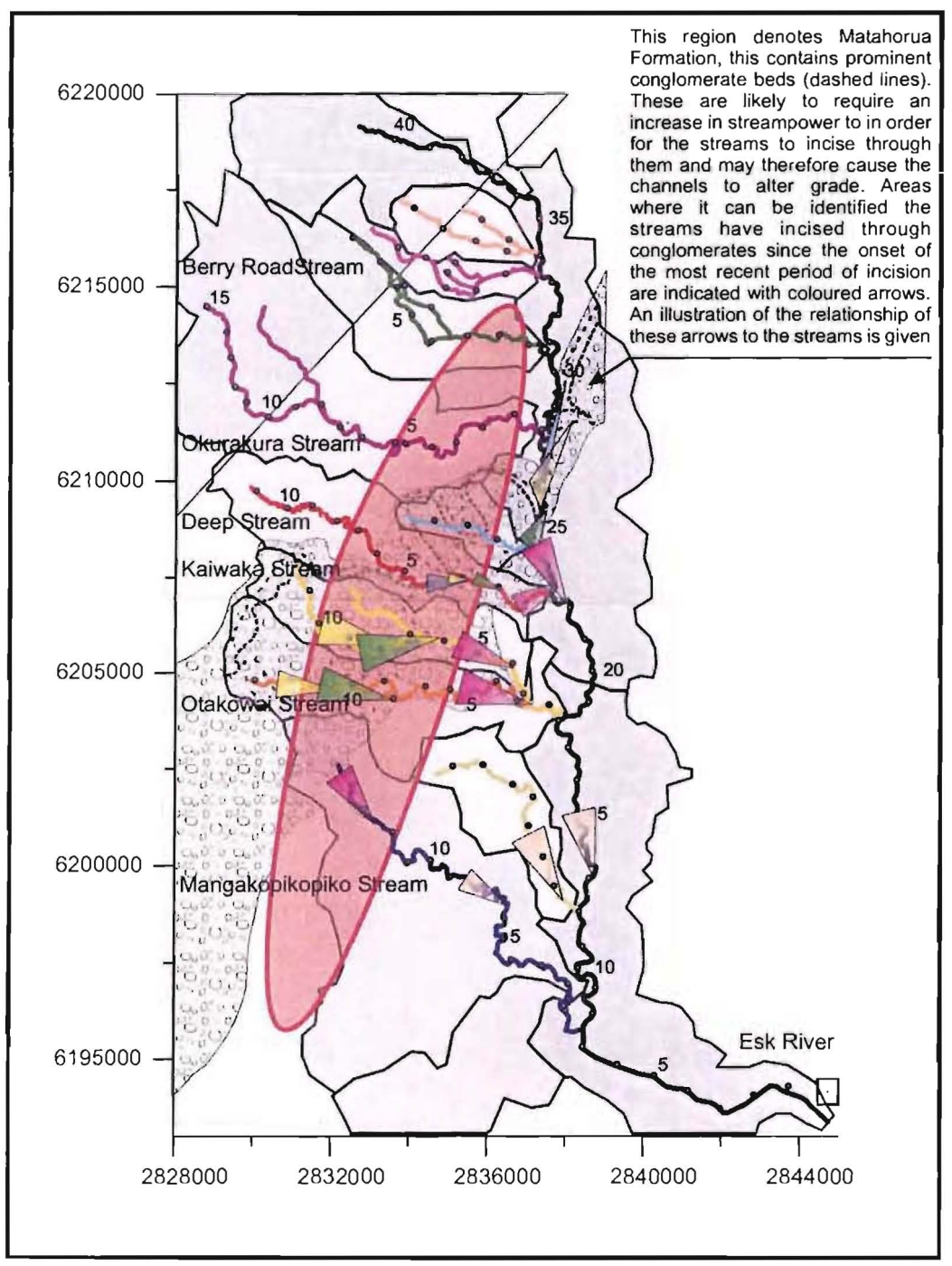

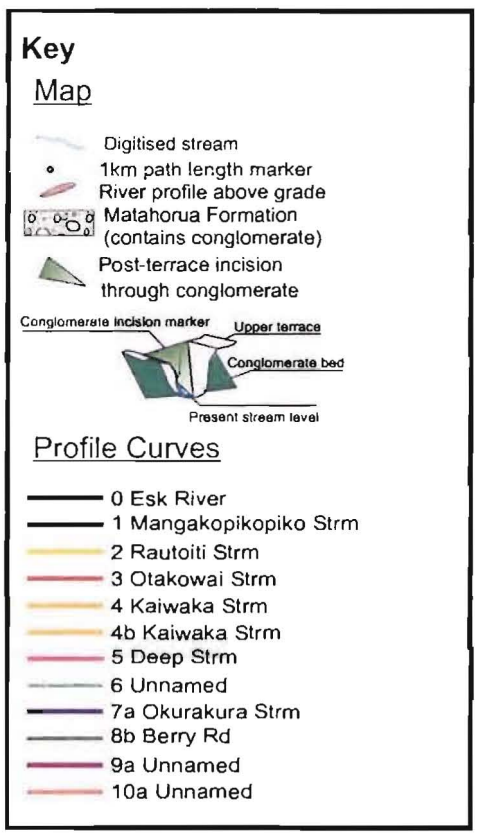

Figure 3.2 Long profiles and location map for Esk Valley rivers
Profiles are based on interpolated 20m contour data. Note coarse data, particularly in lower gradient reaches. Exponential profiles (dashed lines) are automatically fitted to river profiles. Inset shows semi-log plot of profiles illustrating strong correlation to exponential curves, and increased grade in upper reaches.
Deviation of the stream channels above these profiles is high lighted in both the profile curves and map.
Possible conglomerate control is illustrated in the location map, and catchments controlling stream power are also displayed.
The Maungaharuru Range is in the top left of the map.

3.3.1.4 Results

The river profiles fit extremely well with exponential curves, this aided the identification of anomalies in the stream profiles, and classification of stream processes. The profile curves, locations of the rivers, and their spatial relationship with other key geomorphic controls such as conglomerate beds and the Maungaharuru Range are given in Figure 3.2.

Anomalous stream profiles

The most distinctive aspect of the profiles is a region within the middle of the field area where the profile of a number of streams plot above that of the exponential functions. While the average maximum deviation of the profiles is only 20m (the vertical resolution of the contour data the DEM is based on), the consistency of the anomaly in individual profiles, and coherence through the valley lends weight to the inference that the anomaly is not simply a product of the gridding or sampling processes.

While resistant conglomerate beds within the Matahorua Formation may decrease the incision rate and create a local highpoint in the channel profile, only poor outcrop in any channels, and the broad spacing of the conglomerate beds suggests this may not be a strong control on incision. In fact it is possible conglomerates below the water table may not have yet developed significant cements to resist erosion.

The sharp increase in bedload size as a result of the input of resistant greywacke gravels is also likely to be a factor in the adjustment of a channel to grade. However, as shown in Rubey's (1952) equation, the increase in size should lead to a steepening of the reach, increasing the concavity of the profile and therefore appears to be minimal.

Anomalies in both Ohurakura and Berry Rd. Streams detract further from arguments for these two scenarios as these streams run almost entirely through Patoka Formation sandstones and do not incise through, or carry gravels at any stage.

Rapid uplift or a drawing down of base level can propagate a diffuse knickpoint up through the system and may also induce this form. This is however, not supported by the distribution of the anomaly, or the apparent return to grade above the anomaly.

The preferred explanation is for a broad structural warping beneath the anomalies as a result of active compressional stresses present in the forearc. This is discussed in further detail in Section 5.3.

3.3.2 SINUOSITY INDEX

3.3.2.1 Introduction

While the highly incised rivers of the Esk Valley are very tightly constrained and therefore lack the ability to adjust channel form, studying the sinuosity of the streams and gorges in which they are entrenched offers an opportunity to investigate the response of the rivers to tectonic and lithologic controls since the onset of incision. This can help provide important information on rates of landscape development, as well as controls on the valley system at the time of incision.

3.3.2.2 Review

The sinuosity of meandering streams is a useful indicator of channel processes and can provide evidence on factors such as sediment flux, flow regime, bank erodibility, and tectonic adjustment within a reach (Keller and Pinter, 1996; Knighton, 1998). Meandering within a graded system is viewed as a way of maintaining an equilibrium between channel slope and discharge and/or sediment load and is part of a channel form continuum that runs from straight, through meandering, to braided (Leopold and Wolman, 1972).

This relationship, combined with Equation 3.1 by Rubey (1952) provides an excellent insight into the relationship between channel processes and form. If regional or local slope is increased, the river will increase its meander length in order to maintain channel slope. On reaching a critical slope threshold meandering will then rapidly decrease with increasing slope and channels will tend toward braided forms. Alternatively, an increase in flow resistance such as sediment load and bank resistance will require an increase in channel slope, and decrease sinuosity in steeper channels (Knighton, 1998). Valley slopes in the Esk are considered to be above this threshold and it is suggested an increase in slope will decrease meandering.

The above relationships can be used in conjunction with knowledge of stream inflows and lithological controls to investigate subtle tectonic influences on the system (eg. Adams, 1980; Burnett and Schumm, 1983; Campbell and Yousif, 1985; Ouchi, 1985; Gomez and Marron, 1991; Litchfield, 1995). In a study of a New Zealand river system, Campbell and Yousif (1985) found a distinct increase in sinuosity in a braided river immediately upstream of the axis of an active anticline, while downstream the increase in gradient produced a composite sinuous-braided form. This is illustrated overleaf in Figure 3.3.

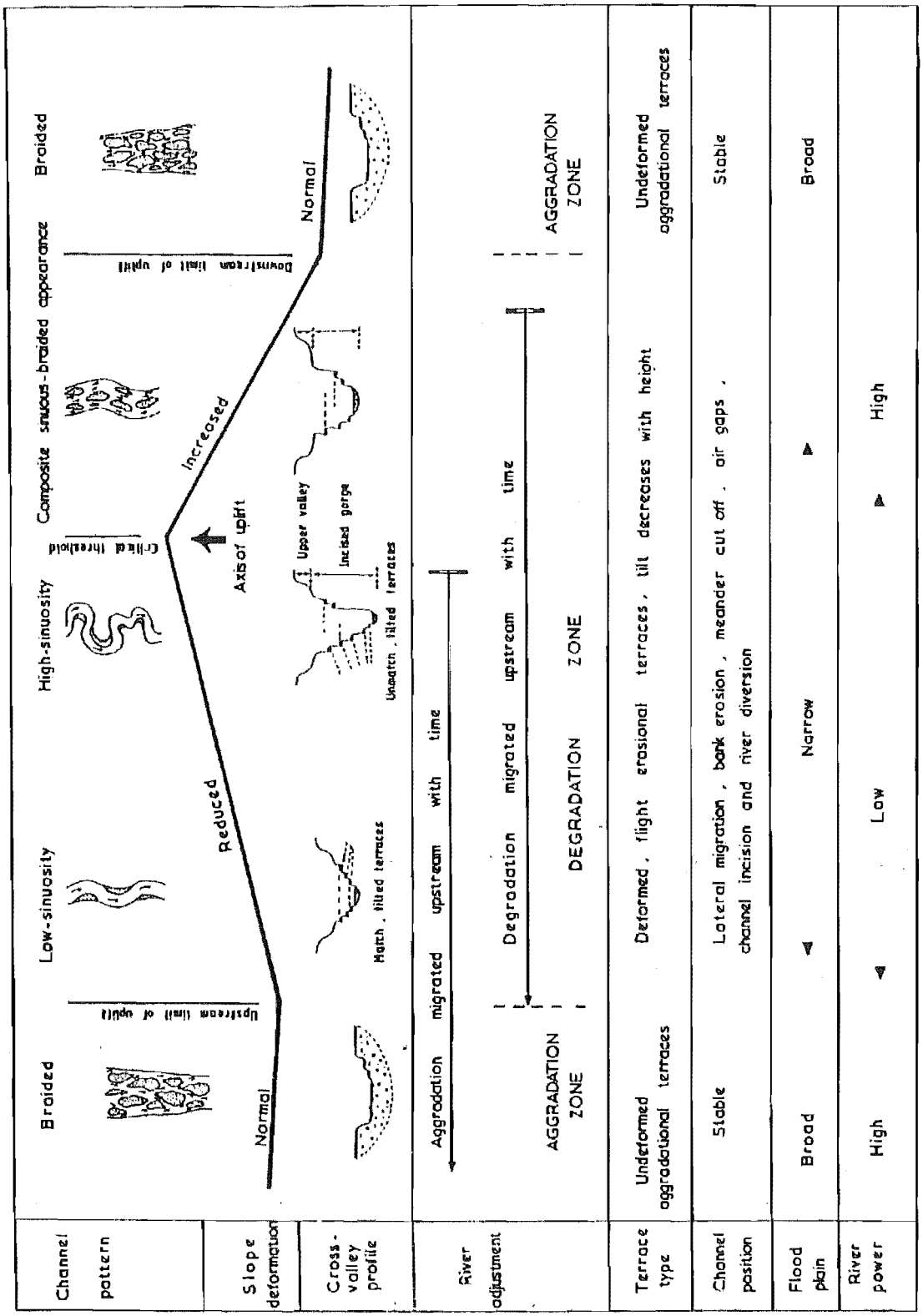

Figure 3.3 Effects on a river as it crosses a growing anticlinal structure (Campbell and Yousif, 1985)

3.3.2.3 Method

Sinuosity is defined as in the equation below:

$$Sinuosity\ (S) = \frac{Channel\ length\ (C)}{Valley\ Length\ (V)} \qquad \text{Equation 3.14}$$

While channel sinuosity is easily identified, quantification can be difficult and time consuming due to difficulties with the variable scale of meanders, superposition of multiple meander wavelengths, and inconsistencies associated with the interpretation of meander form. Traditionally sinuosity is measured by constructing a straight-line valley length (V) through inflection points marking the intersection of adjacent thalwegs along the channel profile, then measuring the stream length between the points (C). The process is usually undertaken by hand; this can be time consuming, introduce measurement errors, and can only be applied over discrete intervals. Automating the task is complicated by the variability in natural channels, and user inputs required to identify meander patterns. A means of partial automation was investigated by Litchfield (1995) in which an "inverted" measure of sinuosity was calculated using set channel lengths calculated from a digitised profile, and then measuring the valley length between points. This was shown to provide good results, however, it still only allowed calculation over discrete intervals and the resultant sinuosity measure is slightly different to that derived from traditional methods.

The method used in this study provides a means of automating the calculation of sinuosity continuously along the stream profile while using user-defined window lengths to determine the scale of meander investigated. This eliminates many errors in the previously described techniques. A line representing the valley length is digitised using straight lines connecting the inflexion points of major thalwegs along the river. A grid is then derived that extends beyond the limit of the widest meander and enables correlation between valley length and channel length continuously along the profile. A running window was chosen that equated to around half the wavelength of the dominant meander, ensuring it was sampled without losing excessive resolution. This agrees with observations made by Litchfield (1995) who suggests a half wavelength interval along the valley length produces results that best describe the channel. Further discussion on this method is presented in Appendix G.

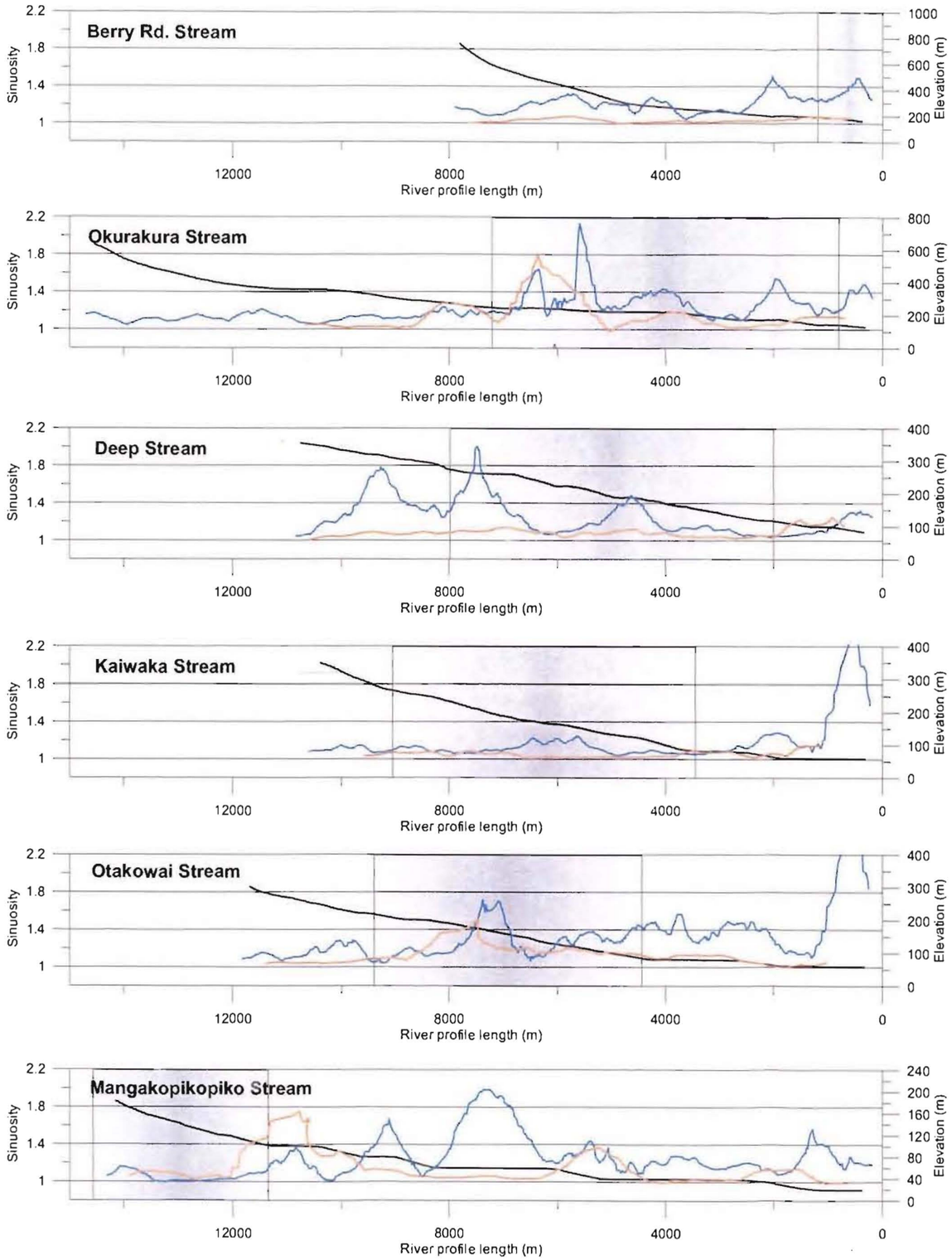

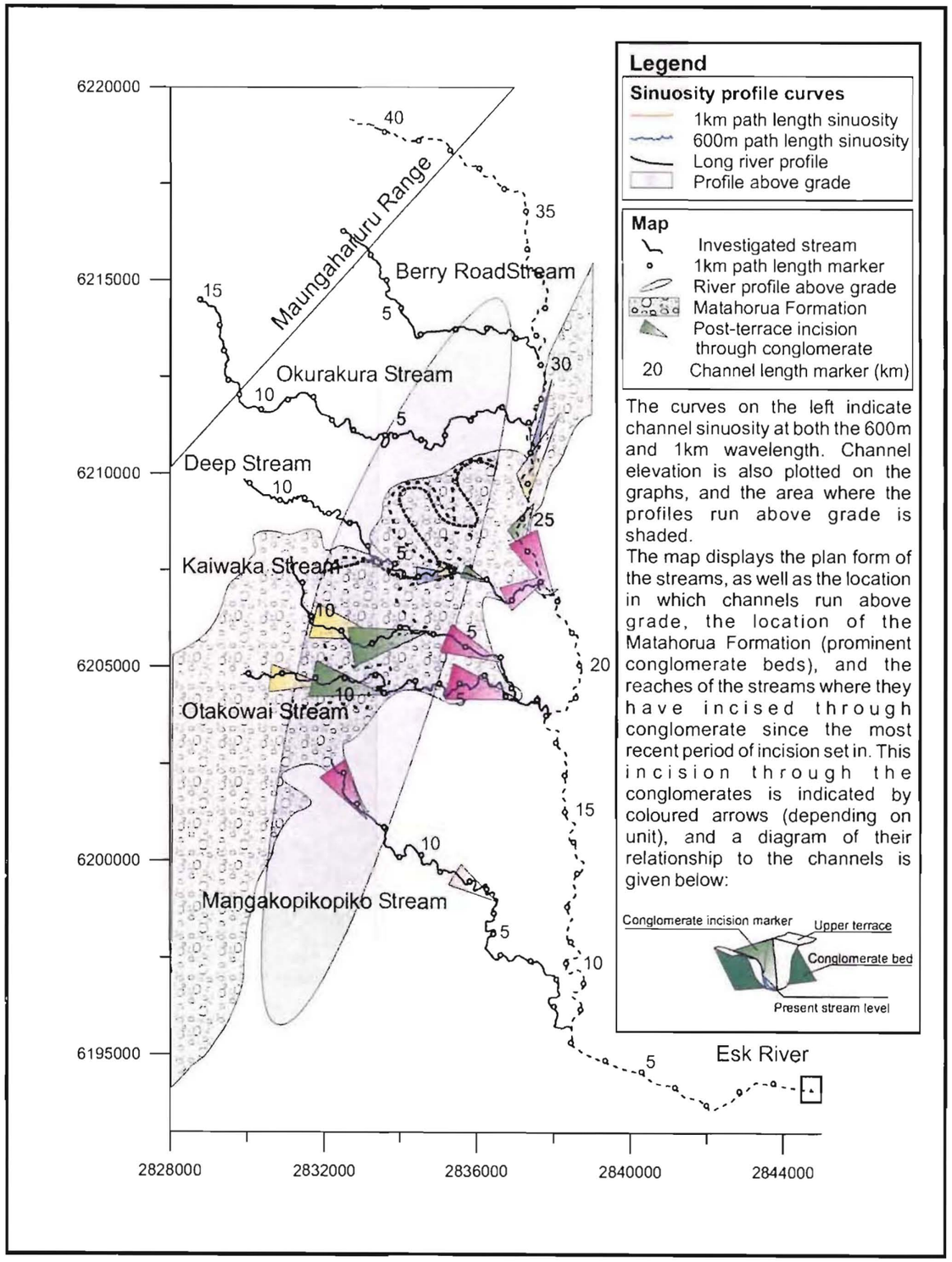

Figure 3.4 Sinuosity curves and location map

3.3.2.4 Results

The results of this investigation are displayed in Figure 3.4. Two scales of meander were noted in the Esk rivers, one with a path length of approximately 1km, and another much tighter pattern superimposed on this with a path length of 600m. These appear to relate respectively to the early form of the incised channels, and to much later forms that have defined the rivers present paths within the valleys.

1km meander

The broad meander pattern in the Esk Valley is preserved at the level of the extensive terrace surface that can be traced throughout the valley (see Section 3.3.3). This indicates the pattern reflects processes and key structural controls active in the valley immediately prior to, and during the first bedrock incision event following terrace formation. IT can therefore provide insights into the initial state of these processes, and can help quantify the development of structural controls over time.

On inspection, meanders that define the form of the gorges are generally very angular and align with defects mapped in the valley (see Section 4.3.3). This suggests the meander pattern is imprinted on structural controls. Field observations indicate these controls are not strong, mainly persistent vertical defects, and weak lithological contrasts. Defects are however, considered to be spaced frequently enough to be readily exploited by meanders of those wavelengths present in the rivers without substantial deviation from their natural form. As a result, the main attributes of the meander pattern – amplitude and wavelength – are considered representative of the natural pattern; however, form, orientation and curvature, are not.

600m meander

The meanders of shorter pathlength generally have an amplitude less than the width of the incised valleys and therefore represent the stream today in greater detail than is preserved of the older form at the upper level. Those within less incised channels e.g. Mangakopikopiko Stream, lower Kaiwaka Stream, and upper Deep Stream, generally have high amplitudes and very short wavelengths, while meanders of similar pathlength in more incised streams have much longer wavelengths and lower amplitudes, apparently due to the effects of the tightly constrained channels. This has the effect of preventing re-grading of the channel through lateral planation and therefore indicates unstable reaches in which aggradation or degradation rates would be heightened.

The shorter pathlength sinuosity almost always has a higher sinuosity index than the long meanders. This implies there has been an increase in meandering over time, and may indicate a general decrease in valley slope related to reduced rates of uplift, or a system reaching grade. This would suggest downcutting rates are not as high as at the onset of incision.

Possible controls on meander pattern

It is interesting to note consistent large meanders in the channels immediately prior to entering the main stem of the Esk River. These are possibly due to a long-term inequilibrium between the Esk and its tributaries, and may reflect higher sediment loads or discharge within the Esk sourced from the Maungaharuru Range forcing a steeper channel profile, or faster incision rate.

Lithologic contrast is often a significant control on channel form. The most important in the Esk Valley is between iron cemented conglomerates and adjacent poorly cemented siltstones or sandstones, this contrast could certainly control local channel grade and sinuosity. However, a lack of conglomerate outcrop adjacent to the sinuous stream channels makes identification of processes difficult. At best, comparisons can be drawn between an increase in sinuosity angularity and Matahorua Formation sediments outcropping elsewhere in the region (Waikoau and Waiiti Rivers) as evidence for lithological control. The conglomerate beds may be expected to "hold up" the rivers and severely inhibit incision as they do for prominent landforms within the valley (see Section 4.2.2.1), this should have the effect of markedly reducing channel sinuosity as the grade is forced to steepen. The rivers have incised up to 4km along the conglomerate beds since the end of terrace formation (Figure 3.4), however, definite trends are not obvious other than an apparent increase in the angularity of the meanders, possibly due to stronger defect controls in the cemented sediments.

Correlations between long river profiles and sinuosity are difficult as a high proportion of the total stream lengths are apparently above grade. This leaves little of the channel experiencing similar conditions in which to observe background levels. However, regions in which the channel profile lies above the exponential profile generally correspond to areas of increased sinuosity (Figure 3.4). The exception to this is Mangakopikopiko Stream in the south, which runs uncharacteristically straight across the inferred region of uplift.

3.3.2.5 Summary

The sinuosity of channels within the Esk Valley streams provides an insight into processes acting since the onset of incision and during the formation of the gorges. It may also provide insight into the geomorphic stability of streams today as described in Section 2.3.1.

Of the two pathlength meanders identified, the longer one appears to indicate conditions at the onset of incision. As this is generally less sinuous than the shorter wavelength meander it may be a result of a steeper system with rivers approaching a braided form.

The shorter pathlength meander is generally more sinuous than the previously mentioned, and may indicate a reduction in incision rate, or system nearing grade.

Defects within the rock mass appear to be a strong control on the formation of meanders, and are inferred to have played an important part since the onset of incision.

The dominant lithological control on sinuosity are the cemented conglomerate beds of the Matahorua Formation. These appear to produce a distinctive angularity in both large and small-scale meanders.

It is difficult to quantify the response of the meander pattern to the region in which rivers run above grade, however, there appears to be a general increase in sinuosity associated with this region.

3.3.3 TERRACE MAPPING

3.3.3.1 Introduction

Terraces are planar surfaces created by the avulsion of river channels. These can be formed during times of degradation, in which the surfaces are generally cut into bedrock; or aggradation when terraces are formed by the deposition of sediments transported by the river. There is at least one aggradational terrace system present throughout most of the Esk Valley. Understanding the distribution, form, and interrelationship between terraces in the valley is important in order to understand previous geomorphic regimes operating in the valley, and the rate of subsequent landscape change.

Terraces in the valley are generally >100m wide and slope gently down to the present day incised stream channels. Upper surfaces are flat and display little evidence of channelisation or disturbance since their formation except in the ephemeral channels. Each terrace often contains up to four c.3-5m risers that step down to the main channels. However, in some areas isolated paleo-channels can be observed bounded on either side by

matched terrace remnants. Terrace risers are often remarkably linear, and may indicate structural control. These were mapped by Black (1991) as fault scarps, though no evidence can be found to support this conclusion.

While only limited field investigation of the terraces has been undertaken in this study, results have shown they are generally composed of 10-15m of matrix supported uncemented greywacke gravel – almost certainly derived from conglomerate members of the Petane Group. Large-scale bedding can easily be identified, and no organic material was found. The gravel appears to lie on broad bedrock straths, gravels at the top of the sequence rapidly grade into c.3m of rarely cross-bedded, slightly pumiceous, volcanic soil.

Terrace drainage is concentrated in the incised ephemeral streams and feeder springs that reflect the high hydraulic conductivity of the volcanic soils and gravels. The intersection of these streams and Esk tributaries is usually marked by a well defined knickpoint as the streams lack the power to match tributary bedrock incision rates.

3.3.3.2 Review

The mapping and correlation of terraces within the North Island has been undertaken by a number of authors. Of these authors, Pillans (1986) provides a good review of terraces formed in the last c.250,000 years, while Litchfield (2002) draws on recent work to study factors driving incision on the East Coast since the formation of the youngest Ohakean Terrace (11-10 ka). Berryman *et al.* (2000) investigates factors associated with the formation of a flight of terraces in the Waipaoa River catchment in northern Hawke's Bay dating from the end of the last interglacial (110ka?) to the Recent.

Aggradation and incision within a catchment is closely linked to glacial and interglacial climate and sea level change. Oxygen isotope and sea level curves for the last 140ka are given in Figure 3.5 below:

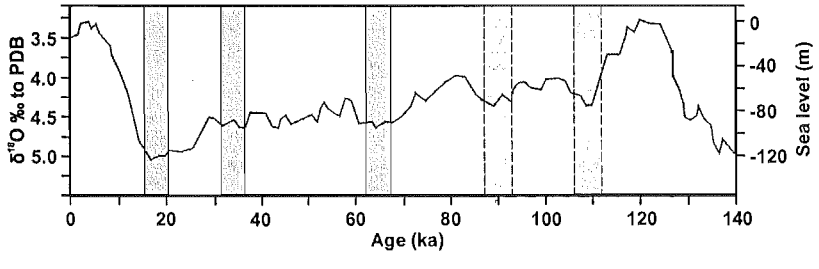

Figure 3.5 Oxygen isotope curve for the last 140ka (Shackleton, 1987)

Shading represents inferred aggradational episodes (Berryman *et al.*, 2000), light grey correlations are uncertain

During the peak of the last glacial sea level was approximately 120m below present day levels (Shackleton, 1987), and the coastline in Hawke's Bay is inferred to have been as much as 30km offshore (Litchfield, 2002). This caused significant incision in downstream reaches of rivers, contrasting with aggradation in upstream reaches.

The terraces in the upper catchment are formed in response to increased sediment supply from periglacial environments during cold glacial periods, they are then preserved by tectonic uplift and/or tilting (Pillans, 1986; Berryman *et al.*, 2000; Litchfield, 2002). Of the twelve terrace treads identified by Milne (1973) in (Pillans, 1986) in the Rangitikei Valley, four sets have been identified in the Ngaruroro River near the Esk Valley (Hammond, 1997) and in the Waipaoa (Berryman *et al.*, 2000). Due to a lack of characteristic ash marker beds overlying older surfaces, the Ohakean Terrace is the only one of these to have been correlated in the Ngaruroro (Hammond, 1997), though Berryman *et al.* (2000) gains age control on the most recent three (c.18ka, c.31ka, c.64ka).

The Ohakean terrace is the most extensive surface in eastern Hawke's Bay, and was abandoned at the end of the last glaciation. This surface is commonly found 60-80m above present river level (Milne, 1973; Pillans, 1986; Hammond and Palmer, 1992), the subsequent incision being the likely effect of reduced sediment input following the termination of the last (Otiran) glaciation (Pillans, 1986). Three terrace risers around 3m in height can be identified on the Ohakean Terrace in both the Mohaka and Ngaruroro Rivers, signifying separate periods of aggradation. These are dated at c.16-14ka, 14-11ka, and 11-10ka (Hammond, 1997). Similar risers have been identified on the Ohakean terrace in the Manawatu (Marden and Neall, 1990), and Waipaoa River catchment (Berryman *et al.*, 2000). Hammond (1997) describes the terrace as "a Nukumaruan mudstone or sandstone strath which is overlain by greywacke sandstone aggradation gravels with sand, silt and clay lenses. Blanketing the aggradation gravels are loess and tephra coverbeds."

3.3.3.3 Method

In order to fit with time constraints, mapping of the terraces within the Esk Valley was undertaken with the aid of aerial photos, a satellite image, and DEM. Likely surfaces were identified in aerial photos, and from field reconnaissance. These were mapped on the satellite image, then overlain on the DEM to provide spatial and elevation control. With the aid of GIS, these points were then plotted on a graph of elevation vs. the stream path

distance to the river outlet. Trends in this data allow individual points to then be correlated with terrace sets, bedding, or unrelated features.

Sources of error in this investigation are similar to those described in the Long River Profiles Section (3.3.1.3), and are related to the coarseness of the DEM vertical resolution, uncertainties when mapping terraces from aerial photos, and also include the impracticality involved in dating surfaces to ensure correct correlation.

Limited field investigation supplemented the aerial photo interpretation. This included observations of terrace morphology and stratigraphy, as well as an attempt to provide age control on the abandonment of the surfaces. The latter was undertaken using a hand auger, and attempted to obtain tephra samples which could be geochemically correlated to ash beds of known age.

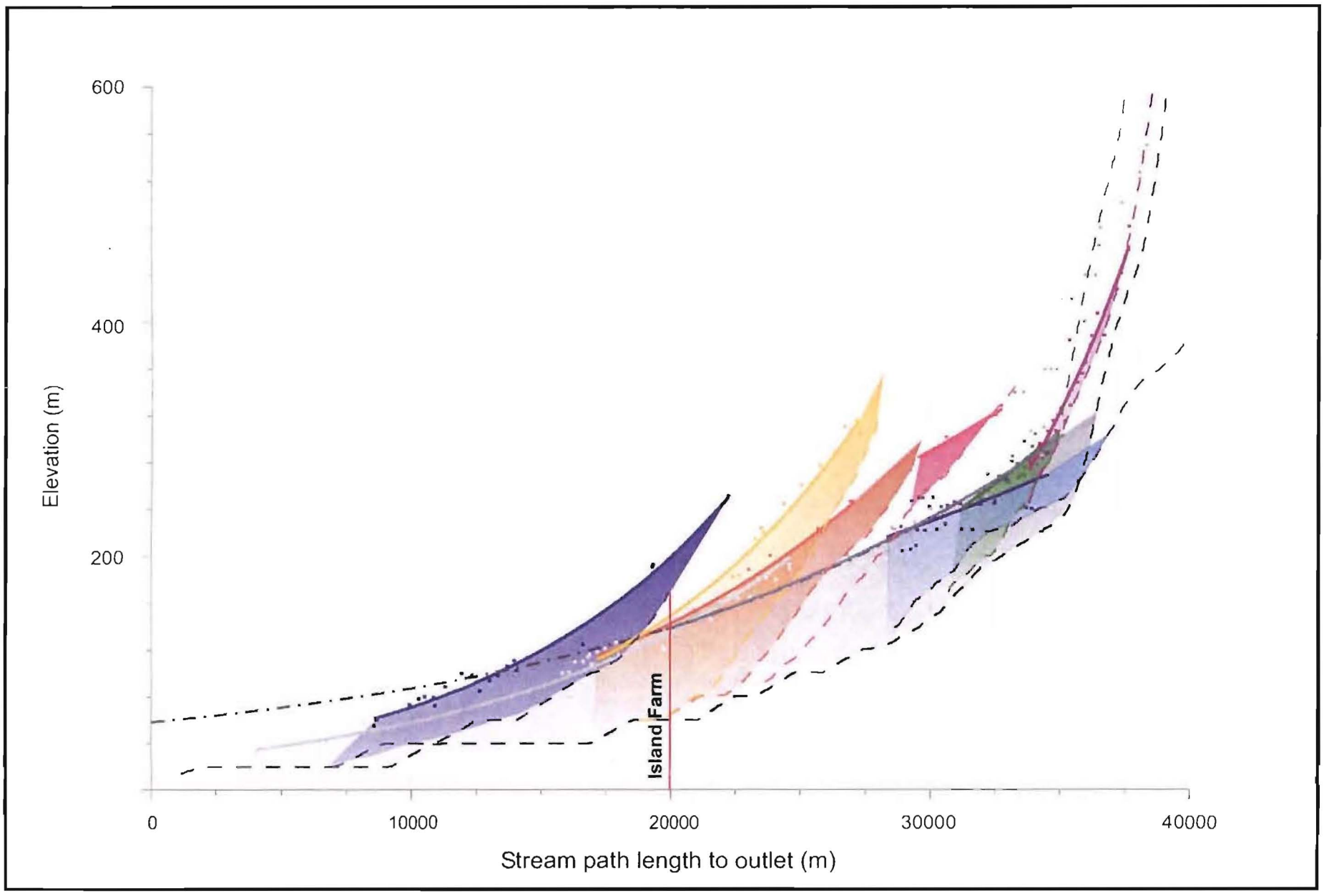

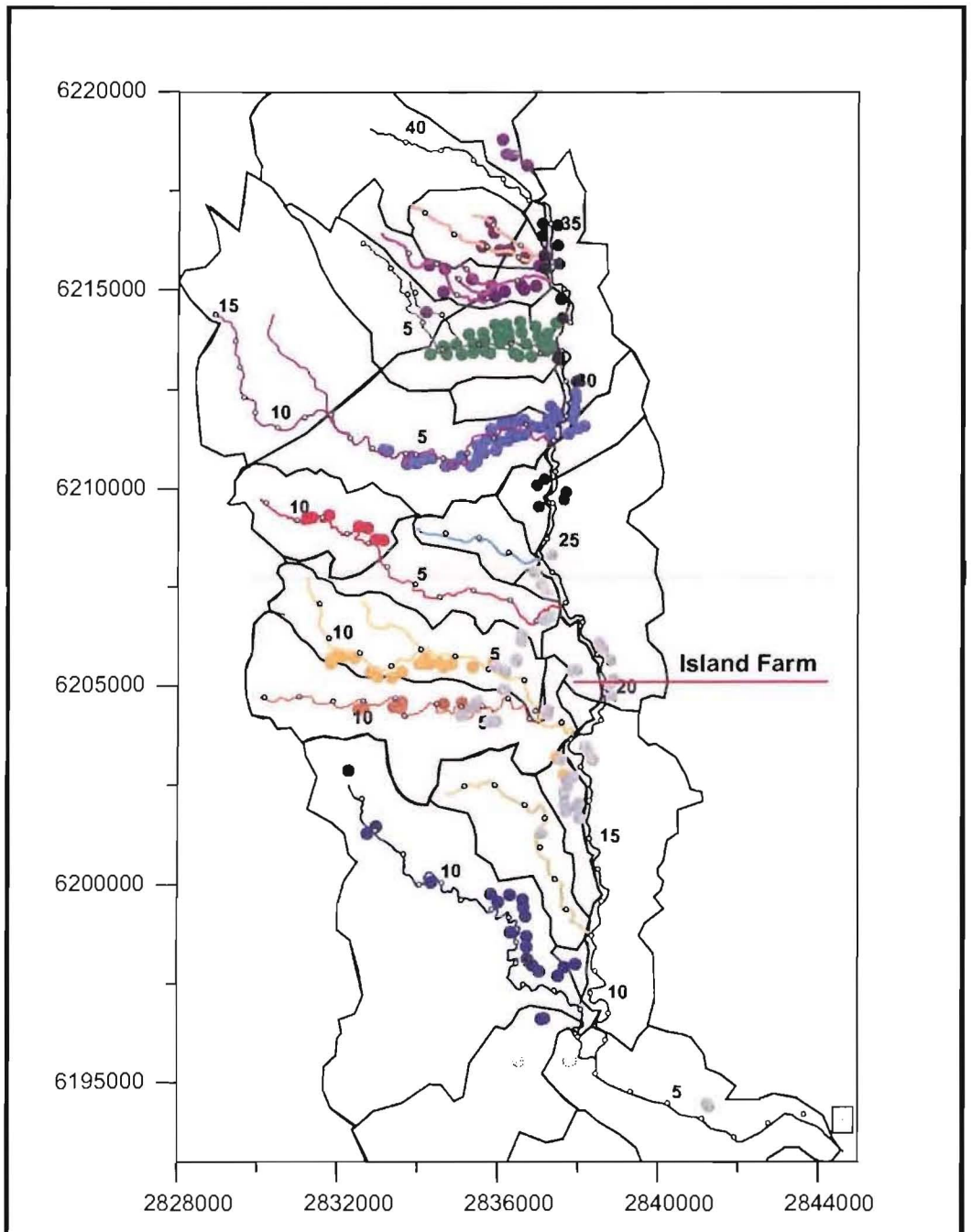

Key

Map

- River
- 1km path length marker
- Data Point
- Catchment
- 25 Channel length marker (km)

Profile Curves

- Data Point
- Post-terrace incision
- Stream Profile
- 12 Upper Esk River
- 11 Lower Esk River
- 1 Mangakopikopiko Strm
- 3 Otakowai Strm
- 4 Kaiwaka Strm
- 5 Deep Strm
- 7a Okurakura Strm
- 8b Berry Rd
- 9a Unnamed

Figure 3.6 Terrace profiles and location map for Esk Valley rivers

Profiles are based on interpolated 20m contour data. Note coarse data, particularly in lower gradient reaches.

Due to scatter in sample data, exponential curves have been fitted to sample points to approximate profile form.

Note the prominent discontinuity in the Esk River profile above Island Farm. The Upper Esk River terrace profile has been extrapolated to the mouth of the river to illustrate it's relationship to the Lower Esk River terrace. No evidence for the upper profile has been found downstream of Island Farm.

3.3.3.4 Results

There appears to be a single terrace set present throughout the Esk Valley (Figure 3.6), this is divided by a prominent breakpoint above Island Farm where the profile shallows markedly. While sampling of the surfaces did not provide sufficient data to constrain the age of terrace formation, based on morphology, elevation, the depth of soil formation, and the extent of the terrace surface it is considered very likely that these correspond to the Ohakean age surfaces that are so extensive throughout the east coast. While individual terrace risers were identified locally in the field, the mapping of these surfaces based on 20m DEM data meant these were unable to be resolved, and the surface mapped represents a combination of these, though is mostly representative of the highest, most extensive surface.

Stratigraphy

Only very limited investigation into the terrace stratigraphy was undertaken, and this was hampered by a lack of exposure on the well-rounded topography. Due to the magnitude and nature of sediment input, terraces can be divided into two main groups, those sourced from the Maungaharuru Range, and those sourced in Matahorua Formation gravels.

Terraces sourced from the Maungaharuru Range are broad, particularly north of Berry Road. Only one exposure of coverbeds was identified below a breached irrigation dam north of Berry Road stream. Within this exposure a 2m thick sequence of cross-bedded reworked fine-grained volcanic soil is exposed. The majority of the sequence is, however, likely to be sourced from the range and composed of fluvial silts, sands and limestone cobbles. Based on observations of the bedrock/terrace surface relationship exposed in the cliffs that define the incised stream channels, it is considered unlikely coverbeds adjacent to the channels exceed 10m in thickness. This is backed up by spring and ephemeral stream flows on the terraces that commonly coincide with inferred bedrock highs – indicating perched watertables are able to intersect the surface, and that coverbed thickness is probably therefore significantly reduced by the minor elevation changes (~6m).

While gravel terraces sourced from Matahorua Formation gravels are extensive in the region south of Deep Stream, the only region investigated was in the Trelinnoe study area (Section 4.2). Here there is 10-15 m of silty gravel, which grades rapidly into 3m of fine sandy and pumiceous soil. This is discussed in more detail in section 4.2.

Profile

The grade of terraces in the Esk appears to be controlled by a combination of lithology, stream power, and bedload. This is not surprising considering they are fluvial landforms, and factors controlling their formation are the same as those discussed in Section 3.3.1. While fluvial controls at the time of formation are not studied in depth, an investigation into the profile form provides important insights into processes active in the Esk since the time of formation. The mapping and correlation of individual sample points to exponential profiles also aided correlation within catchments, and enabled anomalous locations to be discarded.

As with the long river profiles, there is a distinct disparity between the profile of terraces in the upper part of the catchments and those below the Deep Stream area. However, in contrast to the long river profiles, terrace gradients in the upper Esk Valley are much lower than those in the lower valley. The most notable disparity is in the Esk River itself where a sharp upstream decrease in gradient corresponds to a general absence of prominent terrace features between Island Farm and the northern end of Waipunga Ridge as well as the lower reaches of Deep Stream. While the reasons for this disparity are not clear, some suggestions are put forward below:

1. *Abrupt change in ratio of sediment size/volume to stream power* – During cool glacial conditions it is likely elevated regions experience much greater rates of mass wasting as temperature fluctuations are greatest. Orographic effects of the Maungaharuru Range may also not have been as strong as more precipitation fell as snow than in lower catchments. This may have lead to an excess sediment supply in the upper catchments producing a low grade aggradational terrace, lower sediment volumes and higher rainfalls from lower catchments could have dramatically increased the transport rate and steepened the terrace profile.

2. *Resistant lithology in channel creating long-standing knickpoint* – The limestone caprock on Island Farm (see Section 4.1.4) may have extended across the Esk River and produced a resistant knickpoint.

3. *Deep-seated landslides to north of Island Farm may have served as permanent sediment sources preventing incision above this point* – Two large landslides immediately north of Island Farm (see Attachment 1, Section 4.1.4)appear to

have moved a considerable distance, and now discharge directly into the incised Esk River channel. If these were active during terrace formation, they may have constantly choked the channel with sediment, and prevented excavation of sediments from the upper catchment. This may explain the lack of a high terrace in Deep Stream as the outlet to this may have been constantly blocked.

4. *Incorporation of gravel clasts into bedload may have increased bedload size* – The incorporation of Matahorua Formation gravels from the lower catchments may have increased the bedload size, and subsequently required a steeper channel grade.

5. *Drainage in upper catchment was initially to east past Lake Tutira* - The elevation of the broad surface around the toe of Purahotangihia is at the same level as the highest level terrace surfaces in the upper part of the Esk catchment, it is therefore possible streams in this part of the catchment initially flowed out past the present day Lake Tutira and the surface is graded to this path.

6. *Terraces indicate increase in regional uplift rate* – As demonstrated by Whipple and Tucker (2002), an initially steady state river profile can display this sharp decrease in gradient if the regional uplift rate increases suddenly. As incision is driven from the mouth of the river system, terraces in the upper catchment can be uplifted without grade modification while the newly adjusted steepened channel profile propagates up through the system. In the case of the Esk this readjustment would have reached the discontinuity point when deglaciation and rapid incision set in, preserving the terrace form.

7. *Post-formation tectonic warping of the terrace profile* – A structure such as the Wakarara Fault (discussed in section 4.3.3) may have locally uplifted terraces in the region of the discontinuity, and the profiles of the lower tributary streams (from Deep Stream down). This should show up as a convexity in the terrace profiles.

Arguments can be put forward for and against each of these cases, and possibly the answer lies in a combination of two or more scenarios. This requires a much more comprehensive investigation of the system.

From the terrace profiles we can confirm we are looking broadly at one, possibly two, periods of prolonged steady-state behaviour within the system. The profiles also show that, during this steady-state behaviour, rivers in the Esk Valley graded to exponential profiles. This helps support the argument for an exponential profile in the Esk Valley rivers today when under steady-state conditions.

Incision

Incision since terrace formation varies throughout the valley, however, it is in general very high. The terrace profile for the lower Esk River can be extrapolated to intersect the present day coastline c.30m above present day sea level, excluding the headwaters of catchments, this is the minimum level seen. Incision is at a maximum in the centre of the Esk Valley beneath the terrace discontinuity where it is around 80m. This level is fairly consistent throughout the mid to upper Esk Valley. Conservatively assuming terrace abandonment at c.18 ka (Litchfield, 2002) this level of incision equates to minimum and maximum average incision rates of 1.7 and 4.5mm/yr – equivalent to rates of 4-7mm/yr identified in the lower reaches of the Mohaka River to the north, and 2-5mm/yr in the mid reaches of the Tutaekuri to the south (pers. comm Litchfield, 2003). The majority of this incision appears to have, however, occurred since the abandonment of the youngest terrace at c.10-11ka (Hammond, 1997; Berryman *et al.*, 2000; Litchfield, 2002), average incision rates since this time are therefore much higher, approximately 3 and 8mm/yr respectively.

The volume of sediment removed since the onset of incision can be calculated by producing a grid surface interpolated from the data points defining the terraces, then calculating the volume between the DEM surface and this interpolated terrace surface. This was undertaken using Golden Software Surfer 8 and provided a volume of approximately $1055x10^6m^3$. Based on a c.10-11ka age of terrace abandonment, this equates to an average sediment flux of 96,000 m^3/yr.

3.3.3.5 Summary

Terrace composition, distribution, and elevation all suggest the features in the mid to lower Esk Valley are Ohakean Terraces related to the last glaciation. Most locations mapped off aerial photos can be correlated with a single terrace set running up through the Esk Valley. While a prominent breakpoint occurs dividing terraces in the upper and lower Esk Valley, the close correlation to exponential profiles indicates the system was probably at or nearing steady state both above and below the breakpoint.

Perturbations since terrace formation must be either on a regional scale, or produce very little elevation change as these cannot be resolved from deviations of terrace data from the exponential profiles.

Incision rates since the abandonment of the terrace surface(s) at approximately 10ka are high, and therefore required a similarly high sediment flux to transport the sediment out of the system.

4 FIELD INVESTIGATIONS

Due to the large scale of the Esk Valley (>250km^2), target areas for a more intensive field investigation were determined in the reconnaissance stage. These were chosen to provide the best representation of the valley geomorphology and active processes, and included a condensed study area 3x1.5km referred to here as the Trelinnoe study area, selected parts of the Maungaharuru Range, and various other locations throughout the valley.

This chapter is divided into three parts in order to best summarise observations, including:

Section 4.1 *Geomorphic domains* provides a comprehensive overview of key aspects of the Esk Valley geomorphology within five separate domains;

Section 4.2 *Trelinnoe Study Area* details observations on fluvial and hillslope geomorphology in a condensed study area. Particular attention is given to morphology and processes relating to four deep-seated landslides identified in this area; and

Section 4.3 *Defect analysis* presents results from a survey of rock mass defects undertaken in the valley.

4.1 GEOMORPHIC DOMAINS

Geomorphic domains are regions in which similar geomorphic characteristics are displayed. These characteristics can include landforms, active processes, and structural controls. Dividing an area into geomorphic domains contributes to the overall understanding of the area by directing a focus toward important geomorphic factors in each domain, highlighting spatial variations in geomorphology, and most importantly enabling the identification of key interactions by observing similar domains that may lack one or more contributors.

The valley can be divided into six distinct geomorphic domains identified in Figure 4.1:

- Waipunga Ridge
- Lower Esk Aggradational Valley
- Tributary domain 1
- Tributary domain 2
- Tributary domain 3
- Maungaharuru Range mass movement

Processes, landforms, and key geomorphic controls are markedly different in each domain, however, crossovers of individual aspects often allows the relative impact of each factor to be considered in the absence of others. The following section discusses observations of key geomorphic processes, controls, and landform morphology in each domain in order to provide an overview of the current geomorphic state of the Esk Valley.

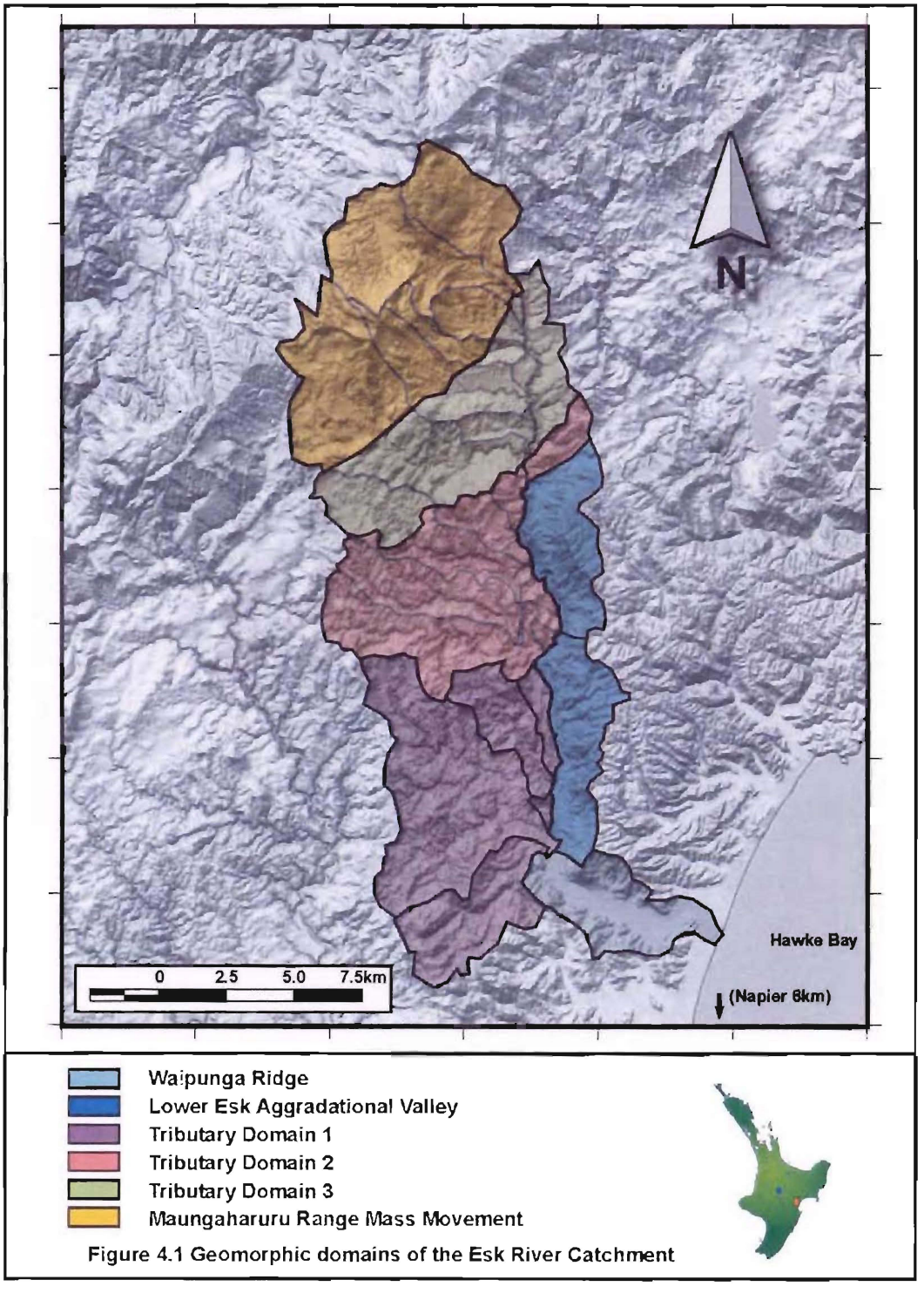

Figure 4.1 Geomorphic domains of the Esk River Catchment

4.1.1 WAIPUNGA RIDGE

This forms the eastern margin of the Esk Valley, the scarp slope presents a topographic barrier that directs the Esk River south to the end of the ridge before turning sharply eastward and running out to the coast. The ridge is on average 200m above the channel of the Esk River, and slopes are steep – around 20°. The spur is capped by a laterally continuous gently eastward dipping sandy limestone which forms the prominent ridge, and plays an important part in affecting the drainage within the domain. Drainage density on the slope face is low as streams run unimpeded downhill into the Esk. Relatively low drainage density on the top of the spur, and stream capture across the ridge indicates a large amount of subsurface flow typical of limestone terranes.

Other characteristic features of this domain are a large rotational landslide at the southern end (1), and a prominent break in slope along the length of the spur corresponding to the level of terraces observed elsewhere in the valley (2).

Figure 4.2 Waipunga Ridge Digital Terrain Model

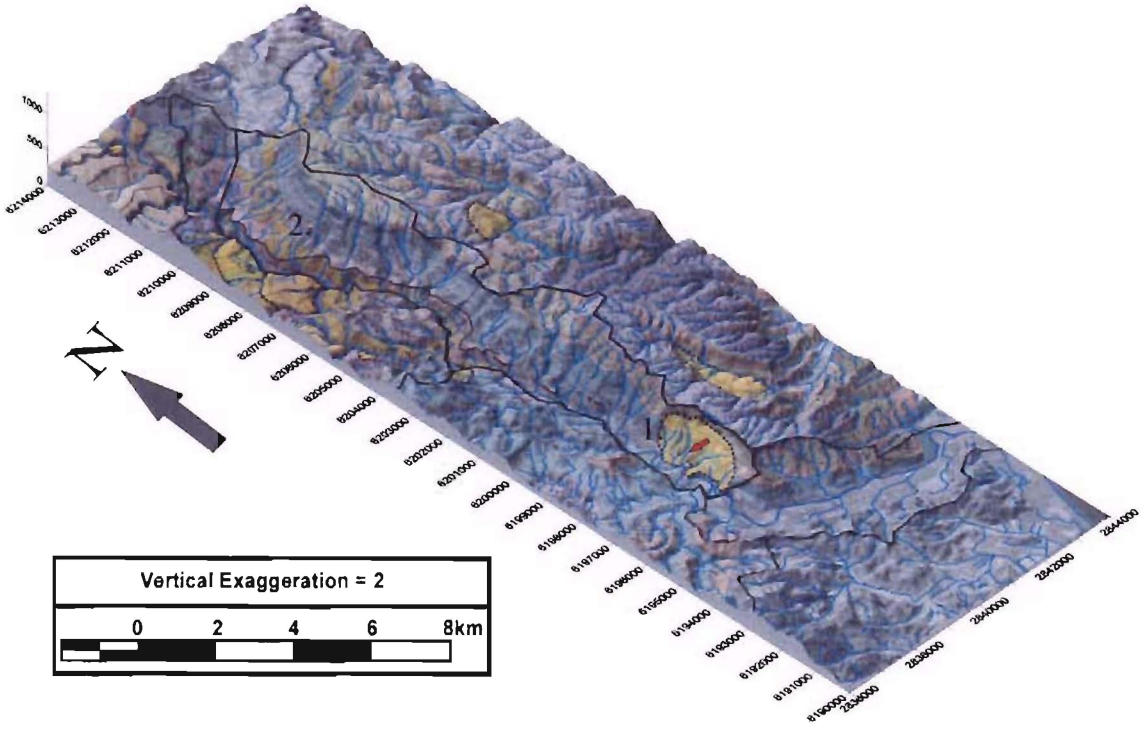

Figure 4.3 Lower Esk Aggradational Valley geomorphic domain DTM
Figure includes detail of the aggradational domain and surrounding area, as well as cross-section through valley fill based on slope profiles and well data.
See Figure 2.6 for full stratigraphic column.

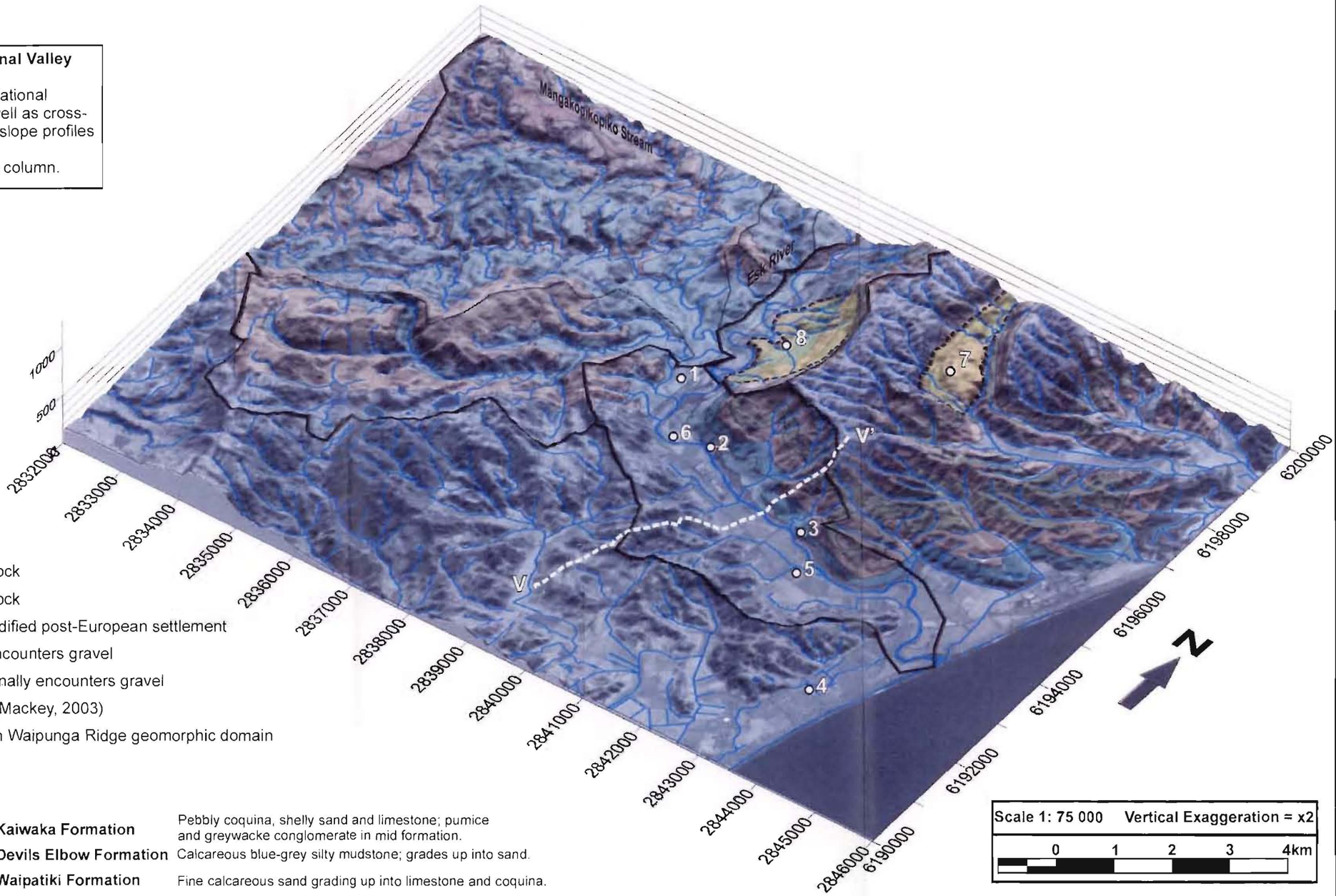

Legend

1. 20m high terrace
2. Channel intersects bedrock
3. Channel intersects bedrock
4. Early outlet channel. Modified post-European settlement
5. Water bore frequently encounters gravel
6. Water bore only occasionally encounters gravel
7. Rocky Basin Landslide (Mackey, 2003)
8. Deep-seated landslide in Waipunga Ridge geomorphic domain

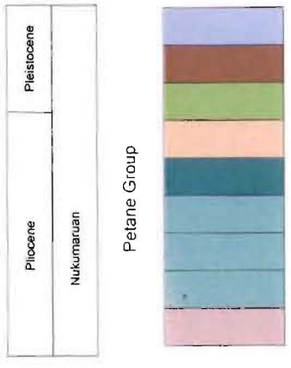

Kaiwaka Formation	Pebbly coquina, shelly sand and limestone; pumice and greywacke conglomerate in mid formation.
Devils Elbow Formation	Calcareous blue-grey silty mudstone; grades up into sand.
Waipatiki Formation	Fine calcareous sand grading up into limestone and coquina.
Te Ngaru Formation	Calcareous blue-grey silty mudstone; grades up into sand.
Tangoio Formation	Fine calcareous sand grading up into limestone and coquina.
Mairau Formation	Calcareous blue-grey silty mudstone; grades up into sand.
Darkys Spur Formation	Laminated fine siliciclastic sand with shell beds and scattered calcareous concretions.
Aroapaonui Formation	Massive blue-grey silty mudstone grades up into fine sand.
Tutira Formation	Poorly sorted greywacke conglomerate, fine sand and silt. Thick pumice near top.

(after Haywick, 1991)

Scale 1: 75 000 Vertical Exaggeration = x2

0 1 2 3 4km

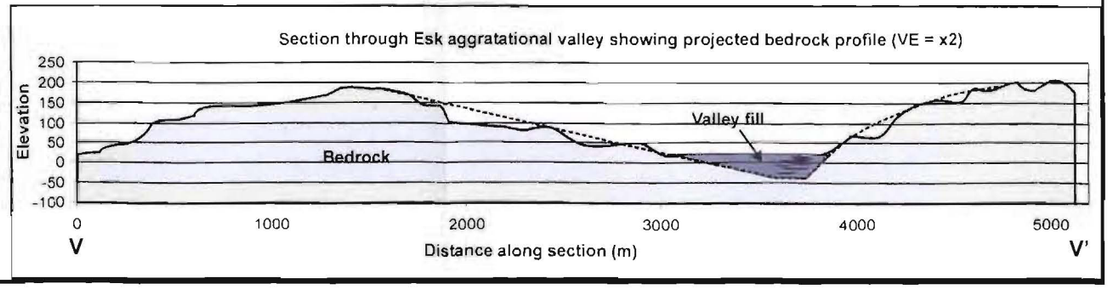

4.1.2 LOWER ESK AGGRADATIONAL VALLEY

The lower Esk River valley consists of a relatively broad alluvial plain (Figure 4.3). This is constrained on the northern margin by steep bedrock slopes of the Tangoio block, an elevated terrain of gently eastward-dipping emergent Plio-Pleistocene interbedded shallow marine limestones, siltstones, sandstones, and conglomerates (Haywick *et al.*, 1991). A relatively low, dissected terrain composed of the same shallow marine strata defines the southern margin of the valley, however slope angles are much lower than those on the northern margin of the domain.

At the upper extent of the domain a broad, 20m high terrace separates Mangakopikopiko Stream from the Esk River (Figure 4.3 (1)). While the valley floor is reasonably flat, the Esk hugs the northern side of the valley, intersecting bedrock twice (2,3). The channel is well defined, and typically 35-40m wide – "within estimates of natural channel width" (Williams, 1986). This is generally around 2m below bank level, the low flow channel meanders within the main channel and is typically incised another 2m. The channel slope is around 0.0025, steep for at least one set of regime equations (Williams, 1986), and over twice the expected grade based on long river profiles (see Section 3.3.1.4). This is likely to be a result of both uplift during the 1931 earthquake, and the redirection of the lower reach, initially south to the estuary (4) (see Section 2.3.3.3) – effectively steepening the channel.

Apart from the broad terrace noted earlier, there is no obvious evidence for the presence of terraces formed as a result of glacial climates. While these would have almost undoubtedly been formed in the valley during these conditions, they may have been eroded as a result of subsequent channel avulsion, buried by aggradation, or lie close to the current valley floor level and require a more detailed investigation to locate.

Preliminary analysis of twelve water well logs for bores deeper than 30m in the valley indicate the bedrock profile beneath the alluvial sediments approximates the extrapolation of slope profiles from above the surface. This suggests the maximum depth of alluvium is c.70m and it is thickest on the northern margin of the valley. Alluvial gravel lenses are apparently only encountered on the northern side, the majority of sediments being silts and clays with occasional sands. The gravel lenses are typically thin (c.2m), and increase in frequency to the east, regularly occurring at c.4m intervals in a bore near the centre of the valley (Figure 4.3 (5)), and only twice (7.5 & 21m) in a 65m bore at the western end (6).

Figure 4.4 Tributary Domain 1 DTM
Figure shows detail of Tributary Domain 1 and main lithological contrasts. Indurated limestones and conglomerates are delineated with darker lines.
See Figure 2.6 for full stratigraphic column.

Localities

1. Prominent conglomerate-controlled dip-slope
2. Eland Landslide
3. Northlands Landslide
4. Eskmount Landslides
5. Deep-seated landslide in upper Matahoura Formation (Grassy Knoll Member)
6. Ponding suggests impermeable conglomerate(?)
7. Extreme sinuosity in streams underlain by conglomerates
8. Linear incised valleys and ridges indicates defect control
9. Steep slopes along western margin of the catchment

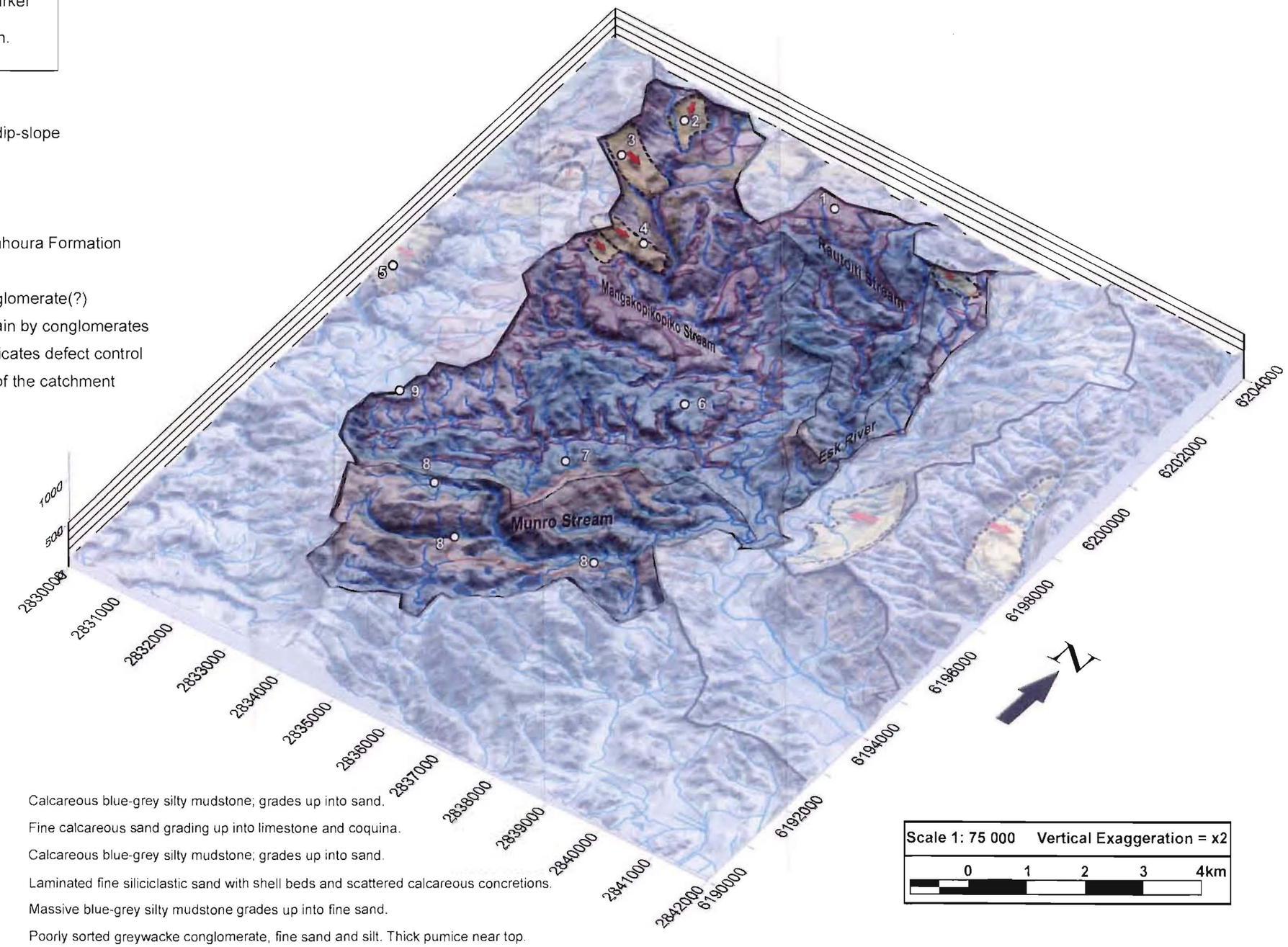

Petane Group

Te Ngaru Formation	Calcareous blue-grey silty mudstone; grades up into sand.
Tangoio Formation	Fine calcareous sand grading up into limestone and coquina.
Mairau Formation	Calcareous blue-grey silty mudstone; grades up into sand.
Darkys Spur Formation	Laminated fine siliciclastic sand with shell beds and scattered calcareous concretions.
Aroapaonui Formation	Massive blue-grey silty mudstone grades up into fine sand.
Tutira Formation	Poorly sorted greywacke conglomerate, fine sand and silt. Thick pumice near top.
Esk Formation	Massive blue-grey silty mudstone, fine sand and pumice layers.
Waipunga formation	Siliciclastic fine sand, rare pumice and silt beds. Scattered calcareous concretions.

(after Haywick, 1991)

4.1.3 TRIBUTARY DOMAIN 1

This is the domain nearest to the lower Esk Valley, and includes landforms that provide a transition from the low relief rolling hills of the Lower Esk Aggradational Valley to highly incised/terraced topography in tributary domains 2 and 3. Figure 4.4 gives an overview of the domain.

While the majority of this domain is comprised of the easily eroded blue-grey silty mudstones of the Esk, Aropaoanui and Mairau Formations, the Tutira Formation conglomerate and thin limestone units in the upper parts of the Petane Group have a strong influence on the topography. Basic geological mapping was undertaken using aerial photos to identify high contrast indurated, erosion resistant conglomerates or limestones. Rapid lithologic changes and strong competence contrasts within this Group produce a characteristically more dissected landscape than that of the Maungaharuru Group.

Essentially a semi-circular basin with short, steep, meandering streams; the outer extents are delineated by short, sharp oversteepened slopes and a prominent ridge. This is almost certainly an effect of conglomerate and limestone cap rocks sheltering underlying lithologies, especially along the northern boundary of the basin where conglomerates have been mapped (Bland, 2001). The contrast in the level of topographic dissection across the drainage divide between the Mangaone River to the west, and Mangakopikopiko Stream in the Esk catchment is likely to be a reflection of more active erosional processes within this domain (Attachment 1). Much shorter stream paths on the Esk side of the divide are likely to provide more efficient sediment transport mechanisms and promote active basin expansion and increased sediment yields. This is evidenced in the large number of shallow failures in the region, particularly along the margins.

There are four deep-seated landslides within the domain, all in the upper part of the catchment. Eland and Northlands landslides (localities 2 & 3) are both situated in the Grassy Knoll Member sandstones and siltstones. This is the same Member as that underlying Trelinnoe and Little Ice-cream slides in Tributary domain 2, as well as another slide to the SW of the catchment (locality 5). Both of these slides occur down-dip and appear to be lithologically controlled. Similar scarp morphologies to the east and west of the Northlands slide suggest similar failures have taken place here, but the sediment has subsequently been totally evacuated by fluvial processes.

Incision increases markedly up the valley, with broad, moderately incised (<40m) sinuous channels in the lower half of the valley, and deep, narrow valleys in the upper reaches reflecting a much more rapid incision. Tributaries to the two main branches of Mangakopikopiko Stream are short and steep, they show a high degree of connection with adjacent slopes, and this is reflected in apparently high sediment loads. Where these tributaries rest on, or have incised through conglomerates, sinuosity becomes tortuous as the tributaries are caught on the indurated lithologies and forced to run above grade.

The presence of these extensive conglomerates complicates the mapping of river terraces as they dip close to the ancient stream grade in its lower reaches, and appear to have trapped the channel on this surface. This probably forced the stream to begin a broad meander pattern, and is the reason for the very broad surfaces we see in this catchment today. The conglomerate steepens in the head of the catchment this would have forced the stream to straighten and incise more rapidly-producing the steeper slopes and narrower valley we see today.

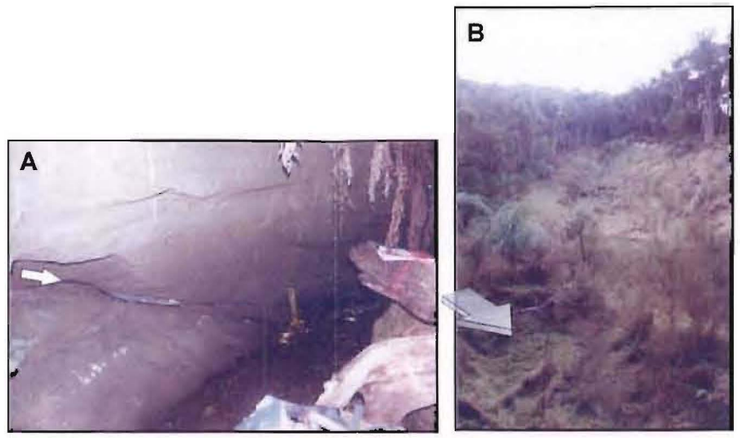

Secondary landslide in Deep Stream
Both photos are taken looking north, photo A is located around ~30m upstream of B, and illustrates a landslide failure surface crossing sub-horizontal bedding, and dipping at around 30° below the stream bed (note geological hammer for scale). Photo B illustrates a shallow, relatively recent failure around 60m in height. The mass is moving down the hill at an angle of around 60° and is probably related to the failure surface shown in A. The arrow indicates the approximate relative orientation of photo A. This is typical of a number of "small" secondary failures identified in Deep Stream.

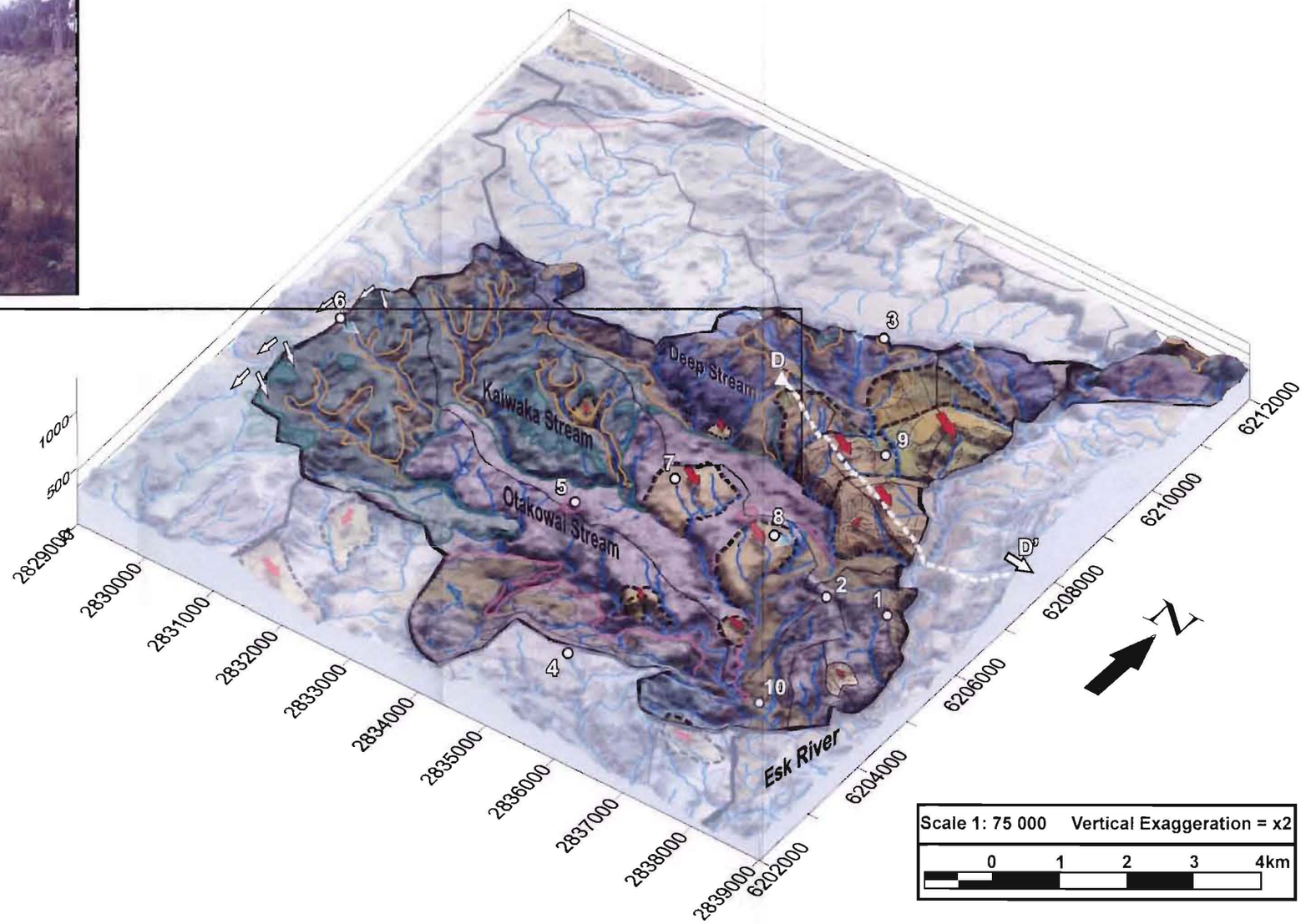

Localities

1. Sharp defect or fault controlled ridge
2. Limestone cap on Island Farm
3. Wind gaps
4. Steep conglomerate controlled ridge (100-150m relief)
5. Good stream correlations may suggest drainage capture
6. Conglomerate capped "grassy knoll"
7. Trelinnoe Landslide
8. Little Icecream Landslide
9. Deep Stream landslide complex

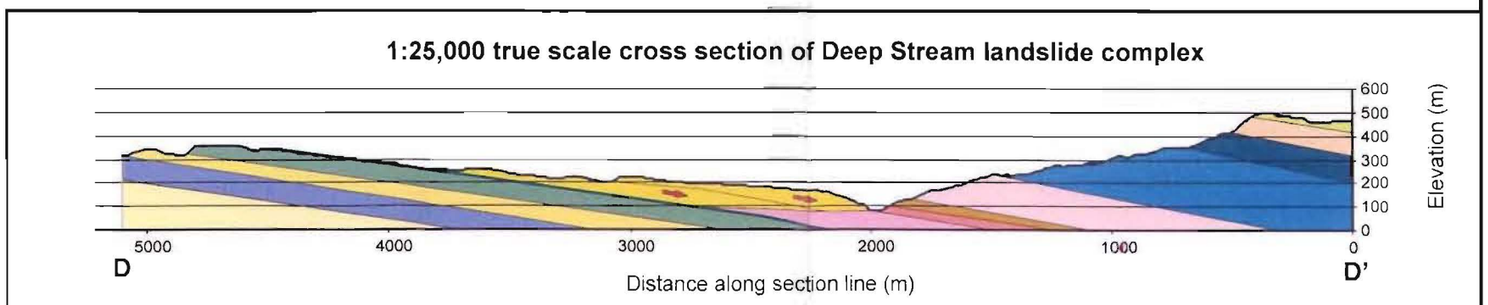

Figure 4.5 Tributary domain 2 DTM
Figure includes detail of Tributary Domain 2, true scale cross section of landslide complex north of Deep Stream, and field evidence for parasitic slides and bedding plane shear. See Figure 2.6 for stratigraphic column.

4.1.4 TRIBUTARY DOMAIN 2

This domain includes Otakowai, Kaiwaka, and Deep Streams, as well as the first of the unnamed streams in the Esk catchment. Much of the domain is included in the Trelinnoe Study Area and is discussed in detail in Section 4.2, this section will concentrate on relevant features of the domain outside of the detailed study area. These include the landslide domain to the north of Deep Stream, and structural control and morphology of the surrounding area.

The 3.8km^2 landslide complex (Figure 4.5 (9), and cross-section D-D') is one of the most prominent features in the domain. Extensive bedding-controlled dip-slopes to the west indicate source areas for the adjacent landslides. The dip-slopes are controlled by Papariki Member conglomerate, however, the basal failure may in fact coincide with one of the thin tuffaceous horizons within the overlying Grassy Knoll Member, similar to that found at the Trelinnoe slide (7) (Section 4.2.3.1). While the subdued morphology of the slides does not suggest current activity, the toe of the southernmost slide shows some strong relief, and is considered the most active failure in the complex. The base of this failure is likely to be very close to the uncemented sandstone horizon that is inferred to form the failure surface to the Little Icecream slide (8) (see Section 4.2.3.2).

Considering the scale and orientation of the southern slide, it is likely it would have had a major influence on the development of Deep Stream. Indeed it is possible that a landslide dam event may have blocked the drainage, the knickpoint found upstream at the domain boundary may be a result of such an event.

A recent lateral failure shown in Figure 4.5 A and B may be due to increasing stresses along the margins of the landslide complex as a result of differential motion within the slide. This would indicate the slide complex continues to creep slowly. The lateral failure is associated with a prominent terrace surface. Approximately 20m high at its maximum upstream extent, the terrace dips steeply downstream (~15° below local stream grade) for c.1km. Such terraces were not observed in other streams within the domain, and the location, form, and very large debris clasts within the terrace suggests it may have been formed as a result of a dam generated by one of these secondary lateral failures.

Along the western margins of the domain, possible wind gaps and a strong correlation between the location of streams on either side of the divide (Figure 4.5 locations 3&6)

suggest strong structural control or stream capture. These features lie above the current level of the extensive upper terrace surface (see Section 3.3.3), and apparently relate to a drainage system present prior to terrace formation. If these are related to a stream capture event, the fact streams have been captured by drainages in Pohue Formation sandstone may indicate a much greater incision rate in this lithology.

Island Farm is located in the SW corner of the domain, and is an isolated limestone capped hill (2). An abundance of landslides on this feature suggest it is currently geomorphically active, and is yet to reach the degree of stability attained by the rest of the catchment. While the limestone cap cannot yet be correlated to units elsewhere in the basin (pers. comm. Bland, 2003) it is posible it once stretched across the present Esk River, and has been "holding up" the area. Similar terrace elevations, and an isolated basin within the block support a complex drainage history, and suggest stream flow during Ohakean times may have been around either side of the "island". The close proximity to the Deep Stream landslide complex, as well as unusual features such as the limestone cap, the internal basin, and a strong lineament that terminates in a discordant lithology in the Esk River (1) means the possibility of this being a large bedding controlled landslide, similar to those in Deep Stream cannot be ruled out.

Localities

1. Remnant bedrock ridges indicate strong NE-SW defect control
2. Highly sinuous channels displaying only limited incision. Dominant meander orientation matches inferred defect orientation from locality 1.
3. Major increase in incision.
4. Broad surface with moderate slope dips down to stream channel.
5. Probable landslide shows strong defect control about it's margins.
6. Conglomerate -controlled ridge above Berry Rd.
7. Angular meanders in sinuous streams.
8. Catchments extend up to Maungaharuru Range.
9. Strong lineaments on terraces consistently step down toward stream locations
10. Remnant bedrock ridge to north of Berry Rd. Stream may indicate prior terrace surface.
11. Lineaments step down from both the NW and SE to form probable NE trending paleo-channel.

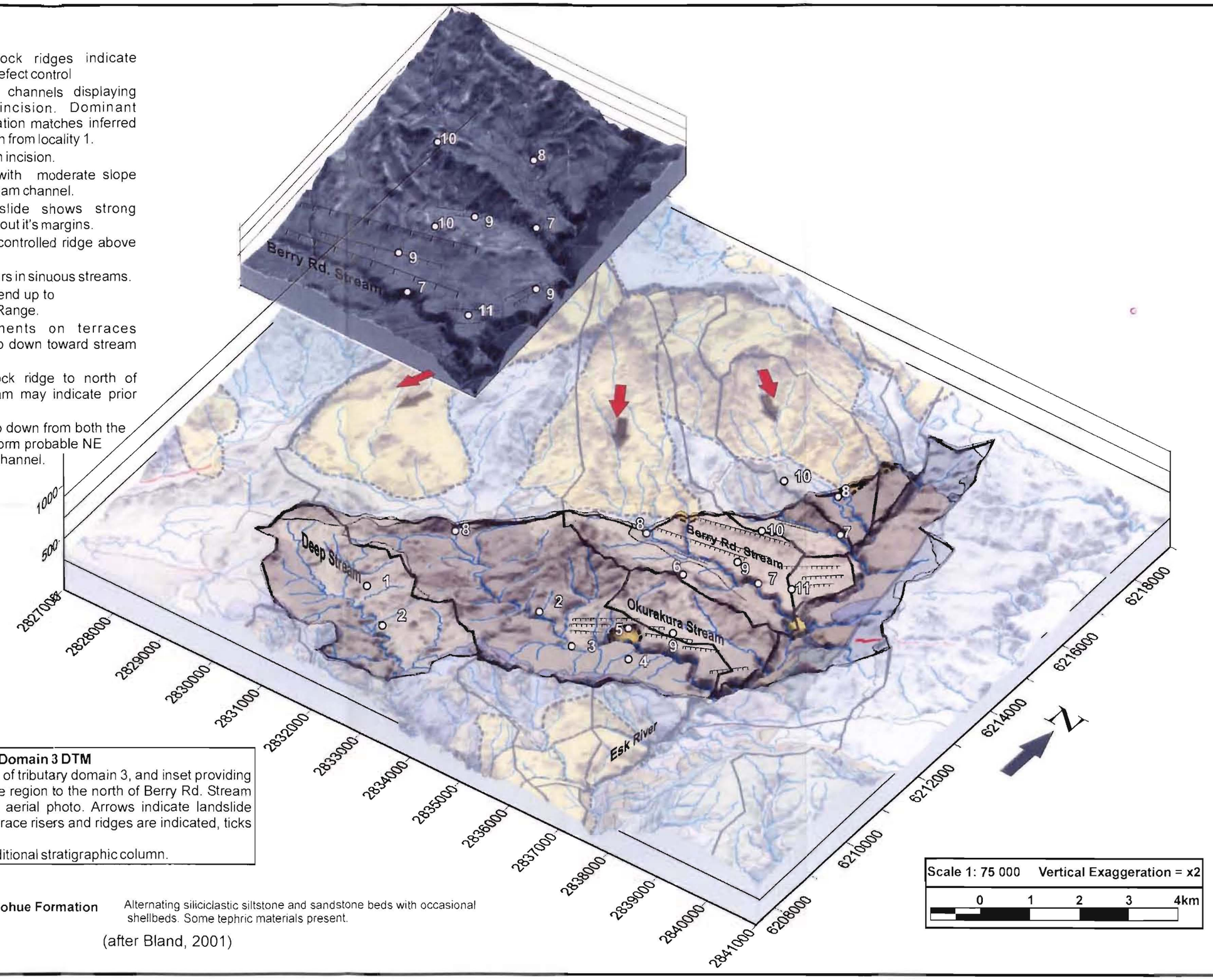

Figure 4.6 Tributary Domain 3 DTM
Figure includes detail of tributary domain 3, and inset providing additional detail of the region to the north of Berry Rd. Stream based on a rectified aerial photo. Arrows indicate landslide movement. Linear terrace risers and ridges are indicated, ticks are on the scarp side.
See Figure 2.6 for additional stratigraphic column.

Pohue Formation Alternating siliciclastic siltstone and sandstone beds with occasional shellbeds. Some tephric materials present.

(after Bland, 2001)

4.1.5 TRIBUTARY DOMAIN 3

This domain incorporates the section of the Esk catchment entirely underlain by alternating sandstones and siltstones of the Pohue Formation. The homogeneity and low resistance to weathering of these sediments is probably responsible for the characteristically low relief, little dissected terrain. This is also the only domain to derive sediments and streamflows directly off the Maungaharuru Range. Prominent features include the ridge south of Berry Road, the most extensive terraces in the valley, and low amplitude, highly angular, sinuous stream channels, and many linear terrace risers.

Deep Stream is the only catchment in the domain not to be sourced from the Maungaharuru Range. The upper part of this catchment shows strong evidence of defect control both in NE trending low, linear ridges, and a similarly oriented strong meander pattern (Figure 4.6 1&2).

To the north of Deep Stream, Okurakura Stream lies in a typically broad, low relief valley. Like Deep Stream, the sinuous channel in upper reaches shows strong defect control. A knickpoint approximately halfway along the reach (3) marks a transition from this highly sinuous form to a more typical highly incised channel.

Strong lineaments are present on the terraced surface around Okurakura and Berry Rd Streams, as well as the unnamed stream immediately to the north of these (9,11). Orientations of the lineaments change, apparently depending on the orientation of the adjacent stream reach, and each marks a rise of over 5m away from the current main stream channel. These were mapped by Black (1991) as fault traces, and while their strongly linear nature suggests this may be the case, the consistency of the rises away from stream channels suggests it is unlikely displacement observed across each of the lineations is related to tectonic activity, and is rather an effect of stream erosion. It is probable that they were initially formed by tectonic processes as defects in the rock mass, and have subsequently been enhanced by stream processes. The orientation of defects exploited therefore depends on the orientation of the particular incising channel.

A prominent ridge south of Berry Road Stream (6) forms the divide between this and Ohurakura Stream catchments. The ridge is capped by a continuation of Matahorua Formation greywacke conglomerates, a prominent band of which can be seen extending to the NE from below Purahotangihia at the top of Waipunga Ridge.

Streams in the domain are characterised by a highly angular sinuosity (7,2), this is particularly evident in Berry Rd. Stream. While the pattern is not clearly apparent on the DTM, the aerial photo in Figure 3.1 provides clear evidence. The magnitudes and orientations of the strongest meanders can be correlated from stream to stream suggesting the principal control is infact persistent defects. The angularity is greatest in upper reaches of the streams, possibly a result of increasing defect concentrations and/or persistence during the propagation of incision up the channels.

With a lack of mechanical contrast between lithologies within this domain, landscape form appears largely defect controlled. Lineaments on terraces are strong, streams are angular, and ridges commonly match defect orientations. It is difficult, however, to determine whether this evidently strong defect control is purely related to a lack of lithological contrast, or whether tectonic influence – and therefore structural control – is in fact stronger in this domain than elsewhere in the catchment.

Figure 4.7 Maungaharuru Range Mass Movement geomorphic domain DTM
Figure includes detail of the Maungaharuru Range Mass Movement geomorphic domain and adjacent deep-seated failures as well as location of cross-sections given in Figure 4.11. Red arrows indicate landslide movement, white arrows delineate an arcuate graben inferred to indicate extension into the basin. Broken white lines are inferred "in-situ" outcrop of Te Waka limestone.
See Figure 2.6 for full stratigraphic column.

Localities

1. Southern landslide
2. Central landslide complex
3. Northern Landslide
4. Large basin on top of Maungaharuru Range
5. Very large rotational failure
6. Erosion at toe of slide currently faster than sediment is contributed
7. Beheaded streams
8. Te Pohue Landslide
9. Limestone carapace
10. Exhumed bedding surface

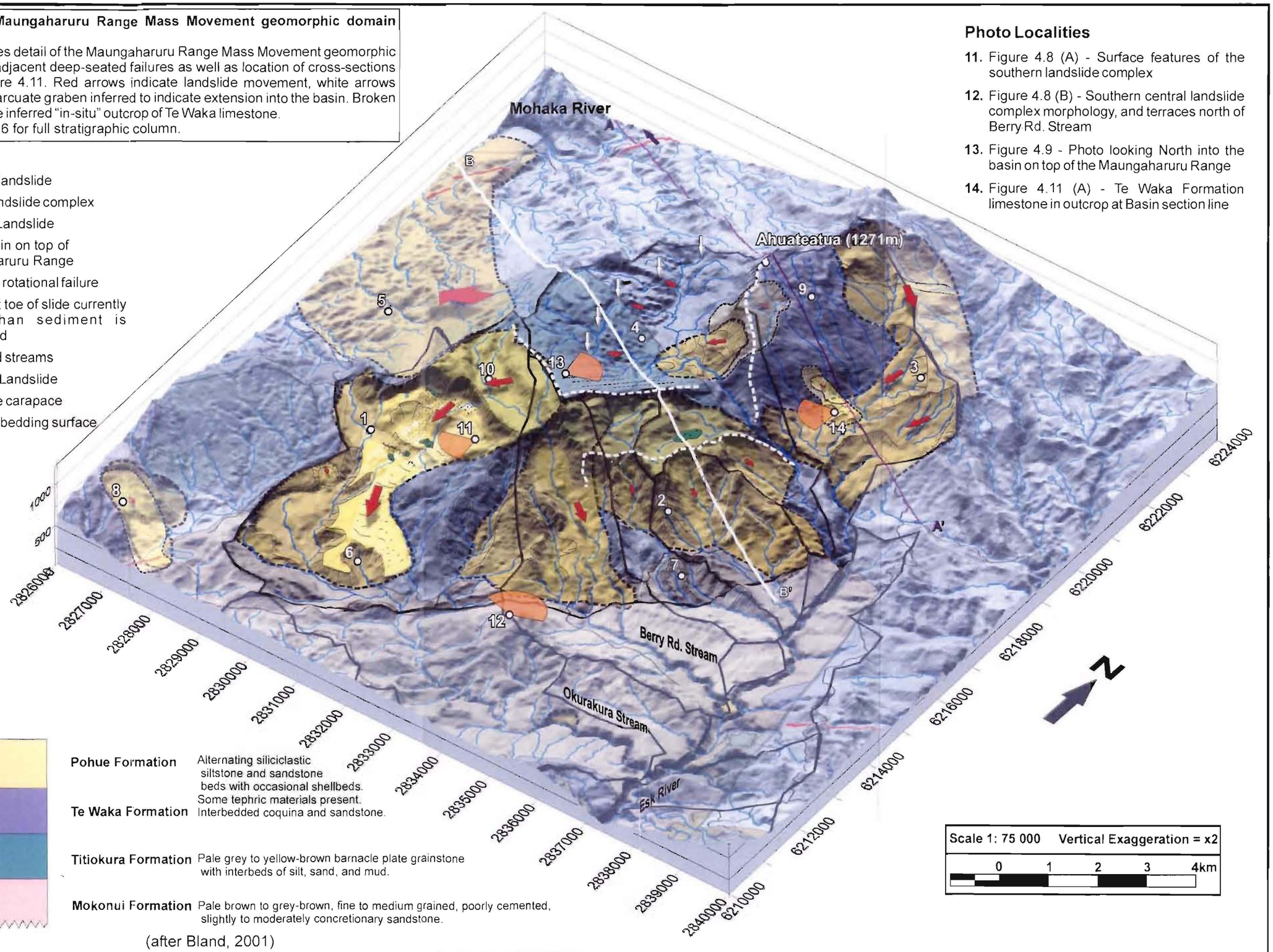

Photo Localities

11. Figure 4.8 (A) - Surface features of the southern landslide complex
12. Figure 4.8 (B) - Southern central landslide complex morphology, and terraces north of Berry Rd. Stream
13. Figure 4.9 - Photo looking North into the basin on top of the Maungaharuru Range
14. Figure 4.11 (A) - Te Waka Formation limestone in outcrop at Basin section line

Maungaharuru Group
Waipipian
Opotian

Pohue Formation Alternating siliciclastic siltstone and sandstone beds with occasional shellbeds. Some tephric materials present.

Te Waka Formation Interbedded coquina and sandstone.

Titiokura Formation Pale grey to yellow-brown barnacle plate grainstone with interbeds of silt, sand, and mud.

Mokonui Formation Pale brown to grey-brown, fine to medium grained, poorly cemented, slightly to moderately concretionary sandstone.

(after Bland, 2001)

Scale 1: 75 000 Vertical Exaggeration = x2

0 1 2 3 4km

4.1.6 MAUNGAHARURU RANGE MASS MOVEMENT

This upland part of the catchment is characterised by very steep slopes, rapid erosion, and very large landslide complexes. Morphology is dominated by the presence of these landslides which extend to the limestone lined basin at the summit of the range. Very large limestone blocks (>1000m^3) are incorporated into the hummocky terrain of the large slides, which mostly appears to be composed of mobilized sandstones and siltstones.

There are four separate landslide complexes within this domain, each having an area of approximately 6km^2. Surface features within the landslides are consistent with those of translational slides; gradients are relatively linear, transverse ridges are common, and there is little evidence of back-tilting. These degrade into earthflows as material becomes increasingly chaotic downslope.

Morphology of the southern landslide (Figure 4.7 (1), Figure 4.8-A) suggests it is an active translational failure and that the material is accelerating downslope. Beneath the main headscarp, very large limestone blocks (>30m^3) form a tract down the centre of the slide, the volume of the individual blocks decreases downslope as they are broken up and incorporated into the mass. The blocks are highly disjointed, show no preferred orientation, and are not considered to be in contact with the principal failure surface, but rather are embedded in the mobile landslide mass.

Swamp areas on the slide currently act as sediment traps, and indicate a perched watertable and localised areas of backtilting. A lake may have existed in the upper region of the slide (in the basin above the prominent graben), and appears to have breached rapidly (Figure 4.8-A). The toe of the slide is highly eroded, indicating a long-term – though not permanent – dominance of fluvial processes.

The central slides (Figure 4.7 (2), Figure 4.8-B) are located in steep, relatively narrow gullies. Debris within the slides shows little topographic irregularity related to slide movement, and appears to have been substantially reworked by fluvial processes. The individual slides appear to have consisted of multiple regressive failures, however have now receded back to an indurated limestone ridge, and as a result, activity is confined to surface failures.

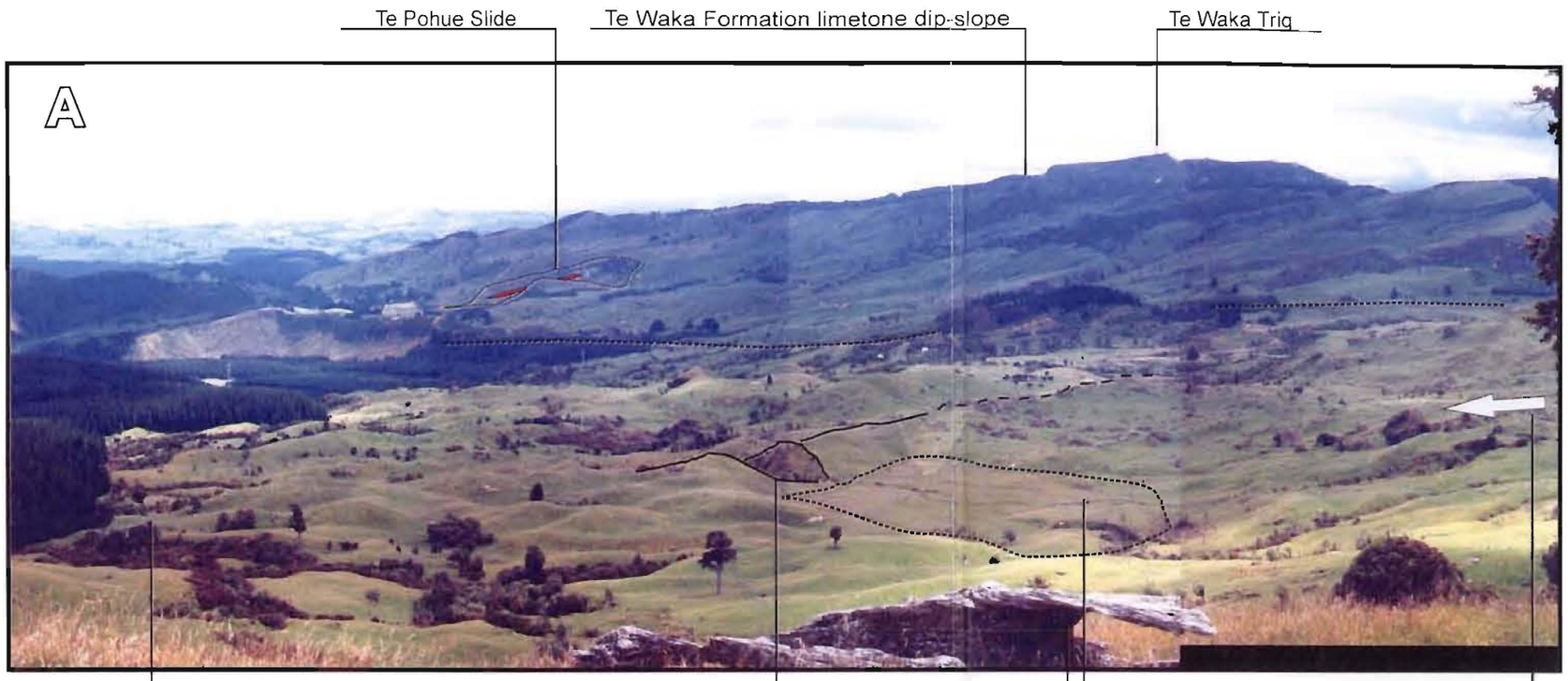

Figure 4.8 Photos of southern and central landslide complexes on the Maungaharuru Range detailing key morphological characteristics

Photo locations are given in Figure 4.7. Photo A is taken looking SW across the southern landslide toward Te Waka Trig; Photo B is taken looking NW-NE from the western end of the prominent conglomerate capped ridge in Tributary Domain 3

Further description of each photograph is given below:

A. The approximate location of the SW margin of the slide is indicated by the broken black line in the farground. Topography on the landslide is chaotic, but slope elements are all remarkably well rounded as a result of the thick tephra and colluvial blanket. Exceptions to this are the limestone blocks that form a tract accross the centre of the image, and the gully cut at the outlet of the lake. This lake is considered a high prioroty for future trenching as it appears to have been a long-term feature, and have breached relatively recently, offering the possibility of investigating current activity on the slide.

B. This shows the southern slide in the central landslide complex and it's relationship with the broad terraces in the region of Berry Rd. Stream. Note the contrast between the dissected topography on the landslide surface and the broad terraces with a single, well defined, highly incised channel. Also note the lack of obvious colluvial material where the "toe" of the landslide may be expected. This may have been removed by fluvial activity, or the majority of displacement may be taking place on upper slopes of the slide, with fluvial activity being an important process in the transport of material downslope.

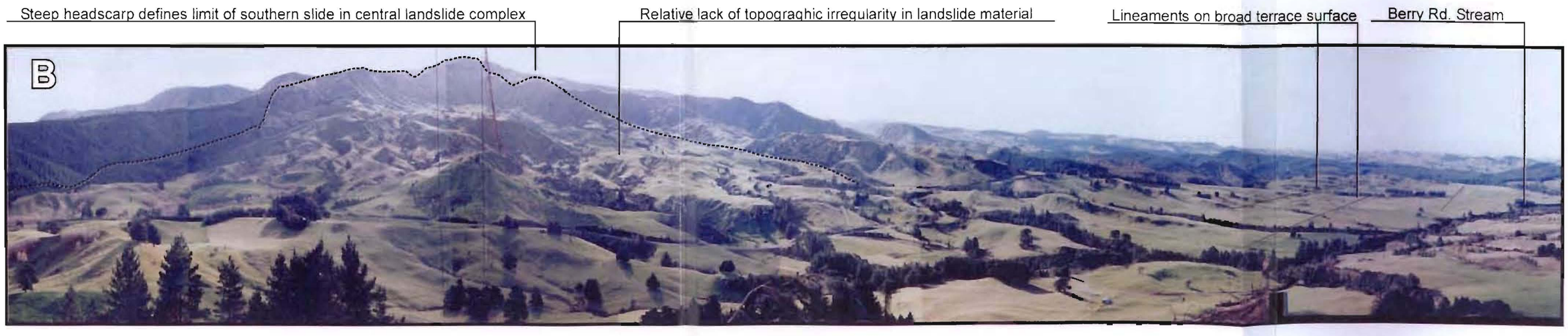

The plateau at the head of these central slides, while marked as landslide area, is not incorporated in the slides. It is, however, being affected by the reduction in lateral confinement, substantial subsurface fluid flow, and destabilisation due to the regressive slides. Sinkholes ~20m in diameter immediately behind the ridge indicate sediment entrained in groundwater is being transported through open subsurface fractures resulting from rockmass dilation parallel to the ridge. There is a high probability of failure associated with the continued relaxation and opening of these fractures. Back from the ridge, swamps reflect poor drainage and subsidence in the area.

The basin on the top of the Maungaharuru Range (Figure 4.7 (4), Figure 4.9) covers an area of 9km^2 and provides baseflow to the Esk River. The basin is lined with highly fractured, disjointed Te Waka Formation limestone that indicates widespread gravitationally induced disturbance. An arcuate extensional graben indicates block movement into the basin. Similarly, defects along the eastern margin indicate stress relief perpendicular to the adjacent scarp. A landslide, possibly related to a larger rotational failure, may have once dammed the outlet to the basin, forming a lake and substantially reduced base flow in the Esk River.

Figure 4.9 View looking north into the basin on top of the Maungaharuru Range

Ahuateatua Peak stands in the centre of the image, the location on the photograph is given in Figure 4.7. The sharp elevation contrast between Te Waka Limestone that forms the ridge below Ahuateatua Peak, and the same limestone unit lining the basin in the foreground (300m below the peak) is clearly evident in this figure. Other notable features include: a large landslide that may have temporarily blocked basin drainage (1); possible lake sediments (2); an arcuate graben indicating bedrock extension into the basin (3); and blocky, dissected Te Waka limestone inferred to be sliding downslope (4)

To the north of the basin is a Ahuateatua Peak defined by a carapace of in-situ Te Waka limestone (Figure 4.7 (9)). The limestone is being undermined along the eastern margin, adjacent to the north slide. This has produced a low (<20m), but angular scarp where the limestone cap has been removed, and now exposes a softer underlying sandstone lithology. Defects visible parallel to the scarp indicate further gravitational relaxation of the rockmass, and fragmentation of the caprock. Regressive failures where the underlying lithology has been exposed are testament to the much lower strength and weathering resistance of the underlying siltstone.

The north slide (Figure 4.7 (3)) is characterised by relatively subdued relief, and evolved, hummocky topography. This is indicative of a slow-moving earthflow. A linear graben near the top of the slide may be fault controlled, or indicate a spatial variation in the movement rate of the earthflow. The lower part of the slide can be divided into two more rapidly moving earthflows, these appear to be separated by a strong bedrock or fault-controlled ridge.

4.1.6.1 Structural analysis

The tectonic and structural process(es) responsible for shaping the southern Maungaharuru Range and driving the large landslides in the domain are not clear. The range forms part of a 50km long linear ridge, defined largely by limestones of the Te Waka and Titiokura Formations (Figure 4.7, Attachment 1). The Maungaharuru section, however, stands anomalously high; Ahuateatua Peak is 200-300 m higher than the linear ridges of the same c.80 m thick Te Waka Limestone that run to the NE and SW of the range.

Beneath Ahuateatua Peak, strata is folded uncharacteristically tightly to form the NE quadrant of NE-SW elongate dome. The folding displaces strata approximately 2km east from the main strike ridge of the range into the Esk Valley. Te Waka limestone forms a carapace over the structure, and the morphology of this section of the range is entirely bedding controlled (9). A steep scarp to the southwest divides the Te Waka limestone from a basin lined with the same unit to the southwest (Figure 4.7 (4), Figure 4.9) (pers. comm. Bland, 2003). The limestone to the east of the basin is once again displaced eastward from the dome structure, this time sharply, and by around 1km. Landslides disguise bedrock outcrop at the southern end of the range, however limestone at the southern end of the basin dips gently to the north-east, contrasting strongly with the steep south-easterly dip of beds on the Te Waka Range to the south. The limestone in the basin also projects between

1.3 and 2km further eastward than that on the Te Waka Range, as this must dip below the Pohue Formation at the foot of the range, it must have been displaced at least 1.3km, probably up to 2 km to the east.

A number of investigators have attempted to explain the structural morphology of the range, however, hypotheses to date are inconclusive. Francis (1991) mapped the area in a reconnaissance investigation prior to seismic surveying being undertaken. He infers the Titiokura Fault Zone to run in a NW-SE direction in the location of the SH5 cutting; Ahuateatua is to have been emplaced by an eastward dipping thrust fault (the Taraponui Thrust) which divides the peak from the basin, and a continuation of the Ngatapa Syncline, mapped to the north of the range, extends into the basin and is responsible for the synclinal form of strata within basin.

Studies undertaken since by Cutten (1994) and Bland (2001) challenge this view somewhat as in their investigations the Taraponui Thrust is not mapped, and the Ngatapa Syncline is inferred to be located well to the west of the basin, and other structures mapped by Francis (1991) on the eastern side of the range have been suggested to in fact be based on displaced landslide material.

Only dat tapes produced from the seismic survey across the range following Francis' investigation (EC91 5,6&7 – see Attachment 3) are available. The processing of these is time consuming, and beyond the scope of this study. However, an initial report by Wylie (1993) based on these lines infers a NNE trending cross fault along the foot of the range. NW trending strike-slip faults at either end of this cross fault are inferred to accommodate displacement on this structure, although it appears no faults are evident in the lines (see Frontier, 1995). A basement high at 400m below sea level is interpreted below the main ridge on the eastern side of the range, within the region bounded by these faults. A later report based on the same survey data (Frontier, 1995) gives a surprisingly different interpretation for what is presumably the same horizon (the "Top Cretaceous Unconformity"). This shows no faults, and an unconformity that dips at twice the angle of the previous report. The variation in interpretations may indicate data from the seismic surveys is of particularly poor quality, and interpretations are therefore uncertain.

Irrespective of the actual structure(s) contributing to the form of the range, a number of factors are evident:

- The form is tectonic in origin, and a result of tectonic activity since the deposition of the Waipipian Te Waka Formation Limestone (3-3.6Ma) which shows no significant variation in thickness over the entire range,
- Limestone within the basin was once continuous with the same units now forming Ahuateatua Peak, pesently 300m higher,
- Structures that displace limestone in the region of the southern and central landslide complexes east from the strike of the corresponding units on the main rangefront are likely to be discrete and trend/strike NW,
- The blocky, disjointed limestone within the basin has experienced much more deformation than the intact beds forming the peak,
- Active landslides on the slopes of the range surrounding the basin indicate this region is currently far more geomorphically active than the in situ strata surrounding the adjacent Ahuateatua Peak;
- Seismic reflectors beneath the range may be extremely poor, unusual for the bedded sedimentary strata underlying the range.

As the steep scarp on the SW side of Ahuateatua Peak prevents a traditional syncline/anticline pair from fitting this situation, and the basin limestone displays a much higher degree of disruption and deformation than that on the peak, it is inferred this limestone was initially at the level of Ahuateatua Peak, and the range was in the form of a NE-SW symmetric tight anticline. The southern end of the anticline is inferred to have had a similar form to that of Ahuateatua Peak; this is based on an exhumed bedding surface above the headscarp on the southern slide indicating an area in which large limestone blocks appear to have been excavated through bedding-controlled slip (Figure 4.7 (10)). As stream power here is low with no catchment, the most likely mechanism for removing these blocks is through translational landsliding on a weak horizon within the limestone unit, similar to the style of failure seen within the same Te Waka limestone at the Te Pohue slide (see Section 2.2.2.6). This would require at least a moderate southerly dip – opposite to the northerly dip observed today.

Additional deformation of the basin limestone is inferred to have occurred as a result of the subsequent subsidence or downwarping of the unit into the basin. In order to accommodate this, either the compressional tectonic regime must reverse and be locally extensional, sediments beneath the basin must have reduced in volume, or the range must have expanded laterally. As the first two mechanisms are considered highly unlikely, the third is the preferred option.

The cross-section in Figure 4.11-B indicates profiles of the Te Waka limestone across Ahuateatua, and through the basin at a location 2.5km to the south (the location of these is given in Figure 4.11-C and Figure 4.7). While the prominent arcuate scarp in the shaded relief map (Figure 4.11-C) appears typical of a rotational failure, the presence of the steeply dipping in-situ Te Waka limestone in Figure 4.10-A indicates sediments east of this scarp are infact in-situ – excluding this possibility. In order to match the limestone bed photographed with the corresponding unit in the basin, it must be extrapolated west in a tight anticline (blue shaded region in Figure 4.11-B).

4.1.6.2 Deep-seated gravitational slope deformation hypothesis

Introduction

This investigation puts forward the suggestion that a **"deep-seated gravitational slope deformation"** (DSGSD), as described by Agliardi *et al.* (2001), may be a viable means of describing some of the structural complexities evident in the Maungaharuru Range, and provide for a driving mechanism to initiate the large failures present along the eastern margin of the range. Little is known about these phenomena, however, Agliardi *et al.* (2001) suggest some useful diagnostic features include:

- Morpho-structures (doubled ridges, scarps, counterscarps, etc.) similar to those observable, at a smaller scale, in cohesive soils landslides,
- Size of the phenomenon comparable to the slope,
- Present day low rate of displacement (mm/y, in alpine and prealpine areas); and
- Presence of minor landslides inside the deformed mass and ancient collapses of the lower part of the slope.

(Agliardi *et al.*, 2001)

The DSGSD inferred here is in the form of a large rotational landslide. However, the high confining pressures involved at depths of up to 2km result in a plastic deformation of the entire sliding mass, significantly changing the distribution of strain throughout the slide.

In a in "typical soil mechanics" approach to rotational failures, a failure ellipse is described through the base of the sliding mass. This represents a discrete shear surface formed as stress localises along this plane, material within the slide is then dealt with as a rigid (brittle) block. Gravity forces driving and resisting sliding are then balanced taking into account friction in the failure plane, and a factor of safety value is obtained to describe the stability state of the mass. However, in a collapse of the scale evident here, confining pressures acting on the sediments are extremely high (<50MPa); this has been shown to cause a change in the behaviour of sediments when placed under lateral loads, altering the style of deformation from brittle to ductile. The transition has been described in chalk at pressures over 30MPa by Leddra et.al (1993), and in London Clay at over 10MPa by Petley and Allison (1997). While results of these investigations were obtained under lab conditions and cannot be directly applied to field situations, they do provide an analogue to describe the behaviour of material at depths in the order of 100-250+m (Petley, 1996). This effectively invalidates the "rigid block" approach to analysing landslides at this scale.

In a ductile deformation, once interparticle bonds in the material are broken and the initial elastic phase of deformation is overcome, the material reaches a steady state plastic deformation phase where it cannot sustain increases in load, but also cannot strain weaken further. In this situation strain is distributed throughout the mass, and the slide can undergo a prolonged period of very stable creep at constant stresses (Petley and Allison, 1997).

Agliardi *et al.* (2001) used an elasto-plastic material model to describe fractured schistose phyllites when modelling a DSGSD in the Rhaetian Alps, Italy (Figure 4.10). This lithology has a Young modulus considerably higher (11GPa) than average siltstones (~5GPa), though otherwise mechanical properties are similar. The phyllites may therefore be expected to behave similarly, though exhibit less elastic or plastic deformation than sediments in the Maungaharuru Range.

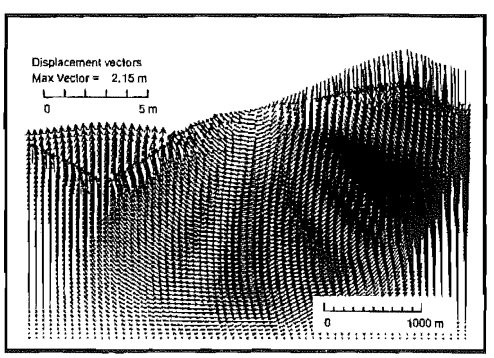

Figure 4.10 Elasto-plastic deformation modelled for a DSGSD in Phyllite (Agliardi *et al.*, 2001)

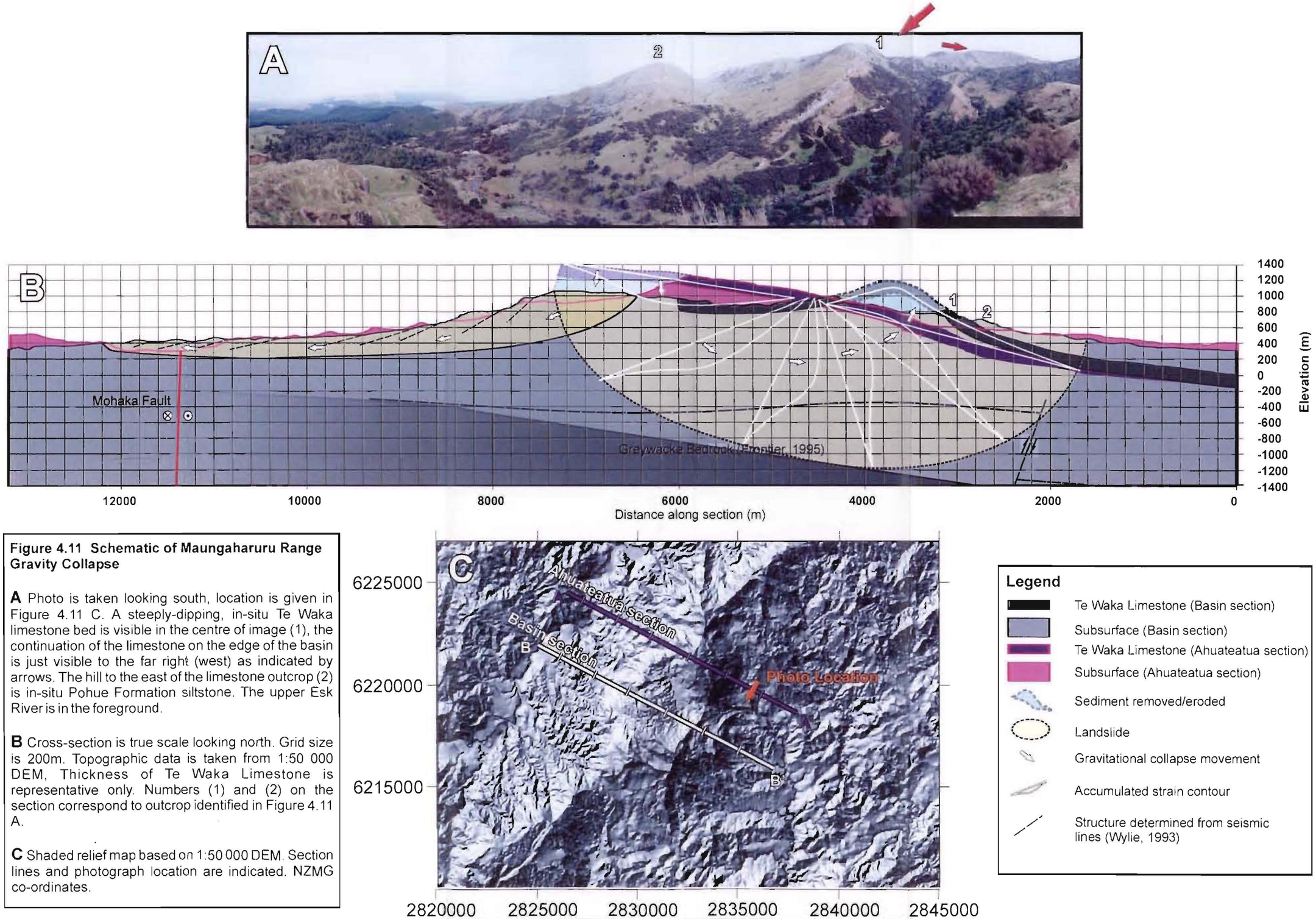

Figure 4.11 Schematic of Maungaharuru Range Gravity Collapse

A Photo is taken looking south, location is given in Figure 4.11 C. A steeply-dipping, in-situ Te Waka limestone bed is visible in the centre of image (1), the continuation of the limestone on the edge of the basin is just visible to the far right (west) as indicated by arrows. The hill to the east of the limestone outcrop (2) is in-situ Pohue Formation siltstone. The upper Esk River is in the foreground.

B Cross-section is true scale looking north. Grid size is 200m. Topographic data is taken from 1:50 000 DEM, Thickness of Te Waka Limestone is representative only. Numbers (1) and (2) on the section correspond to outcrop identified in Figure 4.11 A.

C Shaded relief map based on 1:50 000 DEM. Section lines and photograph location are indicated. NZMG co-ordinates.

Failure model

The inferred failure in the Maungaharuru Range is best described by a rotational movement, with the long axis of the failure ellipse oriented down-dip. This is required in order to accommodate the transfer of strain from the basin to the face of the range. By having the elongate axis of the ellipse down-dip it is inferred preferential zones of weakness, and grain orientations in the bedded sediments partially control the style of deformation. The sediments, however, deform plastically, and the maximum strain occurs through the centre of the mass. The failure ellipse describes the extent of movement, and is associated with minimal displacement where many inter-particle bonds remain intact. This style of motion is indicated by the strain contours in Figure 4.11-B.

Based on an initial slope profile similar to that of the limestone remaining to the east of Ahuateatua, and a rotational mass transfer, the cross-sectional area lost through subsidence in the basin equates to the projected area increase on the eastern face of the range (c. 2400m^2). The area of each of the strain contours in Figure 4.11-B also equates to this value. These indicate a slightly eccentric down-dip transfer of maximum strain, most likely a reflection of near-surface variations in confining pressure imposed by the geometry of the range.

Basic analysis suggests the failure may extend as far as 1200m below sea level, 2.1km below the lowest point in the basin, coinciding with the approximate elevation of local basement as interpreted from seismic profiles by Frontier (1995). This may be expected as the much stronger greywacke basement is unlikely to deform in the same style as the much weaker Neogene strata. If this basement is therefore assumed to be fixed, then a semi-linear increase in total strain may be expected in order to maintain a consistent shear stress through the plastically deforming slide mass.

The centre of the ellipse matches a point of minimal change where the profile of the basin limestone intersects that of the limestone defining the hillslope below Ahuateatua.

Proposed sequence of events

1. Tectonic development of NE-SW trending anticline.
2. Block sliding off the southern quadrant of the anticline (Figure 4.7 (10)). Tectonic activity induces WNW trending shear south Ahuateatua.
3. Elastic then plastic deformation of sediments begins adjacent to southern side of the shear zone.
4. Deformation propagates southward. Full-plastic deformation is achieved south of shear. Significant subsidence of ridge crest. Eastern margin of range begins to dilate leading to enhanced sediment stripping, this is at a maximum in the region of the tight anticline where extensional defects begin to form in limestone cap. Continued block sliding at southern end of anticline.
5. Ridge starts to achieve concave profile, substantial joints form in limestone cap, infiltration begins to increase markedly. Full plastic deformation beneath much of the range. Tight anticline continues to form and releases large limestone blocks which topple and slide down the oversteepened rangefront. Mass movement becomes prevalent as dilation continues along eastern rangefront. Deep-seated, though relatively shallow (<150m) rotational slide begins along western ridge as response to increased shear stress from main collapse.
6. Basin now formed above northern section of slide. Plastic deformation continues to develop throughout range. Limestone cap largely removed from tight anticline and easily erodable underlying sediments begin to be rapidly eroded, this continues to deplete resisting forces. Intense deformation of sediment on southern shoulder of range now allows formation of large mass movement complexes and rapid evacuation of sediment. Rate of rotational failure on western flank matches that of main failure.
7. Continued plastic deformation throughout range. Medium sized landslide at the outlet of the basin blocks drainage and creates 3km^2 lake. This markedly increases pore pressures and leads to period of increased plastic deformation and associated deep-seated landslide activity. Subsequent breach of dam returns pore pressures to normal and substantial erosion from eastern face may be required to return stress balance to normal state and continue movement.

Discussion

While this model is largely theoretical, and backed up by minimal field data other than observations of prominent outcrop, and the association of this pattern with the geometry of the Maungaharuru Range, it does provide a viable means with which to facilitate the very difficult apparent transfer of mass from the range crest through to the eastern face. A number of additional observations help back up this model, including – possibly – results from the EC91 seismic survey. These are discussed along with the inevitable uncertainties and complications in the following section.

The homogeneous form of deformation may explain the variation in the interpretation of seismic data across the range (Wylie, 1993; Frontier, 1995). Macroscopic variations in strain within the mass are likely to severely complicate reflection patterns. The progressive decrease in strain toward the slide margins would prevent the delineation of a discrete zone of disturbance and further complicate identification. The reflector identified by Wylie (1993) neither fits the basement reflector identified by Frontier (1995), or surface outcrop patterns. It does, however, correlate relatively well with inferred areas of similar strain, suggesting it may relate to some form of strain partitioning, or other slide-related phenomena. This is supported by the cross-fault inferred by Wylie (1993) which terminates the reflector in a similar place to the failure ellipse, before the bed is inferred to continue once again 800m lower (Figure 4.11).

Additional supporting observations:

- There is no true "toe" or break-out at the foot of the range as deformation may be concentrated in less confined sediments further up the slope (Figure 4.8).
- A possible increase in defect concentrations in valley sediments below the foot of the range is inferred from strong lineations and stream sinuosity patterns (see Section 4.1.5). This may be related to the eastern extent of deformation.
- Based on morphological evidence, including the inferred degree of subsidence and current activity of landslides, deformation on the range appears to have been a long-term process. This supports the steady-state plastic deformation inferred in the model.

- Vectors representing the maximum accumulated strain coincide with the maximum convexity of the Ahuateatua slope profile, possibly indicating the initiation of a similar process beneath the peak.
- The arcuate scarp noted within the basin in Figure 4.7 and 4.9 corresponds with the intersection of the main failure and the western rotational slide in Figure 4.11-B, and may provide evidence of the inferred structural division about this boundary.

Complications:

- A lack of precedent – Petley and Allison (1996) state "...there is virtually no evidence that geomorphologists have considered the implications of the stress-strain regime relevant to large failures." The implications of this observation, combined with the scale of this particular failure means literature describing similar investigations is sparse.
- Minimal driving force – While the "initial" (Ahuateatua) slope profile provides what is considered sufficient driving force to enable the initiation of this process, the current profile indicates a much lower driving force – especially if erosion of the tight anticlinal structure was not as rapid as is inferred. Consideration must however be given to the plastic nature of the deformation; while the strain contours indicate the current total strain, a plastic substance need not fail in a predetermined manner as in brittle failure, and the principal zone of deformation may migrate over time. In this case the zone of maximum deformation may flatten as sediment is stripped from the face of the range, and related confining pressures decrease.
- Lack of subsurface data – while this is not strictly a complication, the acquisition of subsurface information such as seismic data could provide valuable information on important controls such as bedding attitudes and thicknesses, which may easily confirm or discredit this model.
- No control on initial tectonic inputs – Whether active or not, these are likely to play a significant part in the structural evolution of the range. Until the mechanism responsible for the initial anticlinal form of the Maungaharuru Range is known, the effect of these can – at best – be assumed negligible. This may be possible if the rate of sliding is great enough to allow plastic deformation of the sediments to mask structural inputs.

4.2 TRELINNOE STUDY AREA

Selected as a region in which to undertake an intensive field investigation, the Trelinnoe study area displays a large number of features characteristic to the Esk Valley, these include:-

- Strong lineaments, easily identified from satellite imagery and vertical aerial photos
- Steep, highly incised streams with limited contributing catchment
- Broad terraces. While these are more dissected than in many other areas of the valley, they are still largely unmodified, and concordant ridge crests in the areas of greatest dissection allow the correlation of an enveloping terrace surface.
- Both Kaiwaka and Otakowai Streams run above their graded exponential profiles in mid to upper reaches.
- The sinuosity of the streams is high, particularly in Otakowai Stream where several strong reversals in channel direction take place.
- Strong lithological control, particularly from conglomerates along the margins of the catchments, and isolated hills within the area.
- Several large-scale mass movements

A location map for this area is provided below

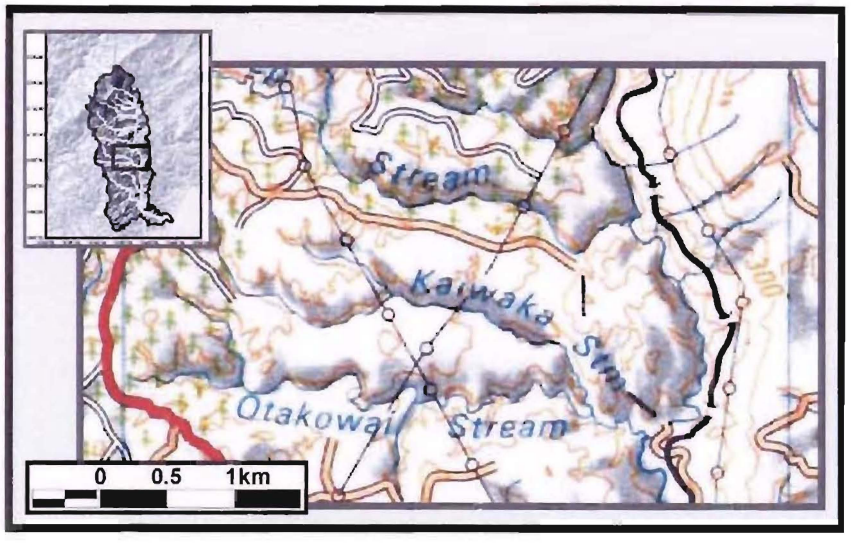

Figure 4.12 Detail of Trellinoe study area. See inset of the study area and Esk catchment for location.

Morphologically the area is dominated by a well-defined upper surface with generally subdued well-rounded landforms and prominent conglomerate capped remnants. This surface is cut west to east by two highly incised (80-100m) tributaries to the Esk River – Kaiwaka Stream in the north, and Otakowai Stream to the south. These streams converge at their eastern ends and flow to the south round the pronounced form of Island Farm before discharging into the Esk River.

Vegetation in the area has changed dramatically since the mid 1900's. Vertical aerial photos taken in 1943, five years after the Esk Valley flood, detail a barren landscape largely devoid of vegetation other than an apparent pastoral cover and small pockets of scrub. Shallow landslides, indicated in photos by bright white scars of exposed bedrock, are prevalent – covering approximately 10% of the land surface, and 80% of slopes over 30°, many of these scars remain in the landscape today. This is a sharp contrast to current vegetation cover, and is typical of changes throughout the Esk Valley. Island Farm and Little Ice-cream Slide are now planted in commercial pines, dense native bush has revegetated gorge walls and riparian zones, and improved farming practices maintain good grass cover year round.

While vegetation may have prevented many shallow failures, it also hides many geological features, and for this reason older 1943 photos are used in a detailed air-photo interpretation. High levels of distortion in these photos related to lens and topographic effects have been removed by manual rectification of the images. This is however not ideal, and some distortion remains – particularly around the perimeter of images, and in areas with high topographic contrast.

Geomorphic mapping was undertaken at a scale of 1:15,000 to highlight important morphological features within the area. These included lithological controls, drainage patterns, river incision, and landslide features. Results are presented in Attachment 2, and an oblique view of the area including geomorphic interpretations is given in Figure 4.13.

Due to the level of incision in the river system, the field investigation was undertaken in two parts:

1. *Geological mapping and the investigation of bedrock features along the stream channels.* This provided the best insight into the structure of the area, and errors associated with the aerial photo investigation. It was, however, hampered by limited access points (stream outlets, and two steep tracks approximately halfway

along each channel), slow progress in the gorges, and few landmarks to locate mapping. This affected both coverage and accuracy of location in much of the work; and

2. *An investigation into landforms and processes of the upper surface above incised channels.* This was complicated by tephra cover, vegetation, and evolved rounded slopes, all of which severely limited exposure. This investigation did, however, provide important ground truth to support the aerial photo interpretation.

Four deep-seated landslides are identified in the study area; Trelinnoe, Little Ice-cream, Kaiwaka, and Otakowai landslides, these are discussed in a later section (4.2.3 Landslide investigation).

4.2.1 STREAM CHANNEL FEATURES

Both Otakowai and Kawaka Streams transition downstream from relatively broad, steep sided valleys with shallow fine gravel fills, through to incised gorges with a mixture of bedrock, fine alluvium, and moderate sized siltstone boulders, and finally into highly incised, very narrow bedrock gorges.

Valleys and gorges are generally delineated by smooth, near vertical valley walls particularly in upper reaches; these often run very straight and suggest defect control. Vegetation is present to near stream level. Abandoned terraces are generally not seen in either stream, though in lower reaches small recent terraces are present – probably related to flood events. This indicates rapid incision, and negligible variation in long-term aggradation/degradation rates.

Oversteepened channel reaches up to 50m in length may relate to highly degraded knickpoints, tectonic controls, or resistant lithologies. These oversteepened reaches are characterised by rapid flows in sinuous bedrock channels up to 0.5m wide by lm deep and serve as an indication of the rapid incision occurring within the system (Figure 4.14F). The form of these features suggests rapid planation of a surface followed by relatively recent incision. While knickpoints greater than 1-2m are not present in the system, it is considered unlikely these features are evidence of degraded knickpoints as local bedding orientations are typically steep, and the form is not consistent with the steady upstream migration of a channel perturbation. These reaches are more likely to be a result of tectonic and lithologic controls. Subsurface faulting leading to deformation and uplift of the stream channel

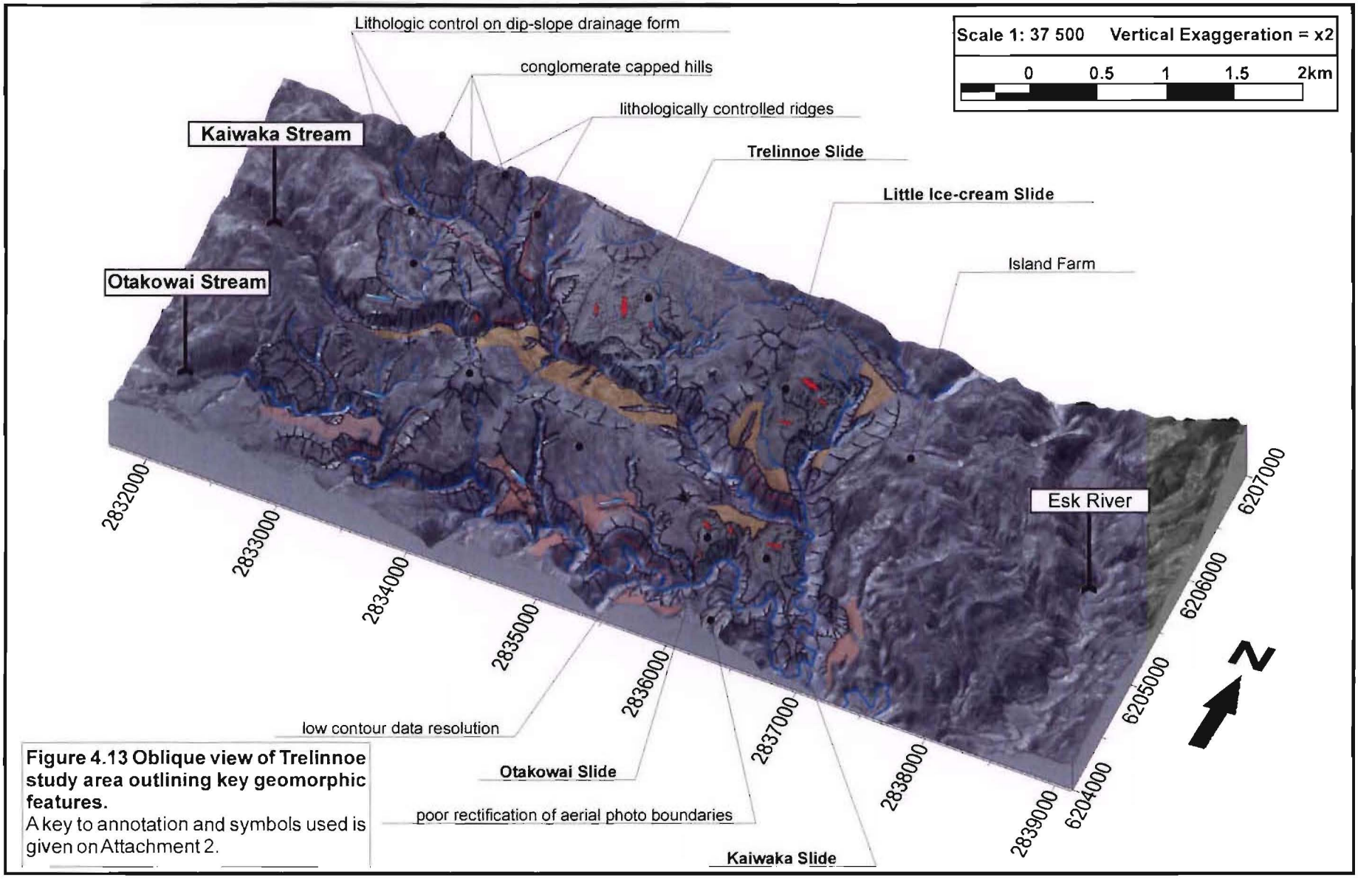

Figure 4.13 Oblique view of Trelinnoe study area outlining key geomorphic features.
A key to annotation and symbols used is given on Attachment 2.

initiates lateral migration and downcutting during low flows; high flows easily fill the channel and rapidly produce planed bedrock surfaces. These processes are controlled by slight variations in bedrock resistance and increased defect concentrations, the latter related to the initial tectonic folding.

Few faults are identified in the stream channels; this is likely to be due in part to vegetation cover along much of the valley walls, and preferential fluid flow enhancing vegetation growth along fractures and faults. Three faults are identified cutting the channel in the upper reaches of Kaiwaka Stream, and while a sense of motion could not be determined, similar orientations of the fault planes suggest they may be related to a single style of deformation. Each fault is sub-vertical and strikes approximately N-S (see Appendix H for details); they occupy zones of deformation ~1m wide, while increased numbers of joints are identified up to 100m away from the fault. Each fault was marked by a waterfall indicating the strong control on drainage formation. The orientation, persistence, and other details were measured for joints within the valley walls were surveyed – these are discussed in section 4.3. The location and orientations of the faults compliment similar structures identified by Black (1991), and Bland (2001) in strata elsewhere in the region.

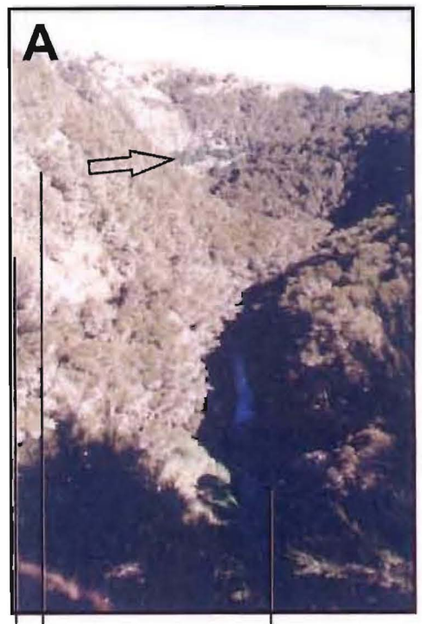

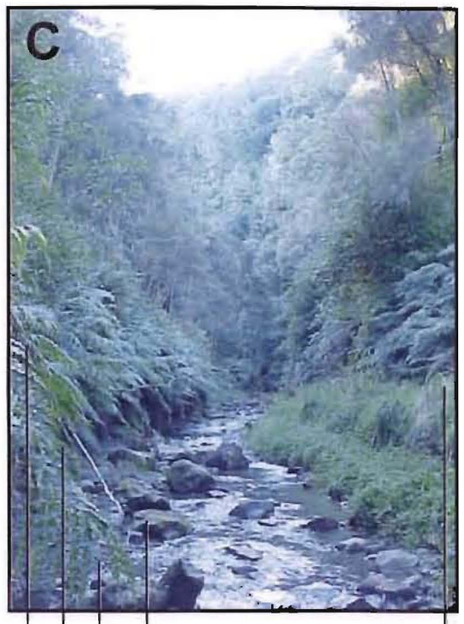

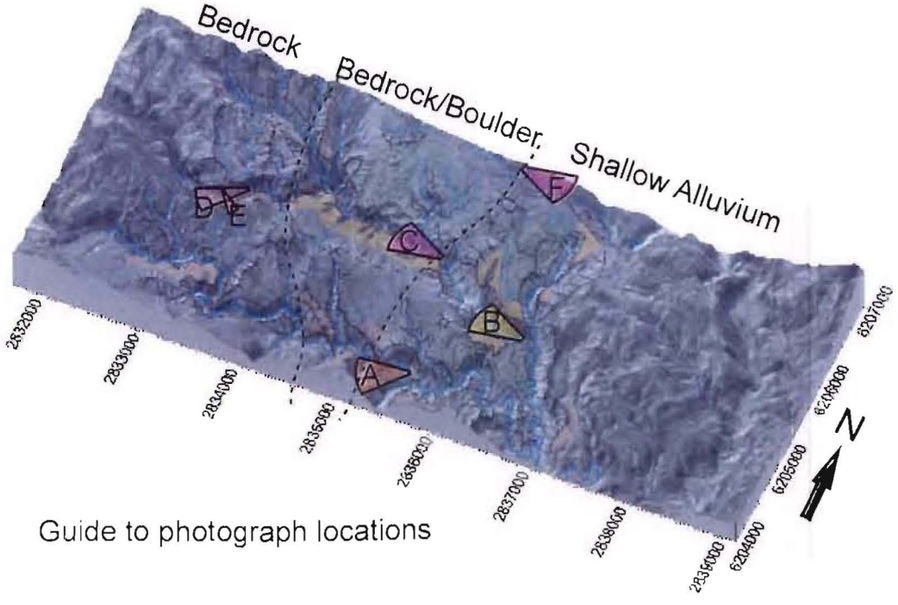

Figure 4.14 Photographs detailing key geomorphological characteristics of stream channels within the Trelinnoe Study Area.

4.2.2 UPPER SURFACE FEATURES

As mentioned earlier, landforms of the upper surface are generally subdued and well rounded compared to features within the valleys. This is in part due to the tephras that blanket the landscape, however, it is mostly a result of a disassociation of hillslopes from the fluvial system and the dominance of slow geomorphic processes – such as soil creep – associated with this lack of strong geomorphic influence. Landforms can be divided into two groups, those associated with lithological control, and those related to ancient and modern fluvial systems.

4.2.2.1 Lithological features

Lithology influences slope morphology and drainage form, and is responsible for the presence of many landforms in the area. The upper Papakiri Member conglomerate forms strong, erosion resistant ridges in the north-west of the area as well as a cap on remnant hills. The Grassy Knoll Member conglomerate also forms prominent caps, most notably in the centre of the region, and along ridges to the south of Otakowai Stream. Island Farm (Figure 4.13, Figure 4.16-B) is capped by a resistant limestone unit that appears to be very localised, and cannot be correlated with any other unit in the valley (pers. comm. Bland, 2003). This unit may help explain the unusual isolated form of the hill.

Slope drainage is also influenced by lithology, this is most likely a result of both weathering resistance and permeability contrasts. Drainage preferentially develops in the down-dip direction. Papakiri Member sediments in the west of the area appear highly dissected, and drainage forms in small, steep basins with high topographic variation. In the north-east of the area, an uncemented sandstone unit produces linear drainages in very steep sided gullies, this unit can be traced SSW to just north of Otakowai Stream where a similar pattern occurs on a broad dip-slope.

Lithology controls slope form, and dip-slopes are commonly gentle and grade at, or very close to the dip of bedding. This is most often a result of slightly more indurated beds sheltering underlying lithologies. In contrast, scarp slopes are consistently ~20-25° and concave upward, a result of the resistant lithology standing at a much higher angle than underlying strata are able to maintain (Figure 4.16).

4.2.2.2 Fluvial features

Fluvially related features are dominated by broad Holocene gravel terraces that gently dip toward current channels and can be traced through much of the Esk Valley. The gravel sequence may overly strath surfaces, and appears to be between 10 and 15m thick. It is incised to bedrock in places by ephemeral streams (Figure 4.15). The terraces are covered in a 3m thick blanket of reworked loess soil and tephra. This was augered in an attempt to identify tephra markers for age correlations, however the reworked nature of the soil made identification extremely difficult and the exercise was subsequently abandoned.

A lower terrace surface, approximately 6m below the upper one is occasionally present, and may indicate the gradual onset of stream incision. This is almost always adjacent to the current incised gorge, however, in places an apparent migration of the stream channel is visible where low-level terrace surfaces are separated from the current gorge by small "islands" of what appears to be outlying bedrock. A lack of outcrop prevented further investigation.

Figure 4.15 Holocene gravels exposed in an incised ephimeral stream channel adjacent to Kaiwaka Stream.

The person at bottom right is 1.6m tall. Note the currently dry channel. Siltstone bedrock is approximately 2m below the lowest channel level to the left of the image. Kaiwaka stream lies ~50m away in the direction of the photograph and is incised c.60m below this level; its far bank is marked by the band of thick vegetation in the middleground.

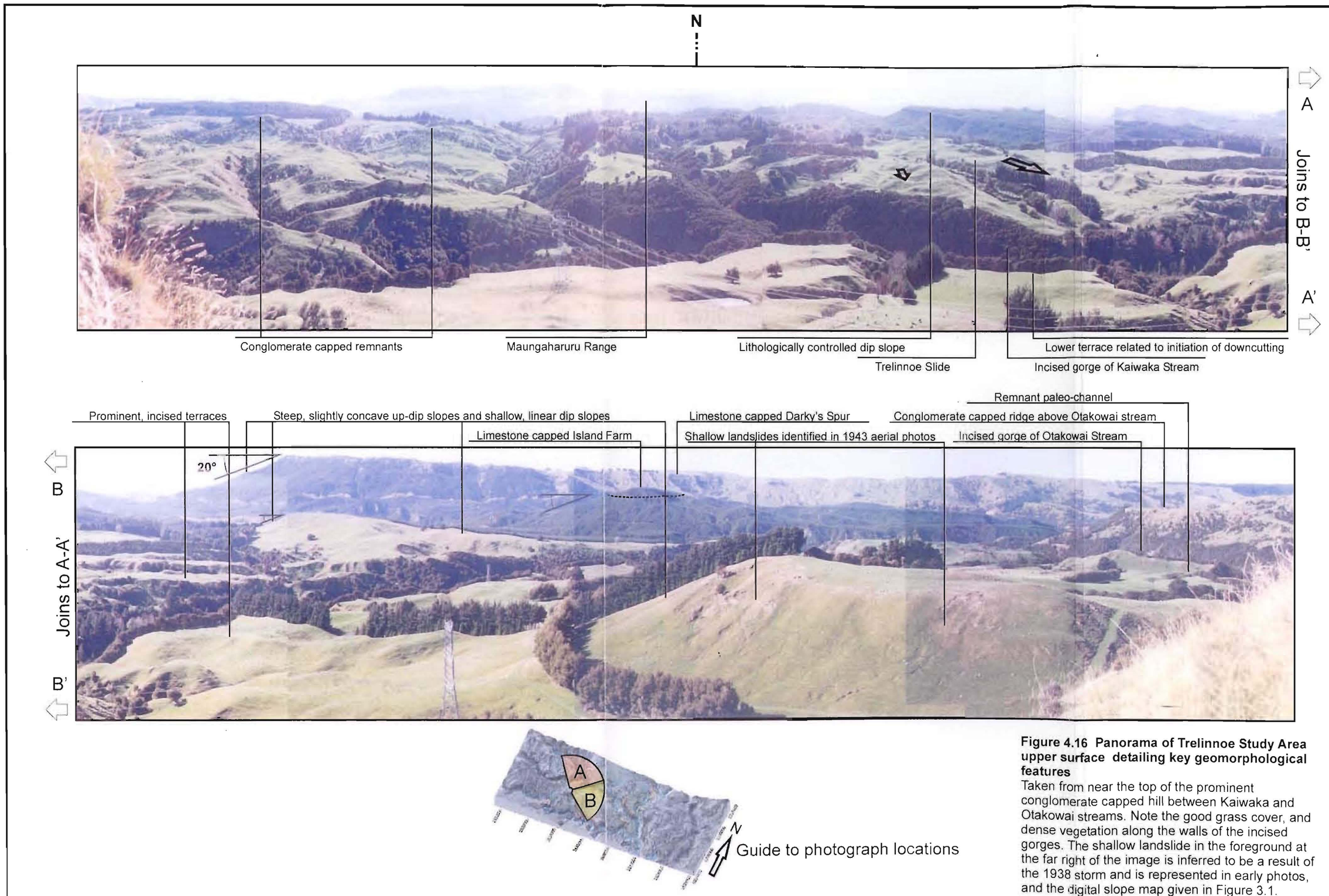

Figure 4.16 Panorama of Trelinnoe Study Area upper surface detailing key geomorphological features
Taken from near the top of the prominent conglomerate capped hill between Kaiwaka and Otakowai streams. Note the good grass cover, and dense vegetation along the walls of the incised gorges. The shallow landslide in the foreground at the far right of the image is inferred to be a result of the 1938 storm and is represented in early photos, and the digital slope map given in Figure 3.1.

4.2.3 LANDSLIDE INVESTIGATION

Four deep-seated landslides were identified in the Trelinnoe study area; Trelinnoe, Little Icecream, Kaiwaka, and Otakowai landslides. While spatially separate, many features of these slides are similar. Each is discussed below and parallels are drawn at the end of this section.

4.2.3.1 Trelinnoe Landslide

The Trelinnoe slide (Attachment 2, Figure 4.16-A, Figure 4.19) is the most extensive, accessible, and in many ways most typical slide in the area. The slide covers 780,000m^2 and has an estimated volume of 31.2x$10^6$$m^3$. It is essentially a translational dip-slope slide and at least one failure surface can be identified at river level. The surface in the middle of the slide is dominated by transverse extensional grabens that indicate a dilation of the slide mass, while in other regions compressional ridges are prominent. These features can be used to define three zones of differential slide motion, the most rapid of which lies adjacent to Kaiwaka Stream. Minimal movement occurs within the most "inland" zone to the northeast.

The toe of the landslide can be identified at bed level in Kaiwaka Stream (Figure 4.17), although vegetation cover severely limits exposure. The failure surface here is a 50cm thick coarse sandy tuffaceous horizon, this is in-situ and dips steeply downstream at 050/20° SE. At the time of investigation, this was saturated with a very high seepage rate. A highly fractured moderately indurated siltstone band is present around the toe of the slide and fractures dip into the toe at around 40°, the strike rotates through 30° downstream. This change in strike indicates a component of lateral movement (supported by local dip direction), and the dip of fractures back into the face indicates a sharp upward rotation of the failure surface. These are probably releasing structures, and indicate the level of the bedrock river bed at the time of failure was at least 3m higher than present (Figure 4.17, Figure 4.19). By inferring an average stream incision rate of 3.5-4.5mm/yr (Section 3.3.3.4) an approximate age of between 670y.BP and 860y.BP is given for the formation of this failure surface.

Anecdotal evidence suggests the slide remains active. Mr John Wills – the landowner at Trelinnoe Station – noted a large slip of at least 400m^3 at the toe of the slide less than ten years ago, apparently unrelated to any climatic or tectonic disturbance. While sampling a

similar region the author also noted an area on the slide face in which joints are fully relaxed (i.e. the normal stress across the planes is negligible), and toppling failures are common.

Figure 4.17 Outcrop of Trelinnoe Slide failure surface in Kaiwaka Stream

Photo taken looking north just downstream of the Kaiwaka Stream bridge (NZMS 260-V20 348058).Note pack and A3 map board on left hand side for scale. The tuffaceous horizon is underlined in orange and marks the base of the slide. Defect planes are highlighted in the toe zone. It is inferred that bedrock in the stream at the time of failure was at least 3m higher than current stream level and these defects represent a rotation of the toe toward the surface. Large siltstone boulders are present in the stream bed material as a result of continued slide movement.

It is difficult to determine the failure surface for the whole slide. The failure occurs in indurated siltstones that suggest a maximum friction angle (~32°) far in excess of the 6° average slope of the slide (Figure 4.19). The failure surface must therefore be either on siltstone reduced to residual shear strength, or a thin interbed of a much weaker lithology. The tephra on which the failure occurs in the toe zone is a very good candidate for the latter as results of sample testing indicate the material rapidly disaggregates in water, and when saturated, has negligible internal friction. It is difficult, however, to confidently extrapolate this below the slide mass as dip measurements taken around the slide are sparse, and vary greatly from 0-20°. The steep scarps and basins within the lower 400m of the slide reflect extension of the mass, and indicate a dramatic increase in slide velocity (Attachment 2, Figure 4.19). The surface of the slide here rises at an angle similar to that of the local tephra bedding suggesting the steeply dipping strata may be the primary control on the failure in this region. However, the transition to less variable topography more characteristic of translational landslides further up-slope suggests either the bedding dip

must increase significantly, or the primary failure surface must be transferred to another, shallower dipping, though similarly weak, structure.

4.2.3.2 Little Icecream Landslide

The Little Icecream slide is the second largest in the study area (Attachment 2, Figure 4.20). Also a translational slide, it covers 700,000m^2 and has an estimated total volume of 17.5x10^6m^3. Unfortunately, forestry has recently been established over the surface of the slide making field investigation impractical. Observations are therefore based largely on air-photo interpretations and basic structural mapping in the surrounding area.

In planimetric view the slide extent defines a parabolic shape, the axis of which lies along a low ridge that runs down the centre of the slide mass. A smaller failure within the slide reproduces this form and indicates highest movement rates are probably associated with increased overburden pressure from material forming this ridge.

Movement has been facilitated by the deep incision of an unnamed stream at the toe of the slide. The degree of stream incision is disproportionately high for the catchment size and suggests highly erodable bedrock. This has been mapped by Bland (2001) as uncemented sands of the lower Waipunga Formation. However, it may also incorporate the cohesionless sands near the upper contact of the Matahorua Formation Grassy Knoll Member which outcrops close to the toe region of the slide. Here the siltstone that comprises most of the unit grades into a 10m thick fine grained clean massive uncemented sandstone that is then overlain by a thin (5m) poorly cemented greywacke conglomerate (Bland, 2001). Moderately- to well-sorted, poorly cemented, slightly micaceous siliciclastic sandy siltstones and sandstones of the Waipunga Formation lie unconformably upon the upper Matahorua Formation conglomerate, and at their base grade over several metres from a sandy siltstone to a fine grained sandstone (Bland, 2001).

The slide can be partitioned into four domains based on apparent total displacement and mechanics (Attachment 2). The northernmost appears to have moved very little, though the graben at the head of the slope indicates up to 50m of extension. This lack of movement is probably due to incision in the toe region being the lowest of any part of the slide. Two domains can be defined along the central ridge, these are the most active in the slide and display several diffuse, arcuate extensional grabens indicating internal disturbance of the masses and possibly some rotation. The western unit appears to have moved up to 150m downslope from the adjacent hill, and is marked by an incised stream in its northern lateral

margin and a prominent scarp on the southern edge. The eastern of the two central domains appears the most active of the entire slide, it also appears to have a stronger component of rotation than any other region. This may be related to the appearance of a secondary shear surface related to increasing degrees of rotation as blocks move downslope, or possibly a change of lithology on the shear surface inducing different deformational characteristics within the slide. Total movement is likely to be only ~20m. The southernmost section is the least disturbed and one of the less active regions of the landslide. This is surprising as stream incision begun adjacent to this region and it should have therefore had the longest time to develop and may indicate the landslide was triggered a significant time after the onset of incision. Possible triggers include: co-seismic shaking, the development of a network of low shear strength persistent defects, or a variation in rock properties across the slide which may prevent the release of this section before the movement of central regions have created a favourable geometry. Displacement in this area is truly translational, although apparently only in the order of 20m.

A lineation visible in early aerial photographs runs along the valley walls in Kaiwaka Stream and appears to indicate a strong lithological contrast, most likely the base of the 10m thick, clean sandstone in the Grassy Knoll Member (Attachment 2). This marker may coincide with the primary basal shear within the landslide. Interestingly, another lineation along the Kaiwaka Stream wall marks the Old Coach Road, a route established in 1861 to provide access to Te Pohue (and eventually Taupo) from Napier (Parsons, 1997). The route crosses from apparently stable ground on the southern margin of Little Icecream Slide through the slide and back onto stable ground on the northern side. While the road cuts one of the most inactive parts of the landslide, it does provide a good tie point across which to judge movement for the 122 years between 1861 and recent aerial photos in 1983. This period covers both the 1931 earthquake and 1938 storm. Interestingly, although a detailed survey was not undertaken, there is no obvious offset across the slide margin indicating this portion of the slide has been stable for the entire period.

4.2.3.3 Kaiwaka Landslide

Kaiwaka Landslide (Attachment 2, Figure 4.21) is a large, extensional, translational slide located at the eastern end of the Trelinnoe Study Area. Only a very limited investigation of the slide was able to be undertaken due to a lack of outcrop. While still a dip-slope failure, unlike other slides in the region, the direction of slide movement cuts obliquely across

local dip, deviating by up to 70° to the north. As a result, the basal failure is likely to be near horizontal (see Figure 4.21). Lithologies here are the same as those underlying Little Icecream Slide, and it is inferred internal shear strength in the same uncemented sandstone is likely to be sufficiently low enough to facilitate failure at such low angles (<5°).

The surface of the slide shows evidence of a sinuous stream channel cut c.10m below the terrace surface. While this channel obviously pre-dates the slide, and has been heavily modified by its movement, it appears the initial incision was controlled by strong lineaments as depicted in Attachment 2. The landslide boundaries also adhere strictly to these lineaments suggesting defect control, typical of Esk Valley landslides.

Figure 4.18 Kaiwaka Landslide from Island Farm

Photo is taken looking WSW, and clearly shows Kaiwaka Landslide at the end of the extensive terrace surface between Kaiwaka and Otakowai Streams.

4.2.3.4 Otakowai Landslide

Otakowai landslide is located just to the west of the Kaiwaka slide (see Attachment 2, Figure 4.21). This slide appears to be more typical of those evidenced in the area, and is inferred to be a simple translational slide with basal shear occurring on a Grassy Knoll Member tephra, as detailed in Section 4.2.3.1.

A number of medium sized bedrock failures in Otakowai Stream between Otakowai Slide and easting 2835000 may be evidence for a strong underlying instability in the region (Attachment 2). These failures typically occur on the northern margin of the stream, and contain fragmented bedrock and surficial deposits. Where underlying bedrock is visible, it is often intensely sheared or contains imbricate defects at less than 1m spacings. This may indicate a deeper-seated control on the landslides than is apparent from their surface expression, possibly a strong tectonically induced defect control, or extensive bedding controlled slide similar to that to the north of Deep Stream (see Section 4.1.5). More detailed mapping is required to investigate the relationship between these medium scale and surficial landslides, and a more regional (~2km^2) instability.

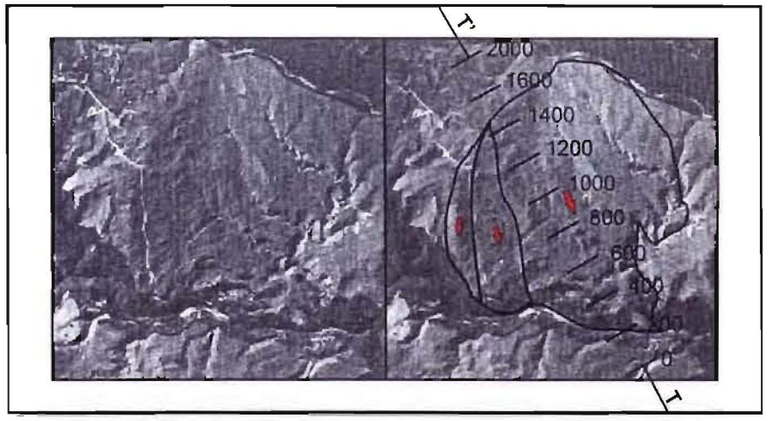

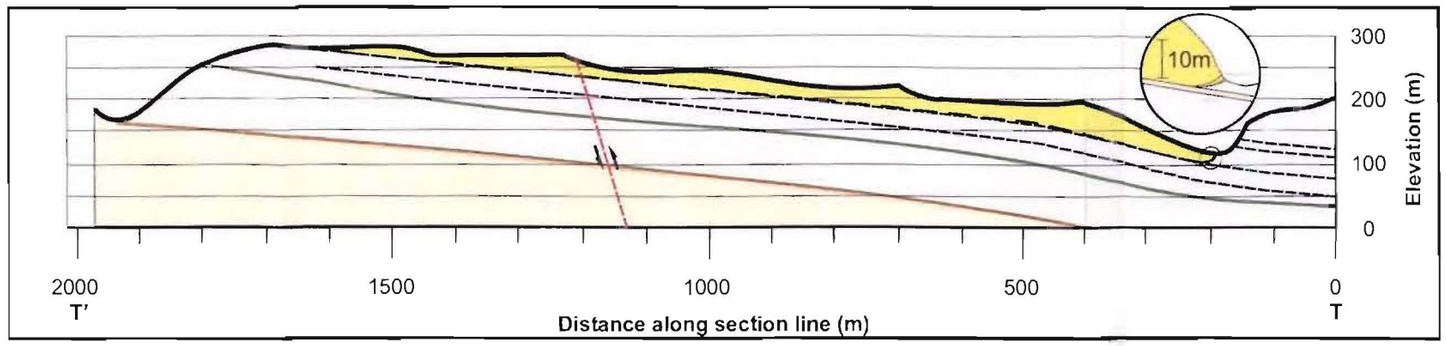

Figure 4.19 Stereo photo pair and true scale cross section of Trelinnoe Landslide
Note three zones of motion, and apparently rapid movement towards toe in the photos. Failure is inferred to be on a thin tephra horizon as noted in the toe zone (Figure 4.17), and is illustrated in the inset (The inferred channel level at the time of the last failure is shaded in light grey). Warping of beds is due to combination of the Wakarara Fault - Trelinnoe Sector (WFTS) and the Eastern Patoka Fault. The minor fault indicated is likely to be a backthrust related to the WFTS (see Figure 5.6 and Attachment 2).

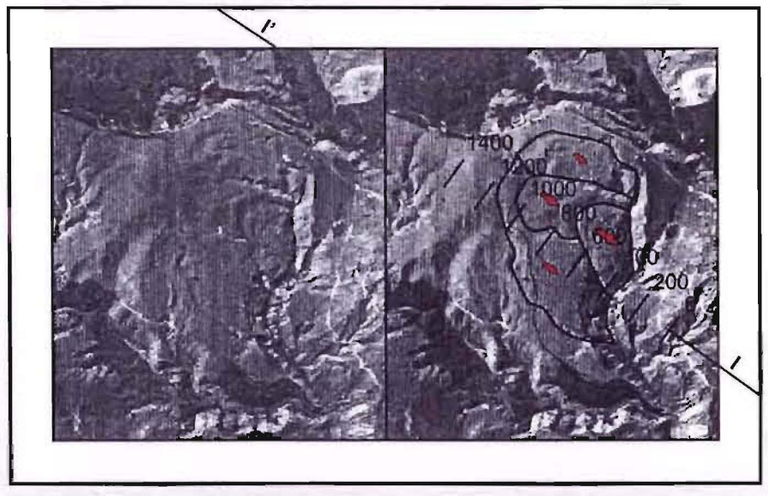

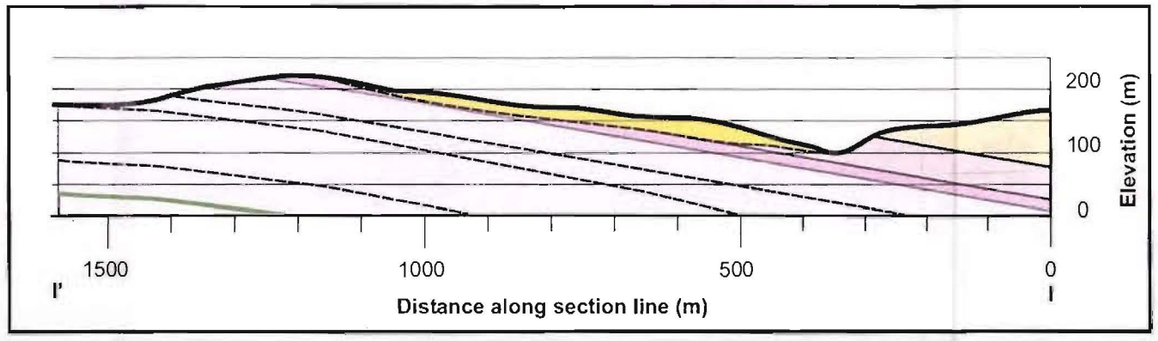

Figure 4.20 Stereo photo pair and true scale cross section of Little Icecream Landslide
Upper part of landslide is likely to be failing on uncemented sandstone bed immediately below upper conglomerate of Grassy Knoll Member. A change in the style of motion from translational to rotational part way down the slide is thought to be related to a change of basal lithology. Note Old Coach Road running through the western margin of the slide

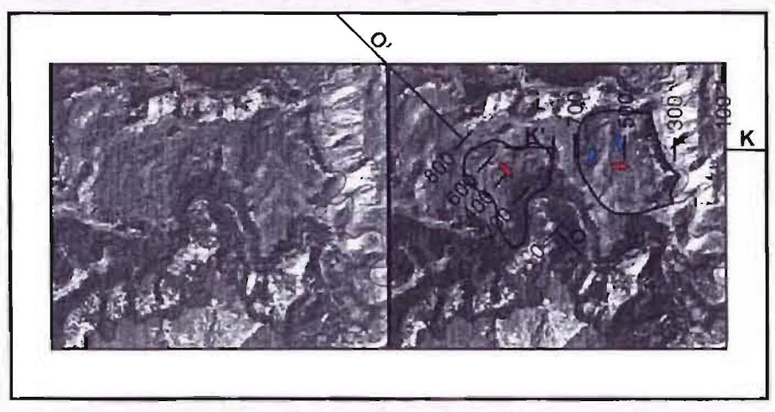

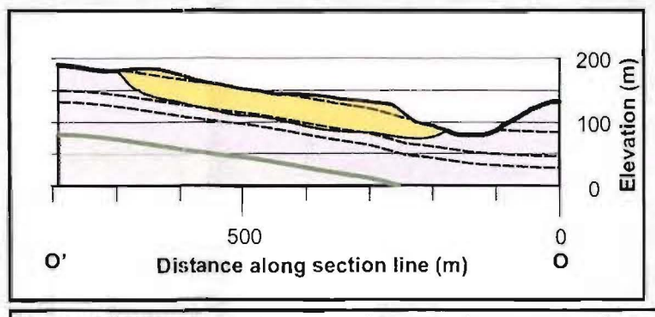

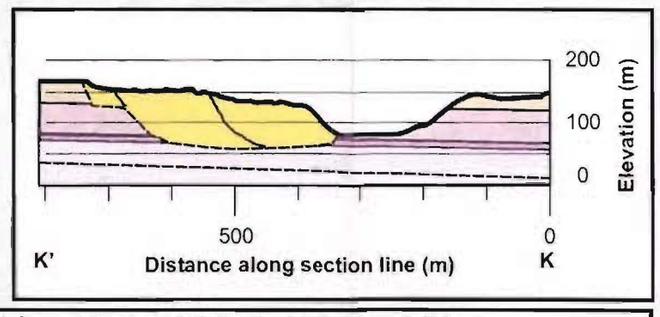

Figure 4.21 Stereo photo pair and true scale cross sections of Otakowai (left) and Kaiwaka (right) Landslides
Otakowai landslide is inferred to be failing on a tephra layer within the Grassy Knoll Member. Kaiwaka Landslide is unusual as failure is only obliquely down-dip. Poor outcrop hampers accurate location of the failure surface, however it is likely to be within the same uncemented sandstone as Little Icecream Landslide (above). Note deformation of sinuous stream channel on landslide surface

4.3 DEFECT ANALYSIS

4.3.1 INTRODUCTION

Defects are discontinuities in a rock mass. Their orientation and persistence reflect stresses in the rock since formation. They affect the geomorphic development of a region by providing surfaces or zones of weakness that may be preferentially eroded by fluvial processes, conduits for subsurface fluid flow, and planes of low frictional resistance that promote block failure and landsliding. An investigation into the defects within a region can therefore provide valuable insight into previous tectonic stresses as well as current geomorphic processes.

4.3.2 METHOD

Defect analysis was mainly confined to the Trelinnoe study region and involved the recording of:

- *Location* - On aerial photos in the field then transferred to GIS format.
- *Orientation* - Strike and dip
- *Persistence* - Persistence is the "length" of the defect on the rock face. While only the most persistent defects are mapped, noting this is important in order to record the significance of the feature.
- *Spacing* - Where defects are evenly spaced on the rockface, they are listed as "sets" and an average orientation taken. This, combined with defect persistence, can help determine the significance of features.
- Defect information is analyzed using a combination of stereonet plots in the Dips computer program and GIS.

Stereographic analysis in Dips was used to identify defect sets. Poles to defect planes were plotted on a lower hemisphere equal angle stereonet, and concentrations of poles then used to identify each defect set. (see Appendix H – Figure H.3).

Data taken from Dips was then transferred to GIS and spatial relationships of the defects were investigated. Sets are compared with lineaments identified in the reconnaissance stage of the investigation.

4.3.3 RESULTS

The majority of bedrock in the study area is massive to weakly bedded, unjointed siltstone. The limited defects present are often therefore prominent features, and easily distinguishable. Highly persistent defects are relatively common and often extend the entire height of a c.40m cliff. Defect sets are also commonly visible in the field, and spacing can vary from tens of centimetres to tens of metres. Care was taken when sampling the orientation of defects to avoid exfoliation defects related to relaxation of the rock face as these secondary features are primarily a result of - rather than a possible contributor to - geomorphic processes. A typical example of surveyed defects is given in Figure 4.22.

Sampling of defect orientations was sparse, partly due to dense vegetation cover along much of the valley walls, and partly a reflection of the massive, unjointed nature of the bedrock. Vegetation also hampered the recording of defect persistence and spacing as poor exposure often did not allow reliable identification. This made interpretation extremely difficult and these aspects were subsequently ignored. No spatial relationship could be identified between the sets. Eighty-five defects were sampled in all; their locations are recorded in Appendix H.

Fisher Concentrations on the stereonet (Figure 4.23), while low, are considered to be statistically significant. They are interpreted to be the effect of several sets of sparse, regionally persistent, controlling defects within a broad zone of disturbance. In ideal circumstances where only defects related to the five sets were sampled; allowing for a $\pm 5°$ deviation in strike and/or dip, Fisher Concentrations could only be expected to average around 2.8%. This is calculated based on the fact the above deviation accounts for 7% of the total plot area, and assumes each defect set contains 20% of the total points. The average concentration given above is therefore calculated as the percentage of plots per 1% stereonet area.

Five defect sets are identified, four sub-vertical, and one steeply dipping. All but set four correlate extremely well with the orientation of lineaments identified in aerial photos. A summary is given in Table 4.1.

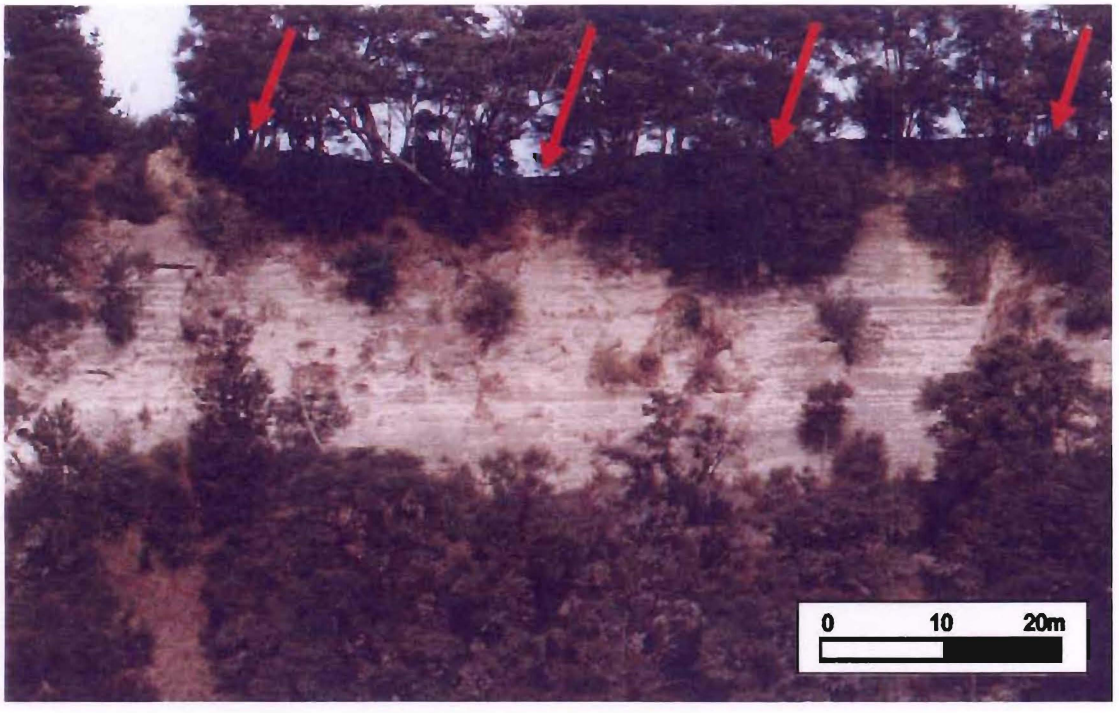

Figure 4.22 Typical defect set identified in Kaiwaka Stream.

Defects can be traced through the full height of the cliff. There is no evident dilation of defects, shearing, or displacement of beds. The traces are strong and continuous and are generally marked by vegetation due to slightly elevated groundwater flows.

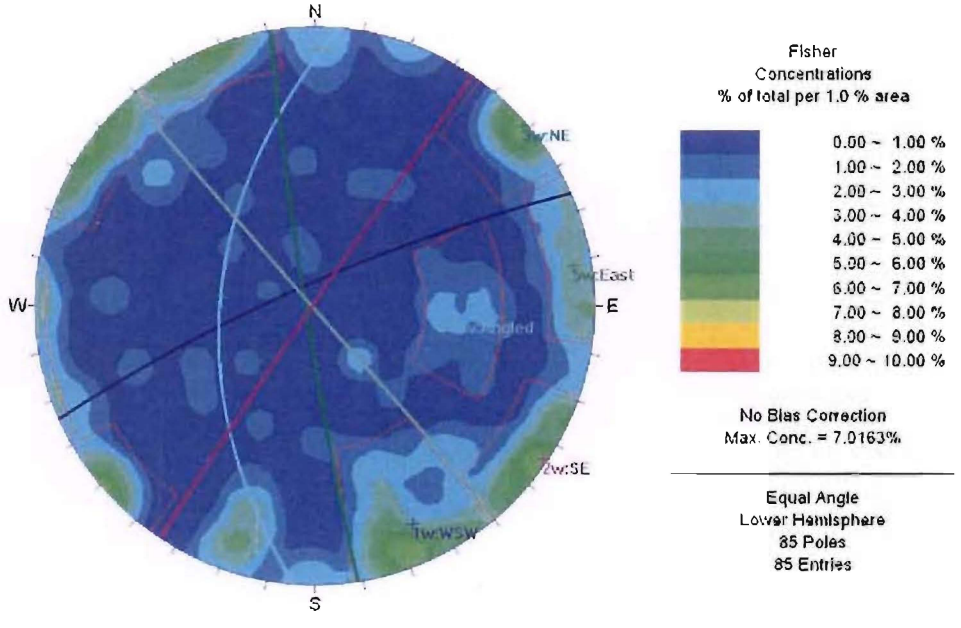

Figure 4.23 Defect concentrations plotted on equal-angle stereonet

Defect set	Strike	Dip	Dip Direction	Count
1	246°	81°	WSW	17
2	214°	89°	SE	11
3	139°	89°	NE	6
4	185°	53°	Angled	9
5	170°	86°	East	9

Table 4.1 Identified defect sets

A final set of defects was identified, though not included in the dips analysis. These defects were infrequent, though where identified they were very persistent and oriented sub-parallel to bedding (Figure 4.24). They were almost always associated with active groundwater flow and commonly bright orange mineralization(?). The sub horizontal nature of these surfaces makes them particularly difficult to identify in the field as they readily accumulate debris and encourage vegetation growth. The defects are inferred to be associated with flexural shear as a result of tectonic activity. This is discussed later in Section 6.1.1.

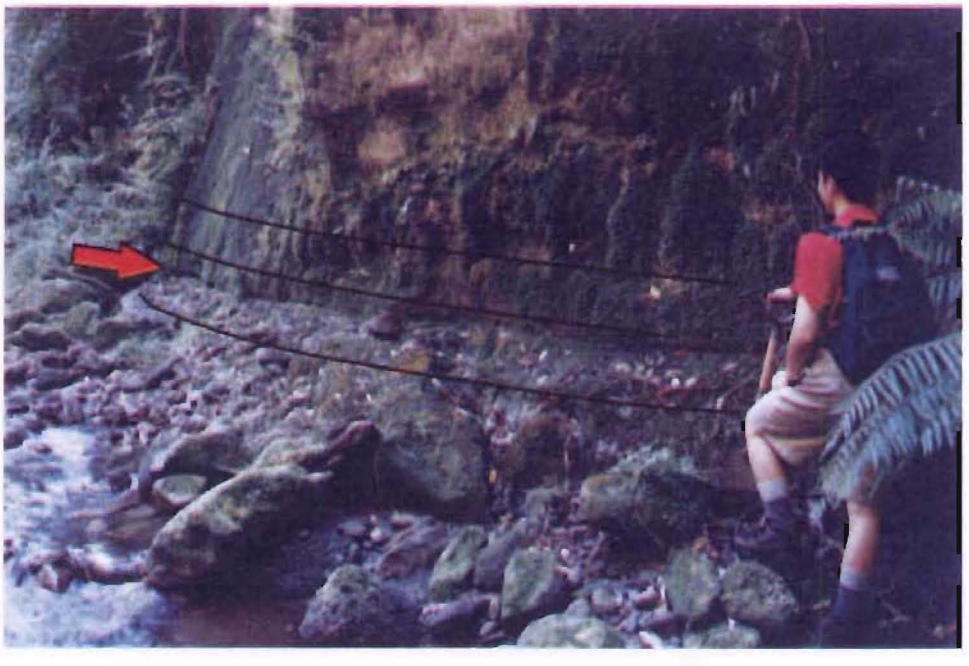

Figure 4.24 Flexural shear defect sub-parallel to bedding

Persistent defect typical of those identified elsewhere in field area. It continues across the stream channel, and can be traced at least 40m downstream. Approximate bedding attitude is indicated in black. Defect orientation is horizontal.

4.4 SUMMARY

The Esk Valley can be divided into five distinct geomorphic domains. Division is based primarily on lithology, followed by the degree of landscape maturation (as described in Section 2.3.1), and hydrology. The lithology and hydrology are the two most important geomorphic controls in the valley, and the high variation in landscape maturity reflects a similarly high degree of disequilibrium in the system.

Indurated lithologies such as limestone and cemented greywacke conglomerates play an important part in defining slope angle and topographic variation.

The entire valley is currently in a state of geomorphic disequilibrium. An evolved upper surface morphology is not currently responding to the high rates of incision taking place in the deep bedrock gorges. This is due to the poor connection between streams within the gorges, and the hillslopes of the upper surface, and can largely be attributed to the broad terraces within the system which act as a buffer zone between the two elements.

A general increase in hillslope stability up through the catchment is matched by greater incision and apparently less stable streams. Narrow bedrock gorges dominate the fluvial system within the upper valley, while sinuous streams in shallow alluvial channels are common toward the mouth.

Irrespective of the complex structure defining the Maungaharuru Range, geomorphic activity in the region is higher than has been seen today. Nonetheless it is an actively evolving geomorphic environment, and continues to be a major long-term sediment contributor to the Esk system as a whole.

Lithologically controlled deep-seated landslides take place on low gradient bedding surfaces are prevalent throughout the central valley, and lie largely within the upper Grassy Knoll Member of the Matahorua Formation. These appear to be sliding on weak, permeable tuffaceous horizons, a similarly weak clean, uncemented sandstone, and tectonically-induced defects in siltstone and sandstone units. Generally, although slide initiation post-dates the onset of incision, activity on the slides is not currently high.

Sediments within the valley display evidence of tectonic influences including faulting, broad folding, and defect generation. Defect orientations align with lineaments described in Section 3.2.

5 STRUCTURAL INVESTIGATION

5.1 INTRODUCTION

Seismic reflection profiles are used in this study to provide insight into subsurface structure. Discrepancies observed during both reconnaissance and field investigations suggested there may be a stronger tectonic influence on basin sediments and active geomorphic processes in the Esk Valley than considered by previous workers (Grindley, 1960; Bland, 2001). These discrepancies included:

- Well-developed lineaments observed in both satellite and aerial photos
- Long river profiles indicating a distinct region in which streams are running above grade
- High sinuosity and incision of rivers
- Faults and persistent defects mapped within the valley
- Highly variable dips within the central region
- Steep dip of Tutira Formation conglomerate in the vicinity of Eland Station
- Uplift of Tangoio block during 1931 earthquake
- Location adjacent to the active Mohaka Fault
- Faults mapped immediately to the north and south

In order to elucidate some of these discrepancies, an interpretation of three seismic reflection lines acquired as part of a 1997 Westec Petroleum survey was undertaken. This was combined with limited results from a 1991 Petrocorp Exploration Limited survey, and work by Beanland *et al.* (1998) approximately 30km to the south.

5.2 METHOD

Interpretation of Westec lines WEC97-1 to 3 formed the basis of this investigation as the raw stacked and migrated data is now open file and readily available. They are located largely within the Esk Valley -- WEC97-2 runs along the boundary of the Trelinnoe study area – and cover approximately 50km (see Attachment 3, Figure 5.4).

As these seismic reflection profiles were undertaken for the purpose of petroleum exploration, the survey and processing was designed to highlight deeper structures. This has resulted in good data extending down to 5s **two-way-time** (TWT), however, data within the upper 0.3s TWT is unfortunately either not available or of very poor quality. The best quality data is in well bedded sediments above the basement greywacke between 0.3 and 3s TWT, and reflectors can easily be traced for several kilometres. Below this, the profile becomes very "noisy". The structural simplicity of the area means the stacked profiles are by far the clearest and therefore used in interpretation – migration, used to restore dipping reflectors, severely reduces visible detail, and is unnecessary for such continuous, sub-horizontal stratigraphy .

Interpretation and correlations were undertaken using Kingdom Suite 2-D and 3-D seismic packages. This was important as the lines surveyed were constrained by available roading, and are therefore not straight. Units were correlated to outcropping stratigraphy mapped by Bland (2001), and interpretation in Beanland *et al.* (1998) based on projected surface outcrop and reflection pattern. As sediments within this section are very similar to those present in the Beanland *et al.* (1998) study, the same average wave velocity of 2200m/s is used to determine approximate thicknesses, and enable clear correlation between the studies.

Unfortunately, only low quality scanned images of sections of Petrocorp seismic lines EC91-2, -3, -4, and NW88-10 are available in Wylie (1993). These have only minimal preliminary interpretation, and little control on the identified structures. A follow-up report (Frontier, 1995) provides two structure contour maps indicating the top of a "Cretaceous unconformity", and the base of an "Oligocene unconformity". These were determined from Te Hoe 1 well data immediately to the north of this study area, and are likely to be accurate ages. The Cretaceous unconformity map was digitised and imported into Kingdom Suite as a surface to allow correlation with WEC97 results.

5.3 RESULTS

Interpreted seismic sections used in this study are provided on Attachment 3 and Figure 5.1, a composite seismic section is provided in Figure 5.3. As described previously, the basin in which the Esk Valley is located contains a thick sequence of largely conformable sedimentary strata that dip gently to the southeast. Beds generally also thin in this direction, reflecting the westerly sediment source of the uplifting axial ranges. The

sediments rest unconformably on westward dipping strata of inferred Miocene (?) age sediments (Beanland *et al.*, 1998), which are in turn cut by steep, westward dipping thrust faults.

A relatively good correlation can be made with outcrop mapped in the Esk Valley, particularly in the upper 1s TWT where a disconformity appears to separate the cyclic sediments contained within the Matahorua Formation from the underlying early- to mid-Mangapanian siltstones and sandstones of the Pohue Formation. This early-mid Mangapanian age disconformity (referred to from here as the **Matahorua Horizon**) is marked by a complex progradational sequence that appears to downlap onto the underlying boundary in the region above the **Wakarara Fault-Trelinnoe Sector** (WFTS) and **Eastern Patoka Fault** (EPF) (discussed later), as well as above deformed Miocene sediments in the east.

Other inferred unconformities in the sequence lie below the Opoitian Maungaharuru Formation, and at the upper contact of the Mesozoic basement greywackes.

The unconformity that marks the boundary between the deformed Miocene sediments and overlying Maungaharuru Group is referred to in Cutten (1994) as the Mokonui Unconformity, and is Kapitean to Opoitian in age (6.5-3.6Ma). This is supported by Opoitian sediments overlying it in the Esk region, however, these are complicated here as the initiation of the Raukumoana fault produces a thick wedge of sediment that extends eastward across the section, and an overlying reflector thins to the east before terminating above the faults deforming Miocene sediments.

The Cretaceous unconformity identified in Frontier (1995) which marks the upper contact of the greywacke basement is supported by a good correlation with both the lower unconformity marked on the seismic sections provided with Wylie (1993) (Figure 5.1), and geological mapping to the north of the region in Cutten (1994). Combined with interpretation of EC91-3 and WEC97-1, this indicates a relatively consistent Miocene sediment thickness to the west of the WFTS of around 700m (Figure 5.3). The unconformity lies on the boundary between discontinuous reflectors sub-parallel to the overlying Mokonui Unconformity, and the typically scattered reflections relating from basement greywackes. There is no evidence on the western side of the WFTS for the formation of the prominent fault-bounded basins evident in the eastern extents of WEC-1 and 3 (Attachment 3).

There are three active tectonic structures within the region. These are all westward dipping reverse faults, and are usually marked by an associated broad doming of the Cenozoic sediments. Due to the homogeneity of sediments in the basin, components of possible dextral strike-slip cannot be identified.

The structures identified are illustrated in Attachment 3 and Figure 5.3, a brief description of each from west to east follows:

5.3.1 PATOKA FAULT ZONE

While the Mohaka Fault appears to have been the dominant structure in the formation of the western ranges, rangefront structures within the **Patoka Fault Zone** (PFZ) have accommodated a substantial amount of contraction. This zone comprises the westernmost faults in the Esk Valley, and the fault strands can be clearly seen in copies of EC91-2 to 4 and WEC97-2 stretching along the foot of the Maniaroa and Te Waka ranges (Attachment 1).

The zone consists of the steep Rukumoana Fault to the west, and two prominent splays, which can be observed on each of the EC91 surveys (Figure 5.1). At the location of EC91-4 these splays are approximately 1.5 and 4.5km to the east of the main fault. They are incorrectly labelled in this section and fault B in fact appears to be the normal Te Waka Splinter Fault discussed in Section 2.2.2.4, indicating the Rukumoana Fault in fact runs north-east along the eastern foot of the range. Displacement increases on each structure as the faults flatten and diverge to the north.

The easternmost of the PFZ splays, the Eastern Patoka Fault is inferred from a strong, gently westward dipping reflector at around 2s TWT in EC91-4, this correlates well with a similar reflector at the western end of WEC97-2 – immediately below a broad c.5km wide anticlinal structure which dominates the profile (Figure 5.2). This structure is likely to be responsible for many of the defects and lineaments noted earlier (see Section 4.3). While the maximum vertical displacement of any single reflector across the anticline is only 0.2s TWT (~220m), it is permeated by a myriad of small faults which criss-cross the section, generally with less than 20m of vertical displacement. They are associated with minor warping of the sedimentary sequence above the inferred termination of the EPF at depth.

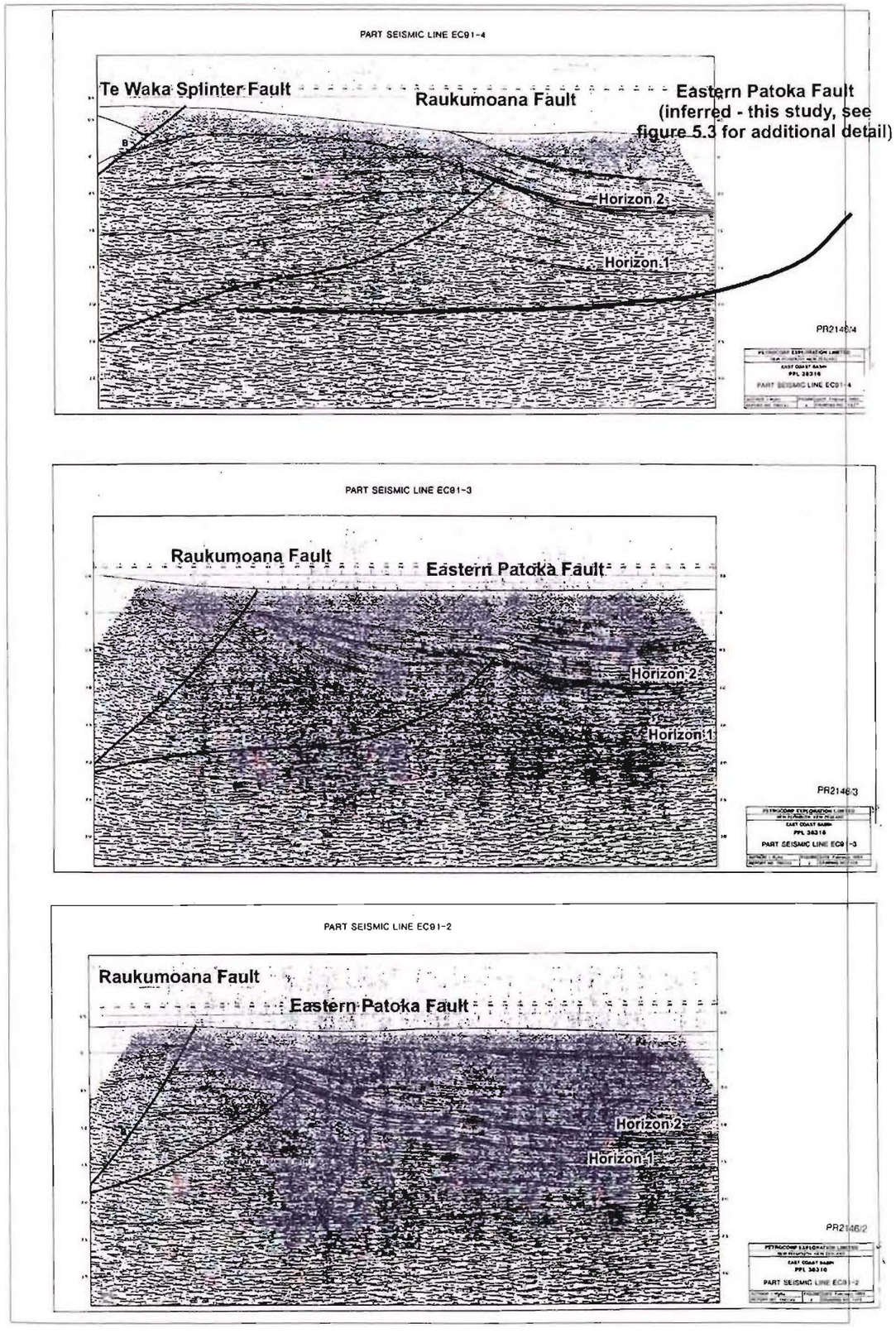

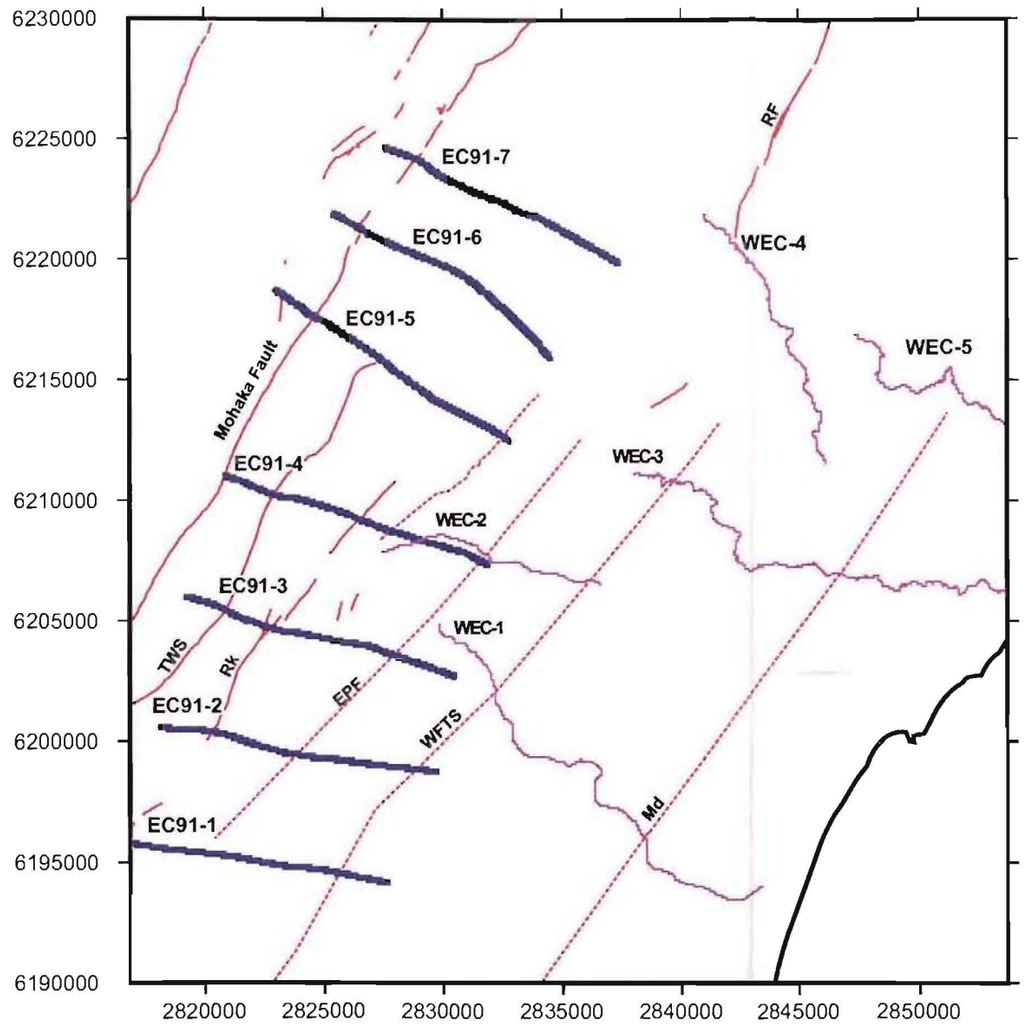

Figure 5.1 EC91 seismic lines indicating location of Raukumoana and Eastern Patoka Fault structures. Seismic lines were acquired as part of the 1991 Petrocorp Exploration Ltd. East Coast Basin seismic survey. Initial interpretation undertaken by Wylie (1993). Re-interpretation of the structures identified in EC91-4 was undertaken in this study, and the Eastern Patoka Fault is inferred from a strong reflector at 2s TWT observed in both this section and WEC97-2 (see Attachment 3). Limited data is available for the 2km at either end of each line, the intial and final 1km is omitted. Horizon 1 is inferred to correlate to the top of the greywacke basement identified in Frontier (1995), Horizon 2 correlates with the Mokonui Unconformity identified in WEC97-1 to 3. Seismic lines and identified fault structures are located on the map above. Solid lines indicate previously identified structures - Mohaka Fault, Te Waka Splinter Fault (TWS), Rangiora Fault (RF), and the Raukumoana Fault (Rk) (adapted from Cutten (1988), Kamp (1988), Neall *et al.* (1995), Begg *et al.* (1994)), dashed lines indicate structures identified in this study - Eastern Patoka Fault (EPF), Wakarara Fault - Trelinnoe Sector

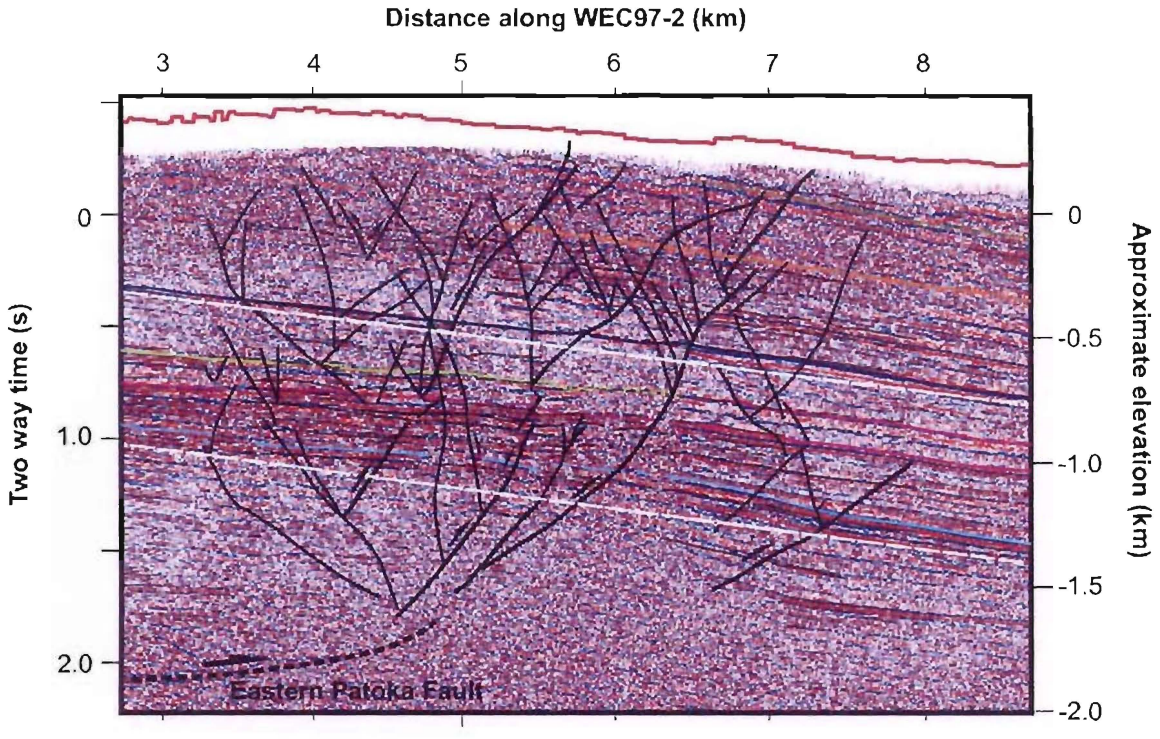

Figure 5.2 Detail of WEC97-2 showing broad anticlinal structure, and diffuse fault zone above the Eastern Patoka Fault

Reference lines are indicated in white, and stratigraphic horizons detailed in Figure 5.3 are also highlighted. Note the dominance of thrust faulting across the axis of the anticline.

5.3.2 WAKARARA FAULT – TRELINNOE SECTOR

The structure identified in the central region of the survey is unlikely to produce coherent surface traces, instead it has developed a c.3km wide zone of minor faulting and jointing as part of a broad eastward dipping monocline (Attachment 3, WEC-1&3). While poor quality data at depth prevents the accurate location of the fault plane, the effects on reflectors above are easily recognisable. Approximately 700m of vertical displacement can be observed from the gently tilted western limb of the monocline across to the sub-horizontal undeformed sediments on the east (see Figure 5.6). Further discussion on this and implications for surface expression are given in section 5.5 (Impact on valley geomorphology).

5.3.3 MIOCENE DEFORMATION STRUCTURES

The easternmost structures in the region are visible at the eastern ends of WEC97-1 and -3 (Attachment 3). Subtle deformation of sediments in this area allows at least two active

westward dipping thrusts to be inferred. These are likely to be a slow continuation of the structures controlling deformation of the Miocene sequence.

These appear to have been active since the Mokonui Unconformity, and are not reactivated structures as might be expected to have occurred during the first recorded uplift event in the forearc (see Section 2.2.2.1). Evidence for this is seen in the distinct thinning of beds over the faults, and downlap relationships which are common throughout the sequence, though particularly in lower parts (Maungaharuru Group).

Petane Group sediments thicken significantly to the east, probably due to the onset of uplift, however a slight thinning of beds can still be identified across the structures. Post-depositional deformation of stratigraphy is evident throughout the sequence, however, it reduces significantly toward the surface – possibly due to a broader distribution of strain in sediments remote from the propagating tip of the structures.

There is considerably more deformation associated with these structures visible to the north in WEC 3 (Attachment 3).

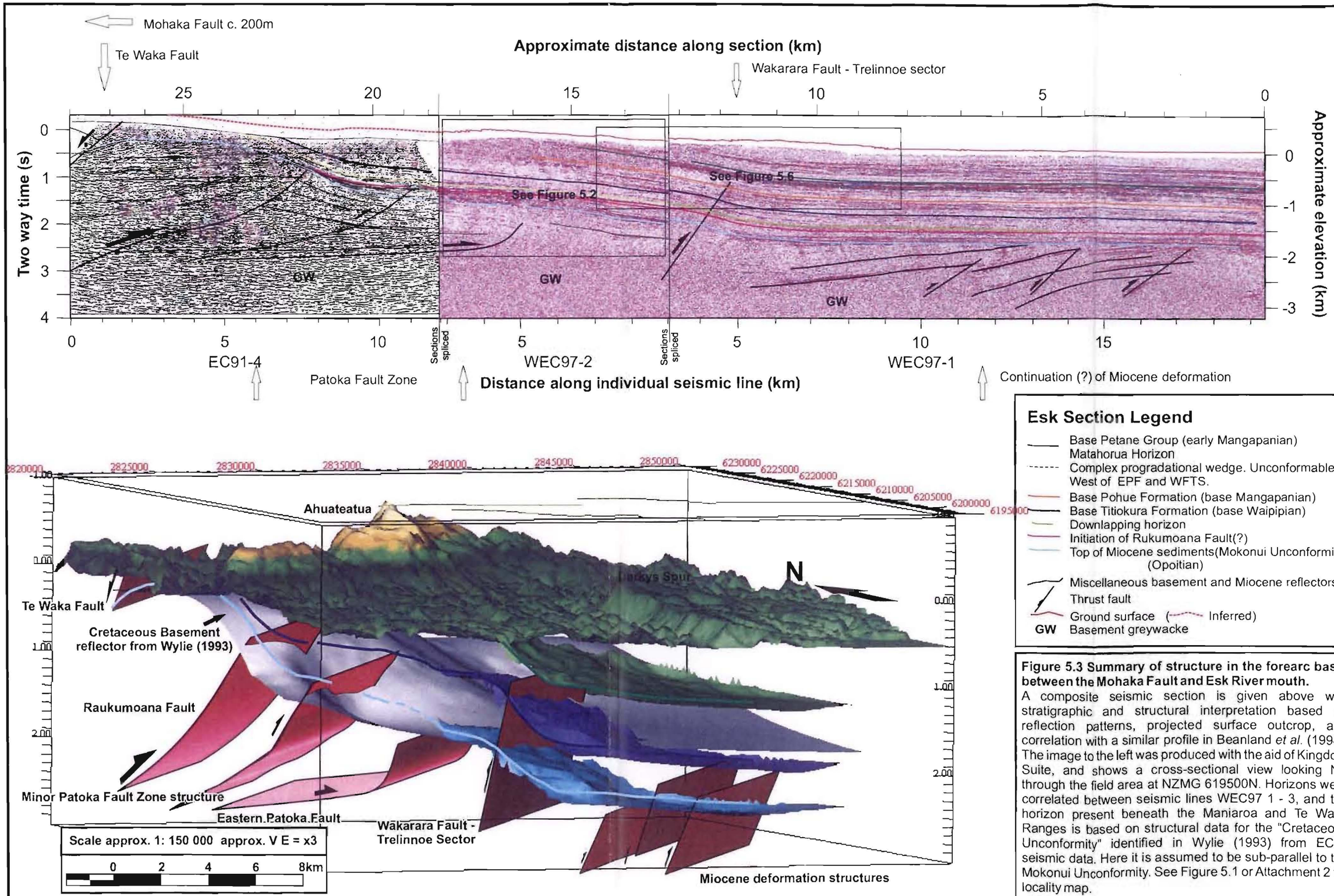

Esk Section Legend

- Base Petane Group (early Mangapanian) Matahorua Horizon
- Complex progradational wedge. Unconformable(?) West of EPF and WFTS.
- Base Pohue Formation (base Mangapanian)
- Base Titiokura Formation (base Waipipian)
- Downlapping horizon
- Initiation of Rukumoana Fault(?)
- Top of Miocene sediments(Mokonui Unconformity) (Opoitian)
- Miscellaneous basement and Miocene reflectors
- Thrust fault
- Ground surface (Inferred)
- GW Basement greywacke

Figure 5.3 Summary of structure in the forearc basin between the Mohaka Fault and Esk River mouth.
A composite seismic section is given above with stratigraphic and structural interpretation based on reflection patterns, projected surface outcrop, and correlation with a similar profile in Beanland *et al.* (1998). The image to the left was produced with the aid of Kingdom Suite, and shows a cross-sectional view looking NE through the field area at NZMG 619500N. Horizons were correlated between seismic lines WEC97 1 - 3, and the horizon present beneath the Maniaroa and Te Waka Ranges is based on structural data for the "Cretaceous Unconformity" identified in Wylie (1993) from EC91 seismic data. Here it is assumed to be sub-parallel to the Mokonui Unconformity. See Figure 5.1 or Attachment 2 for locality map.

5.4 CORRELATION WITH STRUCTURAL STYLE TO THE SOUTH

Structures identified in this study bear a striking resemblance to those detailed in Beanland *et al.* (1998) near the Ngaruroro River, 30km south of the Esk Valley. These southern structures have been investigated in much more detail than those in this study, and a comparison between the two regions provides confirmation of observations as well as important further insight into the nature and activity of the structures. A composite seismic section produced for the Esk Valley (**Esk Section**) is compared with a similar section produced by Beanland *et al.* (1998) (**Ngaruroro Section**) in Figure 5.4.

The scale of the two surveys is markedly different. The composite section for the Esk indicates a maximum depth to the Miocene strata of c.2.3s TWT, the distance between the prominent monoclinal structure in the centre of the line, and the axis of the first active Miocene anticline is c.9km giving a time to width ratio of 1:2.5 . Alternatively, these dimensions for the Ngaruroro Section are c.1.6s, 4.7km respectively, giving a ratio of 1:3.4. This must be considered when comparing the two lines in Figure 5.4, as structures in the Esk Section line are effectively far less steep, and broader than those in the Ngaruroro Section.

Sedimentary thickness and structure correlates well between the lines, however, the actual sediments present obviously vary. East of the major monoclinal structure, Miocene strata dip and thicken in a westerly direction in both lines, and the total vertical displacement on these beds is comparable. The base Waipipian unconformity (c.3.7Ma) identified in the Ngaruroro Section is slightly younger than Opoitian Mokonui Formation sediments resting on the corresponding Mokonui Unconformity (c.5.3Ma) in the Esk, and the base Nukumaruan horizon (c2.4Ma) is similarly younger than cyclic Matahorua Formation sediments (base c.3Ma) downlapping on the relevant Esk Section horizon. Despite this, the thickness of sediments and superficial reflector patterns at each location are very similar. This indicates similar changes in basin environment at each location, and suggests the age discrepancies may be related to diachronous transgressions in a northward dipping basin, a margin-parallel southward propagation of basin subsidence, or sampling errors may be involved in dating and correlating the strata.

Figure 5.4 Comparison between composite seismic profiles in the Esk Valley, and south of the Ngaruroro River (Beanland *et al.* (1998))
Section N-N' is from the southern study. The overlay indicates units and structures identified in this investigation along composite section E-E' within the Esk Valley, and highlights similarities between the sections. For clarity the base Nukumaruan (bWn), base Mangapanian (bWm), and base Waipipian (bWp) reflectors are highlighted in the Ngaruroro Section according to their inferred correlatives in the Esk Section.
Ages given in timescale are equivalent to New Zealand stage boundaries in Morgans *et.al* (1996) (adapted from Beanland *et al.* (1998))

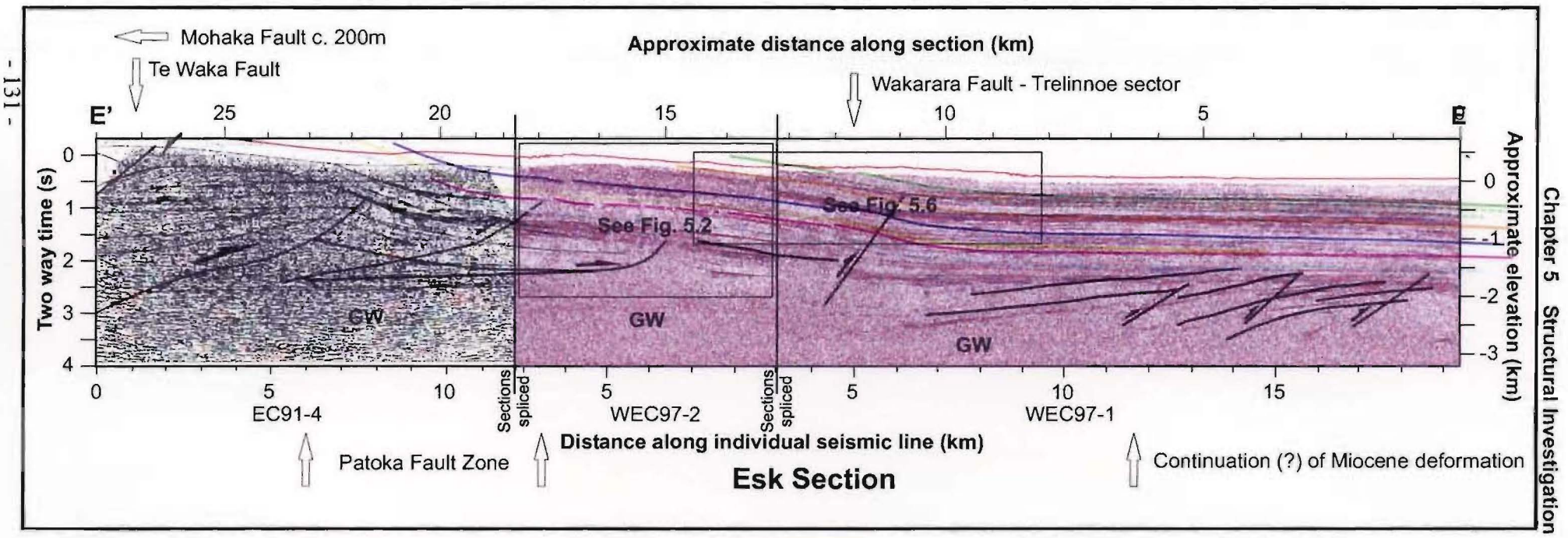

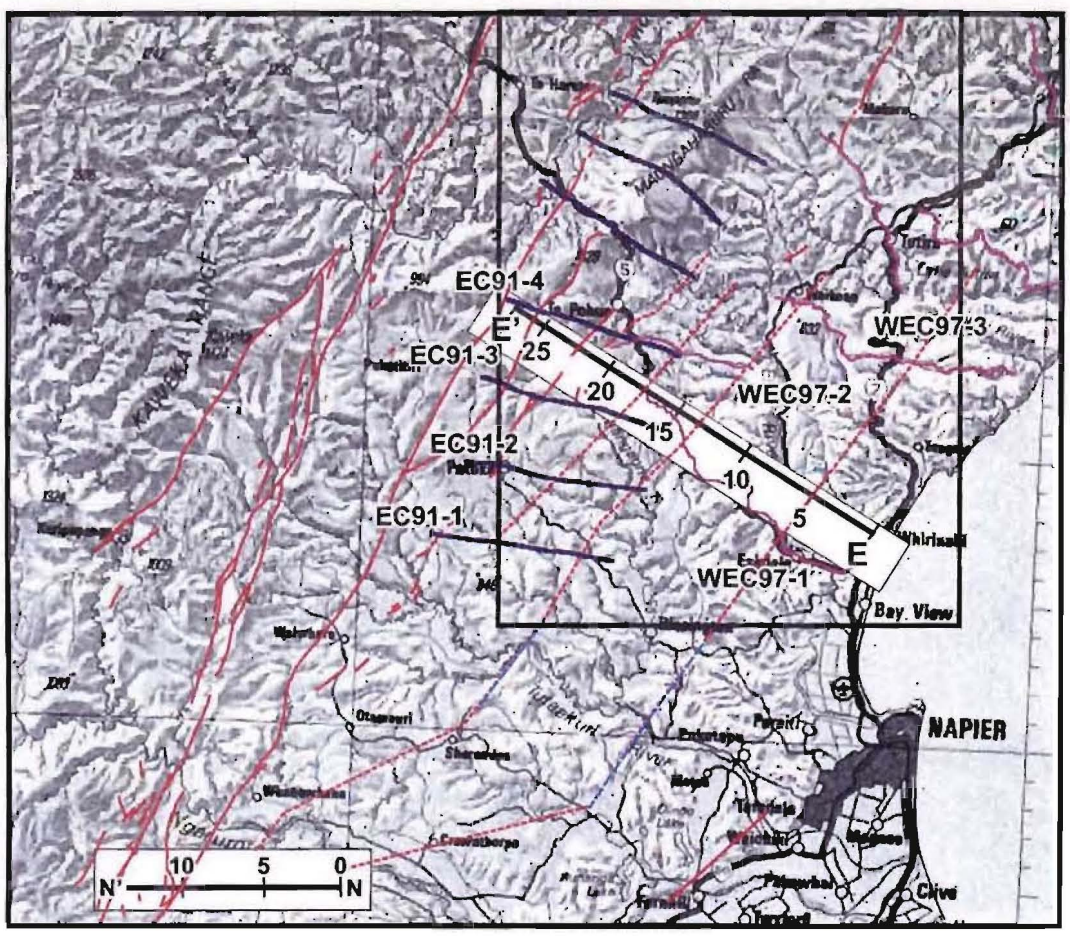

Esk Section Legend

- Base Petane Group (early Mangapanian) (Matahorua Horizon)
- Complex progradational wedge. Unconformable(?) West of EPF and WFTS.
- Base Pohue Formation (base Mangapanian)
- Base Titiokura Formation (base Waipipian)
- Downlapping horizon
- Initiation of Rukumoana Fault(?)
- Top of Miocene sediments(Mokonui Unconformity) (Opoitian)
- Miscellaneous basement and Miocene reflectors
- Thrust fault
- Ground surface (Inferred)
- GW Basement greywacke

Map Legend

- EC91 seismic line
- WEC97 seismic line
- Surface fault trace
- Subsurface fault (Frontier, 1995)
- Subsurface fault (this study)
- Field area

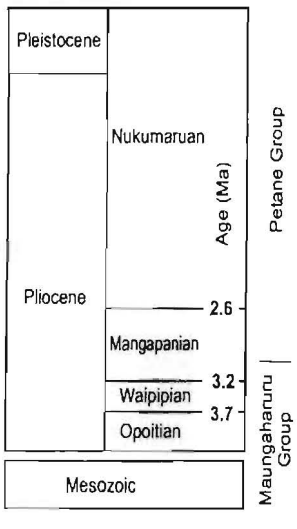

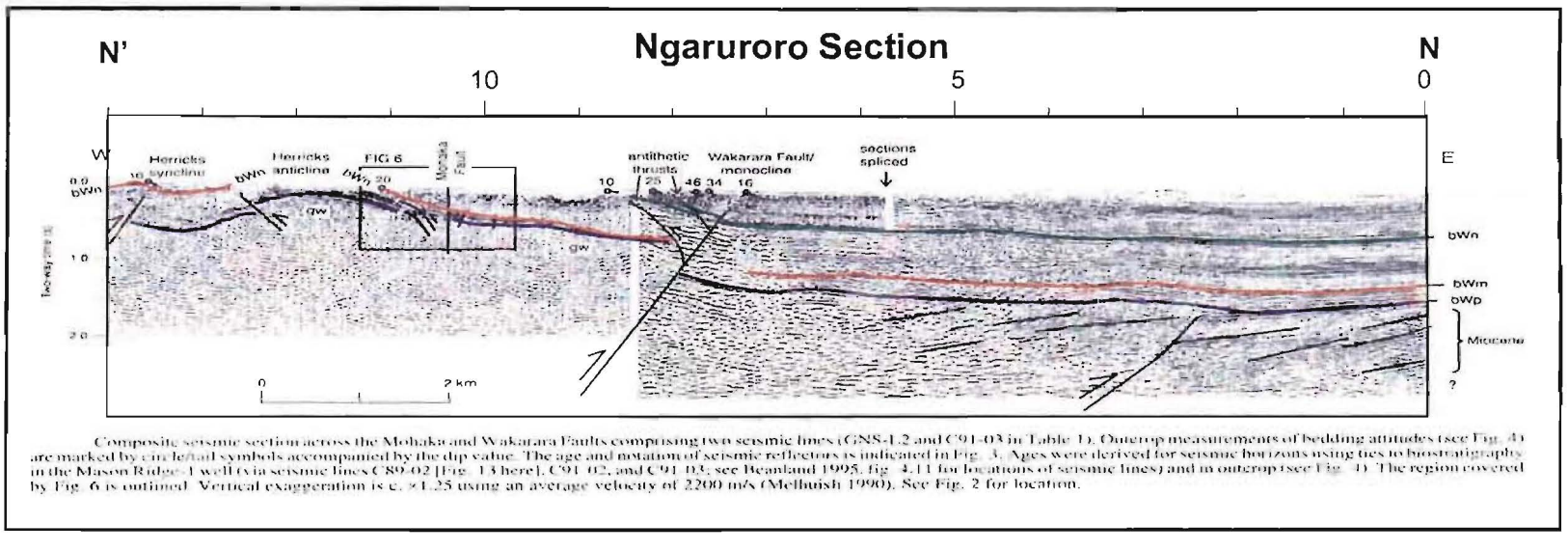

Composite seismic section across the Mohaka and Wakarara Faults comprising two seismic lines (GNS-L2 and C91-03 in Table 1). Outcrop measurements of bedding attitudes (see Fig. 4) are marked by circle/tail symbols accompanied by the dip value. The age and notation of seismic reflectors is indicated in Fig. 3. Ages were derived for seismic horizons using ties to biostratigraphy in the Mason Ridge-1 well (via seismic lines C89-02 [Fig. 13 here], C91-02, and C91-03; see Beanland 1995, fig. 4.11 for locations of seismic lines) and in outcrop (see Fig. 4). The region covered by Fig. 6 is outlined. Vertical exaggeration is c. ×1.25 using an average velocity of 2200 m/s (Melhuish 1990). See Fig. 2 for location.

Interestingly, deformation of the Miocene succession above the basement greywacke is minimal on the western side of the Wakarara Fault at each locality. It is also interesting fact to note the spacing of the faults identified to the west of the Wakarara Fault on both sections, while these structures do not correlate between the two composite cross-sections, the similar spacing may indicate some degree of structural inheritance or equivalence.

Faults identified in each section are identical when profile lengths are adjusted to overlap the structures. Spacing of the structures normal to the western bounding (Mohaka) fault at the location of the Esk Section profile is approximately 1.5 times that of those in the region of the Ngaruroro Section profile, a value equivalent to the increase in forearc basin width between these two locations (see Figure 5.5). This indicates that while over 30km apart, they are in fact likely to be the same structures at each location, and movement rates are directly proportional.

Structures between these two locations indicated to be cutting Cretaceous strata to the west of Napier (source Frontier, 1995) also support this hypothesis (Figure 5.4); as do basic observations of river form across the Heretaunga Plains which indicate distinct changes in the Tutaekuri, and Mangaone Rivers along the projected strike line of the Wakarara Fault/monocline, these match changes in the Ngaruroro River adjacent to the structure at the location of the Ngaruroro Section. While further field investigation is required to confirm these relationships, the monocline/fault identified as striking through the centre of the Esk Valley is therefore defined as the Waikarara Fault – Trelinnoe sector (WFTS).

A final point to note regarding the correlation of Ngaruroro Section structures to the Esk Section is a distinct decrease in shallow earthquake activity that coincides with the boundary between the two sections as shown in Figure 5.5. These earthquakes occur in or above the subducting Pacific Plate, and the decrease in the density of earthquakes may indicate a significant change in processes relating to its subduction. Reyners (1983) suggests a possible model of subducting plate segmentation based on seismological evidence (stress distribution, rupture patterns, recent shallow seismicity), the best defined of the six boundaries he identifies is the southern of the two indicated in Figure 5.5. The intersection of this boundary with faults that bound the western margin of the Forearc coincides closely with the decrease in earthquake density and inferred divergence of the Wakarara Fault and may in some way be related to structural style seen in the Forearc.

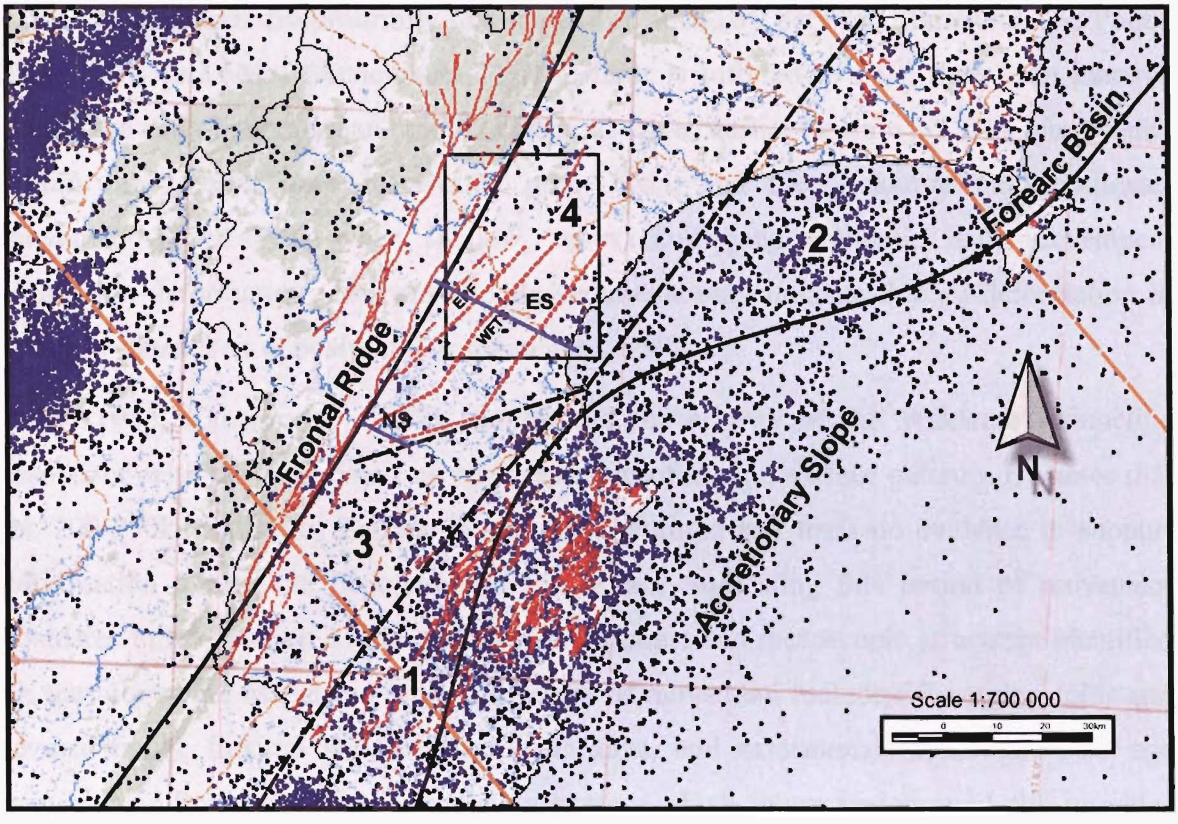

Figure 5.5 Correlation between shallow (<40km) earthquake locations and structure within the central Forearc Basin

Earthquake locations include all those recorded at depths <40km (source Geonet, 2003). The Forearc Basin is divided into four sectors based on the intensity of earthquake activity (1(high) – 4(low)). This activity correlates broadly with the intensity of active faulting in the Forearc (marked in red (Begg *et al.*, 1994)). Faults identified in this study are marked by broken red lines, an abrupt decrease in earthquake density coincides with the region in which the traces are inferred to diverge from the Ngaruroro Section (NS). Note the general lack of seismic activity in the study area. Possible segmentation of the subducting Pacific Plate as noted by Reyners (1983) is indicated by broken orange lines; the area where the southern segmentation boundary intersects the western bounding structures of the Forearc is approximately co-incident with the decrease in seismic activity within the basin and may be responsible for the distinct structural styles.

While accurate slip rates for the Waikarara Fault are not known, a good description and history is given in Beanland *et al.* (1998). It is considered a rangefront contractional structure in their study, and exposures of similar structures show it to dip 60-80° to the northwest, striae on exposures trend within 20° of the fault dip indicating little strike-slip displacement (Erdman and Kelsey, 1992). The fault is a reactivated structure, the timing of formation is not known, however, it was active between 2.8 and 3.2 Ma (early Mangapanian), this correlates well with an up to c.200m thick wedge of sediment that can be traced east from the structure in WEC97-1. This wedge lies immediately below the

early Mangapanian disconformity that marks the boundary between Matahorua and Pohue Formations (c.2.6Ma) (Attachment 3). The fault is inferred to have then been inactive during the early Nukumaruan (c.2.0-2.6Ma). As stated earlier (section 2.2.2.1), many faults within the forearc were reactivated post-1.6Ma, and the Wakarara Fault indicates movement post-2.0Ma, when shallow, eastward dipping antithetic faults developed; significant deformation observed in 1Ma sediments may indicate that all deformation in fact post-dates their deposition (Beanland *et al.*, 1998).

Raub (1985; Raub *et al.*, 1987), investigates the activity of the Wakarara Monocline associated with the fault based on river terrace profiles and surface outcrop. He notes that the 200-750ka Salisbury Terrace is strongly deformed and finds no evidence to support deformation during the deposition of the terrace, indicating this period of movement postdates the deposition of the gravels. Macroscopic and mesoscopic structures identified on the monocline associated with this period of movement include SE verging folds and reverse faults, flexural slip, contractional faults, and extensional faults. The next age control is on Porewan (30ka) aggradation terraces which appear undeformed, this provides a minimum age for the cessation of movement. Finally, he notes localised surface rupture on some terraces during the Holocene indicating limited recent displacement.

While Berryman (pers. comm. in Beanland *et al.*, 1998) notes only "limited evidence of recent faulting or folding" of river terraces near the Wakarara Fault, evidence from river profiles in the Esk valley, and observed changes in river form may suggest the fault is still active.

5.5 IMPACT ON VALLEY GEOMORPHOLOGY

Both active and inactive structures can have an effect on processes operating in a rapidly evolving landscape such as the Esk Valley. Effects can either be direct; in the form of uplift, subsidence, tilting, folding, warping or offset; or they can be indirect and be responsible for the formation of weak zones in rock mass such as defects, shear zones, and favourable bedding orientations which often become the focus for subsequent geomorphic processes. Structures in the Esk Valley, including the Eastern Patoka Fault, Wakarara Fault – Trelinnoe sector, Miocene faults in the east, and the Raukomoana Fault, are all likely to have played a part in controlling geomorphic processes forming the Esk Valley.

5.5.1 EASTERN PATOKA FAULT

The EPF shows very little sign of activity during the deposition of strata that overly it. This indicates, excluding an initial possible movement producing sediments at the time of the Mokonui Unconformity, propagation has been entirely within the last 2My. The pattern of small thrusts appears to become more diffuse toward the surface, and noise in the seismic line makes it difficult to trace any faults much above the Matahorua Horizon (Figure 5.2). It is suggested that at this level contraction related to the propagating thrust begins to give way to extension of the sediments across the crest of the anticline. This, along with the reduction in confining pressure encourages the splaying of the faults. Two ways of accommodating the mass imbalance created through this extension are through normal faulting, and the thinning of beds through flexural shear. Unfortunately neither of these cases can be resolved in the poor quality data of this upper section.

Surface expression of the EPF is likely to mainly consist of many minor extensional structures. It is unlikely that individual splays of the fault zone extend to the surface due to the diffuse nature of the faulting. It is, however, probable that the subtle variations in dip observed in the field are a result of more ductile deformation of sedimentary sequence by faults near the surface. Defects observed are also likely to be the result of this extension. It is unlikely the broad folding would be differentiated in the field purely from surface mapping, however, depending on the timing of deformation, it is considered very possible that stream processes would be sensitive to the degree of deformation.

5.5.2 WAKARARA FAULT – TRELINNOE SECTOR

The Wakarara Fault – Trelinnoe Sector and associated monocline are the easternmost of the range front structures, and mark the boundary between relatively undeformed, flat-lying forearc basin sediments to the east, and those disturbed by the encroachment of contractional rangefront structures from the west. Of the c.700m of vertical uplift observed across this monocline, the vast majority of this (approximately 500m) has taken place since the reactivation of the structure. This deformation therefore affects all strata present above the structure post-2Ma, and is responsible for the marked increase in dips observed in the field to the NW of Eskmount Station. Assuming the structures are in fact related, this vertical displacement on the WFTS since the Matahorua Horizon (2.6Ma) is likely to relate to substantial displacement on the Wakarara Fault between 200ka and 30ka. However, given the large distance between the two sections (30km+), complete lack of data on the

structure relating the two regions, and poorly constrained correlation with the Mangapanian period deformation, timing of displacement may vary by as much as 0.4My (as shown by the variation in unconformity ages in Section 5.4) with movement on one sector of the fault preceding the other.

The WFTS monocline shows little evidence of the incipient faulting so prevalent in the EPF immediately to the west. Instead, sediments generally appear to have been deformed in a more ductile manner. The style of deformation once again appears to change above the Matahorua Horizon, and appears to indicate a significant decrease in stratal strength above the unconformity. Sedimentary formations in the upper portion of the sequence experience the least gravitational loading, and have also experienced less compaction than deeper units. This is likely to have produced less competent lithologies with a lower elastic modulus, that are now held under relatively low confining pressures. All these factors will act to decrease the angle of thrusting within this succession.

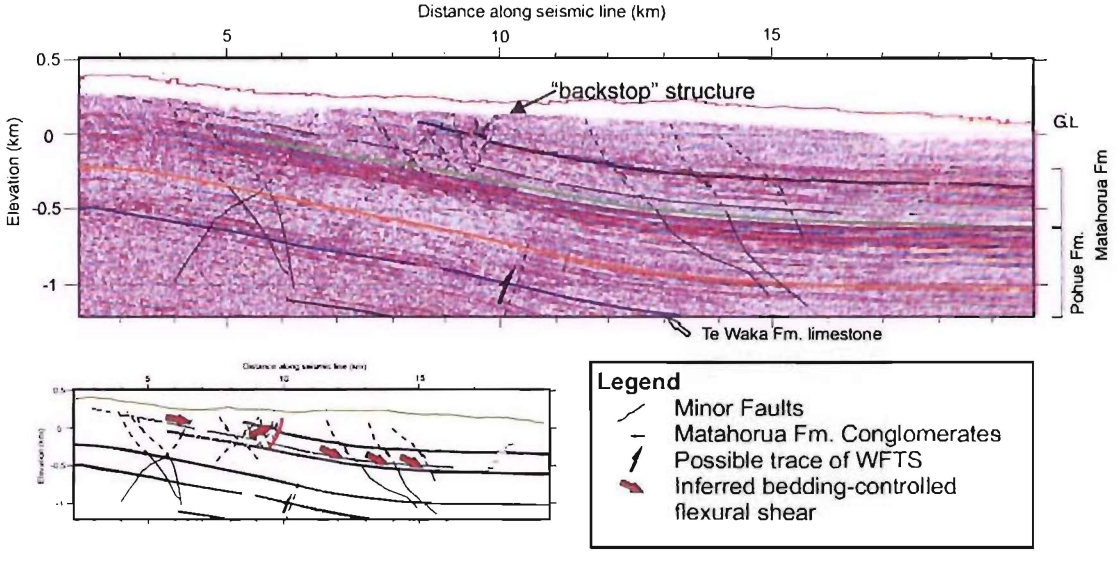

Figure 5.6 Detail of near-surface deformation above WFTS identified in WEC97-1.

Inset indicates backstop mechanism, and possible block sliding on the oversteepened section. Depths are based on an average wave velocity of 2200m/s. A disconformity is inferred to separate the Matahorua and Pohue Formations (green horizon).

Deformation in these upper beds is detailed in Figure 5.6, and can be divided into two zones either side of the 5km mark on WEC97-1, this point marks the steepest part of the fold (average dip of 15°) and is likely to be near the area in which the projected fault plane would reach the surface. A steeply dipping (60°) structure at this point appears to act somewhat like a backstop, dividing the two zones. To the west, reflectors become discontinuous reflecting a high level of disturbance within the sediments. Backthrusts initiated at the junction between this backstop and the disconformity appear to propagate steeply westward, and there may be a slight thickening of sedimentary units in the region. While similar backthrusts are observed on the Waikarara Fault to the south (Beanland *et al.*, 1998), and the quality of data in the upper portion of the profile makes it difficult to confirm the thickening of beds, the contrast between reflection pattern, faulting, and apparent dips across the Matahorua Horizon indicates strong lithological control on the structural processes. It appears that flexural slip and gravitational sliding may be taking place in a wedge of sediment above the disconformity across this relatively steeply dipping section (Figure 5.6).

To the east of the backstop internal deformation of the sediments once again appears to be concentrated in those above the Matahorua Horizon (Figure 5.6). This zone is experiencing compression related to the shortening of sediments in the tightening fold hinge. These faults are well defined, and spaced approximately 200m apart. They dip to the east, and are generally thrust structures. They appear to terminate sharply on the horizon, and the nature of motion suggests these are flexural slip thrusts created by the wedges of sediment slide beneath each other.

5.5.3 RUKUMOANA FAULT

Too little is known about the Rukumoana Fault to determine its influence on the Esk Valley. As is characteristic of many of these structures, while there is little offset of post-Cretaceous sediments evident in seismic profiles, stratigraphy is strongly deformed across the fault indicating considerable dip-slip motion at depth in the basement. The fault has a strong surface trace, whether this is entirely a result of the up to 100m vertical displacement (see section 2.2.2.4), or whether it is related to an unresolved strike-slip component is debatable. As mentioned in section 3.2.2, the strong lineament continues along the foot of the Maungaharuru Range, it is likely this is a continuation of this surface

expression partially obscured by eroded sediments off the range. Unfortunately no seismic lines cross this feature, and its presence is unable to be confirmed.

5.5.4 MIOCENE DEFORMATION STRUCTURES

The Miocene structures to the east of the area show only minimal uplift of surface sediments (~40m). Despite this, they coincide with the sharp bend at the transition from the valley to aggradations plain, and may in some way have influenced the development of this form.

5.6 SUMMARY

The two key structures identified in this study are the Wakarara Fault – Trelinnoe Sector and Eastern Patoka Fault, evidence suggests both of these structures have been active over the last 1my. The influence of these on surface sediments, processes, and landforms is difficult to quantify due to the depth at which they appear to terminate, and diffuse nature of deformation preceding the thrusts. The Eastern Patoka Fault produces a broad (c.5km) anticlinal structure with an associated zone of diffuse thrust faulting. The WFTS induces c.700m of vertical displacement across a gentle monoclonal fold. Brittle deformation appears to be concentrated in the sedimentary sequence above the Matahorua Horizon indicating a change in material properties above this boundary. Both bedding-parallel flexural slip, and significant flexural slip thrusts may be associated with this structure. It it is likely both these structures have been responsible for the formation of defects and steepened dip slopes which have been exploited by river systems and subject to landsliding in the centre of the valley.

The activity and effects of the Rukumoana Fault, and structures associated with the continuation of Miocene deformation, is more difficult to quantify, although it appears these structures have not played a particularly important role in defining basin processes.

6 DISCUSSION

6.1 GEOMORPHIC PROCESS INTERACTIONS

6.1.1 FLEXURAL SHEAR

The process of flexural slip usually occurs in bedded sedimentary strata, and is a result of differential motion between adjacent beds due to tectonic tilting or folding. While this process has long been recognised (eg. Fell *et al.*, 1988; Tanner, 1989; Hutchinson, 1995), the geotechnical implications are only moderately understood, and seldom addressed. This is primarily because the tectonically induced shears have very limited expression in the field, and are not often identified during field investigations – particularly where contributing tectonic influences are muted or not anticipated (Hutchinson, 1995).

Flexural shears are defects in the rock mass parallel or sub-parallel to bedding. Rock mass shear strength across these defects can be reduced to residual levels. The shears are formed as strain – initially accommodated by ductile "flexural flow" – becomes localised along sharp brittleness contrasts in the rock, producing discrete slip planes. Strain is then accommodated along the planes (Hutchinson, 1995) and continued flexure of the beds allows these planes to coalesce and persistent discontinuities to develop.

Strain distribution, and therefore the analysis used, is largely dependant on the geometry of the fold producing the slip. For the analysis of flexural shear Ramsay (1967; Ramsay, 1974) and Hutchinson (1995) subdivide folds into two principal geometries: chevron and rounded. For a rounded fold as produced by the Wakarara Fault – Trelinnoe Sector, the distribution of strain developed in the rock mass is uneven. It is at a maximum at the inflection point of the fold where movement is in a reverse sense with upper beds sliding toward the crest of the fold over lower beds, and drops to zero toward the crest and trough of the fold (Figure 6.1).

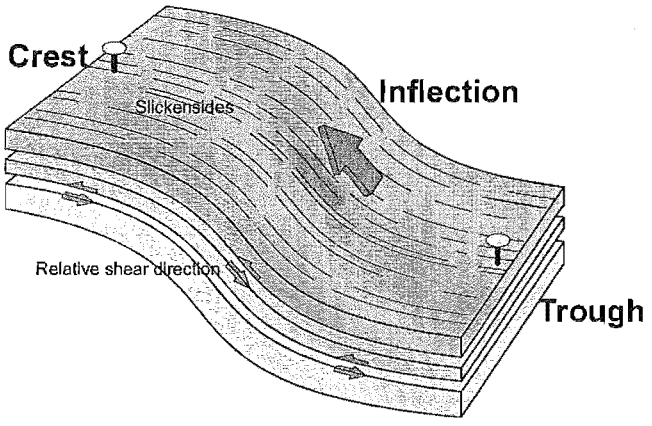

Figure 6.1 Block diagram illustrating shear sense and slickenside formation on a rounded fold.

Shear between beds is in a reverse sense with upper beds moving up-dip relative to underlying beds. Maximum displacement is at the inflection point of the fold. This decreases to zero toward the crest and trough. Slickensides form on slip planes parallel to motion.

Typically flexural shears can be seen as polished, subplanar defects parallel or sub-parallel to bedding. The surface is usually striated in the direction of shearing, and may be associated with strong weathering or elevated groundwater flows. The degree of movement is often difficult to determine due to a lack of "piercing point" indicators on either side of the structure (Skempton and Petley, 1968; Hutchinson, 1988; Tanner, 1989; Hutchinson, 1995). Such defects were identified in the Esk Valley as described in Section 4.3. Striae and slickensides were not visible, however, possibly due to the homogeneous soft sediments producing a fine grit in the gouge zone and evening out surface perturbations. As mentioned in Section 5.4, such shears have been noted within the Pliocene Ashley Mudstone and Upper Sandy Mudstone overlying the Wakarara Fault in the area to the south of the Ngaruroro River (Raub, 1985).

The attainment of a coherent plane on which residual strength exists is critical in terms of the role flexural slip plays in slope stability. This is principally controlled by the degree of displacement of beds across the discontinuity. Skempton and Petley (1968) show that in Pleistocene London Clays more than 10cm of displacement is required to reduce shears associated with faults, landslides, and bedding plane slip to a residual value. This is adopted by Hutchinson (1995), and is also used here as no data is available for Esk Valley materials.

Ramsay (1967) showed that the amount of strain (γ) accommodated across a lithological unit on a rounded fold is directly proportional to the thickness of the unit (t), and is independent of changes in curvature of the surface of the fold – instead depending only on the angle of dip produced by the folding (α) (in radians). This relationship is given below in Equation 6.1.

$$\gamma = t\alpha \qquad \textbf{Equation 6.1}$$

Hutchinson (1988) expanded on this and investigated the effect of brittleness contrasts in adjacent beds. He shows how, theoretically, the degree of displacement (s) imparted on a specific shear plane (initial slip (s_i), and total slip (s_t)) is directly related to the degree of folding (again given by the angle of dip of associated beds (α)), the brittleness index (I_B) of the less competent bed, and the thickness of the beds (competent (t_1), incompetent (t_2), and total ($t = t_1 + t_2$)) (Equation 6.2).

$$s_i = I_B(t_1 + t_2)\alpha \qquad \textbf{Equation 6.2}$$

The brittleness index was first suggested by Bishop (1967), but it is not a widely used descriptor in geomechanics literature. It is simply a measure of the percentage reduction in strength of a material passing from the peak to residual state, and can be derived from a stress-strain curve. It is defined by the equation below (Figure 6.2). Bishop (1967) notes that "this index varies most markedly with stress", and it is therefore of limited use when dealing with shear in a sedimentary sequence as thick as those in the Esk Valley. For near-surface strata in the Esk Valley the value of the brittleness index is assumed to be approximately 0.7, typical of weak siltstones and sandstones.

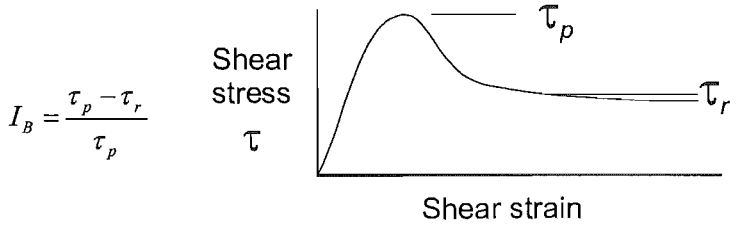

Figure 6.2 Generic stress-strain curve and equation to illustrate brittleness index

Displacement on a flexural shear occurs within the less competent bed, generally at the contact with the more competent one. As the failure within this bed is controlled by the strain distribution across it, the thickness of the bed in relation to that of the competent bed is important. The maximum degree of flexural shear is therefore produced when the pair consists of a thick competent bed and a thin incompetent one (Hutchinson, 1995). The vertical spacing of the shears also plays a part, as the total strain is distributed between them and a large number of closely spaced shears will each have a much lower displacement than a few widely spaced ones.

It is difficult to take the two layer approach of Hutchinson (1995) when calculating the degree of flexural shear across the WFTS simply because of the scale of the disturbance, and inherent difficulties in identifying weak layers and quantifying their shear strengths. Analysis of seismic profiles in section indicates a change in material properties above the Matahorua Horizon. Deformation of the sediments above this appears to be at least partially lithologically controlled-indicating favourable conditions for the formation of flexural shears. The maximum dip of these beds across the WFTS is 15°, and removing the 2° dip induced by regional tilting leaves 13° of WFTS associated folding. Given the c.1km thick sediment pile in this area (see Figure 5.6), and applying Equation 6.1 the total maximum strain accommodated through these sediments is 226m, or 22.6%. While much of this is likely to be accommodated internally as plastic flexural flow, this is considered sufficient to also produce significant flexural shear planes throughout the sequence.

6.1.2 DEFECT GENERATION

Five defect sets were identified in the field investigation. These correspond well to the orientation of lineaments identified in the reconnaissance stage of the investigation, indicating the lineaments are likely to be a result of strong defect control, and defects present are likely to be laterally continuous.

As defects are related to stresses on the rock, it is natural to investigate the relationship between the defects and active structures in the valley (the EPF and WFTS). Monoclinal folding associated with these structures trends NNW at a bearing of 033°. The location of these structures corresponds with the location of the strongest lineaments.

Of the four sub-vertical defect sets identified, set 2 parallels the trend of the structures, set 1 – the strongest set – strikes 32° to the east of this, and set 3 and 5 strike to the west. The strike of these final two is similar, and they are interpreted as being related. The

combination of sets 3 and 5 produces an equivalent number of defects to that of set 1, and the average strike is perpendicular.

This information, combined with the lack of any other local tectonic sources suggests these defects are primarily a result of stresses imposed by the formation of the WFTS. An idealised block diagram showing defect generation as a result of the formation of a rounded monoclinal fold is given in figure. Here, plane **A** is parallel to the fold axis and is an analogue to set 2 identified in the field; this is likely to be produced by extension across the fold. Planes **B** and **C** relate to set 1 and 3+5 respectively; these conjugate defects are localised reflections of the regional stress field responsible for the thrust propagation and indicate a principal stress defined by the bisector of these planes.

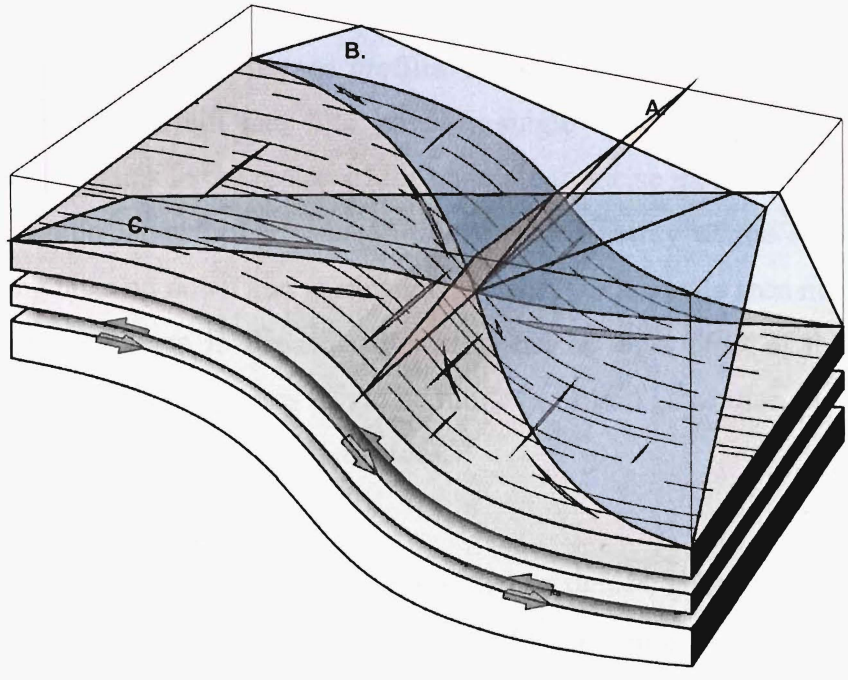

Figure 6.3 Idealised block diagram detailing defect generation across a thrust-propagated fold

In the field plane **B** and **C** represent defect sets 1 and 3+5, and are perpendicular to each other, but rotated 13° anticlockwise from the symmetrical arrangement with plane **A** (set 2). This may be associated with some influence from defect set 4 and local bedding on defect generation.

6.1.3 STRUCTURAL CONTROL ON RIVER FORM

As suggested in Section 5.4, the WFTS has a similar displacement history through the Pliocene as the Wakarara Fault to the south of the Ngaruroro River. This displacement history could possibly be extrapolated to infer the significant post Matahorua Disconformity (2.6Ma) vertical offset in the Esk Valley to have taken place within the last

200ka, as well as a period of minor faulting in the Holocene. However, the age control on the histories, and the understanding of the relationship between the two faults is too poor to confidently make this extrapolation and may involve an error of as much as 400ka (Section 5.5.2).

6.1.3.1 Long river profile

While, as discussed in Section 3.3.1.3, complications associated with the acquisition and grid interpolation of base data inhibits the reliability of the area of inferred uplift, the consistence of the anomaly throughout the valley is inferred to suggest a true perturbation in the river system. This anomaly, initially inferred to relate to a single zone of uplift in the central region, is now known to coincide with a combination of the WFTS and EPF structures. Though it is impossible to tell the degree of uplift from this data, based on the lack of deformation noted on terrace profiles it is unlikely to be high. It is, however, possible an increase in uplift rate – or possibly single uplift event early in the stream incision – forced streams in the region of the anomaly to incise more rapidly than in other reaches. This would have further reduced the restricted ability of the streams to erode laterally, forcing incision down into narrower channels. The anomaly seen may simply be a reflection of this reduction in the channel width, and be an artefact of the cartography process (as visibility into the gorges would be limited), or grid generation (which would be unable to resolve channels less than 25m wide).

6.1.3.2 River Sinuosity

The sinuous form of the rivers is strongly controlled by defects generated by the structural warping. This indicates defects were significant factors in valley morphology at the onset of incision and therefore the WFTS and EPF must have also been substantially developed. This is not surprising considering the degree of displacement evidenced from deformed sediments in seismic section.

There may be a general increase in sinuosity across the EPF and WFTS structures. The lack of a distinct change in the pattern suggests that deformation as a result of activity on either structure during terrace formation is unlikely to be high. Tectonic tilting of the valley as a result of regional uplift combined with low flows and heavy sediment loads is likely to be largely responsible for the highly sinuous form of the Esk tributaries prior to incision. An apparent increase in their sinuosity since incision is likely to reflect a

reduction in the incision rate as the channels are reaching grade and rivers are tending toward a braided form.

6.1.4 SIGNIFICANCE OF TERRACES

6.1.4.1 Geomorphic environment

The terraces throughout the Esk Valley represent a period in which constructional landscape processes – particularly tectonic uplift – were dominant. Streams were transport-limited as sediment produced through degradational processes exceeded the sediment transport capacity of the valley. The manifestation of this was in a landscape consisting of steep meandering streams working across broadening aggradational valleys and facilitating the continued degradation of relatively unstable subaerial landforms and hillslopes recovering from the previous intense fluvially driven degradation of the last interglacial (128-112ka) (Section 3.3.3.2).

While the streams facilitated the degradational process by removing colluvium, they were not actively driving it, being sediment choked and unable to access bedrock. As hillslopes were left to attain equilibrium during late stages of the last interglacial and much of the last glacial, both shallow and deep-seated landslides are likely to have been prevalent. With minimal incision or stream-generated erosion taking place, these slides would have eventually run themselves out, and remaining material then excavated through moderate fluvial activity.

Examples of such relict landslides include the evacuated slide planes noted both to the east and west of the Northlands landslide, and the Deep Stream landslide complex (which lies at the transition point between upper and lower Esk River terrace profiles) (Attachment 1). While the latter of these slides shows evidence of activity since the onset of the current period of stream incision, the degree of movement indicated by the long, linear dip-slope headscarps indicates significant toe erosion has taken place throughout the slide's history. It is likely the failure was initiated during the last interglacial and continued to creep throughout the glacial. The latest period of incision has rejuvenated the failure by creating greater void space at the toe.

The formation of a sequence of periodic aggradational terraces in a system only occasionally incising into a rapidly uplifting last glacial landscape has been noted elsewhere on the east coast by Berryman *et al.* (2000) (Section 3.3.3.2). While limited incision is likely to have occurred since the last interglacial, this sequence has not been

identified in the Esk Valley, and it is possible a combination of limited incision, strong lateral planation, and considerable mass-movement driven landscape adjustment throughout the glacial has overprinted much of the evidence for previous terrace levels. Incision is, however, unlikely to have been sufficient to significantly destabilise hillslopes and generate further periods of deep-seated landsliding.

The current period of incision within the catchment is likely to have been initiated c.10ka as a result of increased precipitation in the headwaters allowing the system to adjust its grade to accommodate regional uplift that took place during the last glacial. Given the sinuosity of both modern and ancient channels throughout the valley, and the relatively strong influence of the defect control on river form, it seems likely that the majority of incision took place during periods of low flow. The reduced power of the stream in this state would have emphasised the minor contrast in strength between the soft bedrock and defect planes, and abrasion, slaking, and dissolution are likely to have been the dominant erosional processes.

Based on an average annual incision-related sediment production of 96,000 m^3/yr (Section 3.3.3.4), and the sediment rating curves discussed in Section 2.3.3.3 (and given in Appendix B), an average flow of 21m^3/s in the lower Esk River channel is required to transport all the sediment, well above the 5.3 m^3/s mean flow. This implies that, although the majority of incision has taken place during low flow conditions, flood flows are required to transport sediment through the system.

As indicated by the sediment rating curves, negligible sediment is transported during normal flow. Given the rate of sediment transport during a normal 2 year flood flow (1.06m^3/s at 200m^3/s) (Williams, 1986), the average volume of sediment produced through incision can be transported out of the system if the river flows at this rate for 2 days per event. While this is considered long for the hydraulically responsive catchment, given other high flow events that take place, it is probable that very high flow (1:10yr+) events are not required to transport the sediment generated through channel incision.

6.1.4.2 Terrace discontinuity

An important aspect of the terrace investigation was the identification of a prominent break in the profile of the main Esk River terrace in the region surrounding the Deep Stream confluence. While the reason for the discrepancy, and ages of the upper and lower terrace surfaces, are not known, the age of abandonment of these surfaces is inferred to be

Ohakean (18-10ka) (Section 3.3.3.4). It seems likely that high sediment inputs from the Maungaharuru Range gravitational collapse and Deep Stream landslide complex played an important part in determining stream processes and therefore defining the terrace profiles, particularly in the region of the Upper Esk terrace. Such significant sediment inputs are absent in the mid to lower Esk Valley catchments.

The trace of the monocline associated with the WFTS crosses the Esk River approximately at the location of the terrace discontinuity. The correlation of activity on the Wakarara Fault with the WFTS as described in Sections 5.4 and 6.1.3 indicates substantial uplift (500m) of the north-western side of the structure may have taken place between 200ka and 30ka. It seems, however, that this uplift may have ceased in the Esk catchment prior to the establishment of the base level defining the upper surface (possibly mid interglacial, c.125ka).

The above conclusion can be tested by investigating possible outcomes if the fault pre-dates terrace formation.

- If the terrace is a single age throughout the valley, the discontinuity in the profile could then be inferred to represent the final stage of uplift on the WFTS. If this were the case, the same distortion should be evident on the terrace surface across the monocline in the Kaiwaka and Otakowai catchments (Attachment 1). These profiles show no apparent distortion associated with the structure (Figure 3.6 Terrace profiles and location map for Esk Valley).
- Alternatively, if the Upper Esk Terrace represents an older level than that in the lower valley and displacement on the anticline has occurred since the older surface, but ceased prior to the younger terrace formation, a similar break in the profiles may once more be expected in the tributary catchments where remnants of the older surface may be expected to be preserved in the upper catchment.

With a localised tectonic effect therefore excluded, it is hypothesised the Upper Esk Terrace surface may represent base level defined by last interglacial incision (not dissimilar to that seen in the catchment today) to which subsequent landscape adjustment occurred. It is possible that, despite the elevated levels of precipitation from the Maungaharuru Range, exceptionally high sediment inputs from both the range and Deep Stream landslide complex overwhelmed the system, and minor glacial period variations in

incision rate were therefore insufficient to drive incision and further reduce base level in the upper catchment.

In the lower catchment (tributary domains 1 and 2), where such large-scale deep-seated landslides are not present, limited incision (c.20m) and profile adjustment was possible during warmer periods, and the catchment re-graded to the Ohakean terrace level.

A comparison of the Upper Esk terrace profile with that of the Esk River today can be used to investigate the possible origin of the Upper Esk terrace profile. If base level in the upper catchment was defined by a hybrid or detachment-limited channel under similar climatic and tectonic conditions as today, then the profile of this – allowing for slight regional tilting – may be expected to have a similar longitudinal profile to the current channel (if this is at grade). Comparing the upper terrace and Esk River longitudinal profiles as given in Figure 3.6 indicates these grades are remarkably similar, affirming the assumption that the upper terrace profile may represent an incising hybrid or detachment-limited system, while also suggesting the modern Esk River may be nearing grade.

A further check on this comparison is to compare the uplift rate as described by the elevation difference between the graded profiles below Purahotangihia to that of Castlecliffian strata that would have been present above the Tangoio block prior to erosion (Figure 6.4). These strata are thought to mark the initiation of regional uplift (Kamp, 1992). Given a vertical separation of the graded profiles of 80±10m and late last interglacial age of 120±5ka, this gives an uplift rate of 0.67±0.11mm/yr; comparable to that of $0.81^{+1.16}_{-0.11}$ mm/yr derived for Purahotangihia since the deposition of the Castlecliffian sediments (based on an elevation of 650±20m and an age of $0.8^{+0.10}_{-0.46}$ Ma).

A similar calculation can be undertaken for the inferred channel levels at the western end of the Lower Esk Aggradational Valley geomorphic domain (Figure 4.3). This provides an uplift rate of 0.37±0.1mm/yr, expectedly lower than that in the upper valley considering the regional tilting taking place. Castlecliffian sediments located below the trig at the SW extent of the Waipunga ridge (Haywick *et al.*, 1991) can again be used to check this rate. These are accurately located at an elevation of 291m; given the same estimated age, an uplift rate of $0.36^{+0.49}_{-0.04}$ mm/yr is obtained. While these figures are based on several assumptions, and errors are large as a result of poor age control, the close correlation at both sites helps strengthen the validity of the assumptions, and suggests uplift may have been relatively constant over the last 800,000 years.

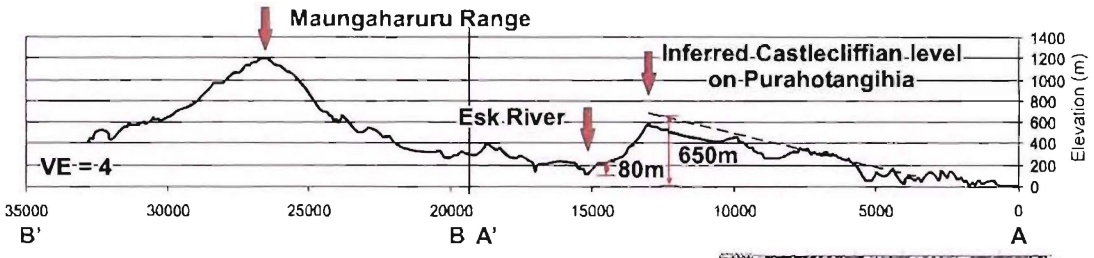

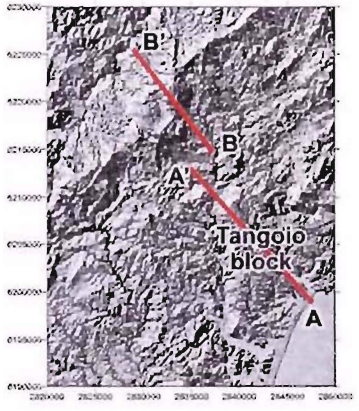

Figure 6.4 Illustration of dimensions used to derive uplift rates in the upper Esk Valley

A lithologically controlled dip-slope dips SW from Waipunga Ridge to the coast. Scattered outcrops of Castlecliffian conglomerate indicate the age of the final depositional event prior to uplift. A bedding surface defined by this outcrop is extrapolated up-dip to Purahotangihia. The uplift rate required to raise this surface 650m at Purahotangihia correlates well with an inferred 80m post-interglacial base level uplift in the Esk Valley.

6.1.4.3 Implications for hillslope development

The form of long-term mass movement driven hillslope evolution postulated in Section 6.1.4.1 for both the upper and lower catchment, has important implications for present day catchment stability. Slopes generated in this regime are likely to be mechanically stable and have well evolved profiles.

As slopes are suggested to have developed largely as a result of post interglacial mass movement into a fluvial system that was primarily transport-limited, deep-seated landsliding is likely to have developed to a stage at which all mechanically and geometrically feasible failures have been exhausted. This explains the lack of deep-seated failures above the Upper and Lower Esk Valley terrace surfaces. As there is currently minimal fluvial activity taking place on this upper surface, it is unlikely further deep-seated failures will be triggered.

While it is suggested that there has been minimal incision in the upper catchment since the last interglacial (excluding that currently taking place), limited incision may have taken place in the lower catchment – as indicated by the lower Esk terrace profile 20-30m below that described by the extension of the upper terrace near the mouth of the river Figure 3.6. This incision may have lead to a slightly less stable lower catchment, and combined with lithological contrasts as described in Section 4.1, may be part of the reason for the disparity in landscape ruggedness between the upper and lower catchments.

Typically vegetation is more sparse during glacial periods, and this is reflected in the lack of organic matter observed in the terrace gravels. (although most would have since been oxidised and therefore not preserved). The lack of substantial vegetation, particularly in the upper catchment, would have produced shallow slope stability conditions not unlike those produced by the pastoral conditions present in the catchment in 1938, and it is likely slopes are therefore graded to a similar level of stability.

The age of terrace abandonment (c.10ka) therefore provides a minimum age for the majority of the landforms in the lower valley (excluding relatively minor subsequent adjustment primarily due to the effects of increasing soil depth related to production through slaking and chemical weathering of the bedrock). It also provides a maximum age for the initiation of many of the processes that currently dominate the catchment today (deep-seated landsliding, river incision).

6.1.5 SUMMARY

Geomorphic processes in the Esk Valley are intimately linked. To develop an understanding of any aspect of the valley system requires an assessment of all the major contributing factors: tectonic activity, climate, fluvial processes, and mass movement.

Tectonic activity has possibly been the single most important process in the Esk Valley over the last 800ka. Consistent regional uplift has differentially uplifted the valley, with maximum rates occurring near the Maungaharuru Range, and dropping off to near zero at the coast. The Wakarara Fault – Trelinnoe Sector has locally increased dips, induced flexural shears, and along with the Eastern Patoka Fault and Miocene deformation structures, induced a persistent pattern of defects in the valley. While the long-term regional pattern of uplift is ongoing, significant activity on the structures beneath the Esk Valley appears to have ceased prior to 120ka. Evidence suggests there may have been a limited rejuvenation of the structures in the last 10ka.

The primary climatic influence on valley morphology is associated with the variation of sediment generation, stream power, and base level adjustment between glacial and interglacial periods. This has affected the rivers' ability to adjust to tectonic influences, and therefore defined their form, and the dominant channel processes. Climate has also had a major effect on vegetation in the valley and therefore helped define hillslope stability and processes.

Fluvial processes have been important in defining valley form, and controlled rates of topographic adjustment as well as the evolution of hillslope profiles. It is inferred that during the last interglacial, incision rates were similar to those today. Once rivers rapidly reached a stable base level (as defined by the profile of the Upper Esk terrace), they began to plane laterally and undercut valley walls. This incision is likely to have triggered the deep seated gravitational slope deformation on the Maungaharuru Range as well as many deep-seated landslides in the channel walls, and initiated a period of rapid hillslope adjustment. This lead to the formation of the Upper Esk Valley terrace we see today, and it is also suggested to have triggered the Deep Stream and Maungaharuru Range landslides.

The end of the interglacial saw stream power reduce, and with active shallow and deep-seated landsliding continuing in the catchment, rivers became sediment choked. Lacking the power to incise and keep pace with tectonic uplift, they developed broad meandering forms to maintain grade with the continued uplift and facilitated the transport of sediment out of the system. Hillslopes were left to adjust through mass movement, and exhausted opportunities for landsliding, creating stable landforms and slopes. Minor incision occasionally took place in the mid to lower catchment, most likely during glacial warm periods. However, high sediment yields from the upper catchment prevented this incision from propagating up the channel.

The onset of the present interglacial marked a return to rapid incision in the catchment. Meandering, low-power streams incised along defects, and today much of the catchment appears to be nearing grade.

6.2 LANDSLIDE INVESTIGATION

Deep-seated landslides investigated in the Esk Valley can be classified in two groups; the massive translational regressive failures on the eastern face of the Maungaharuru Range, and low-angle translational failures within the Grassy Knoll Member.

6.2.1 MAUNGAHARURU RANGE

6.2.1.1 Landslide model

Despite apparent similarities, the landslides on the Maungaharuru Range each display quite different characteristics. This makes it unsuitable to formulate a "typical" model for their mode of failure. Instead their activity, and therefore the value of their sediment input, is better examined in terms of the activity of the underlying driving mechanism and the contribution of recent geomorphic change. Unfortunately the deep-seated gravitational

slope deformation proposed here as the mechanism responsible for the generation of these landslides is only poorly understood; however, some insight can be gained by considering the plastic sediment deformation required for this model and structural control associated with the uplift of the range.

6.2.1.2 Age and activity

It is extremely hard to determine a maximum age for landsliding on the Maungaharuru Range as critical data relating to the rate and nature of the structure uplifting the range is not known. An absolute maximum age can be gained from the presence of Castlecliffian sediments on the Tangoio block, if these sediments were extrapolated across the valley they would overly the Maungaharuru Range (Figure 6.4). Given maximum uplift rates are likely to be adjacent to the Mohaka Fault, and structures within the basin uplift the range with respect to the Tangoio block, the extrapolation of the Castlecliffian sediments indicates the Te Waka limestone that currently defines the form of the range was most likely not yet exposed at the time of this deposition. The age of this unit's deposition therefore probably represents the initiation of uplift and subsequent incision of the Esk Valley at a time when there was negligible relief on the Maungaharuru Range, offering an absolute maximum age for the initiation of any landsliding on the range of $0.8^{+0.10}_{-0.46}$ Ma.

This rather unsatisfactory age control can be improved upon if it is assumed upper surface hillslopes in the Upper Esk Valley are in fact a product of landscape adjustment to a new base level defined by aggressive incision during the last interglacial as suggested in Section 6.1.4. It is possible that the rapid unloading and removal of lateral support around the base of the Maungaharuru Range related to this adjustment is responsible for the initiation of the DSGSD. Given time for sufficient sediment removal in the valley, and the DSGSD to develop, the landslides evident on the slopes of the Maungaharuru Range are likely to have initiated during the early- to mid-glacial period (120-60ka). However, maximum movement rates probably took place during the mid- to late-glacial (c.80-18ka) when all lateral toe support is likely to have been removed and plastic deformation had been fully developed. Excluding unconstrained structural factors, and assuming the 300m of subsidence on the top of the range is wholly related to the development of the DSGSD, this gives an average subsidence rate in the basin on top of the range of 2.5mm/yr.

Landslides in this area do not appear as active as they may have been in the past, suggesting the driving force is in fact no longer sufficient to sustain previous failure rates. Increased gravitational loading as a result of the accumulation of snow during glacial climates could possibly explain the apparent increased activity during the last glacial,

however, this is unlikely given the upper slopes of the range were 500m below the snow equilibrium line altitude (McGlone, 1980; Pillans and Moffat, 1991; Pillans *et al.*, 1993) and substantial accumulation would not have taken place. A possible short- to medium-term factor could be increased pore pressures from the inferred landslide dammed lake (Section 4.1.6).

6.2.1.3 Geomorphological implications

The geomorphological implications for this type of movement on the Maungaharuru Range can be considered in terms of the proposed rotational nature of deformation. This means the deviatoric stress is constantly reducing as material rotated up in the "toe zone" resists movement. While this reduction in deviatoric stress may be facilitated by uplift of the source area, shallowing of the zone of failure, or sediment stripping off the front of the range (see Section 4.1.6.2).

Evidence for the decreased activity can be seen – amongst other factors – in terms of shallow failures where, despite the ruggedness of the range, there are surprisingly few of these either on early aerial photos, or on the landslide susceptibility map (see Appendix E). The major form of erosion instead appears to be through the incision of soft colluvial sediments previously mobilised through deep-seated landsliding. This can be evidenced in the incised gullies that drain the slopes of the range.

The decrease in sediment supply from the range will have major consequences for the Esk Valley as this region both supplies the majority of stream flows, and, as shown in the hypsometric curve (Section 2.3.1) and long river profiles (Section 3.3.1) is the least geomorphically mature region of the catchment and is therefore likely to be a major sediment contributor the rest of the system.

6.2.2 MEDIUM-SCALE TRANSLATIONAL FAILURES

Medium scale deep-seated landsliding in the Esk Valley occupies over 4% of the total catchment land area, and occurs almost exclusively within the Grassy Knoll member of the Matahorua Formation (Attachment 1). The strong influence of the WFTS on bedding within the valley means that exposure of this unit also coincides with the trace of the associated monocline and it is difficult to determine the primary control on the landsliding.

6.2.2.1 Landslide model

A generic model for these medium-scale failures is given in Figure 6.5. Key landslide features and controls identified in the model are discussed below:

1. Material in "shallow" parts of the landslide, often toward the headscarp of the failure, regularly shows evidence of ductile flow and/or is more highly deformed than the rest of the mass;
2. The main landslide block is generally intact, although it often shows evidence of some extension downslope in the form of transverse scarps and grabens;
3. There is possible internal division into zones based on differential rates of movement;
4. One lateral margin is commonly exposed by stream incision. This margin often contains steep secondary failures inferred to be generated by differential motion within the slide (see Figure 4.5 Tributary domain 2 DTM, A&B);
5. The toe zone of the landslide is typically at, or very near, current stream bed level. It is not uncommon for the failure surface to be below bed level, displacement being facilitated by a slight rotation in the toe zone, possibly along flexural shears. Intense shearing and high groundwater flows are often present at the toe of the slide.

6.2.2.2 Geomorphic Controls on landslide development

Important geomorphic controls on landslide development are also illustrated in Figure 6.5, and are discussed below:

6. *Stream incision* – This is particularly important in the toe region where it creates a geometry suitable for the initiation of the landslides with the removal of lateral support. As the landslide failure planes are inferred to be planar surfaces that dip to the east or south-east, incision is required to excavate down to the pre-existing weak surfaces and provide a void into which the slides can move.

   It is important that stream activity continue in the toe region, and that stream power is sufficient to transport sediment produced by the slide, as debris trapped between the slide and the opposing wall of the channel will buttress the slide.

   Stream incision can also cause the drawdown of the watertable in adjacent bedrock spurs. This is likely to have a stabilising effect on the slides as pore pressures, particularly in fractured or permeable rock (i.e. landslide mass) will be decreased, and required rainfall levels to saturate the rock will increase markedly. High seepages from the tephra at the toe of the Trelinnoe slide (Section 4.2.3.1) are evidence for this process.

7. *Weak sedimentary layers* – laterally extensive weak horizons provide planes predisposed to the formation of large deep-seated landslides. Where the angle of

internal friction of the undisturbed strata is at or below that of local bedding, failure is able to occur. Once this takes place, the development of strain rapidly reduces the material to residual strength further reducing slide stability. Permeability typically also increases in mobilised material found along the failure surface of landslides. This can reduce stability by increasing pore pressures and clay content through weathering which is important in long-term deep-seated failures. Field evidence indicates that two principal lithological controls are the frequent 50cm thick tuffaceous horizons, and the 10m thick cohesionless quartz-rich sandstone in the upper section of the Matahorua Formation Grassy Knoll Member.

The tuffaceous horizons are particularly important as they have a much lower shear strength than the adjacent strata, and weather to clays. As a result of their volcanic source and "airfall blanket" deposition they occur frequently within the Matahorua Formation and are laterally extensive.

8. *Defect controls* on the margins are important as they both increase groundwater infiltration, and reduce lateral resistance to sliding. When a slide initiates it has to overcome both the shear strength of the material that is to become the basal failure surface, and the resisting forces of material along the margins. The fact that lateral and headscarp defects are so strictly adhered to indicates that the presence of these may be critical to slide generation, and that the slides may therefore – at least at the time of initiation – be very close to stable state. This may support an initial earthquake triggering hypothesis, as if the angle of the defect or bedding-controlled failure surface was substantially higher than that of the respective friction angles, a pure incision-triggered slide may be more likely to propagate back up the slope inducing lateral shears with orientations beneficial to the slide geometry rather than failing along less favourably oriented pre-existing surfaces.

9. *Flexural shears* are also likely to be important contributors to the formation of the failure surface. However, as these are unlikely to be as extensive or planar as the bedding controls, they are seen as mechanisms to enable the propagation of strain largely transferred in weaker horizons.

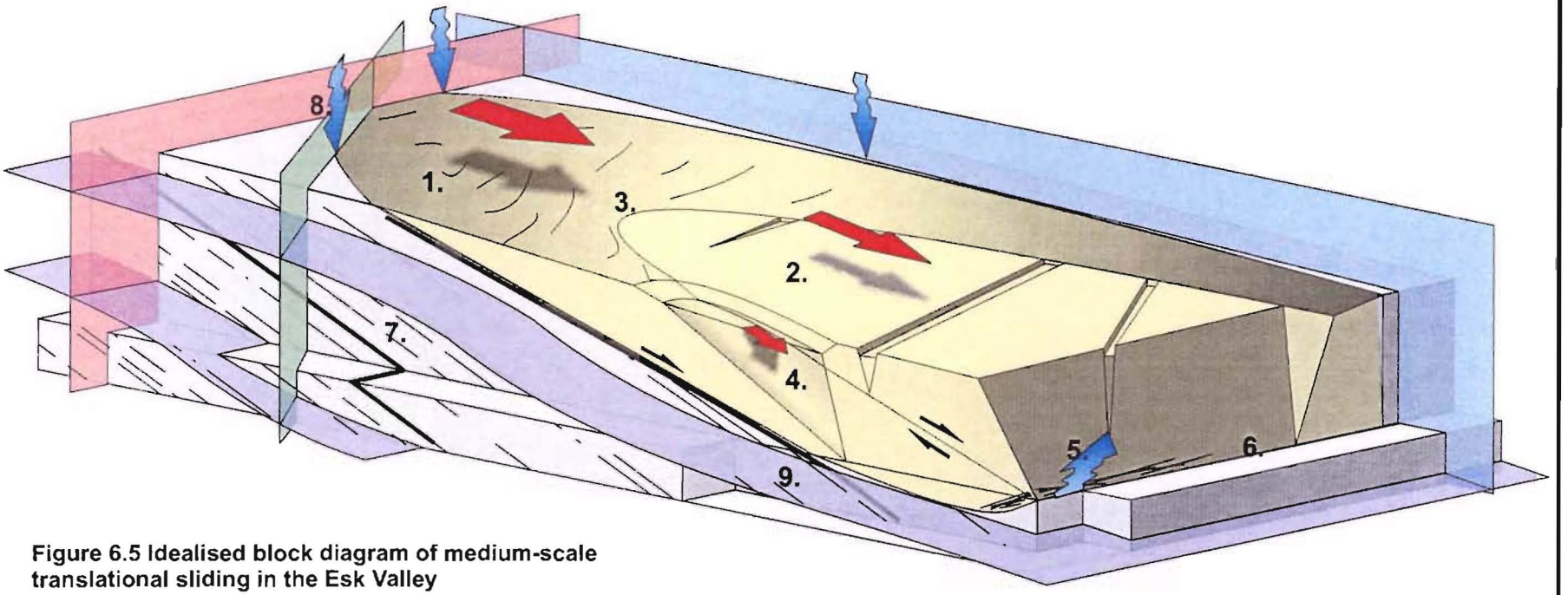

Figure 6.5 Idealised block diagram of medium-scale translational sliding in the Esk Valley

Vertical planes represent the three principal sub-vertical joint sets identified in Sectoin 4.3.3. The colours of the planes corresponds to those identifying the planes on the stereonet in Figure 4.23. These planes increase infiltration, and facilitate lateral release. The purple planes represent flexural shears and cross sub-parallel to bedding. The bedding attitude is indicated with dashed lines sub-parallel to the landslide failure surface. Weak tephra horizons are indicated by heavy black lines.

6.2.2.3 Age and activity

The failure surface for these slides often coincide with stream level, or slightly below the bedrock channel. Assuming terraces were abandoned at 10ka, then these slides must be much younger than this. The incidence of the failure surface with present day stream level suggests that either 1) as rivers have incised they have continually triggered translational failures each time they near a weak surface, or 2) landsliding of this scale is a recent phenomenon, and variation of a controlling process such as increasing tectonic activity or rainfall is responsible for the generation of the failures.

Whilst the continued failure option is in many ways the most likely, a number of factors do not support this inference:

- River channels display little or no evidence of continued disturbance from the slides as may be expected from a situation in which a continuous sediment supply has been provided for thousands of years.
- There is little evidence for multiple stages of failure. Where landslides are zoned, the upper unit does not appear to have moved significantly further than the underlying. It often appears more intact, suggesting less total shear stress through the unit as failure has been concentrated in underlying sediments.

Despite these observations, there is no clear mechanical reason why deep-seated landsliding should purely be a recent occurrence, particularly as most controls on landsliding have either:

a) Remained constant through time i.e. earthquake activity and incision rate (inferred from apparently constant uplift rate, Section 6.1.4.2), and levels of defects (assuming the majority of activity on the WFTS ceased prior to the last interglacial, see Section 6.1.4.2);

b) Developed to increase slope stability i.e. drawdown of groundwater level, and the disassociation of rivers from hillslopes.

It is therefore assumed that deep-seated landsliding has been a consistent input to the river system since the onset of incision. The lack of internal deformation in the slides is thought to be a reflection of the relatively wide spacing of coherent planes of weakness on which sliding can occur; the fact that the failure surface of many of the slides investigated

coincides with current channel level may be coincidental (lateral failure from Deep Stream Landslide Complex, Trelinnoe Landslide, Kaiwaka Landslide), or a reflection of extremely high driving forces migrating the zone of failure with lowering of the stream bed level (Deep Stream Landslide Complex). It is likely the slides are episodic, and the initiation is controlled by incision intersecting widely spaced, discrete weak horizons.

Due to the geometry of a translational landslide, once initiated, the medium-scale failures are likely to remain active until exhausted of landslide material, or external controls such as those discussed earlier in this section act to resist the sliding. These landslides display a wide range of activity levels in the catchment, although surface morphology does not indicate current rapid movement on any of the slides. While some failures, such as the Little Icecream Landslide, may have been partially stabilised through the incision related draw-down of the groundwater level, the majority may be expected to continue to creep slowly and sporadically discharge material off the face to be transported by the fluvial system. There is no evidence to suggest that any of these failures have or will fail rapidly.

6.2.3 SUMMARY

Two styles of deep-seated landsliding were investigated in the Esk Valley; the large regressive failures on the Maungaharuru Range, and medium-scale translational failures in the Matahorua Formation.

The failures on the Maungaharuru Range are investigated with respect to the deep-seated gravitational slope deformation driving subsidence in the basin on top of the range, and landslides off the eastern face. This activity is inferred to have initiated as a result of lateral unloading through landsliding following the incision of the last interglacial (between 120 and 60ka). Average subsidence rates were approximately 2.5mm/yr and are likely to have been substantially higher during peak movement (c.60-18ka). Infilling of a lake on the crest of the range may have accelerated movement, but present-day activity appears low.

The occurrence of medium-scale translational landslides within the catchment corresponds to the trace of the Wakarara Fault – Trelinnoe Sector and outcrop of the Matahorua Formation. Basal failure is primarily lithologically controlled, although flexural shears associated with the WFTS are likely to also play an important role. Critical horizons include regular tuffaceous layers, and a thick (c.10m) uncemented sandstone below the upper contact of the unit. These slides were initiated post-10ka, and progressive failures

have most likely occurred with continued stream incision. They are possibly initially earthquake triggered features.

The Maungaharuru Range was a major sediment contributor to the valley system throughout the last glaciation. The reduced activity indicates a deficit in sediment supply to the valley, probably throughout the last 18ka.

Medium-scale landslides have not contributed a significant volume of sediment to the system and are likely to continue to slowly creep for their duration. The exception to this is the Deep Stream landslide complex which may have been initiated following the last interglacial. Sediment produced from this slide may have played a significant part in preventing incision from propagating up the channel between 120ka and 10ka.

6.3 GEOMORPHIC STABILITY OF THE CATCHMENT

From this study it is possible to derive a model of catchment stability. Geomorphic stability in a landscape such as this can be defined as a measure of the rate of landscape evolution and its sensitivity to perturbations in the geomorphic regime. This section investigates the role of landsliding and stream incision as dominant catchment processes, the interaction between these and tectonic and climatic forcing, and the implications for continued landscape development.

6.3.1 MAUNGAHARURU RANGE

The slopes of the Maungaharuru Range are some of the most geomorphically active regions in the catchment. Although sediment production in this area currently appears to be very high, the majority appears to be sourced from mobilised colluvium, and not related to continued movement of the deep-seated landslides that flank the range. These slides appear to be currently less active than their overall morphology suggests they once were. However, swamps, sinkholes, open fractures, and rockfalls around the crest of the range all indicate possible continued displacement of the underlying structural or DSGSD driving mechanism (Section 4.1.6).

Recent deforestation of the range, particularly in incised valleys, is likely to have played a large part in the destabilisation of soft alluvial or colluvial debris on the range. Anecdotal evidence from forestry contractors and local farmers suggests stream channels on and around the range are rapidly aggrading (as much as 4-5m in 40 years under some bridges on Ohurakura Road). This follows massive degradation in many small streams on the range

during the April 1938 storm where Grant (1939) reports "Many such streams which previously gave good road fords have been scoured into heavy gulches".

6.3.2 MEDIUM TRANSLATIONAL LANDSLIDES

Deep seated landslides provide the crucial link between present-day channel processes and continued hillslope evolution of the upper surface. These slides significantly reduce bedrock strength, produce oversteepened hillslopes, and channelise overland flow. All of these effects provide a means for the incision occurring within incised channels to propagate to the landforms above the terrace surface. An increase in the rate of landsliding could significantly increase the rate of sediment generation in the system, both directly through slide transfer into the channels, and indirectly through the production of shallow landsliding on upper surface slopes. Conversely, if slides cease their motion, the unjointed siltstone cliffs are likely to remain intact, and the primary form of geomorphic adjustment will be through the continued slow undercutting of valley walls. There is very little evidence of this process taking place in the catchment today, particularly in upper, highly incised reaches. Here the vertical nature of the walls suggests these have not been adjusted significantly since the onset of incision. The rate of undercutting will eventually increase as the upper reaches of the catchment attain grade and excess stream power allows the system to cross from detachment-limited incision to transport-limited planation.

The deep-seated translational failures within the Matahorua Formation appear to be relatively stable and are likely to continue their slow creep. There is evidence for a possible landslide dam in Deep Stream as a result of a lateral failure off the Deep Stream Landslide Complex (Section 4.1.5), and rapid secondary failures such as this, or that off the toe of the Trelinnoe slide, are likely to continue to occur episodically.

A lack of morphological evidence in the stream channels for the continued input of these slides over the last 10ka indicates that the streams have been able to keep up with sediment inputs. This is supported by an inspection of the present day channel at the toe of the failures where bedrock is commonly exposed. These slides are not major sediment contributors to the system.

There is no evidence for significant movement during either the 1931 earthquake or 1938 flood, though the toe regions of some do show significant evidence of current activity (e.g. Trelinnoe Landslide, Section 4.2.3.1) .

6.3.3 SHALLOW FAILURES

While these failures occupy only a small portion of the total catchment land area (c.0.4% as a result of the 1938 storm), they are some of the most prevalent active geomorphic features in the valley. This means they have historically had a large effect on the valley geomorphology.

The majority of slopes in the catchment were developed throughout the last glacial period when streams are unlikely to have had access to bedrock and were probably only transporting sediment through the system. These slopes were therefore initially graded through mass movement under the cover of native grasses and shrubs (not too dissimilar to the vegetation in the valley today). Broadleaf forests developed over these slopes with the onset of global warming in the last 14,500 years and would have notably increased soil stability. Much of this forest was replaced by bracken and scrub following the arrival of Polynesian settlers c.1000BP, and slope stability would have suffered as a result (see Section 2.3.4).

The slope history described above has lead to the development of generally evolved, relatively stable hillslopes; present-day shallow landsliding occurs mainly in geomorphically active areas where slopes are connected to the stream system. The shallow landslides are triggered by increased pore pressures in the mixed weathered bedrock/tephra soils as a result of high intensity rainfalls, and were particularly problematic following the conversion of the catchment to pastoralism in the early-mid 1900's (Section 2.3.2.3).

Recent improvements in land management practices and the re-establishment of riparian zones along many streams is likely to have significantly improved the shallow slope stability situation. The process of shallow landsliding is, however, likely to continue at levels significantly greater than pre-European settlement.

6.3.4 STREAM CHANNELS

6.3.4.1 Esk Valley

The high degree of incision in the catchment (c.1.7 – 4.5mm/yr for the last 10ka (section 3.3.3.4)) is evidence for the disequilibrium in the Esk Valley system, and indicates a high degree of instability. However, morphological evidence (channel bed morphology (Section 3.3.1.4), long profile form (Section 6.1.4), and sinuosity (Section 3.3.2.4)) suggests at least the main channels are nearing their equilibrium profile and the rate of incision is

decreasing. As this takes place, the river channels are likely to begin to fill with sediment and plane laterally, providing source material for flood flows, and destabilising the walls of the channels. Evidence for this can be seen in the lower valley today where the broad channel has significant bedload. This is a long-term effect however, and currently much of the channel remains incised into bedrock with very little bed load. This, combined with the lack of water storage in the system will ensure a rapid response to rainfall events, particularly infrequent high magnitude storms.

Today streams are both detachment and transport-limited. These limitations determine the grade of the highly incised streams, and define the rate at which degradational processes are able to operate. While long river profiles indicate tectonic controls within the central reaches of the valley, stream incision appears to have been able to keep up with this by cutting narrower channels more rapidly (Section 6.1.3.1). This localised uplift has not had a huge influence on the valley morphology, and most of the tectonic controls are inherited from previous regimes within the catchment (e.g. the steep Maungaharuru Range, regional uplift, defects and flexural shears associated with the WFTS).

This incision has added a degree of stability in some ways, or at least a buffer zone in which a significant period of time (>1ka) is likely to be required to propagate significant geomorphic change throughout the catchment.

6.3.4.2 Aggradational plain

If the Upper Esk Terrace profile represents the graded profile of the Esk River following a period of rapid incision during the last interglacial (c.125-120ka), and the surface is the result of ongoing hillslope and channel processes adjusting to this profile; then, given the apparent continued uplift of the Esk region following the formation of the surface (Section 6.1.4), incision below this terrace may be assumed to have occurred since 120ka. In the Lower Esk Aggradational Valley this appears to comprise of a significant amount of incision (c.50m) below present valley level (Figure 4.3), before aggradation to the level of the extrapolated Ohakean terrace profile (c.15m above modern level) took place, and finally incision to the current valley level. This interpretation is hampered by the resolution of contour data which inhibits the location of terraces in the lower valley, as well as the lack of evidence for terraces in the lower half of the aggradational valley. The depth of incision in the valley is inferred from the adjacent hillslope profiles and well data (Section 4.1.3).

This situation is remarkably similar to that described in the more in-depth study of the Waipaoa River by Berryman *et al.* (2000) (Section 3.3.3.2). These authors suggest incision occurred in the lower reaches of the river up to and during the period in which deposition of the Waipaoa 1 (correlated with Ohakean) terrace was taking place in the upper catchment. This was approximately 16ka, when sea level had reached a lowstand of c.120m below modern sea level (Shackleton, 1987), and the coastline was located well (30km) offshore from its present position. Aggradation then occurred in the lower reaches of the valley during rapid sea-level rise c. 9-6000yr.BP, burying the incision and lower reaches of the Waipaoa 1 terrace. Since 6ka.BP, however, sea level has been stable (Gibb, 1986), and Berryman *et al.* (2000) therefore relate channel adjustments evident in the Waipaoa River Valley since this time to tectonic adjustment.

If the interpretation of Berryman *et al.* (2000) is applied for the Esk River system, then infilling following incision of the aggradational valley probably also occurred during this 9-6ka rapid sea level rise. Based on the valley profile inferred in Section 4.1.3, the Ohakean terrace surface must therefore be deformed to dip steeply below the aggradational sediments in the valley and grade to the erosional surface (Figure 6.6). This indicates a strong post-formation folding with the downthrown side to the east. A profile of the Last Glacial Maximum (Ohakean) terrace in the Ngaruroro River 30km to the south (Litchfield, in prep.) may show evidence for such post-deposition deformation, where, in the lower 24km of the river the terrace surface dips gently below present-day stream level. It is then located somewhat uncertainly in a water well 10 km downstream and 75m below the surface (Dravid and Brown, 1997). This may indicate faulting and/or folding between the localities with similar significant downthrow to the east.

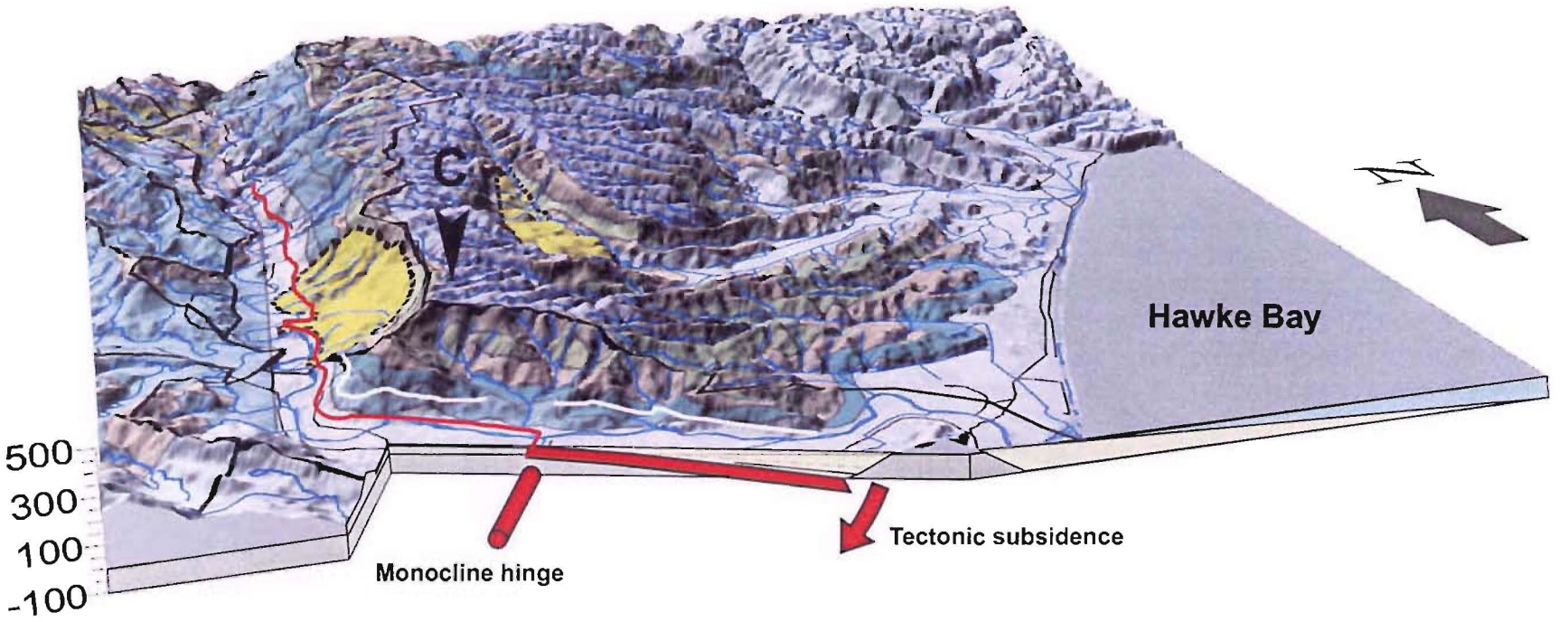

Figure 6.6 Schematic diagram of terrace relationships and monoclinal folding in the Lower Esk Aggradational Valley

The inferred Ohakean (18-10ka) terrace level is indicated in red, the last interglacial level (based on extrapolation from the Upper Esk Terrace) is indicated in white. Folding is inferred to have initiated before or during the deposition of the Ohakean terrace, and ceased at 1750BP. Sedimentary fill is indicated in yellow, bedrock in grey.

"C" denotes Castlecliffian strata outcrop used to derive uplift rates (section 6.1.4.2.)

An examination of seismic evidence (WEC97-3, Attachment 3) indicates a gentle folding of the sediments east of the easternmost Miocene deformation structure (at the 5km mark in the Esk River) assuming a seismic velocity of 2200m/s, this fold induces c.88m (0.4s TWT) of subsidence by the eastern end of the seismic line at the 3km mark on the river channel (Attachment 3). This is inferred to explain the lack of evidence for the Ohakean terrace in the lower aggradational valley noted in Section 4.1.2.

The applicability of this deformation to the deformation of the Ohakean terrace profile is supported by Hull (1986) who notes a net subsidence of 8m at the southern end of the Ahuriri Lagoon over the last 3500 years. The site for this study by Hull is located 9km to the south of the Esk River, along strike of the Miocene deformation structures. The majority of subsidence occurred prior to 1750 years BP (at a rate of 4.6mm/yr), and since then there have been two periods of minor (1m) uplift and one of subsidence. This data is based on radiocarbon dates from a 8m deep trench cut into the lagoon sediments, 8m was therefore the maximum possible subsidence that could be observed.

Based on the data given previously in this section it seems likely that much more substantial subsidence has taken place between the deposition of the 18ka Ohakean surface to 3.5ka when the record in the lagoon begins. In order to facilitate the 88m of displacement calculated from seismic line WEC97-3 at the rate given by Hull (1986), 19ka of constant subsidence is required. This indicates activity on the fold may have initiated at, or slightly before, the formation of the oldest Ohakean terrace.

Contrasting this subsidence at the mouth of the valley is the long-term pattern of consistent regional uplift determined in Section 6.1.4.2, and the effects of the 1931 earthquake (Section 2.2.3). Poorly constrained uplift rates for the mid to upper aggradational valley determined in Section 6.1.4.2 can be applied to suggest the alluvial plain should be c. $2.2^{+0.6}_{-0.3}$ m above the 6000yr. marine highstand level at which the surface was formed. This adjustment is relatively insignificant considering the 2m of uplift that occurred during the 1931 earthquake, and may suggest either that the earthquake uplift is an extremely rare event, that there is considerable error in the assumptions on which the uplift rate is based, or, as described by Hull (1986) in Ahuriri Lagoon, the uplift is part of a continuing cycle of intermittent tectonic uplift and subsidence.

6.3.5 SUMMARY

Climatic and tectonic processes play an integral role in defining the present-day stability of the most active geomorphic processes in the catchment. Gaining an understanding of the activity and nature of these influences can provide significant insight into the form and geomorphic activity of landforms associated with these processes.

Early displacement of landslides on the Maungaharuru Range, and associated instability throughout the last glacial provided significant volumes of sediment to the Esk Valley system. This is likely to have been an ongoing process, but the effect may have been recently enhanced by deforestation. Recent climatic and tectonic controls are not likely to have had a significant impact on the stability of the range.

Translational deep-seated landslides are a slowly emerging feature on the landscape. These provide a geomorphic connection between hillslopes and the channels, and will be important factors controlling future landscape development. Current sediment inputs are, however, not high, and while they have been triggered by climatic and tectonically-induced incision, it is unlikely that continuing activity is altering the stability of the slides.

Shallow landslides occur on slopes evolved during the last glacial. The profile of these slopes, is therefore graded to angles that reflect the poor vegetation coverage during this time. While significant soils are likely to have developed during post-glacial warming, the onset of Polynesian settlement at 1000BP significantly reduced forest cover and initiated the process of hillslopes returning to glacial levels of stability.

Rapid (3-8mm/yr) incision in the catchment has taken place over the last 10ka, and has not significantly destabilised the siltstone valley walls. It appears the streams are reaching grade at present, particularly in the lower catchment, and this is likely to lead to an undercutting of the valley walls and broadening of channels. A degree of stability has been added to the catchments through this incision, and it is likely a response time of c.1000 years will be required to propagate significant geomorphic change from the hillslopes to the streams or vice versa.

The Lower Esk Aggradational Valley shows signs of rapid geomorphic change as a result of the strong influence of tectonic and climatic processes. High rates of tectonic subsidence in the lower valley up to c.1750BP are likely to have lead to significant overbank deposition, while in the upper reaches postglacial incision has seen the Esk River entrench

below the level of the Ohakean terrace, which would limit the degree of flooding in this region. Since c.1750BP tectonic, anthropogenic, and flood-related adjustment has caused the river to incise along the length of the valley.

6.4 FLOOD HAZARD

6.4.1 INTRODUCTION

This section assesses the contribution of catchment evolution to the long-term flood hazard in the lower Esk Valley. The April 1938 Esk Valley flood is used here as a case study as it is the only recorded high magnitude event that posed significant risk to people's life or property. The assessment is based on evidence gathered throughout this investigation, and includes an evaluation of climatic, morphologic, and sediment generation processes (including deep-seated landsliding); and their relationship to the current geomorphic stability of the catchment.

6.4.2 CATCHMENT STABILITY

The uniqueness of the 1938 flood can be investigated by first considering the long-term (10ka+) history of incision and aggradation both in the Esk River catchment, and the aggradational valley.

6.4.2.1 Aggradational valley

Evidence suggests that since c.10ka the Esk River has incised approximately 20m through the Ohakean terrace surface in the upper reaches of the aggradational valley. This incision is likely to have ceased approximately 6ka, allowing the river to achieve a stable form (Section 6.3.4.2). Normal overbank siltation would have developed the banks so the river was confined in all but the most extreme events. During the incision in the upper valley, the lower (eastern) end may have been rapidly subsiding (Section 6.3.4.2), and significant aggradation is likely to have has taken place across the valley floor. It is possible the effects of this can still be seen in the form of the established channel, where it runs very straight across the western side of the fold, before crossing the structure and transitioning to a more sinuous and finally meandering channel in the lower reaches (Figure 4.3, the fold hinge is approximately in the location of cross-section V-V'). As this subsidence ceased just 1750 years ago it is still possible that sedimentation in the lower valley has not been sufficient to raise the valley floor up to a normal floodbank level.

Another important process in the last 10ka is the transport of significant volumes of sediment south along the coast from the mouth of the Mohaka River. This is evident in the large gravel berm present along the coast at the mouth of the Esk River. The generally low stream power of the Esk River was insufficient to overcome this input except during flood flows, and the river mouth migrated southward to Ahuriri lagoon.

Recent tectonic uplift (2m, 1931), aggradation in the valley and channel (c.1m, 1938), and opening of the channel mouth with ongoing gravel extraction to maintain this, all would have had the effect of forcing the channel to incise and increase in sinuosity as it adjusts to a steeper grade. As the form of the channel is suggested to represent adjustment to pre-1750BP tectonic conditions, adjustments since this time are likely to have therefore taken place within the confines of the ancient channel.

6.4.2.2 Esk catchment

All of the aforementioned controls are almost certain to have lead to an entrenchment of the Esk River over the last 6ka, particularly in the upper end of the aggradational valley. Any possible controls affecting aggradation, and enhancing the effect of the flood hazard, must have therefore been sourced from the upper catchment.

Excluding a tectonic influence, there are three significant controls that may generate periods of aggradation in the lower valley and therefore promote flooding: i) a decrease in precipitation and associated stream power; ii) increased sediment yield from the catchment; and iii) the gradual attainment of grade in a stream system.

- Although a reduction in precipitation may initially seem counter intuitive, the highly variable, almost bimodal nature of rainfall in the catchment means that a relatively short-term (c.100yr) decrease in average precipitation within the catchment may not substantially affect sediment yields, but instead may lead to aggradation within channels as stream power is insufficient to move all sediment in the system. This sediment can then be mobilised during flood flows and re-deposited downstream.
- Sediment yield from the catchment is likely to have increased significantly since 1000yr.BP when deforestation began, and once again in the late 1800's with the arrival of Europeans and conversion of the land to pastoralism. The majority of this is likely to be from shallow landsliding and channel erosion off the Maungaharuru Range (Section 6.3.1).

- As the majority of the stream system appears to be nearing grade it will be approaching a transport-limited state (Section 3.3.1.2). Evidence for this can be seen in the accumulation of alluvium in the lower catchment. This will also lead to an accumulation of alluvium in channels, and add to sediment loads during flood events (Section 3.3.1.4).

6.4.2.3 Implications

The long-term tectonic instability in the Lower Esk Aggradational Valley is likely to have meant the lower Esk River has been continually unstable, with periods of rapid incision, aggradation, and avulsion. These were superimposed on long-term aggradation relating to an initially rapid sea level rise between 9-6ka. A stable sea-level since this time, and the general trend of apparently constant uplift since 120ka would have produced incision in the upper aggradational valley, and substantial siltation across the lower valley.

The effects of this long-term tectonic control are, however, likely to have been overprinted by significant recent (<100yr) uplift and aggradation during the 1931 and 1938 events, as well as anthropogenic control initiated after the arrival of Europeans. These are therefore likely to be the controlling factors in present-day channel and valley stability.

Continuous stage recording at the Waipunga bridge site indicate mean water level in the Esk has been consistently decreasing for the duration of recordings (1963-2003) (source: HBRC). This is inferred to indicate the channel has also been downcutting at a rate of 35mm/y. This rate, while rapid, has been remarkably consistent for the 40 year period. A comparison with mean flow data for the same period indicates slight aggradation occurs during periods (c.5yr) of low-flow conditions, and high flow periods increase the incision rate. The consistency of this incision indicates the river in this region is well above grade, and its return to grade is likely to be controlled by mean stream power. Records show this rate was approximately the same between the 1938 flood and the next survey in 1975 (Williams, 1986), indicating little significant incision following the event.

Assuming this incision rate can be extrapolated back to the 1931 earthquake, this would equate to a total incision of 2.2m, above the 1.6m of uplift measured for the same site in 1931 this emphasises the combination of factors required to produce the current regime.

6.4.3 KEY CONTRIBUTORS

6.4.3.1 Climatic

As described in Section 2.4.2.1, the primary contributor to the 1938 Esk Valley flood was three days of particularly heavy rainfall culminating in intense precipitation on the morning of the 25th of April (average of 508mm in 3 days across the catchment, and a peak of 308mm in 14 hours at Tutira (Grant, 1939)). This rainfall was a result of the collision of two weather systems, each commonly associated with very high precipitation levels, in the vicinity of the Maungaharuru Range. The interaction of these systems in association with the orographic effect of the Maungaharuru Range caused a rapid upwelling and condensation of the air masses, rapidly producing intense precipitation.

An event of this scale is very rare in the Esk Valley, and the recurrence interval is approximately 1000 years (Section 2.4.1). It is therefore unlikely the rapidly evolving Esk system could adjust to efficiently transmit flows of such an infrequent event. As a result the catchment response is likely to be poor, and overbank flooding inevitable.

6.4.3.2 Catchment morphology

The main morphologic factors that contribute to flood flows in the Esk Valley are the steep, linear hillslopes that promote rapid runoff, the lack of storage, and the correspondence of the most common channel lengths to channels draining the Maungaharuru Range, producing large flood peaks.

These factors have been constant over the last 10ka, and it is likely the Esk system has adjusted to facilitate them. It is therefore unlikely they played a particularly large part in the 1938 event.

6.4.3.3 Sediment load

From the shape of the hydrograph and sediment transport curve for the 1938 event (Figure 2.9) it is apparent that by far the majority of sediment was transported in the ten hours during which the river rapidly rose and broke its banks. Sediment deposited on the floodplain during this time therefore represents the majority of that transported out of the system during the storm.

As shown in Sections 2.4.2.3, 2.4.2.4, and 3.2.3.3, the volume of sediment produced by shallow landsliding as described by the digital slope map ($2.67 \times 10^{6}{}^{+1.33 \times 10^{6}}_{-0.38 \times 10^{6}}\ m^3$) is considerably less than that likely to have been transported past the Waipunga Road Bridge

($4.51x10^6m^3$), which is in turn less than was deposited on the aggradational valley floor ($6.5x10^6m^3$). Sediment produced by deep-seated landsliding ($0.5x10^6m^3$) is unlikely to have contributed significantly to the total sediment transported during the event. It is easy to resolve the disparity between sediment transported past the bridge and that deposited in the valley simply by considering errors involved. However, when it is considered that not all sediment derived from shallow landslides reached the channel, and of that in the channel, not all was deposited on the valley floor, it seems unlikely that the majority of sediment generated during the storm came from shallow landsliding.

This suggests there must be other significant contributors to flood sediment load. Possible sources include bank erosion, remobilisation of landslide colluvium, bed scour, and sediment entrained in surficial runoff. Each source is investigated further below:

- *Bank erosion* – sediment eroded directly off stream banks can contribute significant volumes of sediment particularly in actively avulsing channels, or those incised into soft alluvial material. Bank erosion is not considered a significant contributor to the Esk flood, principally because banks are largely smooth, unjointed bedrock.
- *Bed scour* in the detachment-limited upper reaches of the catchment appears to occur mostly during low-flow conditions, however, sediment produced by this process requires flood flows to transport it out of the system (section 6.1.4.1). This effectively rules out bedrock incision as a major sediment contributor, and as Grant (1939) notes that scour in the lower reaches of stream channels is "relatively absent" the proportion of sediment eroded from transport-limited reaches is also unlikely to be high.
- *Sediment entrainment in overland flow* is not considered to be a major contributor due to the abundance of broad, low-gradient terraces in the catchment. These are unlikely to sustain flow rates sufficient to transport the large volumes of sediment required, instead accumulating sediment as infiltration reduces overland flow.
- *Colluvium* at the base of slopes derived from previous landslide events is another possible source of sediment. While this is composed of mobilised soils and can therefore produce slumping to depths greater than the average 2m of most shallow landslides, the lack of connection between rivers and the hillslopes in much of the catchment again prevents the entrainment of these deposits in streamflow. This also

means the streams are unable to undercut the base of colluvial deposits, a common method of destabilisation.

It is considered likely that a large proportion of sediment generated during the 1938 storm originated from mobilised colluvial and fluvial deposits on the slopes of the Maungaharuru Range. This region is the most geomorphically active in the valley and slopes are likely to have still been evolving rather then degrading during the mid to late glacial (Section 6.2.1.3). As a result of this the region is likely to have been most severely affected by recent deforestation. It was the focus of the most intense rainfall during the storm, and pore pressures and overland flow are therefore likely to have been very high. These are the two most significant contributors to slope instability, erosion, and sediment transport, – all of which would have been major factors in the production and transfer of sediment during the storm.

Reports by Grant (1939) of severe erosion, and by local farmers of subsequent rapid aggradation support this conclusion (Section 6.3.1). These variations in bed level reflect the degree of erosion that took place on the range, as well as current rates of sediment generation as the transport of sediment into stream channels has aggraded them to levels possibly near to those prior to the 1938 storm.

6.4.4 SUMMARY

The single largest contributor to the 1938 Esk Valley flood was the extreme level of precipitation that fell on the eastern slopes of the Maungaharuru Range between 2am and 5am on the 25th of April. This precipitation marked the culmination of a rare (c.1:1000yr) 3-day rainfall event, and fell on an already saturated catchment contributing to severe channel erosion on the Maungaharuru Range and shallow landsliding in the Esk Valley. All precipitation received on the range entered the main Esk River channel at the same time. As a result, flows in the aggradational valley near the mouth of the Esk River approximately 3 hours later rapidly rose from a very high 600m^3/s to 2000m^3/s in just 3 hours. This caused the river to break its banks, and exceptional volumes of sediment were transported into the aggradational valley and deposited across the floor.

Irrespective of the return interval of the event, evidence suggests that geomorphologically, this is a very rare event. Tectonically induced incision in the upper aggradational valley, and rapid aggradation in the lower aggradational valley are likely to have been the dominant forms of channel adjustment in the last 6ka. It is likely subsidence ceased at

1750BP, and since then it appears the river has remained in the same channel. Much of the long-term tectonic effects have been overprinted by recent anthropogenic channel modification (mid 1800's-present), uplift (1931), and deposition of flood sediments (1938). These have all contributed to the incision of the channel and increasing sustainable flood levels.

6.4.5 RECOMMENDATIONS

The key to minimising geomorphic hazards is to minimise change in the rate of contributing geomorphic processes; rapid change promotes instability in the system and reduces the predictability of system response. This observation can be applied to the Esk River catchment. However, largely as a result of the valley's location in a tectonically active region, natural variation in the rate of geomorphic activity is inherent in the landscape. The most recent evidence of this can be seen in the tectonic uplift as a result of the 1931 Napier earthquake, and indirectly in very high rates of sediment generation and transport as a result of the orographically-controlled 1938 Esk Valley storm.

As these rare natural events are difficult to plan for, and impossible to control, attention must be paid to controlling the rate of geomorphic processes susceptible to anthropogenic activity. The single most important human modification to geomorphic processes in the Esk Valley has been the increase in overland flow and slope instability as a result of deforestation. Another influence includes channel modification in the aggradational valley through straightening the outlet and gravel extraction, although these are both likely to reduce the flooding hazard.

The effects of deforestation are particularly important on the slopes of the Maungaharuru Range and geomorphically active areas characterised by high densities of steep slopes as identified on the Digital Slope Map in Appendix E. In order to prevent significant accumulation of colluvium and alluvium in these regions, and therefore minimise the volume of sediment available for entrainment during flood flows, it is recommended that forestry be carefully managed to minimise the volume of sediment produced through shallow failures and enhanced overland flow during storm events.

Forestry is targeted in the Esk Valley as, although pasture induces similar slope instability issues as cleared or recently planted forestry (Section 2.3.4), commercial plantations are already established in almost all of the most geomorphically active, and therefore areas of greatest sediment contribution. More work is required in order to determine a sustainable

level of sediment production, but it is suggested that maintaining native vegetation and closed-canopy exotic forests (>8yrs) over two thirds of the critically unstable areas could reduce storm-derived sediment production through shallow landsliding by as much as 10%.

The effect of reforestation would be particularly important on the Maungaharuru Range where overland flow rates would also be reduced. Sediment entrained in overland flow and produced through channel erosion is cited as an important contributing factor to the Esk Valley Flood as it is likely to be a large proportion of that transported during the event. In areas of the range where forestry is not established it is proposed that riparian zones are reverted to native vegetation to reduce the transportation of sediment into streams.

7 CONCLUSION

7.1 CATCHMENT PROCESSES AND EVOLUTION

The geomorphology of the Esk Valley is intimately linked to tectonic and paleo-climatic processes. Landscape evolution in the valley is likely to have begun with the onset of the most recent period of Forearc Basin uplift c.800ka. The majority of landforms, however, appear to have evolved throughout the last glacial (120-18ka). Rapid stream incision (up to 80m at c.8mm/yr) has been ongoing since the onset of the current interglacial (c.10ka) and is likely to be a result of increased precipitation and stream power.

The longitudinal profile of a broad terrace in the upper Esk Valley is believed to represent channel base level during the last interglacial. It is suggested that the terrace surface represents a period of significant mass-movement, as well as transport-limited aggradation and lateral planation by sinuous streams throughout the glacial. Limited incision took place in the mid- to lower-catchment during brief glacial warm periods, and these areas re-graded to a c.18-10ka Ohakean terrace.

These conditions have meant that the level of geomorphic connectivity between stream and hillslope processes is low, and these regimes can therefore be considered somewhat independently. Hillslopes on the upper surface are likely to have developed largely during the last glacial, and are generally evolved and relatively stable. Consequently, levels of geomorphic activity are relatively low. The incised streams, however, have rapidly cut into bedrock, and rates of geomorphic change are therefore rapid. Numerous large (c.1km^2) deep-seated landslides provide a degree of connectivity between the stream channels and upper surface, but these are slow moving and significant change is not yet evident.

The angular sinuosity of streams throughout the valley indicates persistent rock mass defects – resulting from deformation by underlying structures (the Eastern Patoka Fault and Wakarara Fault-Trelinnoe Sector) – were well developed by the onset of the current period of incision. The strong influence of these relatively weak defects on stream form indicates incision is likely to have occurred during normal flow conditions. Data from sediment transport curves suggests the sediment generated (96,000m^3/yr) is then transported out of the system during regular flood events.

Deep-seated Landslides investigated in the Esk Valley are classified in two groups:

1. Massive translational regressive failures occur on the eastern face of the Maungaharuru Range. These are inferred to be associated with the development of a deep-seated gravitational slope deformation which affects the entire Maungaharuru Range. However, the understanding of structural control which obviously defines the form of the range is poor, and this interpretation requires more research. The slides are likely to have been triggered as a result of mass wasting in the upper catchment during the early- to mid-last glacial, and show evidence of heightened activity in the past.

2. Low-angle translational failures occur within the Grassy Knoll Member of the Matahorua Formation. The exposure of this unit coincides with the trace of a thrust-propagated monocline associated with the Wakarara Fault – Trelinnoe Sector. Weak, permeable tuffaceous and sandstone horizons within the unit, combined with vertical defects and flexural shears associated with the formation of the monocline provide the mechanical characteristics required for such low-angle (c.6°) translational failures. A favourable geometry is produced by gentle tectonic tilting and the current post-glacial stream incision in the toe zone.

With evolved hillslopes largely detached from a confined but incising river system by stable, largely unjointed valley walls, current geomorphic stability in the valley is relatively high. It is likely to take a substantial period of time (1000yr+) to propagate any significant geomorphic change through the system. However, evidence suggests streams throughout much of the Esk Valley, particularly the Esk River and lower reaches of its tributaries, are nearing grade. As these streams attain grade, they will infill with sediment and excess energy will be available for lateral planation. This will initiate a period of instability where channel walls will be undercut, and deep-seated landsliding will become more prevalent throughout the catchment. Deep-seated landslides have therefore been, and will continue to be, important contributors to landscape evolution within the Esk Valley.

The lower Esk aggradational valley appears to have experienced a significantly different tectonic regime from the upper catchment, and is more susceptible to climatically induced sealevel change. Recent tectonic activity (1931 Napier Earthquake), flooding (1938 Esk Valley Flood), and anthropogenic processes (c.1840-present) have significantly raised channel grade. As a result the river appears confined to an ancient (pre-1750BP) channel and is currently incising at a rate apparently limited only by stream power (3.5mm/yr).

7.2 CONTRIBUTION OF DEEP-SEATED LANDSLIDING TO THE ESK VALLEY FLOOD HAZARD

The volume of sediment currently generated directly through the activity of deep-seated landslides is low. Most sediment is produced either through shallow landsliding in geomorphically active areas within the valley, or the erosion of alluvium, colluvium and loess from the surface of deep-seated landslides on the Maungaharuru Range. The entrainment of this sediment in the river system reduces stream power and blankets bedrock, preventing incision and forcing streams to meander or run above grade. During flood events it contributes to staging levels by adding volume and preventing channel incision.

The April 1938 Esk Valley flood was primarily a response to a rare (c.1:1000yr) rainfall event. Peak flow lasted only half an hour, and the river was beyond it's banks for just seven hours. During this time approximately $4.5x10^6$ – $6.5x10^6m^3$ of sediment was deposited on the valley floor. This sediment is likely to have comprised the majority of that transported by the flood, and was most likely a result of severe erosion on the surface of deep-seated landslides on the Maungaharuru Range, and substantial shallow landsliding on hillslopes within the valley.

Despite reports of reactivation and triggering of deep-seated landslides within the Hawke's Bay Region, there is no evidence to suggest that the deep-seated landslides in the Esk Valley moved significantly during the 1938 storm, or the M_s7.8 1931 Hawke's Bay Earthquake. However, the resolution of this investigation did not allow minor movements (<c.3m) or increases in activity to be identified. These would produce only a relatively small volume of sediment, and hence are unlikely to be significant contributors to flood hazards in the Esk Valley.

7.3 GEOMORPHIC STABILITY AND FLOOD HAZARD ON THE AGGRADATIONAL PLAIN

A study of the Lower Esk Aggradational Valley based largely on the extrapolation of river and terrace profiles indicates the river in the upper half of the domain has incised c.20m over the last 10ka. The river is likely to be sitting on or near a bedrock strath surface, and it is therefore considered very unlikely that overbank sedimentation has been, or will be a significant geomorphic process in this part of the valley. In the lower half of the domain it

appears rapid subsidence up to 1750BP may have promoted significant aggradation across the valley floor. While this now appears to have ceased, it is possible this part of the valley may have been more prone to overbank flooding than the upper valley. Uplift in 1931 and siltation as a result of the 1938 event are likely to have mitigated any preconditioning associated with subsidence in the lower aggradational valley as the Esk River is now incising, and bank levels are elevated as a result of the sedimentation.

While it is considered unlikely that an event of this magnitude will again occur during the design life of any structures in the Esk Valley, forest management in geomorphically active areas, and re-vegetation within gullies on the Maungaharuru Range can significantly reduce the sediment load, and therefore the hazard posed by smaller, more frequent floods.

7.4 ASSESSMENT OF AN ENGINEERING GEOMORPHOLOGICAL APPROACH TO HAZARD EVALUATION

Geomorphic process interactions are complex, particularly in active tectonic regions. Understanding these interactions and identifying the dominant processes within an environment through the study of geomorphology can provide a model for the prehistoric development of landscape elements. By then applying an engineering geological knowledge of soil and rock mechanics, surface and groundwater hydrology, and techniques of hazard evaluation, data gathered through the geomorphological investigation can be used to refine the model of landscape development, assess present-day stability, and investigate the effect of anthropogenic processes.

This investigation has pioneered Quaternary research in the Esk River Valley, and as a result has had little directly relevant geologic or geotechnical research to develop on. This, combined with the large scale of the rapidly evolving valley and its associated hazards, make this an ideal situation in which to implement an engineering geomorphological investigation.

Major achievements of this specific form of investigation in the Esk Valley include:

- The identification of recently, possibly currently, active faulting in the central valley, and the recognition of associated flexural shears and their implications for slope stability;

- The determination of a maximum age for translational landslide development throughout the valley, and the formulation of a model to describe slide evolution and current stability;
- The identification of geomorphically active areas prone to heightened levels of shallow landsliding;
- The development of a model to describe the evolution of landslides on the Maungaharuru Range and assess present-day stability based on a possible deep-seated gravitational slope deformation, a process previously not recognised in New Zealand;
- An assessment of the long-term flooding history in the lower Esk aggradational valley, and evaluation of the potential today;
- The production of a flood hydrograph and identification of major contributors to the April 1938 Esk Valley Flood;
- And the assessment of the April 1938 event with respect to the long-term geomorphic development of the Esk Valley and implications for future hazard management.

All of these observations and conclusions were the direct result of a combined engineering geological/geomorphological investigation and are key to defining hazards in the valley today.

This technique is best suited to the evaluation of regional hazards in geomorphically active regions. In these areas the activity and scale of geomorphic processes mean they are able to be resolved with the c.20+m resolution of data commonly available. The acquisition of more detailed regional data, while both costly and time consuming to obtain, can also cause significant problems with storage and processing and will not necessarily benefit such an investigation. This means the technique may not be suitable for the investigation of localised hazards, or those developing in slowly evolving regions where perturbations are commonly minor, and do not cause significant disruption to the system.

While numerical or similar quantitative methods provide an accurate assessment of hazard susceptibility, these require a significant volume of prior research pertaining to the specific area. In regions such as the Esk Valley, where this data is not available, an engineering geomorphological approach to an investigation can highlight important processes, assess their relative roles in the landscape, provide a qualitative evaluation of hazards, and flag areas in which to concentrate a testing programme and develop quantitative models to better assess hazard potential. This has the potential to make considerable savings in both

time and money, while improving the confidence of any outcomes from a testing programme.

7.5 SUGGESTIONS FOR FURTHER RESEARCH

As this was the first investigation conducted into the Quaternary geology or geomorphology of the Esk Valley, a large amount of "ground had to be covered" in order to develop an adequate understanding of the valley geomorphology and therefore assess landslide and flood hazards. Assumptions are inevitable in such an investigation as funding and time are limited. This section identifies work that is required to confirm or better constrain interpretations made in this investigation, as well as new avenues of research that have been highlighted as a result of findings.

- Terraces – while an attempt was made to date terraces in the valley, this was unsuccessful. Mapping of the surfaces was only at reconnaissance level. The correlation of these surfaces plays an integral part in setting the timeline and identifying the evolution of processes and features in the valley, and accurate age control, and better correlation of the multiple surfaces is essential both in the upper and lower valley.
- Long river profiles – while these were a tool rather than a finding of the investigation, the rivers' close adherence to exponential profiles could offer an opportunity to investigate the development of stream profile. This could also elucidate the source of the inferred area of uplift in the profiles. In order to undertake this investigation better control on the river bed level is required; this is likely to be complicated given the topography, and may not be viable.
- Shallow landslides – as much work has been undertaken into soil stability on the east coast the assessment of conditions for soil stability was not a high priority in this investigation. Shallow landslides were, however, an important contributor to the 1938 flood, and the calibration of a deterministic slope stability model for the catchment could better define at-risk areas, and aid in the development of management practices.
- Translational deep-seated landslides – further work should be undertaken to quantitatively assess the stability of these failures. The role of earthquake ground accelerations and intense rainfall on bedrock pore pressures is not known. Further investigation could develop a model to determine landslide behaviour during

extreme events, and predict future stability. Roadcuts on the Old Coach Road across Little Icecream Landslide could be used to calibrate a long-term "scarp diffusion model" that could be applied to date scarps generated through landsliding.

- Maungaharuru Range – better structural control is required to determine tectonic and gravitational control on deep-seated landsliding off the Maungaharuru Range. This would allow the development and activity of these slides to be better constrained. Two important sites for trenching and radiocarbon dating are in the breached lake on the surface of the southern slide (V20 Esk, 300150), and in the possible lake sediments present-on the top of the range (V20 Esk, 323193). This could provide rates of slide movement and structural development.
- Aggradational valley – Detailed terrace mapping along with a seismic investigation are required to determine the accuracy of inferred terrace relationships and depth to bedrock in the aggradational valley. This would better determine the rate and degree of inferred subsidence in the lower valley, and may have significant implications for earthquake hazards in Hawke's Bay.
- Forearc Basin structure – The interpretation of Westec Petroleum seismic profiles in this study have highlighted some strong similarities between structure in the forearc to the south of the Heretaunga plains, and that in the Esk Valley. Work needs to be done to extend the structures located in the Esk Valley south across the Heretaunga Plains, and determine the relationship of these to those identified in Beanland *et al.* (1998). This could have important implications for groundwater and flood hazard investigations on the Heretaunga Plains, as well as contributing to the scientific understanding of forearc basin structure and evolution.
- Landscape evolution modelling – this is one of the most rapidly developing areas in geomorphologic research, mainly because of the development in computational power that has allowed increasingly complex numerical relationships to be developed and tested and thus providing an increasing degree of understanding of landscape processes. The applicability of these models is broad, with the potential to assess hazards, investigate the effects of climate change, and enable the intelligent management of natural resources. The Esk Valley offers a good opportunity to investigate such a model as the rapidly evolving topography and simple geology largely negate the effects of inherited landforms, and the scale and variation of processes in the valley are likely to be well resolved in a model.

BIBLIOGRAPHY

Adams, J., 1980: Active tilting of the United States midcontinent: Geodetic and geomorphic evidence. *Geology 8*: 442-446.

Adams, J., 1981: Earthquake-dammed lakes in New Zealand. *Geology 9*: 215-219.

Agliardi, F., Crosta, G.B., and Zanchi, A., 2001: Structural constraints on deep-seated slope deformation kinematics. *Engineering Geology 59*: 83-102.

Ballance, P.F., 1993: The New Zealand Neogene Forearc Basins. *In:* Ballance, P.F., *ed.* South Pacific Sedimentary Basins.

Bannister, S.C., 1988: Microseismicity and velocity structure in the Hawke's Bay region, New Zealand: fine structure of the subducting Pacific Plate. *Geophysics Journal 95*: 45-62.

Barnes, P.M., Nicol, A., and Harrison, T., 2002: Late Cenozoic evolution and earthquake potential of an active listric thrust complex above the Hikurangi subduction zone, New Zealand. *Geological Society of America Bulletin 114*: 1379-1405.

Beanland, S., 1995: Role of the North Island Shear Belt in the Hikurangi Margin. *New Zealand Geophysical Society symposium 1995: Subduction systems and processes in New Zealand,* unpaginated.

Beanland, S., and Haines, J., 1998: The kinematics of active deformation in the North Island, New Zealand, determined from geological strain rates. *New Zealand Journal of Geology and Geophysics 41*: 311-323.

Beanland, S., Melhuish, A., Nicol, A., and Ravens, J., 1998: Structure and deformational history of the inner forearc region, Hikurangi subduction margin, New Zealand. *New Zealand Journal of Geology and Geophysics 41*: 325-342.

Beaumont, C., Fullsack, P., and Hamilton, J., 1992: Erosional control of active compressional orogens. London, United Kingdom, Chapman & Hall.

Begg, J.G., Hull, A.G., and Downes, G.L., 1994: Earthquake hazards in Hawke's Bay: initial assessment. *Unpublished Institute of Geological and Nuclear Sciences report no. 333901.10.*

Berryman, K., 1998: Tectonic Geomorphology at a Plate Boundary: a Transect Across Hawke Bay, New Zealand. *Zeitschrift fur Geomorphologie N.F. Suppl.-Bd 69*: 69-86.

Berryman, K., Marden, M., Eden, D.N., Mazengarb, C., Ota, Y., and Moriya, I., 2000: Tectonic and paleoclimatic significance of Quaternary river terraces of the Waipaoa River, east coast, North Island, New Zealand. *New Zealand Journal of Geology and Geophysics 43*: 229-245.

Bishop, A.W., 1967: Progressive failure - with special reference to the mechanism causing it. *Proceedings of the Geotechnical Conference Oslo 2*: 142-150.

Black, R., 1991: Esk River catchment - the influence of lithology and land use on water yield. *In:* Henriques, P.R., *ed.* Sustainable land management : the proceedings of the International Conference on Sustainable Land Management, Napier, Hawke's Bay, New Zealand, 17-23 November 1991, Pp. ix, 503.

Bland, K.J., 2001: Analysis of the Pliocene Forearc Basin Succession Esk River Catchment, Hawke's Bay. Unpublished Master of Science thesis, lodged in the library, The University of Waikato, Hamilton.

Bull, W.B., 1991: Geomorphic responses to climatic change. New York, Oxford University Press, xviii, 326 p.

Bullen, K.E., 1938: An analysis of the Hawke's Bay earthquakes during February 1931. *New Zealand journal of science and technology 19*: 497-519.

Burnett, A.W., and Schumm, S.A., 1983: Alluvial river response to Neotectonic deformation in Louisiana and Mississippi. *Science 222*: 49-50.

Campbell, J.K., and Yousif, H.S., 1985: Tectonic geomorphology of the Lower Waipara Gorge, North Canterbury. *Geol.Soc.Misc.Publ. 32*: 53-65.

Carson, M.A., and Kirkby, M.J., 1972: Hillslope form and process. London, Cambridge Univ. Press; Cambridge Geographical Studies.

Cashman, S.M., Kelsey, H.M., Erdman, C.F., Cutten, H.N.C., and Berryman, K.R., 1992: Strain partitioning between domains in the forearc of the Hikurangi subduction zone, New Zealand. *Tectonics 11*: 242-257.

Clapp, B., and McConchie, J., 2000: Geomorphic response of stream channels to landsliding, Mohaka Forest, Hawkes Bay. *New Zealand Hydrological Society annual symposium, 23-26 November 1999, Napier:* 2-4.

Cole, J.W., and Lewis, K.B., 1981: Evolution of the Taupo-Hikurangi subduction system. *Tectonophysics 72*: 1-21.

Cowie, C.A., 1957: Floods in New Zealand 1920-53 with notes on some earlier floods. Wellington, N.Z., The soil conservation and rivers control council.

Crosby, B.T., and advised by K. Whipple, 2001: Knickpoint Migration in the Waipaoa River and its Tributaries: An examination of the rate and form of transient migration in fluvial systems. Department of Earth, Atmospheric, and Planetary Sciences, Massachusetts Institute of Technology, Massachusetts. p. 17.

Crozier, M.J., Deimel, M.S., and Simon, J.S., 1995: Investigation of earthquake triggering for deep-seated landslides, Taranaki, New Zealand. *Quaternary International 25*: 65-73.

Crozier, M.J., Gage, M., Pettinga, J.R., Selby, M.J., and Wasson, R.J., 1992: The Stability of Hillslopes. *In:* Selby, M.J., *ed.* Landforms of New Zealand, Longman Paul, Pp. 344-366.

Cutten, H.N.C., 1988: Structure of Cretaceous and Tertiary sediments in the vicinity of the Mohaka River, Te Hoe River, Western Hawke's Bay. *Unpublished New Zealand Geological Survey report no. EDS115.*

Cutten, H.N.C. 1994: The Geology of the Middle Reaches of the Mohaka River Institute of Geological and Nuclear Sciences geological map 6. 1 sheet & 38p. Institute of Geological and Nuclear Sciences Ltd., Lower Hutt.

Cutten, H.N.C., Beanland, S., Berryman, K.R., and Boyle, S., 1988: The Rangiora Fault, an active structure in Hawkes Bay. *Unpublished New Zealand Geological Survey report no. 35.*

Dietrich, W.E., Wilson, C.J., Montgomery, D.R., and McKean, J., 1993: Analysis of erosion thresholds, channel networks, and landscape morphology using a digital terrain model. *Journal of Geology 101*: 259-278.

Dravid, P.N., and Brown, L.J., 1997: Heretaunga Plains groundwater study. *Unpublished Institute of Geological and Nuclear Sciences report no.*

Dunlop, J.D., 1992: Catchment: A history of the Hawke's Bay Catchment Board and Regional Water Board. Napier, NZ, Hawke's Bay Regional Council, 84 p.

Earthquake Commission, 2003: *Geonet* www.geonet.org.nz, Institute of Geological and Nuclear Sciences.

Edwards, A.R., 1988: An integrated biostratigraphy, magnetostratigraphy and oxygen isotope stratigraphy for the late Neogene of New Zealand. *Records of the New Zealand Geological Survey 23*: 80.

Erdman, C.F., 1990: Pliocene-Pleistocene stratigraphy and tectonic evolution of the Ohara Depression - Wakarara Range region, North Island, New Zealand. Unpublished M.Sc thesis, lodged in the library, Western Washington University, Bellingham.

Erdman, C.F., and Kelsey, H.M., 1992: Pliocene and Pleistocene stratigraphy and tectonics, Ohara Depression and Wakarara Range, North Island, New Zealand. *New Zealand Journal of Geology and Geophysics 35*: 177-192.

Eyles, R.J., 1971: Mass movement in Tangoio Conservation Reserve, northern Hawkes Bay. *Earth Science Journal 5*: 79-91.

Fell, R., Sullivan, T.D., and MacGregor, J.P., 1988: The influence of bedding plane shears on slope instability in sedimentary rocks. *5th International Symposium on Landslides, Lausanne, Switzerland:* 129-134.

Foley, M.G., 1980: Bedrock incision by streams. *Geological Society of America Bulletin 91*: I 577-578 II 2189-2213.

Forest Research Institute, 1990: Contribution of tree roots to slope stability. *In:* New Zealand Ministry of Forestry, *ed.* What's New in Forest Research.

Formento-Trigilio, M.L., Burbank, D.W., Nicol, A., Shulmeister, J., and Rieser, U., 2003: River response to an active fold-and-thrust belt in a convergent margin setting, North Island, New Zealand. *Geomorphology 49*: 125-152.

Francis, D.A., 1991: Report on the geology of the Te Pohue area, western Hawkes Bay (PPL 38316), with emphasis on stratigraphy and structure. *Unpublished Petroleum Corporation of New Zealand (Exploration) Ltd. report no. PR 1750.*

Frontier, P.T., 1995: Structural maps of PPL38316 area, Hawke's Bay, East Coast Basin, New Zealand. *Unpublished Petrocorp Exploration Ltd. report no. PR 2147.*

Gibb, J.G., 1986: A New Zealand regional Holocene eustatic sea-level curve and its application to determination of vertical tectonic movements. *Bulletin - Royal Society of New Zealand 24*: 377-395.

Golden Software, 2002: *Surfer 8.01*, Colorado.

Gomez, B., and Marron, D.C., 1991: Neotectonic effects on sinuosity and channel migration, Belle Fourche River, Western South Dakota. *Earth Surface Processes and Landforms 16*: 227-235.

Grant, A.P., 1939: Hawke's Bay flood, 23rd-25th April 1938. *New Zealand Institution of Engineers Conference, Auckland, New Zealand:* 55-64.

Grant, P.J., 1996: Hawke's Bay forests of yesterday : a description and interpretation. Havelock North, NZ, Pp. 273.

Grindley, G.W. 1960: Sheet 8 - Taupo. Geological Map of New Zealand Department of Scientific and Industrial Research, Wellington.

Hack, J.T., 1957: Studies of longitudinal stream profiles in Virginia and Maryland. *U.S. Geological Survey Professional Papers 294-B*: 97.

Hammond, A.P., 1997: Late Quaternary landscape evolution of western Hawkes Bay, North Island, New Zealand. Unpublished PhD thesis, lodged in the library, Massey University.

Hammond, A.P., and Palmer, A.S., 1992: Late Quaternary loess and tephras in central Hawkes Bay. *Geological Society of New Zealand and New Zealand Geophysical Society 1992 joint annual conference, Nov. 23-27, Christchurch, New Zealand:* 72.

Harrison, W., 1988: The influence of the 1982-83 drought on river flows in the Hawke's Bay. *Journal of Hydrology (NZ) 27*: 1-25.

Haywick, D.W., Lowe, D.A., Beu, A.G., Henderson, R.A., and Carter, R.M., 1991: Pliocene-Pleistocene (Nukumaruan) lithostratigraphy of the Tangoio block, and origin of sedimentary cyclicity, central Hawke's Bay, New Zealand. *New Zealand Journal of Geology and Geophysics 34*: 213-225.

Henderson, J., 1933: Geological aspects of the Hawke's Bay earthquake. *New Zealand journal of science and technology 15*: 38-75.

Henderson, J., and Ongley, M. 1920: The geology of the Gisborne and Whatatutu subdivisions - Geological Survey Bulletin. New Zealand Department of Scientific and Industrial Research.

Hennrich, K.P., 2001: Probablility of occurrence and extent of rainfall-induced landslides, Hawkes Bay, New Zealand. Unpublished PhD. thesis, lodged in the library, Victoria University of Wellington, Wellington.

Howard, A.D., 1980: Thresholds in river regimes. *In:* Vitek, J.D., *ed.* Thresholds in Geomorphology. Concord, Massachusetts, Allen and Unwin, Pp. 227-258.

Howard, A.D., Dietrich, W.E., and Seidl, M.A., 1994: Modeling fluvial erosion on regional to continental scales. *Journal of Geophysical Research, B, Solid Earth and Planets 99*: 13.

Howard, A.D., and Kirby, G., 1983: Channel changes in badlands. *Geological Society of America Bulletin 94*: 739-752.

Hull, A.G., 1986: Pre-A.D. 1931 tectonic subsidence of Ahuriri Lagoon, Napier, Hawke's Bay, New Zealand. *New Zealand Journal of Geology and Geophysics 29*: 75-82.

Hull, A.G., 1990: Tectonics of the 1931 Hawke's Bay earthquake. *New Zealand Journal of Geology and Geophysics 33*: 309-320.

Hutchinson, J.N., 1988: General report; Morphological and geotechnical parameters of landslides in relation to geology and hydrogeology. *Proceedings of the International Symposium on Landslides 5*: 3-35.

Hutchinson, J.N., 1995: The significance of tectonically produced pre-existing shears. *The interplay between geotechnical engineering and engineering geology : proceedings of the Eleventh European Conference on Soil Mechanics and Foundation Engineering, 28 May - 1 June, Copenhagen, Denmark:* 10.

Johnson, D.M., and Pearce, L.J., 1999: Landslides. *In:* Beetham, D., *ed.* Natural hazards in Hawke's Bay. Napier, Hawke's Bay Regional Council, Pp. 44.

Kamp, P.J.J., 1988: Tectonic Geomorphology of the Hikurangi Margin: surface manifestations of different models of subduction. *Zeitschrift fur Geomorphologie N.F. Suppl.-Bd 69*: 55-67.

Kamp, P.J.J., 1992: Landforms of Hawke's Bay and their Origin: a plate tectonic interpretation. *In:* Selby, M.J., *ed.* Landforms of New Zealand, Longman Paul, Pp. 344-366.

Keefer, D., 1994: The importance of earthquake-induced landslides to long-term slope erosion and slope-failure hazards in seismically active regions. *Geomorphology 10*: 265-284.

Keller, E.A., and Pinter, N., 1996: Active tectonics: earthquakes, uplift, and landscape. New Jersey, Prentice-Hall, Inc., 338 p.

Kelsey, H.M., Cashman, S.M., Beanland, S., and Berryman, K., 1995: Structural evolution along the inner forearc of the obliquely convergent Hikurangi margin, New Zealand. *Tectonics 14*: 1-18.

Kirby, E., and Whipple, K., 2001: Quantifying differential rock-uplift rates via stream profile analysis. *Geology 29*: 415-418.

Knighton, D.A., 1998: Fluvial forms and processes : a new perspective. London, Arnold, 383 p.

Knighton, D.A., 2000: Profile form and channel gradient variation within an upland drainage basin - River Noe, Derbyshire. *Zeitschrift fur Geomorphologie N.F. 122*: 149-164.

Krumbein, W.C., 1937: Sediments and exponential curves. *The Journal of Geology*: 577-601.

Landsat 7 enhanced thematic mapper, 1999: *Rectified Satellite Image ETM3, Path 72 row 86/87,* Landcare Research.

Leddra, M.J., Jones, M.E., and Goldsmith, A., 1993: Compaction and shear deformation of a weakly-cemented high porosity sedimentary rock. *In:* Cripps, J.C.e.a., *ed.* The Engineering Geology of Weak Rock. Rotterdam, Balkema.

Leopold, L.B., and Wolman, M.G., 1972: River Channel Patterns; Braided, Meandering and Straight. *In:* Schumm, S.A., *ed.* River morphology, Dowden, Hutchinson & Ross; Reprint, Pp. 283-300.

Lewis, K.B., 1980: Quaternary sedimentation on the Hikurangi oblique-subduction and transform margin, New Zealand. *In:* Congress, A., *ed.* Sedimentation in Oblique-Slip Mobile Zones. University of Auckland, Blackwell Scientific, Pp. 171-189.

Lewis, K.B., and Kohn, B.P., 1973: Ashes, turbidites and rates of sedimentation on the continental slope off Hawkes Bay. *New Zealand Journal of Geology and Geophysics 16*: 439-454.

Lewis, K.B., and Pettinga, J.R., 1993: The emerging, imbricate frontal wedge of the Hikurangi Margin. *In:* Ballance, P.F., *ed.* South Pacific sedimentary basins. Amsterdam, Elsevier Science Publishers B.V., Pp. 225-250.

Litchfield, N.J., 1995: Structure and tectonic geomorphology of the Lowry Peaks Range - Waikari Valley District, North Canterbury. Unpublished MSc thesis, lodged in the library, University of Canterbury, Christchurch.

Litchfield, N.J., 2002: Distribution, elevation, age, and incision of the Ohakean River Terrace in the Eastern North Island. *Geological Society of New Zealand annual conference, Northland:* 34.

Litchfield, N.J., in prep.: Maps, stratigraphic logs, and age control data for river terraces in the eastern North Island. *Unpublished Institute of Geological and Nuclear Sciences report no.*

Luzi, L., and Pergalani, F., 2000: A correlation between slope failures and accelerometric parameters: the 26 September 1997 earthquake (Umbria - Marche, Italy). *Soil Dynamics and Earthquake Engineering 20*: 301-313.

Mackey, B., 2003: The role of deep-seated landslides in landscape evolution, Tangoio Block, Hawke's Bay. Unpublished Bsc Hons. thesis, lodged in the library, Canterbury University, Christchurch.

Marden, M., and Neall, Y.E., 1990: Dated Ohakean terraces offset by the Wellington Fault, near Woodville, New Zealand. *New Zealand Journal of Geology and Geophysics 33*: 449-453.

Marden, M., and Rowan, D., 1993: Protective value of vegetation on Tertiary terrain before and during Cyclone Bola, East Coast, North Island, New Zealand. *New Zealand Journal of Forestry Science 23*: 255-263.

Marshall, P., 1933: Effects of earthquake on coast-line near Napier. *New Zealand journal of science and technology 15*: 79-92.

Mazengarb, C., 1983: Structure of the Ihungia area (East Coast Deformed Belt). *Geological Society of New Zealand Auckland Conference, Auckland:*

McGinty, P., Darby, D., and Haines, J., 2001: Earthquake triggering in the Hawke's Bay, New Zealand, region from 1931 to 1934 as inferred from elastic dislocation and static stress modeling. *Journal of Geophysical Research-Solid Earth 106*: 26593-26604.

McGlone, M., 1980: Late quaternary vegetation history of central North Island, New Zealand. Unpublished PhD thesis, lodged in the library, University of Canterbury, Christchurch.

McGlone, M.S., 1995: Late Glacial landscape and vegetation change and the Younger Dryas climatic oscillation in New Zealand. *Quaternary Science Reviews 14*: 867-881.

Merz, J., and Mosley, M.P., 1998: Hydrological behaviour of pastoral hill country modified by extensive landsliding, northern Hawke's Bay, New Zealand. *Journal of Hydrology (New Zealand) 37*: 113-139.

Milne, J.D.G., 1973: Upper Quaternary geology of the Upper Rangitikei Drainage Basin, North Island, New Zealand. Unpublished PhD thesis, lodged in the library, Victoria University of Wellington, Wellington.

Moglen, G.E., and Bras, R.L., 1995: The effect of spatial heterogeneities on geomorphic expression in a model of basin evolution. *Water Resources Research 31*: 2613-2623.

Montgomery, D.R., and Dietrich, W.E., 1994: A physically based model for topographic control on shallow landsliding. *Water Resources Research 30*: 1153-1171.

Montgomery, D.R., and Foufoula-Georgiou, E., 1993: Channel network source representation using digital elevation models. *Water Resources Research 29*: 1178-1191.

Morgans, H.E.G., G.H., S., Beu, A.G., Graham, I.J., and Mumme, T.C., 1996: New Zealand Cenozoic Timescale (version11/96). *Unpublished Institute of Geological and Nuclear Sciences report no. 96/38.*

Morris, P.H., and Williams, D.J., 1997: Exponential longitudinal profiles of streams. *Earth Surface Processes and Landforms 22*: 143-163.

Morris, P.H., and Williams, D.J., 1999: Worldwide correlations for subaerial aqueous flows with exponential longitudinal profiles. *Earth Surface Processes and Landforms 24*: 867-879.

Neall, V.E., Hanson, J., and New Zealand Earthquake and War Damage Commission, 1995: The neotectonics of the Ruahine and Mohaka Faults, between the Manawatu Gorge and Puketitiri. Palmerston North, NZ, Dept. of Soil Science, Massey University.

Neef, G., 1999: Neogene development of the onland part of the forearc in northern Wairarapa, North Island, New Zealand: a synthesis. *New Zealand Journal of Geology and Geophysics 42*: 113-135.

New Zealand Aerial Mapping, 1944: *Aerial Photo 471 - 3*, Puketitiri Napier 124.

Nicol, A., Van Dissen, R., Vella, P., Alloway, B., and Melhuish, A., 2002: Growth of contractional structures during the last 10 m.y at the southern end of the emergent Hikurangi forearc basin, New Zealand. *New Zealand Journal of Geology and Geophysics 45*: 365-385.

Ouchi, S., 1985: Response of alluvial rivers to slow tectonic movement. *Geological Society of America Bulletin 96*: 504-515.

Parsons, P., 1997: In the shadow of Te Waka. Napier, Te Pohue History Committee, 248 p.

Pearce, A.J., O'loughlin, C.L., Jackson, R.J., and Zhang, X.B., 1987: Reforestation: On-site effects on hydrology and erosion, eastern Raukumoana Range, New Zealand.

Symposium on Forest Hydrology and Watershed Management, Vancouver: 487-489.

Petley, D.N., 1996: The mechanics and landforms of deep-seated landslides. *In:* Anderson, M., *ed.* Advances in Hillslope Processes. Chichester, Wiley, Pp. 823-836.

Petley, D.N., and Allison, R.J., 1997: The mechanics of deep-seated landslides. *Earth Surface Processes and Landforms 22*: 747-758.

Petrocorp Exploration Ltd, 1991: *Seismic Survey EC91*

Pettinga, J.R., 1982: Upper Cenozoic structural history, coastal southern Hawke's Bay, New Zealand. *New Zealand Journal of Geology and Geophysics 25*: 149-191.

Pettinga, J.R., 1987a: Ponui landslide; a deep-seated wedge failure in Tertiary weak-rock flysch, southern Hawke's Bay, New Zealand. *New Zealand Journal of Geology and Geophysics 30*: 415-430.

Pettinga, J.R., 1987b: Waipoapoa landslide; a deep-seated complex block slide in Tertiary weak-rock flysch, southern Hawke's Bay, New Zealand. *New Zealand Journal of Geology and Geophysics 30*: 401-414.

Pettinga, J.R., and Bell, D.H., 1992: Engineering geological assessment of slope instability for rural land-use, Hawke's Bay, New Zealand. *Landslides*: 1467-1480.

Pillans, B.J., 1986: A late Quaternary uplift map for North Island, New Zealad. *Royal Society of New Zealand Bulletin 24*: 409-417.

Pillans, B.J., McGlone, M.S., Palmer, A.S., Mildenhall, D., Alloway, B.V., and Berger, G., 1993: The Last Glacial Maximum in central and southern North Island, New Zealand: a palaeoenvironmental reconstruction using the Kawakawa Tephra Formation as a chronostratigraphic marker. *Palaeogeography, Palaeoclimatology, Palaeoecology 101*: 283-304.

Pillans, B.J., and Moffat, J., 1991: Pleistocene glaciation of the Park Valley, Tararua Range. *Geological Society of New Zealand Miscellaneous Publication.*

Ramsay, J.G., 1967: Folding and fracturing of rocks, McGraw-Hill book company, 568 p.

Ramsay, J.G., 1974: Development of Chevron Folds. *Geological Society of America Bulletin 85*: 1741-1753.

Raub, M.L., 1985: The Neotectonic evolution of the Wakarara area, Southern Hawkes Bay, New Zealand. Unpublished MPhil thesis, lodged in the library, University of Auckland, Auckland.

Raub, M.L., Cutten, H.N.C., and Hull, A.G., 1987: Seismotectonic hazard analysis of the Mohaka Fault, North Island, New Zealand. *National Society for Earthquake Engineering, Wairakei, New Zealand:* 219-230.

Reyners, M., 1983: Lateral segmentation of the subducted plate at the Hikurangi Margin, New Zealand; seismological evidence. *Tectonophysics 96*: 203-223.

Rubey, W.W., 1952: Geology and mineral resources of the Hardin and Brussels quadrangles (in Illinois). *Unpublished United States Geological Survey report no. 218.*

Shackleton, N.J., 1987: Oxygen isotopes, ice volume and sea level. *Quaternary Science Reviews 6*: 183-190.

Skempton, A.W., and Petley, D.J., 1968: The strength along structural discontinuities in stiff clays. *Geotechnical Conference proceedings vol.2, Oslo:* 29-46.

Sklar, L., and Dietrich, W.E., 1998: River longitudinal profiles and bedrock incision models: Stream power and the influence of sediment supply. *Geophys. Mono 107*: 237-260.

Snow, R.S., and Slingerland, R.L., 1987: Mathematical modeling of graded river profiles. *Journal of Geology 95*: 15-33.

Snyder, N.P., Whipple, K.X., Tucker, G.E., and Merritts, D.J., 2000: Landscape response to tectonic forcing: Digital elevation model analysis of stream profiles in the Mendocino triple junction region, northern California. *Geological Society of America Bulletin 112*: 1250-1263.

Spörli, K.B., 1987: Airphoto lineaments and fracturing in the axial ranges of the Central North Island, New Zealand. *New Zealand Journal of Geology and Geophysics 17*: 139-156.

Spörli, K.B., and Pettinga, J.R., 1980: Mt. Kahurangi, Hawke's Bay, New Zealand: a klippe emplaced by gravity sliding from the crest of the nearby Elsthorpe Anticline. *Journal of the Royal Society of New Zealand 10*: 287-307.

Stirling, I.F. 1979: Esk, sheet V20. NZMS 260 Topographical map Department of Lands and Survey, Wellington, New Zealand.

Stoneley, R., Russell, W.A.C., and Haw, D., 1958: Waikaremoana - Waiakara Mountain Front Reconnaissance. *Unpublished BP Shell and Todd Petroleum Ltd. report no. 307.*

Strahler, A.N., 1952: Hypsometric (area - altitude analysis) of erosional topography. *Geol. Soc. Am. Bull 63*: 1117-11142.

Tanner, P.W.G., 1989: The flexural slip mechanism. *Journal of Structural Geology 11*: 635-655.

Thompson, C.S., 1987a: The climate and weather of Hawkes Bay. Wellington, N.Z., New Zealand Meteorological Service, 46 p.

Thompson, C.S., 1987b: Extreme rainfall frequencies in New Zealand. Wellington, N.Z., New Zealand Meteorological Service, 13 p.

Trustrum, N.A., Gomez, B., Page, M.J., Reid, L.M., and Hicks, D.M., 1999: Sediment production, storage and output: The relative role of large magnitude events in steepland catchments. *Zeitschrift fur Geomorphologie N.F. Suppl.-Bd 115*: 71-86.

Tucker, G.E., Whipple, K.X., Bras, R., and Anonymous, 1998: Impact of tectonic variations on sediment yield and river basin morphology. *Annual Meeting Expanded Abstracts - American Association of Petroleum Geologists.*

Varnes, D.J., 1978: Slope Movement Types and Processes. *In:* Krizek, R.J., *ed.* Special Report 176: Landslides: Analysis and control. Washington D.C., TRB, National Research Council, Pp. 11-33.

Wasowski, J., Keefer, D.K., and Jibson, R.W., 2000: Special Issue from the Symposium on Landslide Hazards in Seismically Active Regions. *Engineering Geology 58*: v-vi.

Westec, 1997: *Seismic Survey WEC-97*

Whipple, K.X., Hancock, G.S., and Anderson, R.S., 2000: River incision into bedrock; mechanics and relative efficacy of plucking, abrasion, and cavitation. *Geological Society of America Bulletin 112*: 490-503.

Whipple, K.X., and Tucker, G.E., 2002: Implications of sediment-flux-dependent river incision models for landscape evolution. *Journal of Geophysical Research 107*: 3-1 - 3-20.

Willgoose, G., Bras, R.L., and Rodriguez-Iturbe, I., 1991: A coupled channel network growth and hillslope evolution model; 1, Theory. *Water Resources Research 27*: 1671-1684.

Williams, G., 1986: Esk River Investigation. *Unpublished Hawke's Bay Catchment Board and Regional Water Board report no.*

Wylie, I.C., 1993: A preliminary interpretation of the subsurface structural style revealed by the 1991 Regional Seismic Survey. PPL 38316, East Coast Basin. *Unpublished Petrocorp Exploration report no. PR 2146.*

APPENDICES

Appendix A
NAPIER AIRPORT AND ESK FOREST RAINFALL RECORD

		Rainfall duration (h)						
		0.5	1	2	12	24	48	72
Return interval	2	18	26	55	72	99	121	131
	10	26	36	77	100	139	171	185
	20	30	41	87	112	156	193	208
	50	34	47	99	128	179	221	239
	34					169.164		
	144							274.32
	1000					253.3024		339.3432

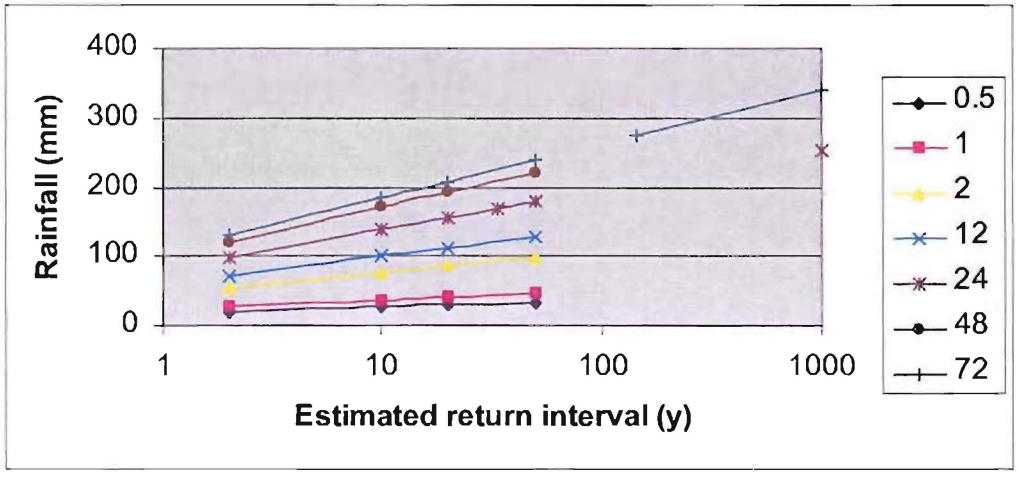

Figure A.1 Comparison of calculated rainfall return intervals for varying intensities at Napier Airport rainfall recorder (Thompson, 1987a) and precipitation recorded at the same location during April 1938 storm (Grant, 1939).

Thomson (1987b) derived rainfall frequencies for fired recorder sites in Hawke's Bay. The record for Napier Airport begins in 1936; Esk Forest in 1951. Figure A.1 Plots 24 and 36 hour rainfalls (mm) for the April 1938 event (highlighted orange) with respect to estimated return intervals at the same site. Figure A.2 plots the April 1938 rainfall recorded at Tutira with respect to the estimates derived for Esk Forest. This is necessary as the Esk recorder was not installed at the time of the 1938 event, and while the Tutira recorder was, it is not a government recorder station, and was therefore not analysed by Thomson (1987b). This comparison, however, is reasonable as each site is a similar distance from the Maungaharuru Range, and Grant (1939) encompasses both sites in the same isohyetal line for the whole 1938 event.

		Rainfall duration (h)						
		0.5	1	6	12	24	48	72
Return interval (yr)	2	17	23	65	101	148	207	234
	10	22	29	88	137	198	282	324
	20	25	32	98	153	220	314	363
	50	28	36	111	173	249	357	414
	551					324		
	1677							611
	1000					343		582

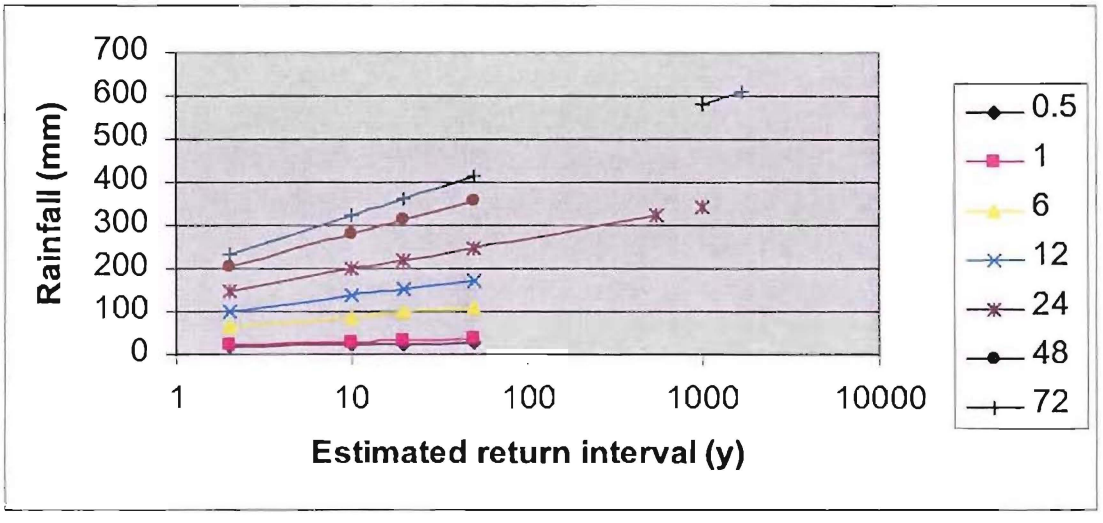

Figure A.2 Comparison of calculated rainfall return intervals for varying intensities at Esk Forest rainfall recorder (Thompson, 1987a) and precipitation recorded at Lake Tutira during April 1938 storm (Grant, 1939).

Appendix B
CALCULATING TOTAL SEDIMENT OUTPUT FOR THE APRIL 1938 FLOOD

Sediment output for the 1938 flood was calculated based on the hydrograph derived from eye-witness accounts (Grant, 1939; Cowie, 1957) and modelled flow stagings at the Waipunga Bridge (Williams, 1986), and sediment rating curves produced for the same section of the Esk River in Williams (1986).

The flood lasted three days, and the rise and fall on the 25th (in Cowie (1957) it is reported as the 24th, however, this appears to be in error as the maximum intensity of rainfall reportedly fell on the morning of the 25th (Grant, 1939; Cowie, 1957), and Grant (1939) notes this was the cause the flood peak) of April is reported by a local settler – presumably living in the lower Esk Valley – and recorded in Cowie (1957) as below:

4 a.m.	rise commenced
7.15 a.m.	bank high
9:30-10:30 a.m.	rising near peak
10 – 10:30 a.m.	at peak
10:30 a.m. – 2 p.m.	falling slowly to bank high
two days later	level back to normal

The peak discharge for the Esk River below the railway bridge (NZMS 260 sheet v20 ref. 386985) was calculated at 1830m^3/s, for Mangakopikopiko stream: 210m^3/s. This gives a combined peak discharge for the Esk River at Waipunga Bridge of approximately 2040m^3/s (Grant, 1939). The peak of the flood is said to have only lasted for half an hour, with the river flowing at over 50% of this for almost two days (Grant, 1939; Cowie, 1957). Total discharge for the Esk River was calculated to be $98x10^6m^3$ (Grant, 1939). Initial sediment volume calculations, also by Grant (1939) suggest sediment loads were over 75% by volume. However Williams (1986) shows the assumptions on which this calculation was based are incorrect, and that the maximum concentration is more likely to be approximately 17.5%.

Stage-flow analysis of the lower Esk River undertaken by Williams (1986) helps determine flows during the April 1938 flood. Maximum flows were reassessed, and the July 1985 event was used to calibrate a hydraulic model for the lower Esk River. The model predicts a maximum flow for the 1938 event of 2000-2500m^3/s, in general agreement with the calculations of Grant (1939) immediately following the event. A check of the models accuracy can be seen in predicted vs. measured flood levels for the event, these are generally within 0.5% of agreement for seven selected sites in the lower 13km of the channel (Williams, 1986). Bank full discharge is currently approximately 600m^3/s, this is possibly slightly higher than the waning bank full flows following the 1938 event as there has been a general degradation of the channel since this time allowing for higher discharges, though not significantly given the inherent errors in this form of derivation.

The values derived in the hydraulic model were used to produce the hydrograph for the 1938 event given in Section 2.4.1. "Rise commenced" is likely to refer to the rise to the main flood peak, flows were most likely already high due to two days' heavy rain in the catchment, and an initial below bank level flow of 500m^3/s was adopted. Peak flow was assumed to be 2000m^3/s, and normal flow nominal. The near "peak flow" was arbitrarily taken as 1800m^3/s. Bank high level was, however, slightly more difficult to determine as interpretations of the river bank may vary along the channel, and with the scale of the event. The river is said to have maintained half its peak flow for almost two days, while even today this would have left the majority of the valley underwater, with the river definitely not within its natural banks. Applying the current bank full discharge value and a simple linear recession of flood waters, however, overestimated the total event outflow as reported by Grant by almost $50x10^6m^3/s$, and left the flow for the two days about the peak at just over 400m^3/s, well below the 1000m^3/s reported by the same author. For the purpose of this investigation a bank full flow of 700m^3/s was adopted, this is probably slightly high as considerable flooding would be likely in the valley, however, it seems a reasonable compromise between eye-witness reports and estimated flows.

Williams (1986) evaluated a suspended sediment rating curve initially produced by the Ministry of Works and Development by comparing predicted sediment loads to actual flows over a range of velocities, including the 725m^3/s March 1985 flood. Results are shown to correspond remarkably well to the predicted curves. He then developed a bed material transport curve based on the hydraulic and sedimentary properties of the channel

using three popular empirical sediment transport equations (Meyer-Peter and Muller, Engelund-Hansen, and Einstein-Brown). These equations gave similar results, and allowed the development of a general bed material transport equation specific to the lower Esk River. Both the suspended sediment and bed material transport equations are given below:

Suspended sediment transport:

$S=1.35x10^{-6}Q^{2.55}$ **Equation B.1**

Bed material transport:

$T=0.00036Q^{0.97}$ **Equation B.2**

Where:

S = Suspended sediment transport rate (m^3/s)

T = Bed material transport rate (m^3/s)

Q = River flow (m^3/s)

These relationships are represented graphically on the sediment rating curves in Figure B.1. This indicates suspended sediment is dominant, particularly at high flows.

A sediment transport curve has been derived for the 1938 event based on inferred flows from the flood hydrograph and empirical sediment transport equations. By calculating the integral of the sediment transport curve, the total sediment output for the event is then determined. Results from this are given in Table B.1.

Table B.1 Calculated flood and sediment output values at Walpunga Bridge for April 1938 Esk Valley flood

Time (h)	Time(s)	Flow (m^3/s)	Suspended load (m^3)	Bed load (m^3)	Total sediment load (m^3/s)
0	0	0	0	0	0
52	187200	500	10.2969186	0.149383766	10.44630237
55.25	198900	700	24.28475747	0.207036825	24.49179429
57.5	207000	1800	269.9470939	0.517507717	270.4646016
58.5	210600	2000	353.1508513	0.573193948	353.7240452
62	223200	700	24.28475747	0.207036825	24.49179429
108	388800	0	0	0	0

Interval (h)	Total outflow (m^3/s)	Suspended load (m^3)	Bed load (m^3)	Total (m^3)
0-52	46800000	542981.1724	14195.24927	557176.4217
52-55.25	4095000	195288.9998	2085.625802	197374.6256
55.25-57.5	10125000	972633.5607	2940.177075	975573.7378
57.5-58.5	6840000	1117505.578	1963.315784	1119468.894
58.5-62	17010000	1881952.306	4927.1467	1886879.452
62-108	57960000	1132832.63	17403.70471	1150236.335
	01.4E+08	5.84E+06	4.35E+04	5.89E+06

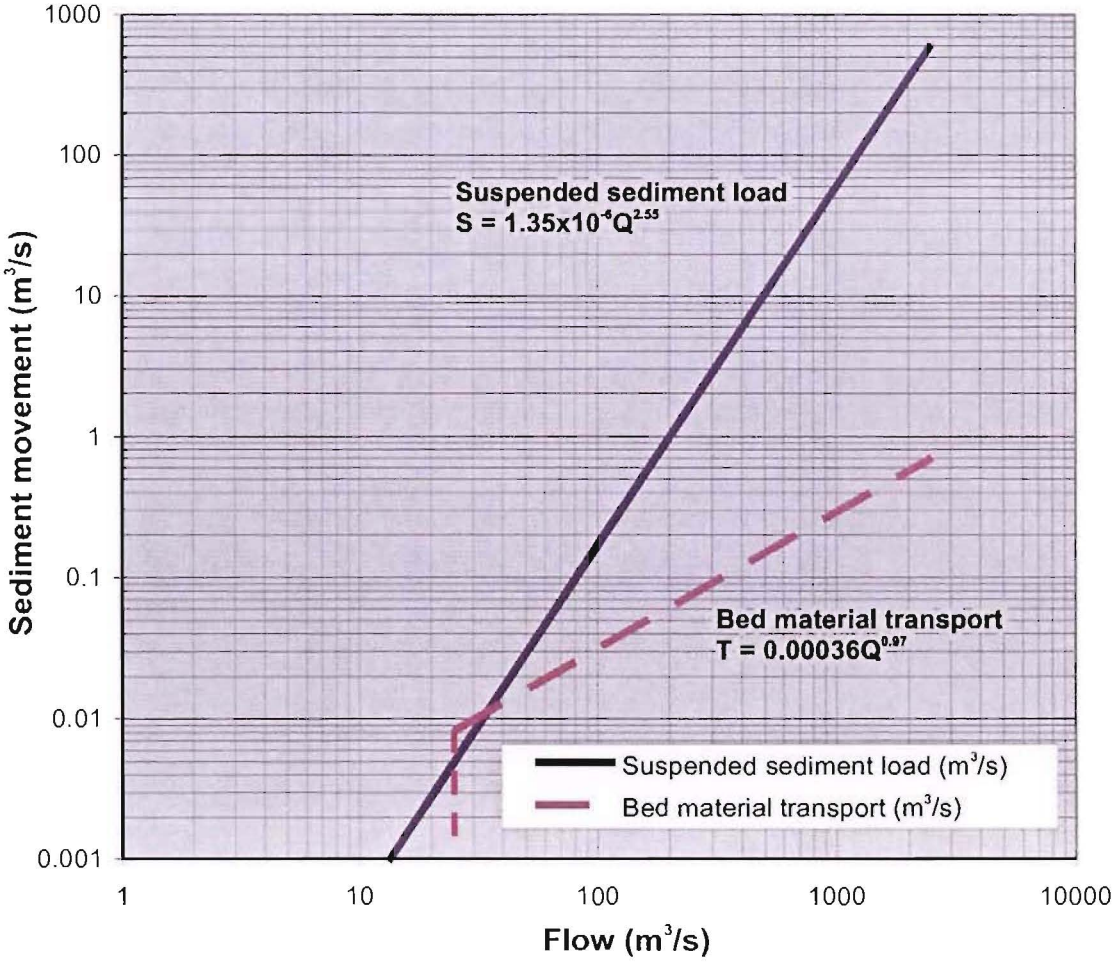

Figure B.1 Sediment transport curves for Esk River at Waipunga Bridge (Williams, 1986)

Appendix C
LINEAMENT ANALYSIS

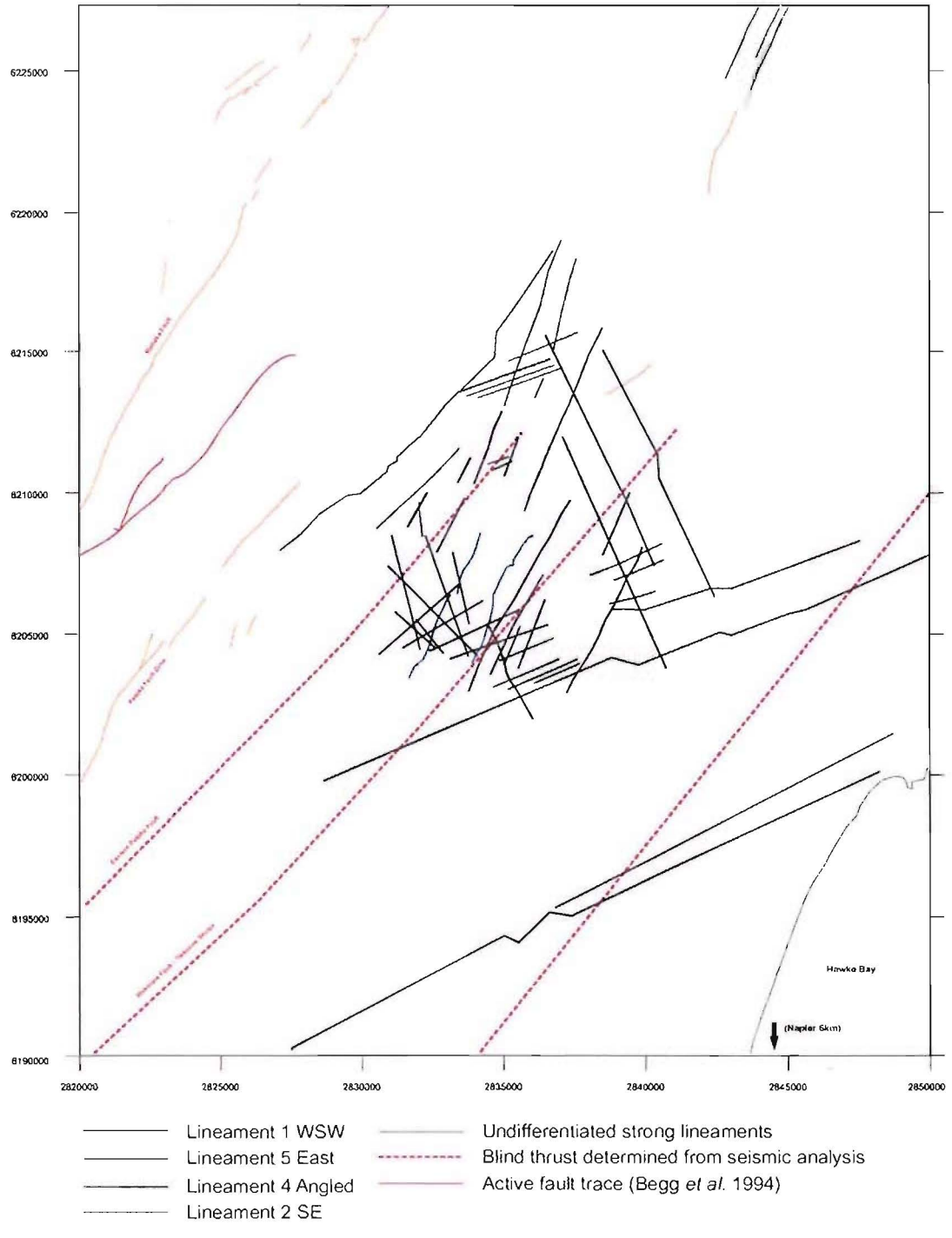

Figure C.1 Representative persistent lineaments identified in the Esk Valley

Lineaments were identified both on aerial and satellite photographs. However, for clarity only a representative set are reproduced here to illustrate the main trends in the valley. These lineaments correlate well with defects measured in the valley, and are labelled accordingly. The maximum intensity appears to correspond with the traces of blind thrusts that deform valley sediments.

Appendix D
LIST OF PHOTOS

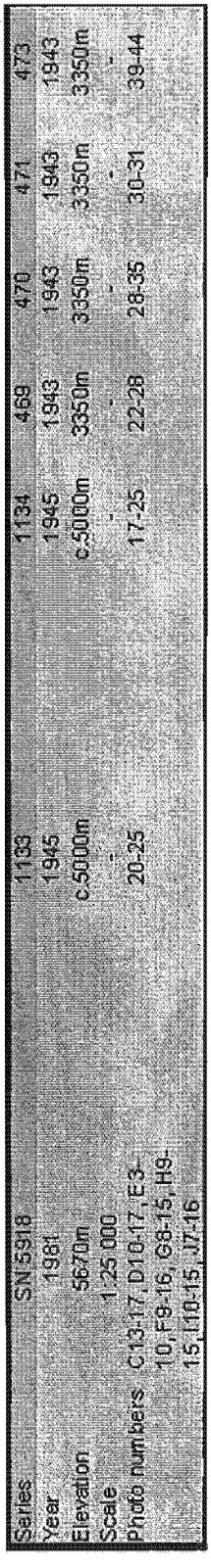

Series	SN 5918	1133	1134	469	470	471	473
Year	1981	1945	1945	1943	1943	1943	1943
Elevation	5670m	c.5000m	c.5000m	3350m	3350m	3350m	3350m
Scale	1:25 000	-	-	-	-	-	-
Photo numbers	C13-17, D10-17, E3-10, F9-16, G8-15, H9-15, I10-15, J7-16	20-25	17-25	22-28	28-35	30-31	39-44

Figure D.1 List of aerial photos used

Figure D.2 List of field photos

XCoord	YCoord	ID	Orientation	Description
2836580	6205240	p4-5-02_1	270	Valley form
2836310	6205270	p4-5-02_2	270	Valley form
2835960	6205390	p4-5-02_3	220	River terrace
2835620	6205570	p4-5-02_4	100	Defects - block failure
2835630	6205560	p4-5-02_5	160	Valley form - defects
2835530	6205620	p4-5-02_6	330	Valley form
2835370	6205810	p4-5-02_8	100	Defects - block failure
2835300	6205790	p4-5-02_9	260	Valley form - defects
2835190	6205830	p4-5-02_10	235	Defects on cliff
2835140	6205810	p4-5-02_11	90	Defects in stream bed
2834800	6205820	p4-5-02_12	90	Failure surface break-out close-up
2834800	6205800	p4-5-02_13	50	Failure surface break-out panorama
2834810	6205820	p4-5-02_16	20	Failure plane - sandstone bed
2833980	6205270	p4-5-02_14	50	Panorama looking NW from flat-top hill
2834790	6207500	p10-5-02_1	175	Possible fault trace, note alteration of dip in beds
2834980	6207400	p10-5-02_2	355	Transition from bedrock to slide debris - note intensely jointed bedrock
2834960	6207430	p10-5-02_3	355	Close-up of bedrock jointing
2835300	6207510	p10-5-02_4	170	Structural control on channel formation in reverse knickpoint
2835290	6207500	p10-5-02_5	50	Dominant structure in stream wall
2835290	6207500	p10-5-02_6	300	Strath terrace surface immediately upstream of reverse knickpoint - highly weathered
2835330	6207480	p10-5-02_7	285	Small knickpoint upstream of small fault
2835280	6207530	p10-5-02_10	150	Receeded cliff-face at reverse knickpoint. note: terrace surface is to immediate right
2835330	6207460	p10-5-02_11	20	Small fault immediately downstream of slide and knickpoint
2835320	6207470	p10-5-02_8	340	Landslide running down to small fault
2834430	6205830	p11-5-02_1	180	Fault splay zone off track. Main fault probably to left (E)
2834430	6205810	p11-5-02_2	180	Close-up of faults
2834720	6205310	p11-5-02_3	115	Panorama looking toward Waipunga Rd cliffs
2834730	6205310	p11-5-02_4	115	Close-up of possible fault disturbing block failure
2834820	6205360	p11-5-02_5	15	Terraces in Trellinoe slide
2835760	6206470	p11-5-02_6	50	Panorama looking at terrace surfaces around cliffs
2835700	6206420	p11-5-02_7	235	Bedding defined ridge within strath terrace
2834470	6205920	p11-5-02_8	170	Widely spaced continuous defects in cliffs above Kaiwaka bridge
2835600	6204450	p12-5-02_1	235	Possible fault traces and dault-sontrolled stream
2835530	6204450	p12-5-02_2	60	Fault or landslide fractured sandstone
2834700	6205880	p5-5-02_1	180	Discontinuity below bridge - continues up face
2832250	6206010	p5-5-02_2	285	Defect crossing stream
2832280	6205990	p5-5-02_3	285	2m high well receeded knickpoint
2832330	6205950	p5-5-02_4	170	Fault trace in south wall
2832330	6205980	p5-5-02_5	350	Fault trace on north wall
2832700	6205590	p5-5-02_7	165	Wood on contact between conglom & siltst. Possible haiatus ~10cm above
2832680	6205600	p5-5-02_8	225	Valley profile (for location)
2832720	6205620	p5-5-02_9	160	3 prominent defects 10m apart
2832490	6205870	p5-5-02_11	190	1m wide fault zone
2832490	6205830	p5-5-02_10	10	1m wide fault zone
2832770	6205560	p5-5-02_12	300	Highly incised stream
2832910	6205530	p5-5-02_14	90	Landslide failure plane
2832970	6205510	p5-5-02_15	350	Looking up at landslide
2842960	6225300	p1-5-02_1	195	Panorama looking up valley
2844480	6224680	p1-5-02_2	185	Looking up at possible fault trace in cliffs
2844570	6224650	p1-5-02_4	150	Interesting weathering pattern in cliffs
2844200	6226690	p1-5-02_5	15	Looking out from valley eroded along fault trace
2830990	6215470	p2001-1	230	Panorama looking toward dip slope
2839530	6203920	p2001-2	330	Panorama looking over Icecream hill
2836630	6215110	p2001-3	260	Looking at fall-off terrace structures
2837600	6213480	p2001-4	220	Fault structures
2840800	6210450	p2001-5	355	Strike ridges
2836890	6213820	p2001-6	75	Fault Structures
2831780	6217640	p2001-7	10	Basin at top of Maungaharuru Range
2832940	6216280	p2001-8	160	Looking out over landslide Debris
2841260	6210100	p2001-9	335	Looking accross at Maungahuruhu Range
2833910	6217340	p2001-10	160	Looking out over landslide debris
2833230	6214910	p2001-11	115	Panorama looking through Esk Valley
2832210	6216910	p2001-12	115	Panorama looking over Esk Valley
2836890	6205640	Trellinoe terrac	230	Panorama looking over main Trellinoe Terrace
2832750	6206410	p7-6-02_1	250	Trellinnoe defects
2835510	6213570	p2001-13	350	Glenlyon step-off surfaces
2835450	6221290	p2-6-02_1	200	Looking back at bedding in southern slides
2837620	6207150	p28-05-02_4	340	Landslide failure surface sub-parallel to bedding
2833580	6212690	p29-05-02_1	0	Panorama of large slide from logging area
2834990	6218870	p01-06-02_1	190	Bedding in Maungaharuru range
2837780	6206800	p28-05-02_3	95	Possible fault/lineation in Esk
2838110	6206390	p28-05-02_2	220	Bedding plane

Appendix E
CALCULATING THE SEDIMENT VOLUME CONTRIBUTION OF SHALLOW LANDSLIDING DURING THE 1938 FLOOD

Inspection of aerial photos indicated approximately 80% of slopes between 27° and 31° on the LINZ DEM exhibited shallow failure during the 1938 Esk Valley storm. While the slope association is primarily a useful tool for identifying areas of potential instability, it can be used to calculate approximate levels of sediment production – though errors are large.

The slope comparison was undertaken by converting the DEM (CD>Appendices/Appendix E/DEM.grd) into a digital slope map for the area using the "Terrain Slope" option in Surfer 8 (CD>Appendices/Appendix E/DigitalSlopeMap.grd). This converts the Z value for each 25m x 25m grid cell to a maximum slope angle for the cell based on the relative elevations of the four adjacent cells (ZN, ZS, ZE, ZW) as given in Equation E.1.

$$S_T \approx \frac{360}{2\pi}.\arctan\left[\sqrt{\left(\frac{Z_E - Z_W}{2\Delta x}\right)^2 + \left(\frac{Z_N - Z_S}{2\Delta y}\right)^2}^2\right]$$

Equation E.1 (Golden Software, 2002)

In order to calculate the volume of material produced by these slides, a distribution map first had to be produced (CD>Appendices/Appendix E/SlopeDist27-31.grd). The Grid>Math command was used to do this by forcing slope values outside the 27° – 31° window to zero, all non-zero values were then made equal to 1, providing a binary grid describing the slope distribution. Calculating the platform area of the cells is complicated in Surfer 8 as it automatically interpolates the Z value between adjacent cells, and areas can only be calculated above or below a set horizon. As most landslide areas constitute a single $25m^2$ cell, this can lead to an overestimation of the true area by as much as 600% Figure E.1. In order to minimise this error, a horizon approximately equal to 1 was selected (0.99999), and the area calculated is between this horizon and 1.

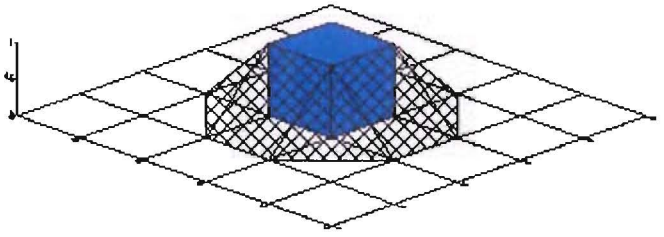

A cube with a coarse grid. Volume error is increased.

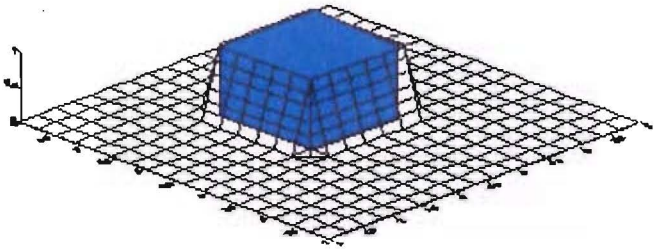

A cube with a finer grid. Volume error is reduced.

Figure E.1 Illustration of grid interpolation derived errors in area and volume calculations (Golden Software, 2002)

The area returned by this method was then divided by the cosine of the average slope (29°), and the average depth of shallow landsliding in the region as reported in literature (Pettinga and Bell, 1992; Merz and Mosley, 1998) to return the total volume of sediment produced.

As well as potential interpolation errors associated with the Surfer program, a number of other substantial sources of error are associated with this approach, these include:

- Actual landsliding as identified in aerial photographs is typically more extensive than that indicated by the slope map. This may have lead to an underestimation by as much as 50%.
- Variation in average landslide depth will substantially affect the total volume calculation, however as the same depth has been reported by separate studies it is unlikely to vary substantially.
- The tendency for the DEM grid to round off sharp cliffs is also apparent as a large number of the slopes are located adjacent to the incised gullies. While the steepness of the terrain in aerial photos makes it impossible to identify landslides in this region, it is unlikely the same processes contribute to landslide generation in these

areas, and distribution is likely to be different. For this reason these slides should not strictly be included in this calculation. However, steep slopes and presumably high pore pressures in this region suggest landsliding is likely to be prevalent along these margins during rainfall events. It is extremely difficult to remove these points from the dataset, an attempt has been made by excluding all elevations below the level of the inferred Ohakean terrace as it would have extended through the valley. This excluded approximately 14% of the area (163,676m^2 in planform area). However, it also excludes many "valid" points below the terrace level and is generally unsatisfactory. For this reason, and for the fact the gorge margins are likely to be inherently unstable, values quoted in the text include these points.

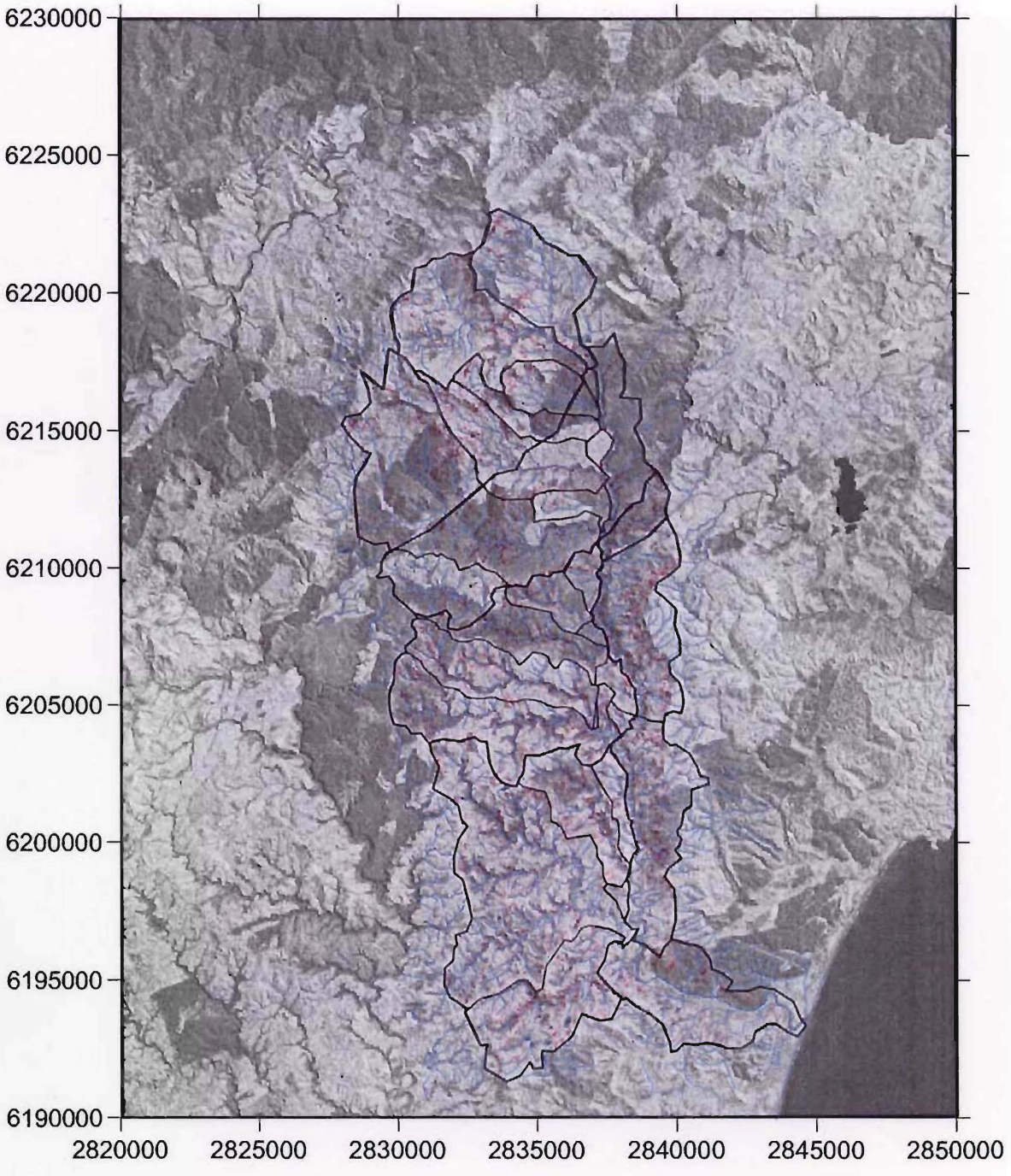

Appendix E.2 Slope distribution map for slopes 27° - 31°

Each point on the overlay represents a 25m^2 cell. Slopes between 27° and 31° are used as a proxy for shallow landsliding following the April 1938 Esk Valley Storm as an examination of aerial photographs taken soon after the event suggest these correspond to 80% of the shallow failures that were present on the landscape. Slopes are derived through interpolation of a LINZ DEM based on 1:50,000 contour data.

Catchment and geomorphic boundaries in the Esk Valley are also outlined. The base image is taken from Landsat 7 ETM (1999). Co-ordinates are in NZMG, units are in meters.

Appendix F
FIT STATISTICS FOR LONG RIVER PROFILE CURVES

Figure F.1 was compiled by Crosby (2001) at a field location NE of Gisborne. The DEM the figure is derived from is the same as that used in this investigation. Contour data is that provided on the NZMS 260 1:50 000 topographic maps. The figure clearly shows the poor grid interpolation, particularly at lower gradients, though also indicates the accuracy of the contour data as it aligns well with the surveyed points.

The profile "smoothing" used in this investigation attempted to partially negate the effect of contamination of the walls in the steep gorges, and this poor grid interpolation by rounding all values down to the nearest 20m interval. This is indicated in red on the lower portion of the diagram. While this removed any contamination, and brought data down slightly – more into line with the true profile – it also emphasised the steps between contours and increased errors associated with correlations with other "unsmoothed" data off the DEM.

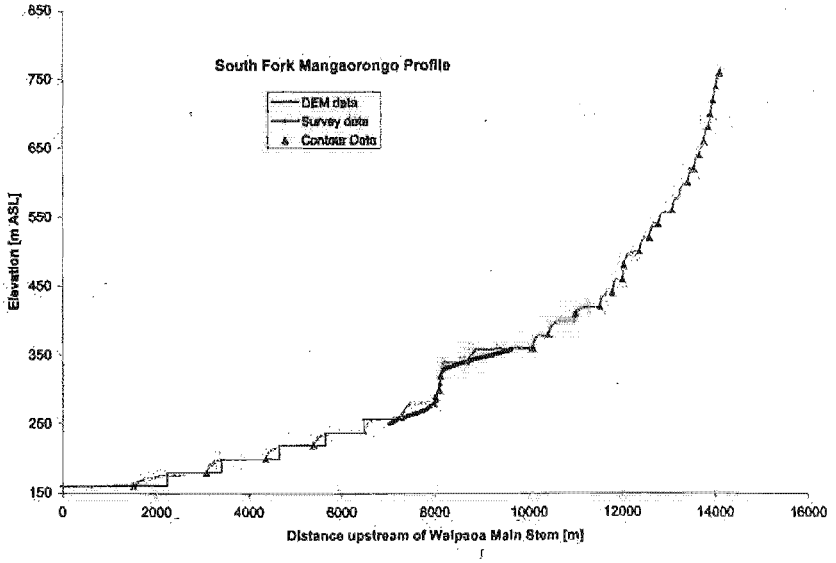

Figure F.1 Long profile of the south fork of the Mangaorongo River showing the relationship between DEM, contour, and survey data (Crosby and advised by K. Whipple, 2001).

(CD>Appendices/Appendix F/DrainageData.xls)

Upper Esk	
Lower Esk	
Mid Esk	
Equation ln(Y)	9.116081842E-005 * X + 2.408758662
Alternate Y	EXP(0.00009116081842 *x) * 11.12014871
Number of data points used	2576
Average X	21155
Average ln(Y)	4
Residual sum of squares	125
Regression sum of squares	2820
Coef of determination, R-squared	0.957435
Residual mean square, sigma-hat-sq'd	0.048712

01 Mangapikopiko Stream	
Equation ln(Y)	0.0001452433939 * X + 2.166752984
Alternate Y	exp(0.0001452433939 * X) * 8.729891872
Number of data points used	986
Average X	13434.9
Average ln(Y)	4.11809
Residual sum of squares	14.9078
Regression sum of squares	362.484
Coef of determination, R-squared	0.960498
Residual mean square, sigma-hat-sq'd	0.01515

02 Rautoiti Stream	
Equation ln(Y)	0.0002443253811 * X + 0.556416446
Alternate Y	exp(0.0002443253811 * X) * 1.744410098
Number of data points used	516
Average X	15842
Average ln(Y)	4.42702
Residual sum of squares	3.54333
Regression sum of squares	146.064
Coef of determination, R-squared	0.976316
Residual mean square, sigma-hat-sq'd	0.006894

03 Otakowai	
Equation ln(Y)	0.0001563822685 * X + 1.072974677
Alternate Y	exp(0.0001563822685 * X) * 2.924064722
Number of data points used	853
Average X	24118.9
Average ln(Y)	4.84475
Residual sum of squares	6.15158
Regression sum of squares	249.156
Coef of determination, R-squared	0.975905
Residual mean square, sigma-hat-sq'd	0.007229

04 Kaiwaka	
Equation ln(Y)	0.0001903152471 * X + 0.4482896111
Alternate Y	exp(0.0001903152471 * X) * 1.565632054
Number of data points used	736
Average X	23427.8
Average ln(Y)	4.90696
Residual sum of squares	4.83261
Regression sum of squares	265.227
Coef of determination, R-squared	0.982105
Residual mean square, sigma-hat-sq'd	0.006584

06 Deep Stream	
Equation ln(Y)	0.0001372268955 * X + 1.371444488
Alternate Y	exp(0.0001372268955 * X) * 3.941039371
Number of data points used	789
Average X	28507.6
Average ln(Y)	5.28345
Residual sum of squares	5.61653
Regression sum of squares	152.862
Coef of determination, R-squared	0.96456
Residual mean square, sigma-hat-sq'd	0.007137

06 Unnamed	
Equation ln(Y)	0.0002294039221 * X - 0.6535284404
Alternate Y	exp(0.0002294039221 * X) * 0.5202070152
Number of data points used	254
Average X	26308.8
Average ln(Y)	5.38182
Residual sum of squares	2.32839
Regression sum of squares	15.8505
Coef of determination, R-squared	0.871918
Residual mean square, sigma-hat-sq'd	0.00924

07 Okurakura Stream	
Equation ln(Y)	9.403044508E-005 * X + 2.281999163
Alternate Y	exp(9.403044508E-005 * X) * 9.79624514
Number of data points used	980
Average X	35237.7
Average ln(Y)	5.59542
Residual sum of squares	6.41824
Regression sum of squares	162.531
Coef of determination, R-squared	0.962011
Residual mean square, sigma-hat-sq'd	0.006563

08 Berry Rd.	
Equation ln(Y)	0.00020085359 * X - 1.164278383
Alternate Y	exp(0.00020085359 * X) * 0.312147832
Number of data points used	615
Average X	34479.3
Average ln(Y)	5.76102
Residual sum of squares	4.96884
Regression sum of squares	142.661
Coef of determination, R-squared	0.966342
Residual mean square, sigma-hat-sq'd	0.008106

09 Unnamed	
Equation ln(Y)	0.0001897809607 * X - 0.9398591958
Alternate Y	exp(0.0001897809607 * X) * 0.3906828413
Number of data points used	412
Average X	36343.4
Average ln(Y)	5.95743
Residual sum of squares	1.0306
Regression sum of squares	42.8612
Coef of determination, R-squared	0.97652
Residual mean square, sigma-hat-sq'd	0.002514

10 Unnamed	
Equation ln(Y)	0.0002366413077 * X - 2.599319126
Alternate Y	exp(0.0002366413077 * X) * 0.07432416636
Number of data points used	307
Average X	36225.9
Average ln(Y)	5.97323
Residual sum of squares	0.968619
Regression sum of squares	26.9049
Coef of determination, R-squared	0.96525
Residual mean square, sigma-hat-sq'd	0.003176

Appendix G
CALCULATING CHANNEL SINUOSITY

G - I INTRODUCTION

A new method of calculating channel sinuosity was developed for this investigation. This method enables a user to quickly and accurately calculate channel sinuosity continuously along a channel profile. The method utilises two popular software applications; Golden Software Surfer, and Microsoft Excel, and results can be easily incorporated in a GIS database.

The calculation of channel sinuosity requires only two variables, channel path length and straight-line valley length. While neither of these is particularly difficult to measure, there are two fundamental problems associated with applying the calculation to a river channel:

1. Delineating a path that is representative of the valley length
2. Choosing a meander length that is representative of those in the channel

These are related by a single complicating factor: geometry in nature is inherently complex. Commonly, meanders of different length and amplitude are superimposed on one another, and structural controls can play an important part in the definition of the meander form, constantly varying their shape and scale. A simple means of dealing will this problem is to perform many iterations along the profile, varying the scale of meander chosen. A computational approach is the obvious choice for this technique as each iteration adds to an already tedious task.

G - II METHOD

1. Examine sinuosity form using a map and/or aerial photos to determine orders of sinuosity present
2. Create a map in Surfer from XYZ topographic data. If no data is available, create a Base Map using an image file of a topographic map, then define image co-ordinates in the properties dialog. Create a grid (originalmap.grd) of the same dimensions using the grid-function command, and set the function to "z=0" or similar.

3. Digitise the stream profile (stream.bln) (SP) from the map, create a "slice" from this profile (stream.dat) using the initial grid used to produce the map (originalmap.grd).
4. Digitise valley length profiles (VLP) connecting inflection points of smallest pathlength meanders (VLPxx.bln)
5. Repeat step 4 for all identified pathlengths
6. Produce a grid (stream.grd) from the SP (stream.dat) that extends laterally beyond the maximum deviation of the coarsest VLP line using the stream path length for Z values. This is done using the Kringing algorithm as an exact interpolator, and produces a corridor of equal length values that extend laterally from the stream path while still honouring the initial values. The selected search radius defines the width of the corridor produced and therefore maximum deviation from the channel. This reduces resolution however, and should be kept to a minimum.
7. Produce a "slice" of the grid from each of the digitised VLPs (VLPxx.bln), this produces individual .dat files with x, y, stream pathlength, and valley length values.
8. This is enough data to produce sinuosity curves from the VLP relating to the shortest pathlength meanders.
9. For the next VLP repeat step 6, substituting the previous VLP "slice" (.dat) for the stream path and using the valley length column for Z values. Step 7 is also repeated; however as a "slice" has already been produced, an additional column of 0's must be added to the VLP .dat file and the grid-residuals option is used instead. This produces a .dat file for the VLP with columns as below:

X	Y	SP length	VLP length	Check value	0	Residuals (previous VLP length)

10. The residuals column is negative, multiply by -1 to restore to normal.
11. If other scales are identified, repeat steps 6-9

12. Open the VLP .dat files in Excel, and add a row of cells at the top of the page. In one of these cells place a value which will represent a sampling interval for the sinuosity calculation. This should approximate the path length of the meanders.

13. In new columns – using the MATCH command and the sampling interval value entered above, find the values in the SP length column that lie half a sampling interval above and below each cell. This will obviously not be possible for the rows near the start and the end of the VLP and will return null values. The formula in cell I28 in Figure G.1 is as follows: =MATCH((G28+D$1/2),$G$4:$G$575,1)

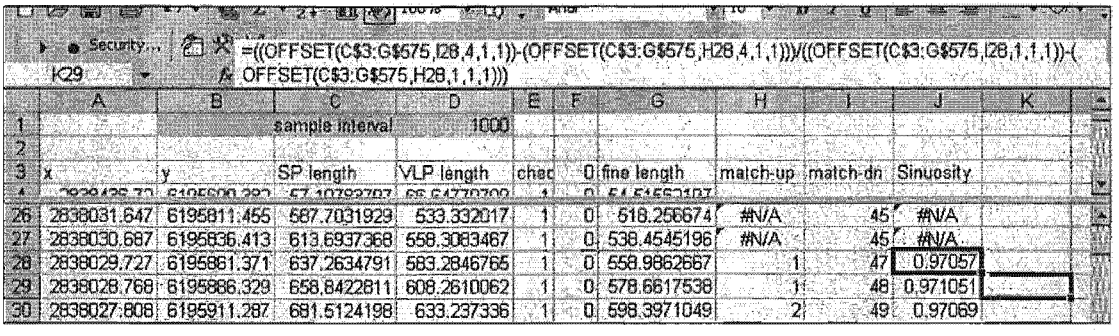

Security... =((OFFSET(C$3:G$575,I28,4,1,1))-(OFFSET(C$3:G$575,H28,4,1,1)))/((OFFSET(C$3:G$575,I28,1,1,1))-(
I29 OFFSET(C$3:G$575,H28,1,1,1)))

	A	B	C	D	E	F	G	H	I	J	K
1			sample interval	1000							
2											
3	x	y	SP length	VLP length	chec	0	fine length	match-up	match-dn	Sinuosity	
26	2838031.647	6195811.455	587.7031929	533.332017	1	0	618.256674	#N/A	45	#N/A	
27	2838030.687	6195836.413	613.6937368	558.3083467	1	0	536.4545196	#N/A	45	#N/A	
28	2838029.727	6195861.371	637.2634791	583.2846765	1	0	558.9862667	1	47	0.97057	
29	2838028.768	6195886.329	658.8422811	608.2610062	1	0	578.6617538	1	48	0.971051	
30	2838027.808	6195911.287	681.5124198	633.237336	1	0	598.3971049	2	49	0.97069	

Figure G.1 Excel spreadsheet used to calculate sinuosities

14. The OFFSET command is then used in conjunction with references returned from column H and I to calculate the sinuosity.

15. Finally, sinuosity should be plotted against SP length

16. The sample interval can then be adjusted to highlight trends or particular meander pathlengths.

A line representing the valley length was digitised using straight lines connecting the inflexion points of major thalwegs along the river. A grid was then derived that extended beyond the limit of the widest meander and enabled correlation between valley length and channel length. A running window of 300m was chosen as a sampling interval along the valley length as results best describe channel sinuosity. This value equates to around half the wavelength of the largest meander, ensuring it is sampled without losing excessive resolution on smaller meanders, and agrees with observations made by Litchfield (1995).

Appendix H
DEFECT ANALYSIS DATA

Figure H.1 Defect orientation and location data

XCoord	YCoord	Strike	Dip	Symbol_typ	Spacing__m	Displaceme	Set	Motion	Notes
2835650	6205560	341	68	Defect	0	0	0		
2835370	6205790	251	65	Defect	0	0	1		
2835360	6205790	92	80	Defect	0	0	0		
2835360	6205790	185	85	Defect	0	0	5		
2835190	6205800	270	52	Defect	1.5	0	0		
2835170	6205800	210	90	Defect	2	0	2		
2835150	6205780	238	62	Defect	0.5	0	1		
2835140	6205770	340	88	Defect	1.5	0	5		
2834690	6205840	250	85	Defect	8	0	1		
2834680	6205840	285	75	Defect	0	0	0		
2832120	6206070	335	85	Defect	0	0	0		
2833030	6205480	320	90	Defect	0	0	3		
2832600	6205660	160	85	Defect	10	0	5		
2832370	6205910	168	88	Defect	0	0	5		
2834740	6207350	18	20	Defect	0	0	0		
2834750	6207350	232	85	Defect	0	0	1		
2834730	6207360	82	18	Defect	0	0	0		
2834860	6207420	136	86	Defect	1	0	3		
2834950	6207380	182	60	Defect	0	0	4		
2834950	6207380	255	85	Defect	0	0	1		
2834940	6207450	145	90	Defect	0	0	3		
2834950	6207480	20	88	Defect	0	0	2		
2835110	6207440	180	88	Defect	0	0	5		
2835160	6207520	255	90	Defect	0	0	1		
2835300	6207500	90	90	Defect	0	0	0		
2835300	6207500	55	82	Defect	0	0	1		
2835310	6207490	216	90	Defect	1.2	0	2		
2835320	6207480	185	90	Defect	0	0	5		
2835610	6207380	248	80	Defect	0	0	1		
2834410	6205800	255	57	Defect	0.6	0	1		
2834410	6205810	3	72	Defect	10	0	0		
2835530	6204570	255	72	Defect	0	0	1		
2835890	6204400	230	70	Defect	0	0	0		
2835770	6204540	138	85	Defect	0.65	0	3		
2835770	6204540	50	88	Defect	0.65	0	2		
2835740	6204520	286	80	Defect	0	0	0		
2835740	6204520	200	85	Defect	0	0	2		
2835720	6204580	111	90	Defect	0.4	0	0		
2835720	6204570	232	28	Defect	0	0	0		
2835550	6204450	316	88	Defect	0	0	3		
2835560	6204470	188	62	Defect	0.15	0	4		
2835550	6204470	195	50	Defect	0.3	0	4		
2835410	6204420	35	40	Defect	0.6	0	0		
2835390	6204420	272	90	Defect	0.6	0	0		
2835400	6204360	320	35	Defect	1.5	0	0		
2835400	6204370	210	88	Defect	0	0	2		
2835390	6204370	244	90	Defect	0	0	1		1m wide gut in hillside.
2835250	6204250	38	70	Defect	0	0	0		Face defect
2835160	6204250	288	88	Defect	0	0	0		
2835160	6204250	75	28	Defect	0	0	0		
2835170	6204500	152	80	Defect	0	0	5		Approx. Left face in photo
2835200	6204480	255	80	Defect	0	0	1		Approx. Right face in photo
2835190	6204510	170	60	Defect	0	0	4		Approx. Middle face in photo
2830900	6203930	204	65	Defect	1	0	4		
2830900	6203920	64	88	Defect	0	0	1		
2830900	6203910	55	50	Defect	0	0	0		
2830930	6203880	42	75	Defect	0	0	0		
2830930	6203880	60	88	Defect	0	0	1		
2830990	6203830	56	68	Defect	2	0	0		Spaced about every 2m up to fault
2838790	6204910	230	45	Defect	0	0	0		
2838790	6204900	178	45	Defect	0	0	4		
2838800	6204920	26	90	Defect	0	0	2		
2837860	6206830	320	90	Defect	0	0	3		
2838100	6206290	42	90	Defect	3	0	2		
2838060	6206290	320	55	Defect	1	0	0		
2838440	6206030	230	27	Defect	0	0	0		
2838720	6205380	158	47	Defect	0.05	0	4		
2838720	6205360	207	45	Defect	0.2	0	4		
2838730	6205330	235	83	Defect	0.6	0	1		
2843830	6213820	245	70	Defect	0	0	1		
2835410	6218190	290	68	Defect	0	0	0		
2834710	6218450	280	80	Defect	15	0	0		
2836790	6204900	180	65	Defect	0	0	4		
2836840	6204610	295	50	Defect	0	0	0		May be exfoliation

Figure H.2 Fault orientations and localities

XCoord	YCoord	Strike	Dip	Symbol_typ	Spacing__m	Displaceme	Motion	Notes
2832480	6205850	190	85	Fault	1	2.8	Normal	
2832320	6205940	165	80	Fault	0.35	3	Normal	
2835320	6207460	210	80	Fault	0	0.4	Normal	
2834430	6205810	354	32	Fault	2.2	0.25	Reverse	
2835100	6209700	0	0	Fault	0	1.5		From Kyle Bland
2832800	6206900	0	0	Fault	0	3		From Kyle Bland
2841450	6206470	45	0	Fault	0	0		From D.Haywick
2846150	6207880	55	0	Fault	0	0		From D.Haywick
2846150	6207850	190	0	Fault	0	0		From D.Haywick
2830910	6203900	199	70	Fault	0	0.2	Normal	
2830930	6203870	60	88	Fault	0	0.25	Reverse	
2830970	6203840	18	90	Fault	0	0.1	Reverse	
2831030	6203800	235	60	Fault	0	0.15	Normal	
2837770	6204040	88	80	Fault	0	0		Appears to be fault, though can't tell motion

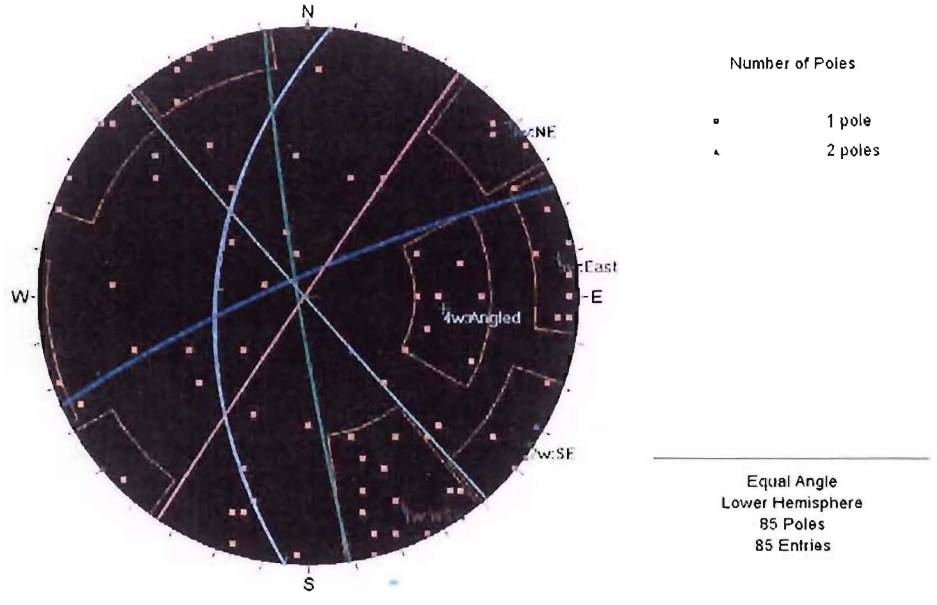

Figure H.3 Stereographic plot of defect poles

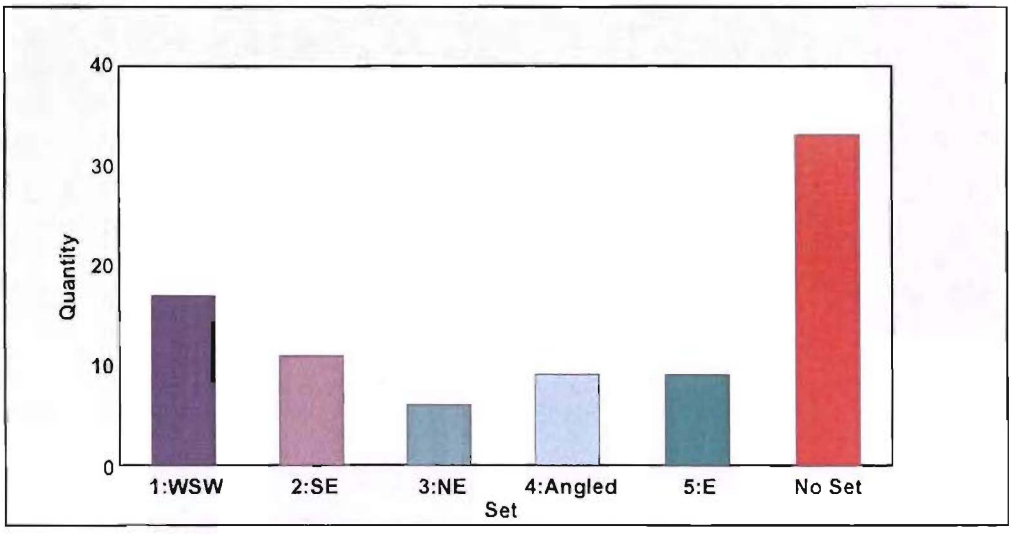

Figure H.4 Relative weightings of defect sets

Appendix I
CD CONTENTS

Directory		File	Opens with	Description
Volume		Hawkes Bay.enl	EndNote	Bibliographic references
		1-Leith-Introduction.pdf	Adobe Acrobat	Chapter 1
		2-Leith-Overview.pdf	Adobe Acrobat	Chapter 2
		3-Leith-Reconnaissance.pdf	Adobe Acrobat	Chapter 3
		4-Leith-Field.pdf	Adobe Acrobat	Chapter 4
		5-Leith-Structure.pdf	Adobe Acrobat	Chapter 5
		6-Leith-Discussion.pdf	Adobe Acrobat	Chapter 6
		7-Leith-Conclusion.pdf	Adobe Acrobat	Chapter 7
		8-Leith-Appendix.pdf	Adobe Acrobat	Appendix
		9-Leith-Bibliography.pdf	Adobe Acrobat	Bibliography
		10-Leith-FullText.pdf	Adobe Acrobat	Full Thesis Text
	Maps	Attachment1.cdr	Corel Draw 11	Field area overview
		Attachment2.cdr	Corel Draw 11	Trelinnoe Study Area geomorphic map
	Georeferenced Images	ETM3Panchromatic.tif	ArcView	Landsat Panchromatic image
		ETM3Panchromatic.tfw	Notepad	Georeferencing information for above image
		ShadedRelief.tif	ArcView	Shaded relief map derived from 20m contours
		ShadedRelief.tfw	Notepad	Georeferencing information for above image
		47029.tif	ArcView	1943 Aerial photo of Trelinnoe Study Area
		47029.tfw	Notepad	Georeferencing information for above image
		47031.tif	ArcView	1943 Aerial photo of Trelinnoe Study Area
		47031.tfw	Notepad	Georeferencing information for above image
		47033.tif	ArcView	1943 Aerial photo of Trelinnoe Study Area
		47033.tfw	Notepad	Georeferencing information for above image
		47035.tif	ArcView	1943 Aerial photo of Trelinnoe Study Area
		47035.tfw	Notepad	Georeferencing information for above image
		113423.tif	ArcView	1943 Aerial photo of Tributary Domain 3
		113423.tfw	Notepad	Georeferencing information for above image
		HawkesBay.tif	ArcView	Regional map of Hawke's Bay. Source: LINZ website
		HawkesBay.tfw	Notepad	Georeferencing information for above image
		2147Cretaceous.tif	ArcView	Contours of Cretaceous unconformity in Frontier (1995)
		2147Cretaceous.tfw	Notepad	Georeferencing information for above image
Appendices	Appendix A	DrainageData.xls	Microsoft Excel	Fit statistics for long river profiles
	Appendix B			
	Appendix C	See photo ID		See photo Description
		Photos.xls	Microsoft Excel	Photo location and orientation
	Appendix D	DEM.grd	Golden Software Surfer	
		eskvalley_a	xyz	ASCII grid data
		DigitalSlopeMap.grd	Surfer	Digital slope map
		SlopeDist27-31.grd	Surfer	Binary grid of slopes 27-31deg
		SlopeDist27-31.dat	xyz	Binary grid of slopes 27-31deg
	Appendix E			
	Appendix F	Sinuosities.xls	Microsoft Excel	Channel sinuosity calculations
	Appendix G	DefectsAndFaults.xls	Microsoft Excel	Defect and fault orientation data
Misc Data	GPS	UppertceASCII.grd	Surfer	grid of GPS survey of terrace north of Berry Rd. Stream
		UppertceASCII.xls	Microsoft Excel	GPS survey of terrace north of Berry Rd. Stream
	Software	s8demo.exe		free demo of Surfer 8
		Acrobat6.exe		free Acrobat reader
		Endemo.exe		free demo of EndNote